



# SAPIENZA

UNIVERSITA' DI ROMA

**Dottorato di Ricerca in Medicina Sperimentale**

XXVIII Ciclo

**Novel cell-based assays identify new metabolic targets to  
block *Plasmodium falciparum* transmission**

DOTTORANDA  
Giulia Siciliano

DOCENTI GUIDA  
Dott. Pietro Alano  
Dott. Andrea Cara

COORDINATORE DEL DOTTORATO  
Prof.ssa Maria Rosaria Torrisi

ANNO ACCADEMICO  
2014/2015



Thesis performed at Istituto Superiore di Sanità

## Contents

|  |     |
|--|-----|
| <b>General introduction</b> .....  | 1   |
| Malaria.....   | 1   |
| <i>Plasmodium falciparum</i> life cycle.....   | 1   |
| <i>Plasmodium falciparum</i> gametocytogenesis.....  | 3   |
| <i>Plasmodium falciparum</i> blood stage metabolism.....   | 5   |
| Hemoglobin digestion.....  | 5   |
| Redox equilibrium.....   | 7   |
| The glutathione system in <i>P. falciparum</i> .....   | 8   |
| The thioredoxin system in <i>P. falciparum</i> .....   | 9   |
| Resistance of <i>P. falciparum</i> to current antimalarial treatments and the need of new drugs....  | 10  |
| <b>Aim of the thesis</b> .....   | 18  |
| <b>A simple and predictive phenotypic High Content Imaging assay for <i>Plasmodium falciparum</i> mature gametocytes to identify malaria transmission blocking compounds</b> ..... | 19  |
| Enlightening the malaria parasite life cycle: bioluminescent <i>Plasmodium</i> in fundamental and applied research.....  | 43  |
| Multicolor bioluminescence boosts malaria research: quantitative dual-color assay and single-cell imaging in <i>Plasmodium falciparum</i> parasites.....                           | 58  |
| Synergy of drugs affecting the redox equilibrium of <i>Plasmodium falciparum</i> mature gametocytes investigated with a bioluminescence assay specific for late sexual stages..... | 79  |
| PfMDR1 mutations protect <i>Plasmodium falciparum</i> asexual blood stages and mature gametocytes against a piperazine-containing antimalarial.....                                | 98  |
| <b>General discussion and conclusions</b> .....  | 118 |

## General introduction

Malaria is the most common and severe parasitic mosquito-borne disease, whose burden is still huge for human population. Poor communities are the most affected in the countries where malaria is endemic. Globally, an estimated 3.3 billion people are at risk of being infected and developing disease, and 1.2 billion are at high risk. According to the last estimates, 200 million cases of malaria occurred globally in 2013 leading to 600 000 deaths, with 90% of the cases located in Africa and with the 78% of the annual deaths occurring in children aged under 5 years, with the pregnant woman at higher risk (WHO World Malaria Report 2014).

Recent efforts to control and even eradicate malaria have involved insecticide-treated bed-nets, indoor residual spraying, and antimalarial treatments, such as artemisinin-combined therapies. These efforts have contributed to a reduction of 42% in malaria-related deaths since 2000, however the growing problem of artemisinin resistance and the absence of an effective malaria vaccine make malaria difficult to be eradicated.

To complicate this task malaria is caused by several parasites of the protozoan *Plasmodium* genus. In fact five species are known to cause malaria in humans: *Plasmodium ovale*, *Plasmodium knowlesi*, *Plasmodium malariae*, *Plasmodium falciparum* and *Plasmodium vivax*. Most research is focused on the latter two strains, which are the deadliest and the most widespread, respectively (Siu & Ploss 2015).

### ***Plasmodium falciparum* life cycle**

In the *P. falciparum* life cycle, a female of the *Anopheles* mosquito transmits microscopic motile sporozoites to the human host during its blood-meal (Figure 1). The sporozoites travel to the liver and invade hepatocytes, where parasites replicate as hepatic schizonts until several thousands of merozoites are produced, in about 8 days. With the rupture of the hepatocyte all the merozoites are released in the human bloodstream, where they invade red blood cells (RBCs). The invasion of the erythrocyte is a complex cellular process that requires the interactions between many proteins both on the parasite and host surfaces, and that starts the asexual blood cycle of the parasite (Bartholdson et al., 2013). During this stage, responsible for the symptoms of malaria disease, the parasite undergoes cycles of growth and division inside the red blood cells of the host. Each intraerythrocytic asexual cycle takes around 48 hours. The intraerythrocytic parasite grows through the ring and mature trophozoites stages divides during the shizont stage and ruptures the host cells to release from 10 to 20 merozoites that invade new erythrocytes, spreading the infection.

During the asexual blood stage the intracellular parasites ingest small packets of the host cell cytoplasm using endocytic structures, known as cytoosomes, at the surface of the parasite, and transfer the hemoglobin content of the RBC to the acidic digestive vacuole (Tilley et al., 2011). Trophozoites sequester to various organs by binding to the capillary endothelium. *P. falciparum* is able to remodel the RBC surface and structure, also presenting adhesins at the RBC surface, enabling infected RBC (iRBC) to adhere to blood vessels walls, in order to avoid spleen clearance.. This sequestration is due to the *P.*

*falciparum* erythrocyte membrane protein 1 (PfEMP1), encoded by the *var* multigene family. PfEMP1 is exposed on structures protruding from the surface of the infected erythrocyte, called knobs, where it binds to some host endothelial receptors including the thrombospondin receptor (CD36), the intercellular adhesion molecule 1 (ICAM-1) and chondroitin sulfate A (CSA) (Tilley et al., 2011) (Tiburcio et al., 2015).

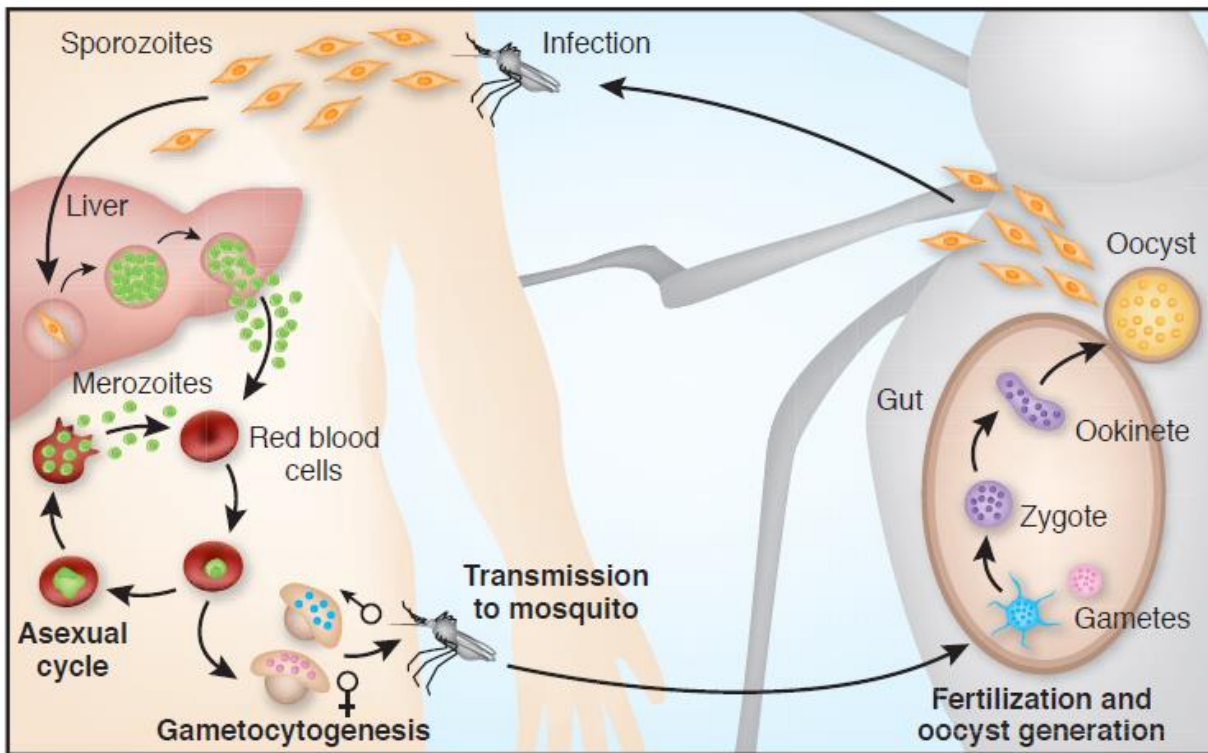


**Figure 1.** Life cycle of *Plasmodium falciparum*. Adapted from (Pasvol, 2010)

The parasite's asexual blood stage is responsible for the clinical symptoms of malaria. These range from uncomplicated fever, anemia, acidosis, renal failure and cerebral and placental malaria. The latter symptoms are due to the adhesion of iRBCs to brain venule endothelial cells or, in pregnant woman, to placental syncytiotrophoblasts (Tilley et al., 2011). In cerebral malaria, the main cause of coma, beside obstruction, is that the sequestration of the iRBCs can be associated with microvascular pathology as demonstrated by endothelial damage and perivascular ring hemorrhages. Monocytes with malaria pigment and fibrin-platelet thrombi are also associated with iRBCs sequestration, contributing to the congestion. The microvasculature congestion leads to severe endothelial damage, causing disruption of the vessel wall with the consequent myelin and axonal damage and breakdown of the blood brain barrier (BBB) (Storm, and Craig, 2014). Placental malaria is a common complication of malaria in pregnancy in areas of stable parasite transmission, particularly severe for primigravidae. The sequestration of iRBCs in the maternal vasculature of the placenta leads to the infiltration of maternal immune cells. This can lead in turn to the upregulation of inflammatory cytokines and to large-scale fibrin deposits within the placenta. The inflammatory immune response, although could limit parasite replication, produces a prolonged chronic infection, associated with both severe anemia and foetal growth restriction (Walker et al., 2013).

Plasmodium asexual blood stages are not directly responsible of parasite transmission from the human host to the mosquito, which is ensured by the parasite sexual blood stages, the gametocytes. In *P. falciparum*, after the rupture of an asexual schizont, the released merozoites invade new erythrocytes, and a small portion of the newly invading parasites differentiate into gametocytes. Sexually committed ring stages start the gametocytogenesis: in 10-12 days parasites pass through five stages of maturation (stage I to V) in which they differentiate into male and female gametocytes. From stage I to stage IV, the gametocytes are sequestered into internal organs, whereas only mature stage V gametocytes are released into the peripheral blood where they can be uptaken by an Anopheles female mosquito biting during its bloodmeal the infected person.

Once in the mosquito midgut, the gametocyte receives the signals for starting the gametogenesis. Such signals include a drop of temperature (by approximately 5°C) and the presence of the mosquito-derived molecule xanthurenic acid (XA). Both male and female gametocytes lose their elongated morphology ('round up') and egress from human erythrocyte. The male gametocyte replicates its genome three times producing eight motile microgametes, while the female gametocyte transforms into a single macrogamete. Then the macrogamete is fertilized by a male microgamete and forms a zygote which develops into a motile ookinete that traverses the midgut cell wall and enters into the mosquito hemocel where it transforms into an oocyst. Inside the oocyst thousands of sporozoites are produced which, after the oocyst rupture, they migrate to the mosquito salivary glands, ready to be injected into the human host during the following bloodmeal (Kuehn and Pradel, 2010).

All the parasite blood stage parasites (both asexuals parasites and gametocytes) can be grown *in vitro* and hepatic stage parasites can be kept in human hepatocyte cultures. It is possible to induce, *in vitro*, the exflagellation of male gametocytes and the rounding up of female gametocytes. Recently, together with the growing need to eradicate malaria, it's becoming of huge importance to induce, *in vitro*, also some mosquito stages, especially zygotes and ookinetes.

### ***Plasmodium falciparum* gametocytogenesis**

Gametocytes are the only sexual stage of the malaria parasite that develops in human erythrocyte and that is responsible for the transmission of the parasite from the human host to the mosquito vector. These nonreplicating forms circulate at lower densities and peak at different time during infection than asexual parasites, generally appearing, in the case of *P. falciparum*, 10-14 days after the first appearance of asexual parasites in the host bloodstream.

While in most *Plasmodium* species the sexual stages mature within 2 days, the gametocytogenesis of *P. falciparum* takes 10-12 days. (Tiburcio et al., 2015; Butterworth et al., 2013; Nilsson et al., 2015) During this period the gametocytes pass through five stages of maturation (Figure 2): from 24 to 30 hours after the invasion of the host cell, the stage I gametocyte is a round cell, morphologically indistinguishable from an asexual trophozoite; the stage II gametocyte is a half-moon-shaped cell (day 2); the stage III gametocyte is a symmetric, elongated cell (day 4); this cell stretches and acquires pointed edges at stage IV (day 6); the stage V gametocyte displays rounded ends (day 10).

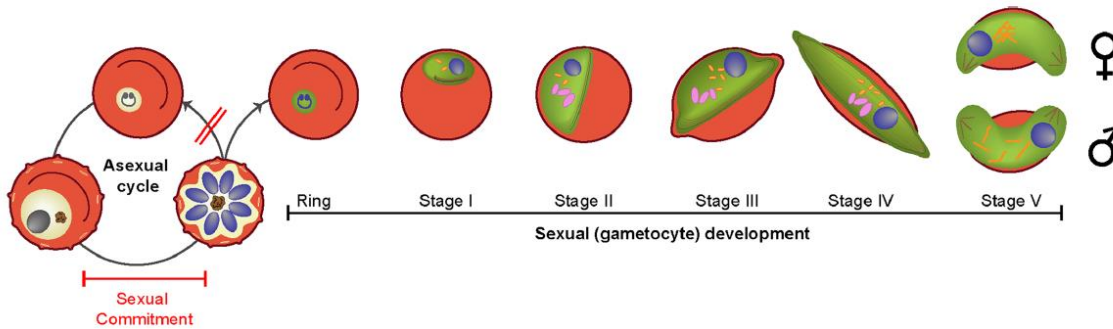


**Figure 2.** Scheme of *P. falciparum* gametocytogenesis. Modified from (Nillson et al., 2015)

This morphological differentiation is accompanied by several cellular rearrangements, including the appearance, from late stage I, of a subpellicular membrane complex subtended by microtubule array connected with an F-actin cytoskeleton, the upregulation of approximately 200 gametocyte-specific genes (Young et al., 2005), specific production of approximately 200 proteins (Silvestrini et al., 2010) and the disassembly of the subpellicular microtubular network at the transition from stage IV to stage V of gametocytogenesis (Dearnley et al., 2012; Tiburcio et al., 2015), making mature gametocytes very specialized cells.

A *P. falciparum* parasite shows adaptive strategies regarding both the proportion of asexual parasites that develop into gametocytes (conversion rate) and the ratio of male to female gametocytes formed. The precise point in which both these decisions occur is still unclear but is thought to be prior to merozoites formation. Only recently it has been identified a master gene, *ap2-g*, responsible for triggering the transcriptional cascade that initiates gametocytogenesis in *P. falciparum* (Kafsack et al., 2014). In asexual parasites the conserved member of the AP2 transcription family is epigenetically silenced by the *P. falciparum* histone deacetylase 2 (PfHda2) and the *P. falciparum* heterochromatin protein 1 (PfHP1) (Coleman et al., 2014; Brancucci et al., 2014).

Another important decision in gametocyte development is the sex ratio. The sex ratio is female-biased (Delves et al., 2013; Teboh-Ewungkem and Wang, 2012). This is explicable with the fact that, in the mosquito, each male gametocyte produces up to 8 flagellated motile microgametes and that each female gametocyte produces only one non-motile macrogamete, so the parasites ensure to produce enough males to fertilize female gametes. The developmental mechanism behind the sex decision is still unknown, but has been suggested that merozoites from a single shizont are destined to form either all male or all female gametocytes (Silvestrini et al., 2000).

Unlike early stage gametocytes (from stage I to stage IV), only mature *P. falciparum* stage V gametocytes are detectable in human peripheral blood. Maturation of immature gametocytes occurs sequestered in human internal organs, mainly in the extravascular space of the human bone marrow. These evidences come from recent analysis of biopsies and aspirates (Joice et al., 2014) (Farfour et al., 2012), and also by qPCR-based detection analysis of sexual stage specific transcripts (Aguilar R et al., 2014). Although it is still unclear whether gametocyte formation occurs in the vasculature before the committed asexual parasites home to the bone marrow or whether it takes place specifically in the hematopoietic system, the sequestration of the immature gametocytes from the circulation is considered a survival strategy for these cells to escape both from immune cells system and from the

mechanical filtration by the spleen. In fact, the onset of gametocyte sequestration seems to be completely different from the one of asexual stage parasites, considering that immature gametocytes completely lack knobs (Tiburcio et al., 2013). A combined study of ektacytometry and microspiltration demonstrated that immature stage II, III and IV gametocytes are less deformable and more stiff than stage V gametocytes, with an important switch in deformability during the maturation of gametocytes from stage IV to stage V. This switch in deformability is directly associated to a dynamic association-dissociation of proteins of the STEVOR family with the erythrocyte membrane compartment during gametocytogenesis, with a direct association shown in stage III/IV gametocytes, which confer the cell rigidity, no more detectable in stage V gametocytes (Tiburcio et al., 2012). Because of their deformability, stage V gametocytes are not retained by the spleen's filtration system and can freely circulate in the human bloodstream where they are ingested by the mosquito.

### ***Plasmodium falciparum* blood stage metabolism – Hemoglobin digestion**

During the intraerythrocytic stage, the parasite consumes up to 80% of the erythrocyte cytoplasm, using a cytostome to ingest packets of hemoglobin. The hemoglobin is for the parasite a source of amino acids and osmolytes and, by its degradation, the parasite creates the sufficient space for growth and division (Klonis et al., 2007). The hemoglobin degradation process occurs in the parasite's digestive vacuole (DV), an acidic organelle with an estimated pH of 5.0-5.4, maintained by a proton gradient activated by an ATPase pump (Saliba et al., 2003).

It is thought that hemoglobin digestion in the malaria parasite is mediated by two aspartic proteases (plasmepsin I and II) and one cysteine protease (falcipain) which have been isolated and purified from the DV and that function optimally at an acidic pH (Goldberg et al. J Exp Med. 1991).

The proteolytic process of hemoglobin degradation releases free heme (ferriprotoporphyrin IX), which is toxic for the malaria parasite. *Plasmodium species* lack a heme oxygenase, the enzyme that in all the vertebrates is responsible for degradation of the heme moiety. For this reason the parasite converts the heme monomer into an inert biocrystal called malaria pigment or hemozoin, a molecule with paramagnetic properties that is retained into *P. falciparum* digestive vacuole (Coronado et al., 2014).

In 2012 Hanssen and colleagues utilized soft X-ray microscopy analysis of cell volume and hemoglobin content in erythrocytes infected by *P. falciparum* asexual and sexual stages (Hanssen et al., 2012). They demonstrated that the hemoglobin concentration in erythrocytes infected by asexual parasites shows a biphasic pattern: it remains constant during the ring stage and decreases 24h after invasion, when the parasite starts the nuclear division (corresponding to an increase in hemoglobin digestion). In trophozoites and in early shizonts hemoglobin concentration is sustained at a constant level because the parasite exhibits the most intensive hemoglobin digestion and to decrease more in erythrocytes infected by segmented shizonts (Figure 3).



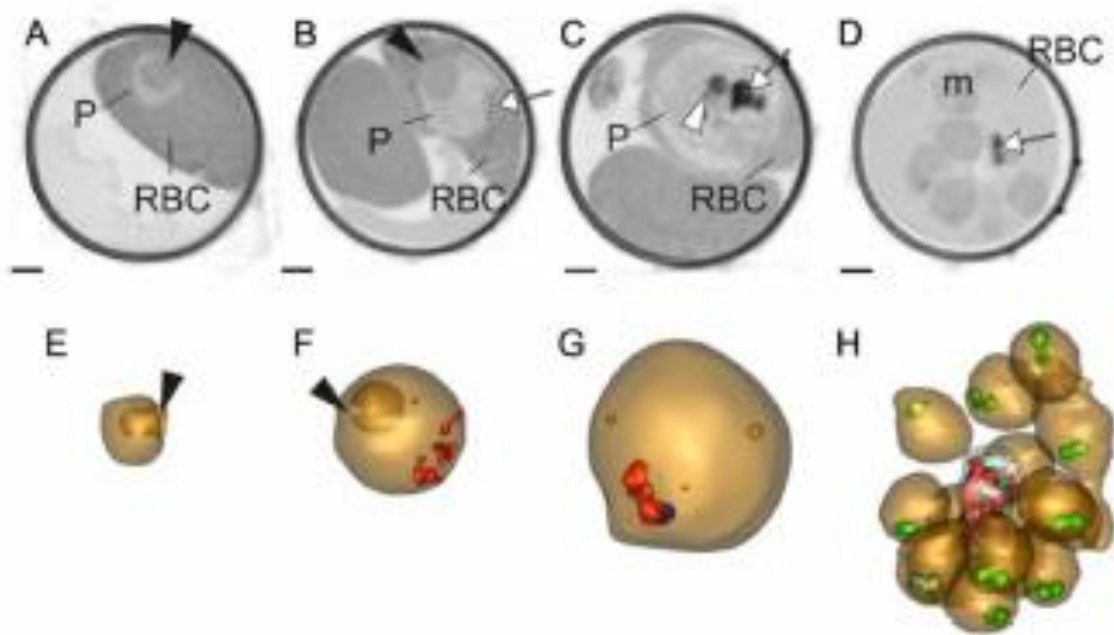


**Figure 3.** Transmission X-ray tomography of asexual stages of *P. falciparum* (Hanssen et al., 2012).

During the asexual blood cycle of *P. falciparum*, the change in hemoglobin content of the infected erythrocyte is accompanied by an increase in volume of the parasite and by the concomitant decrease of the host red blood cell, so that the total volume of the infected erythrocyte is kept constant until early schizogony,.

In parasite sexual development, the concentration of hemoglobin in the host erythrocyte decreases gradually during differentiation from stage II to stage V of gametocytogenesis. By contrast, the total amount of hemoglobin in an erythrocyte infected by stage II gametocytes is lower than that for uninfected erythrocytes, similar to that of erythrocyte infected by mid-late trophozoite. The quantity decreases in stage III and IV of gametocytes development, to remain stable in stage V gametocytes (Figure 4), where hemozoin crystals are dispersed in male mature gametocytes and more condensed in the center of female mature gametocytes. This suggests that hemoglobin digestion is completed by stage IV of gametocytogenesis, which is also supported by the observation that the volume of hemozoin crystals remains constant in the later stages of gametocyte development.

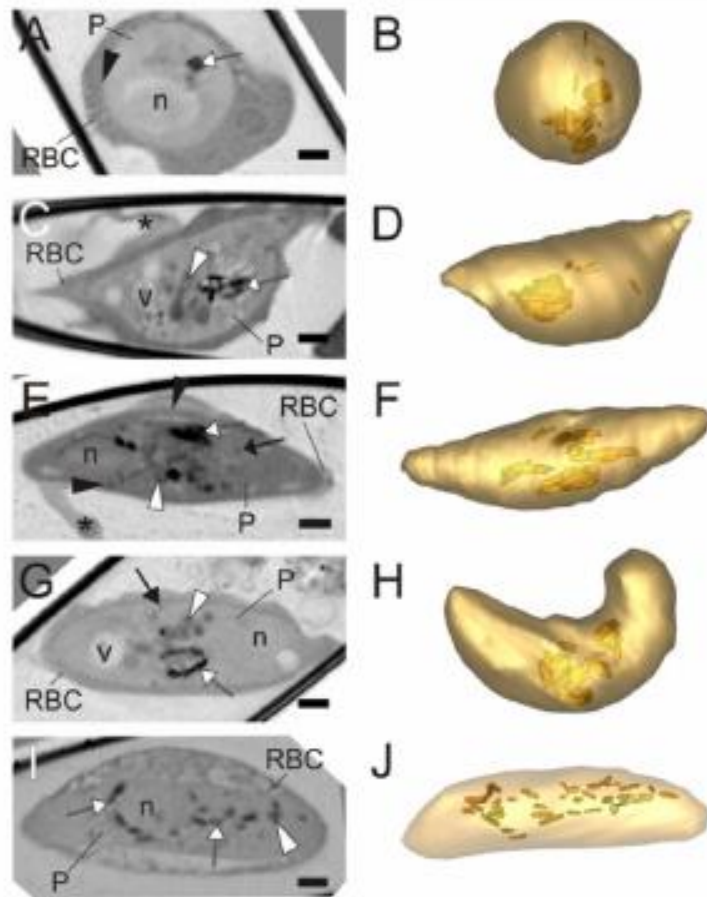


**Figure 4.** Transmission X-ray tomography of sexual stages of *P. falciparum* (Hanssen et al., 2012).

These evidences show that, although about 50% of the host hemoglobin is digested by the time the parasite reaches the stage II of gametocytogenesis, the digestion seems to continue until the gametocyte reaches stage IV of development.

### ***Plasmodium falciparum* blood stage metabolism – Redox equilibrium**

During the erythrocytic life, *P. falciparum* parasites are subjected to a large amount of oxidative stress, coming both from the host immune response and from hemoglobin degradation.

When hemoglobin is taken up by the parasites into their acidic digestive vacuole, it is converted into amino acids and free heme (ferriprotoporphyrin IX). Toxic heme must be detoxified from the parasite and up to 90% is biomineralized to form inert hemozoin. Some of this heme is however not converted into hemozoin and is released into the parasite cytoplasm where it is oxidized with the production of superoxide and hydrogen peroxide ( $H_2O_2$ ) that must be degraded or sequestered to prevent membrane damage and parasite death (Muller 2004; Jortzik and Becker 2012).

In order to counteract the oxidative stress and to maintain controlled redox equilibrium, parasites use a NADPH-dependent thioredoxin and glutathione system (Figure 5).

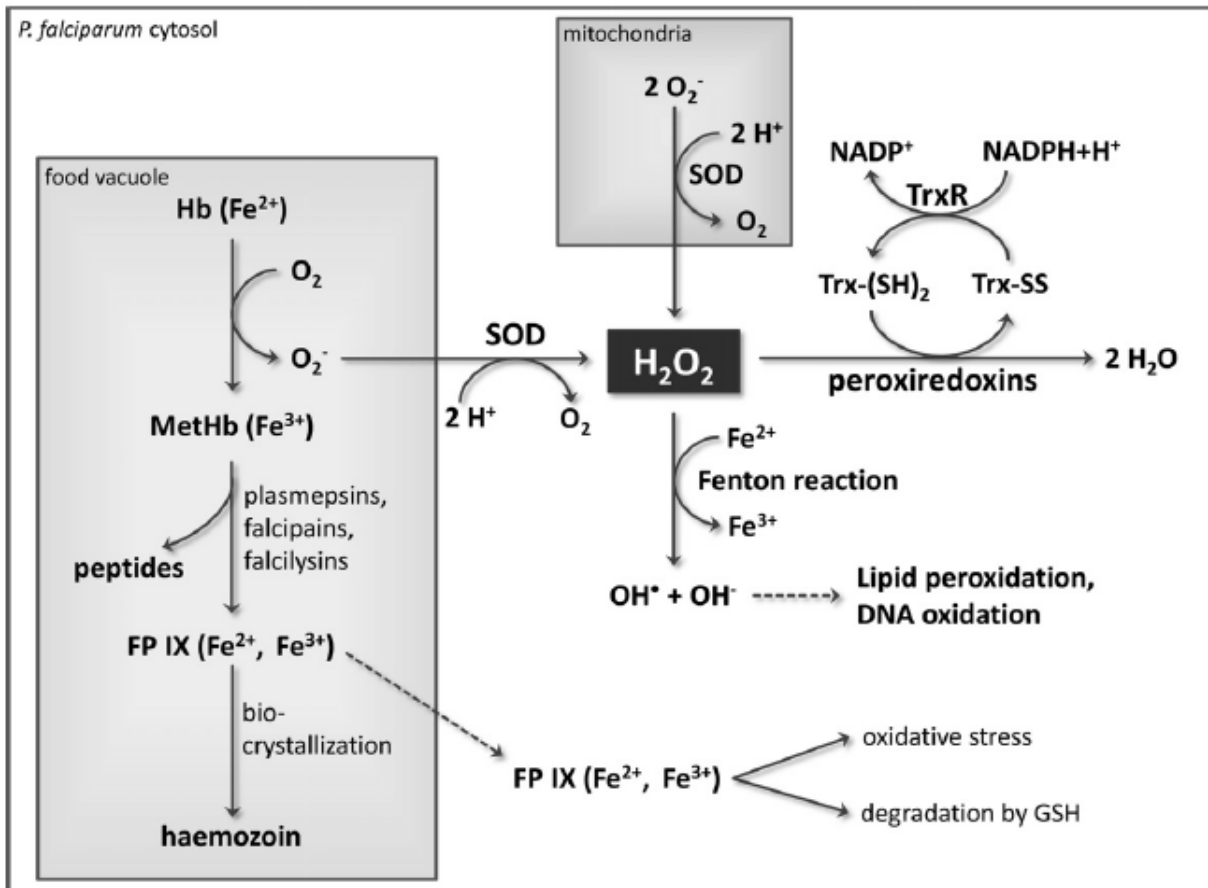


Figure 5. Sources of oxidative stress in *P. falciparum* (Jortzik and Becker 2012).

### -The glutathione system in *P. falciparum*

The redox equilibrium of *P. falciparum* mostly depends on glutathione, which cycles between an oxidized (GSSG) and a reduced (GSH) form (Becker et al., 2003) (Figure 6). The GSSG results from many reactions and it is toxic for the cell at high concentration (above 100µM). It is in part exported from the parasite cell to the host erythrocyte and in part is recycled by the glutathione reductase (GR) or by thioredoxin and plasmoredoxin (Becker et al., 2003).

The GSH is synthesized *de novo* by the  $\gamma$ -glutamyl-cysteine synthetase ( $\gamma$ GCS) and glutathione synthetase (GS) and its synthesis is essential for the development of *P. falciparum* in the host red blood cell (Patzewitz et al., 2012).

The *P. falciparum* glutathione reductase (GR) is a member of a group of enzymes known as flavo disulphide oxidoreductases, that specifically reduce oxidized glutathione in a FAD and NADPH-dependent reaction in order to maintain most of the glutathione in its reduced form.

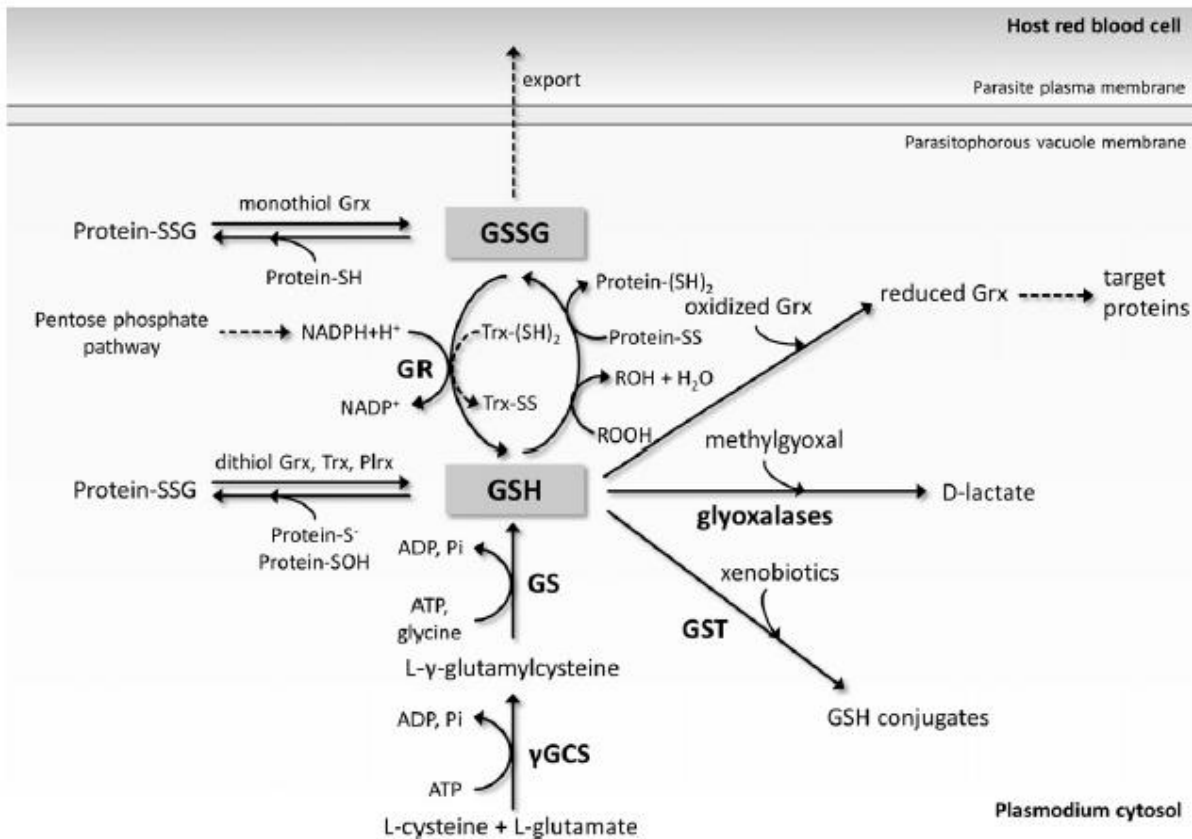


**Figure 6.** The glutathione system in *P. falciparum* (Jortzik and Becker 2012).

Glutathione is involved in many vital detoxification pathways in *P. falciparum*. GSH is the major reductant of the oxidoreductase glutaredoxin (Grx) which in turns reduces a number of target proteins. GSH also functions as a co-factor for the glutathione S-transferase (GST) for the detoxification of electrophilic compounds and for glyoxalase, which detoxify methylglyoxal (Figure 6) (Tripathi et al., 2007; Gallo et al., 2009; Jortzik and Becker 2012).

### **-The thioredoxin system in *P. falciparum***

*P. falciparum* expresses two thioredoxin reductase (TrxR) isoforms which are located in the cytosol and in the mitochondria, respectively (Kehr et al., 2010). TrxR reduces the thioredoxin (Trx) transferring electrons from NADPH via FAD to the disulphide substrate. So the Trx activity, which strictly depends on TrxR, is based on modifying the redox status of protein targets via its Cys-xx-Cys active motif (Figure 7). In *P. falciparum* three Trx have been identified that can be reduced by TrxR. Trx1 is located in the cytosol and can directly and efficiently reduce oxidized glutathione, acting as a backup for the glutathione system. PfTrx1 counteracts the parasite's oxidative stress by directly detoxifying H<sub>2</sub>O<sub>2</sub>, *tert*-butylhydroperoxyde (tBuOOH), cumene hydroperoxydes (CHP) and S-nitrosoglutathione and by maintaining the antioxidant capacity of ascorbate, lipoic acid and lipoamide (Kanzok et al., 2000). Furthermore, PfTrx1 reduces Trx-dependent peroxidases and the Plasmodium-specific dithiol protein plasmoredoxin (Plrx) (Becker et al., 2003).

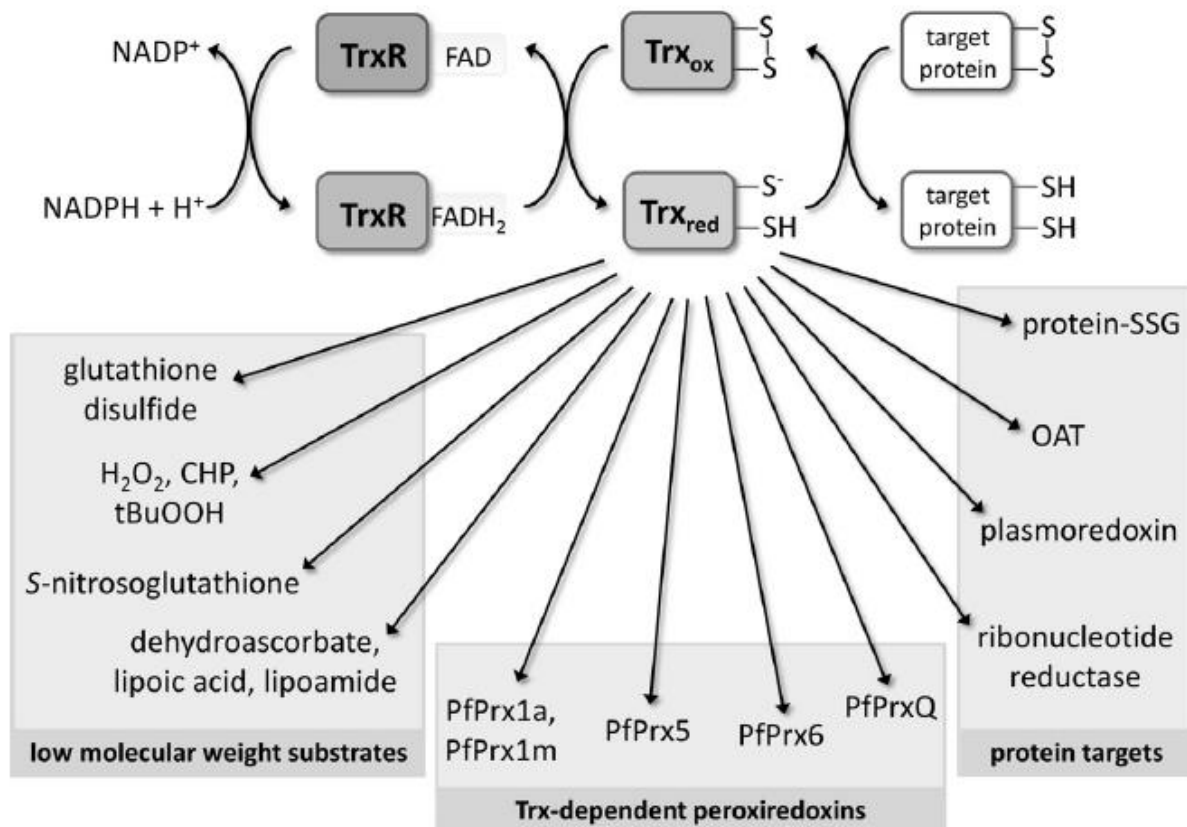


**Figure 7.** The thioredoxin system in *P. falciparum* (Jortzik and Becker 2012).

PfTrx1 interacts also with proteins involved in protein folding, transcription and translation, glycolysis, hemoglobin catabolism and signal transduction and specifically reduces S-adenosylmethionine synthetase, S-adenosyl-L-homocysteine hydrolase, and ornithine  $\delta$ -aminotransferase (OAT).

The *P. falciparum* detoxifying system relies on NADPH-dependent enzymes that use electrons from the NADPH to balance the oxidative stress of the cell. At least the 80% of NADPH in the parasite-infected red blood cell is produced by the *P. falciparum* glucose-6-phosphate-dehydrogenase 6-phosphogluconolactonase (PfGluPho). This is a bifunctional enzyme that catalyzes the first two steps of the pentose phosphate pathway (PPP) and shows major structural and functional differences with respect to the human monofunctional counterpart glucose-6-phosphate-dehydrogenase (G6PD) (Jortzik et al., 2011).

### **Resistance of *P. falciparum* to current antimalarial treatments and the need of new drugs**

The first antimalarial treatment was discovered 400 years ago, with the observation that acutely ill patients were cured of specific periodic fevers after treatment with infusions of the bark from the ‘chinchona’ plants growing in the Peruvian Amazon. Such an activity was later attributed to the alkaloid quinine (QN), which is still important for treating severe and complicated *P. falciparum* malaria. Based on the quinine, several 4-aminoquinolines were then synthesized and used as antimalarial drugs with, among them, chloroquine (CQ). Chloroquine interferes with hemozoin crystals formation (Fitch 1998)

and was used for hundreds of millions of treatments annually before resistance appeared in 1960s (Miller et al., 2013; Aguiar et al., 2012). Chloroquine resistance is conferred by mutations in the *P. falciparum* gene encoding the chloroquine resistance transporter (PfCRT), expressed on the membrane of the parasite digestive vacuole (Fidock DA et al., 2000). The *pfcr*t gene shows an extraordinary sequence diversity among geographically distinct isolates and codes for a 45-KDa with ten transmembrane domains (Valderramos and Fidock 2006).

Chloroquine resistance can be modulated also by mutations or changes in the expression of a *P. falciparum* P-glycoprotein homolog (PfPgh1 or PfMRD1) encoded by the *P. falciparum* multidrug resistance 1 gene (*pfmdr1*). This gene encodes a 162-KDa protein that resides in the membrane of the digestive vacuole of the parasite and that consists of two homologous halves, each with six transmembrane domains and a conserved nucleotide-binding domain (Valderramos and Fidock 2006). Both PfMDR1 and PfCRT1mutant parasites show resistance to other antimalarial drugs, including mefloquine, quinine, lumefantrin, halofantrine and artemisinin (Mu et al., 2003).

The process of hemoglobin digestion is the target also for the action of artemisinin-class antimalarials on *Plasmodium* species. The artemisinins have been developed from the ancient Chinese herbal remedy qinghaosu, used to cure periodic fevers. The artemisinin structure is characterized by a superoxide pharmacophore with a peroxide bridge that is cleaved and activated by ferrous heme or free ferrous iron causing the production of reactive carbon-centered radicals that kill the parasite (Hartwig et al., 2009). Because of it was described a hypersensitivity to artemisinin also for very early parasite (2-4 hours post-invasion) (Klonis et al., 2013) when hemoglobin digestion not appears to occur, alternative pathways for artemisinin activation have been hypothesized. One possibility is that artemisinin activation occurs via one hemoglobin-dependent pathway, dominating in trophozoites, and one hemoglobin independent pathway in rings, suggesting, for example, the sarco/endoplasmic reticulum  $Ca^{2+}$ -ATPase (PfSERCA) as a potential direct artemisinin target (Eckstein-Ludwig et al., 2003; Cardi et al., 2010) or a possible metal-independent artemisinin direct association with cofactors involved in the maintenance of redox omeostasis (Haynes et al., 2007).

Artemisinin was isolated in the 1970s, and from the original molecule several analogues such as sodium artesunate, dihydroartemisinin, arteether and artemether have been developed.

Atovaquone is a naphthoquinone-derivative and a structural analogue of coenzyme Q (ubiquinone) in the mitochondrial electron transport chain. It interferes with the transfer of electrons generated by pyrimidine synthesis and was shown to collapse the membrane potential. *P. falciparum* resistant lines show point mutation in the cytochrome *b* gene (Korsinczky et al., 2000).

The appearance of *P. falciparum* resistance to many drugs led to the necessity of finding new drug targets between the different metabolic pathways of the parasite, and also to introduce therapies that combine two different drugs (combination therapies) in order to attack the parasite on different sides.

Until few years ago the interest in finding new drugs mostly aimed to cure the symptoms of malaria caused by the asexual erythrocytic stages of *P. falciparum* and to counteract the widespread resistance to the known most effective antimalarials. Since the past decade, a new attention has been given to the ambitious objective of eradicating malaria. This requires to combine: 1) renewed efforts to develop insecticides that overcome known resistance pathways and kill all mosquitoes; 2) the delivery of effective vaccines that protect infant and children (nowadays almost totally absent); 3) the delivery of

appropriate and sensitive diagnostic tools to guide health care tactics, and 4) the discovery, development and delivery of new drugs that not only clear the asexual blood parasites to cure patients, but also kill the asymptomatic and vector stage forms, the gametocytes, that allow the transmission of *P. falciparum*.

So far, the only drug which has been described as active against *P. falciparum* immature and mature gametocytes, *in vivo*, is primaquine, an 8-aminoquinoline which however has known gastro-intestinal side effect and presents risk of haemolytic anemia to patients who have low activity of G6PD (G6PD-deficiency). For these reasons it is not recommended for infants or for pregnant women.

Finding new drugs means also to employ high throughput screening (HTS) assays that allow to simultaneously screen several thousands of compounds, *in vitro*, at low cost. Most of these assays have been used to screen drugs against asexual blood stages parasites, and were based on the possibility to incorporate [<sup>3</sup>H] hypoxanthine or the non-radioactive SYBR green, during parasite DNA replication. These assays are being replaced by enzymatic assays as luciferase assays (Siciliano and Alano 2015). The need of anti-gametocyte drugs imposes to develop different types of assays. For these reasons new enzymatic assays, as one based on the parasite lactate dehydrogenase (pLDH) detection (D'Alessandro et al., 2013), specific luciferase assays (Adjalley et al., 2011; Cevenini, Camarda et al., 2014) and functional assays such as the functional imaging assay (Lucantoni, Silvestrini et al., 2015) have been developed.

## References

Adjalley, S.H., Johnston, G.L., Li, T., Eastman, R.T., Ekland, E.H., Eappen, A.G., Richman, A., Sim, B.K., Lee, M.C., Hoffman, S.L., and Fidock, D.A. (2011). Quantitative assessment of Plasmodium falciparum sexual development reveals potent transmission-blocking activity by methylene blue. *Proc Natl Acad Sci U S A*. 108, 1214-23.

Aguiar ,A.C., Rocha, E.M., Souza, N.B., França, T.C., and Krettli, A.U. (2012). New approaches in antimalarial drug discovery and development: a review. *Mem Inst Oswaldo Cruz*. 107, 831-45.

Aguilar, R., Magallon-Tejada, A., Achtman, A.H., Moraleda, C., Joice, R., Cisteró, P., Li Wai Suen, C.S., Nhabomba, A., Macete, E., Mueller, I., Marti, M., Alonso, P.L., Menéndez, C., Schofield, L., and Mayor, A. (2014). Molecular evidence for the localization of Plasmodium falciparum immature gametocytes in bone marrow. *Blood*. 123, 959-66.

Bartholdson, S.J., Crosnier, C., Bustamante, L.Y., Rayner, J.C., and Wright, G.J. (2013). Identifying novel Plasmodium falciparum erythrocyte invasion receptors using systematic extracellular protein interaction screens. *Cell Microbiol*. 15, 1304-12.

Becker, K., Rahlfs, S., Nickel, C., and Schirmer, R.H. (2003). Glutathione--functions and metabolism in the malarial parasite Plasmodium falciparum. *Biol Chem*. 384, 551-66.

Brancucci, N.M., Bertschi, N.L., Zhu, L., Niederwieser, I., Chin, W.H., Wampfler, R., Freymond, C., Rottmann, M., Felger, I., Bozdech, Z., and Voss, T.S. (2014). Heterochromatin protein 1 secures survival and transmission of malaria parasites. *Cell Host Microbe*. 16, 165-76.

Butterworth, A.S., Skinner-Adams, T.S., Gardiner, D.L., and Trenholme KR. (2013). Plasmodium falciparum gametocytes: with a view to a kill. *Parasitology*. 140, 1718-34.

Cardi, D., Pozza, A., Arnou, B., Marchal, E., Clausen, J.D., Andersen, J.P., Krishna, S., Møller, J.V., le Maire, M., and Jaxel, C. (2010). Purified E255L mutant SERCA1a and purified PfATP6 are sensitive to SERCA-type inhibitors but insensitive to artemisinins. *J Biol Chem*. 285, 26406-16.

Cevenini, L., Camarda, G., Michelini, E., Siciliano, G., Calabretta, M.M., Bona, R., Kumar, T.R., Cara, A., Branchini, B.R., Fidock, D.A., Roda, A., and Alano, P. (2014). Multicolor bioluminescence boosts malaria research: quantitative dual-color assay and single-cell imaging in Plasmodium falciparum parasites. *Anal Chem*. 86, 8814-21.

Coleman, B.I., Skillman, K.M., Jiang, R.H., Childs, L.M., Altenhofen, L.M., Ganter, M., Leung, Y., Goldowitz, I., Kafack, B.F., Marti, M., Llinás, M., Buckee, C.O., and Duraisingh, M.T. (2014). A Plasmodium falciparum histone deacetylase regulates antigenic variation and gametocyte conversion. *Cell Host Microbe*. 16, 177-86.

Coronado, L.M., Nadovich, C.T., and Spadafora, C. (2014). Malarial hemozoin: from target to tool. *Biochim Biophys Acta*. 1840, 2032-41.

D'Alessandro, S., Silvestrini, F., Dechering, K., Corbett, Y., Parapini, S., Timmerman, M., Galastri, L., Basilico, N., Sauerwein, R., Alano, P., and Taramelli D. (2013). A Plasmodium falciparum screening assay for anti-gametocyte drugs based on parasite lactate dehydrogenase detection. *J Antimicrob Chemother*. 68, 2048-58.

Dearnley, M.K., Yeoman, J.A., Hanssen, E., Kenny, S., Turnbull, L., Whitchurch, C.B., Tilley, L., and Dixon MW. (2012). Origin, composition, organization and function of the inner membrane complex of Plasmodium falciparum gametocytes. *J Cell Sci*. 125, 2053-63.

Delves, M.J., Ruecker, A., Straschil, U., Lelièvre, J., Marques, S., López-Barragán, M.J., Herreros, E., and Sinden RE. (2013). Male and female Plasmodium falciparum mature gametocytes show different responses to antimalarial drugs. *Antimicrob Agents Chemother*. 57, 3268-74.

Eckstein-Ludwig, U., Webb, R.J., Van Goethem, I.D., East, J.M., Lee, A.G., Kimura, M., O'Neill, P.M., Bray, P.G., Ward, S.A., and Krishna, S. (2003). Artemisinins target the SERCA of Plasmodium falciparum. *Nature*. 424, 957-61.



Farfour, E., Charlotte, F., Settegrana, C., Miyara, M., and Buffet P. (2012). The extravascular compartment of the bone marrow: a niche for *Plasmodium falciparum* gametocyte maturation? *Malar J.* 11, 285.

Fidock, D.A., Nomura, T., Talley, A.K., Cooper, R.A., Dzekunov, S.M., Ferdig, M.T., Ursos, L.M., Sidhu, A.B., Naudé, B., Deitsch, K.W., Su, X.Z., Wootton, J.C., Roepe, P.D., and Wellems, T.E. (2000). Mutations in the *P. falciparum* digestive vacuole transmembrane protein PfCRT and evidence for their role in chloroquine resistance. *Mol Cell.* 6, 861-71.

Fitch, C.D. (1998). Involvement of heme in the antimalarial action of chloroquine. *Trans Am Clin Climatol Assoc.* 109, 97-106.

Gallo, V., Schwarzer, E., Rahlfs, S., Schirmer, R.H., van Zwieten, R., Roos, D., Arese, P., and Becker, K. (2009). Inherited glutathione reductase deficiency and *Plasmodium falciparum* malaria--a case study. *PLoS One.* 4, 7303.

Goldberg, D.E., Slater, A.F., Beavis, R., Chait, B., Cerami, A., and Henderson GB. Hemoglobin degradation in the human malaria pathogen *Plasmodium falciparum*: a catabolic pathway initiated by a specific aspartic protease. (1991). *J Exp Med.* 173, 961-9.

Hanssen, E., Knoechel, C., Dearnley, M., Dixon, M.W., Le Gros, M., Larabell, C., and Tilley L. (2012). Soft X-ray microscopy analysis of cell volume and hemoglobin content in erythrocytes infected with asexual and sexual stages of *Plasmodium falciparum*. *J Struct Biol.* 177, 224-32.

Hartwig, C.L., Rosenthal, A.S., D'Angelo, J., Griffin, C.E., Posner, G.H., Cooper, R.A. (2009). Accumulation of artemisinin trioxane derivatives within neutral lipids of *Plasmodium falciparum* malaria parasites is endoperoxide-dependent. *Biochem Pharmacol.* 77, 322-36.

Haynes, R.K., Chan, W.C., Lung, C.M., Uhlemann, A.C., Eckstein, U., Taramelli, D., Parapini, S., Monti, D., and Krishna, S. (2007). The Fe<sup>2+</sup>-mediated decomposition, PfATP6 binding, and antimalarial activities of artemisone and other artemisinins: the unlikelihood of C-centered radicals as bioactive intermediates. *ChemMedChem.* 2, 1480-97.

Joice, R., Nilsson, S.K., Montgomery, J., Dankwa, S., Egan, E., Morahan, B., Seydel, K.B., Bertuccini, L., Alano, P., Williamson, K.C., Duraisingh, M.T., Taylor, T.E., Milner, D.A., and Marti, M. (2014). *Plasmodium falciparum* transmission stages accumulate in the human bone marrow. *Sci Transl Med.* 6, 244.

Jortzik, E., Mailu, B.M., Preuss, J., Fischer, M., Bode, L., Rahlfs, S., Becker, K. (2011). Glucose-6-phosphate dehydrogenase-6-phosphogluconolactonase: a unique bifunctional enzyme from *Plasmodium falciparum*. *Biochem J.* 436, 641-50.

Jortzik, E., and Becker, K. (2012). Thioredoxin and glutathione systems in *Plasmodium falciparum*. *Int J Med Microbiol.* 302, 187-94.

Kafsack, B.F., Rovira-Graells, N., Clark, T.G., Bancells, C., Crowley, V.M., Campino, S.G., Williams, A.E., Drought, L.G., Kwiatkowski, D.P., Baker, D.A., Cortés, A., and Llinás, M. (2014). A transcriptional switch underlies commitment to sexual development in malaria parasites. *Nature.* 507, 248-52.

Kanzok, S.M., Schirmer, R.H., Turbachova, I., Iozef, R., and Becker, K. (2000). The thioredoxin system of the malaria parasite *Plasmodium falciparum*. Glutathione reduction revisited. *J Biol Chem.* 275, 40180-6.

Kehr, S., Sturm, N., Rahlfs, S., Przyborski, J.M., and Becker, K. (2010). Compartmentation of redox metabolism in malaria parasites. *PLoS Pathog.* 6, 1001242.

Klonis, N., Tan, O., Jackson, K., Goldberg, D., Klemba, M., and Tilley, L. (2007). Evaluation of pH during cytosomal endocytosis and vacuolar catabolism of haemoglobin in *Plasmodium falciparum*. *Biochem J.* 407, 343-54.

Klonis, N., Xie, S.C., McCaw, J.M., Crespo-Ortiz, M.P., Zaloumis, S.G., Simpson, J.A., and Tilley L. (2013). Altered temporal response of malaria parasites determines differential sensitivity to artemisinin. *Proc Natl Acad Sci U S A.* 110, 5157-62.

Korsinczky, M., Chen, N., Kotecka, B., Saul, A., Rieckmann, K., and Cheng, Q. (2000). Mutations in *Plasmodium falciparum* cytochrome b that are associated with atovaquone resistance are located at a putative drug-binding site. *Antimicrob Agents Chemother.* 44, 2100-8.

Kuehn, A., and Pradel, G. (2010). The coming-out of malaria gametocytes. *J Biomed Biotechnol.* 2010, 976827.

Lucantoni, L., Silvestrini, F., Signore, M., Siciliano, G., Eldering, M., Dechering, K.J., Avery, V.M., and Alano, P. (2015). A simple and predictive phenotypic High Content Imaging assay for *Plasmodium falciparum* mature gametocytes to identify malaria transmission blocking compounds. *Sci Rep.*

Miller, A.K., Harrell, E., Ye, L., Baptiste-Brown, S., Kleim, J.P., Ohrt, C., Duparc, S., Möhrle, J.J., Webster, A., Stinnett, S., Hughes, A., Griffith, S., and Beelen, A.P. (2013). Pharmacokinetic interactions and safety evaluations of coadministered tafenoquine and chloroquine in healthy subjects. *Br J Clin Pharmacol.* 76, 858-67.

Mu, J., Ferdig, M.T., Feng, X., Joy, D.A., Duan, J., Furuya, T., Subramanian, G., Aravind, L., Cooper, R.A., Wootton, J.C., Xiong, M., and Su, X.Z. (2003). Multiple transporters associated with malaria parasite responses to chloroquine and quinine. *Mol Microbiol.* 49, 977-89.

Müller, S. (2004). Redox and antioxidant systems of the malaria parasite *Plasmodium falciparum*. *Mol Microbiol.* 53, 1291-305.

Nilsson, S.K., Childs, L.M., Buckee, C., and Marti, M. (2015). Targeting human transmission biology for malaria elimination. *PLoS Pathog.* 11, e1004871.

Pasvol, G. (2010). Protective hemoglobinopathies and *Plasmodium falciparum* transmission. *Nat Genet.* 42, 284-5.

Patzewitz, E.M., Salcedo-Sora, J.E., Wong, E.H., Sethia, S., Stocks, P.A., Maughan, S.C., Murray, J.A., Krishna, S., Bray, P.G., Ward, S.A., and Müller, S. (2013). Glutathione transport: a new role for PfCRT in chloroquine resistance. *Antioxid Redox Signal.* 19, 683-95.

Saliba, K.J., Allen, R.J., Zisis, S., Bray, P.G., Ward, S.A., and Kirk, K. (2003). Acidification of the malaria parasite's digestive vacuole by a H<sup>+</sup>-ATPase and a H<sup>+</sup>-pyrophosphatase. *J Biol Chem.* 278, 5605-12.

Siciliano, G., and Alano, P. (2015). Enlightening the malaria parasite life cycle: bioluminescent *Plasmodium* in fundamental and applied research. *Front Microbiol.* 6, 391.

Silvestrini, F., Alano, P., and Williams, J.L. (2000). Commitment to the production of male and female gametocytes in the human malaria parasite *Plasmodium falciparum*. *Parasitology.* 5, 465-71.

Silvestrini, F., Lasonder, E., Olivieri, A., Younis, S., and Alano, P. (2010). Protein export marks the early phase of gametocytogenesis of the human malaria parasite *Plasmodium falciparum*. *Mol Cell Proteomics.* 9, 1437-48.

Siu, E., and Ploss, A. (2015). Modeling malaria in humanized mice: opportunities and challenges. *Ann N Y Acad Sci.* 1342, 29-36.

Storm, J., and Craig, A.G. (2014). Pathogenesis of cerebral malaria--inflammation and cytoadherence. *Front Cell Infect Microbiol.* 4, 100.

Teboh-Ewungkem, M.I., and Wang, M. (2012). Male fecundity and optimal gametocyte sex ratios for *Plasmodium falciparum* during incomplete fertilization. *J Theor Biol.* 307, 183-92.

Tibúrcio, M., Niang, M., Deplaine, G., Perrot, S., Bischoff, E., Ndour, P.A., Silvestrini, F., Khattab, A., Milon, G., David, P.H., Hardeman, M., Vernick, K.D., Sauerwein, R.W., Preiser, P.R., Mercereau-Puijalon, O., Buffet, P., Alano, P., and Lavazec, C. (2012). A switch in infected erythrocyte deformability at the maturation and blood circulation of *Plasmodium falciparum* transmission stages. *Blood.* 119, e172-80.

Tibúrcio, M., Silvestrini, F., Bertuccini, L., Sander, A.F., Turner, L., Lavstsen, T., and Alano P. (2013). Early gametocytes of the malaria parasite *Plasmodium falciparum* specifically remodel the adhesive properties of infected erythrocyte surface. *Cell Microbiol.* 15, 647-59.

Tibúrcio, M., Sauerwein, R., Lavazec, C., and Alano, P. (2015). Erythrocyte remodeling by *Plasmodium falciparum* gametocytes in the human host interplay. *Trends Parasitol.* 31, 270-8.

Tilley, L., Dixon, M.W., and Kirk, K. (2011). The *Plasmodium falciparum*-infected red blood cell. *Int J Biochem Cell Biol.* 43, 839-42.

Tripathi, T., Rahlfs, S., Becker, K., and Bhakuni, V. (2007). Glutathione mediated regulation of oligomeric structure and functional activity of *Plasmodium falciparum* glutathione S-transferase. *BMC Struct Biol.* 7, 67.

Valderramos, S.G., and Fidock, D.A. (2006). Transporters involved in resistance to antimalarial drugs. *Trends Pharmacol Sci.* 27, 594-601.

Walker, P.G., Griffin, J.T., Cairns, M., Rogerson, S.J., van Eijk, A.M., ter Kuile, F., and Ghani, A.C. (2013). A model of parity-dependent immunity to placental malaria. *Nat Commun.* 4, 1609.

WHO World Malaria Report 2014.  
([http://www.who.int/malaria/publications/world\\_malaria\\_report/en/](http://www.who.int/malaria/publications/world_malaria_report/en/))

Young, J.A., Fivelman, Q.L., Blair, P.L., de la Vega, P., Le Roch, K.G., Zhou, Y., Carucci, D.J., Baker, D.A., and Winzeler, E.A. (2005). The *Plasmodium falciparum* sexual development transcriptome: a microarray analysis using ontology-based pattern identification. *Mol Biochem Parasitol.* 143, 67-79.

## Aim of the thesis

- Development of a functional imaging assay specific for testing compounds against mature stage V gametocytes of *P. falciparum*.
- Development of a dual-color luciferase assay for testing compounds against both immature and mature gametocytes of *P. falciparum*.
- Development of a bioluminescence assay specific for testing compounds against mature stage V gametocytes of *P. falciparum*.
- Study of the mechanism of action of methylene blue against mature gametocytes of *P. falciparum* and of the parasite redox metabolism.
- Evaluation of the activity and of the mechanism of action of a piperazine-containing compound, Actelion-451840, against asexual and immature and mature sexual blood stage parasites of *P. falciparum*.

These aims are developed throughout the following manuscripts.

# A simple and predictive phenotypic High Content Imaging assay for *Plasmodium falciparum* mature gametocytes to identify malaria transmission blocking compounds

Leonardo Lucantoni<sup>1</sup>, Francesco Silvestrini<sup>2</sup>, Michele Signore<sup>3</sup>, **Giulia Siciliano**<sup>2</sup>, Maarten Eldering<sup>4</sup>, Koen J Dechering<sup>4</sup>, Vicky M Avery<sup>1</sup>, Pietro Alano<sup>2</sup>.

1) Discovery Biology, Eskitis Institute for Drug Discovery, Griffith University, 4111 Nathan, Queensland, Australia. 2) Dipartimento di Malattie Infettive, Parassitarie ed Immunomediate, Istituto Superiore di Sanità, Viale Regina Elena n. 299, 00161 Roma, Italy. 3) Dipartimento di Ematologia, Oncologia e Medicina Molecolare, Istituto Superiore di Sanità, Viale Regina Elena n. 299, 00161 Roma, Italy. 4) TropiQ Health Sciences, Geert Grooteplein 28, huispost 268, 6525 GA Nijmegen, The Netherlands.

This work is published in Scientific Reports, volume: 5 pages: 16414; 2015 doi: 10.1038/srep16414.

**Abstract:** *Plasmodium falciparum* gametocytes, specifically the mature stages, are the only malaria parasite stage in humans transmissible to the mosquito vector. Anti-malarial drugs capable of killing these forms are considered essential for the eradication of malaria and tools allowing the screening of large compound libraries with high predictive power are needed to identify new candidates. As gametocytes are not a replicative stage it is difficult to apply the same drug screening methods used for asexual stages. Here we propose an assay, based on high content imaging, combining “classic” gametocyte viability readout based on gametocyte counts with functional viability readout, based on gametocyte activation and the discrimination of the typical gamete spherical morphology. This simple and rapid assay has been miniaturized to a 384-well format using acridine orange staining of wild type *P. falciparum* 3D7A sexual forms, and was validated by screening reference antimalarial drugs and the MMV Malaria Box. The assay demonstrated excellent robustness and ability to identify quality hits with high likelihood of confirmation of transmission reducing activity in subsequent mosquito membrane feeding assays.

## Introduction

Malaria is a disease resulting from infection by the intracellular protozoan parasite *Plasmodium*. It remains the most significant parasitic disease in the world, causing ~200 million clinical cases and up to 750,000 deaths each year (WHO World Malaria Report 2014). Substantial efforts are being made not only to reduce the number of clinical manifestations and deaths attributed to malaria, but also to achieve eradication of this disease. *Plasmodium falciparum*, responsible for the most severe form of malaria, is transmitted by female *Anopheles* mosquitoes, which inject sporozoites into humans causing an asymptomatic hepatic infection, followed by the intra-erythrocytic parasite proliferation responsible for the symptoms of malaria and fatal complications of the disease such as severe anaemia and cerebral malaria. Within the host red blood cells, parasites undergo several rounds of asexual replication, while a small proportion develops into sexual forms called gametocytes. Male and female *P. falciparum* gametocytes undergo five stages of maturation (stage I to V), which last about 10 days. Mature

gametocytes persist in the peripheral circulation for several weeks (Bousema and Drakeley 2011; Bousema et al., 2010), where they can be taken up by a mosquito during a blood meal. Inside the mosquito midgut mature gametocytes are triggered within a few minutes to differentiate into female and male gametes, followed by mating. Fertilization produces a motile ookinete which further develops, eventually leading to the generation of infective sporozoites migrating to the insect salivary glands.

Malaria control is mostly achieved by prevention of mosquito bites (insecticide-treated nets, indoor spraying) (Karunamoorthi 2011), plus prophylactic and drug treatment, presently based on artemisinin-based combination therapy (ACT). However, emerging resistance to artemisinins in the field is a pressing issue (Petersen et al., 2011; Dondorp et al., 2009; Mok et al., 2015). In this context, the development of new antimalarial drugs is critical, as the current choice of drugs is limited. In addition to activity against blood stage asexual parasites, inhibition of gametocyte viability and a cognate block in parasite transmission, is a necessary complementation for an integrated program of antimalarial intervention.

The last four years have seen the emergence of a considerable number of different approaches to determine the impact of compounds on gametocyte development (Chevalley et al., 2010; Peatey et al., 2009; Tanaka et al., 2011; Lelievre et al., 2012; Lucantoni et al., 2013; Ruecker et al., 2014; Bolscher et al., 2015; Duffy and Avery 2013; Sanders et al., 2014; Cevenini et al., 2014; D'Alessandro et al., 2013; Wang et al., 2014; Miguel-Blanco et al., 2015). Some of these assays are focused specifically on stage IV-V gametocytes, with the aim to identify compounds active against the mature sexual stages, the only ones able to survive and further develop in the mosquito blood meal. While many schizonticides, such as chloroquine, retain some efficacy against young gametocytes (stages I, II, and III) (Lucantoni et al., 2013), gametocytes at late stages of maturation are less/not sensitive to them (Duffy and Avery 2013; Butterworth et al., 2013). The insensitive stage V gametocytes remain quiescent but infectious in the peripheral bloodstream for at least three weeks (Bousema et al., 2010; Eichner et al., 2001). These cells are directly responsible for malaria parasite transmission as they are programmed to sense the environmental changes in the transition from human circulation to the mosquito midgut and to readily transform into male and female gametes. The first event in gamete formation, induced by a decrease in temperature and the presence of the gametocyte-activating factor xanthurenic acid (XA), is the rapid morphological transition from the typical crescent shape of mature gametocytes to a round cell (Billker et al., 1998), in a process, essential for the progression of gametogenesis (Taylor et al., 2008), defined as "rounding-up" (Figure 1).

Current screening assays for compounds active against gametocytes use a variety of detection methods, including measurement of parasite ATP levels (Lelievre et al., 2012), parasite enzymatic activity (D'Alessandro et al., 2013) or expression of a gene reporter (Lucantoni et al., 2013). Additional image based approaches ascertain gametocyte viability with Mitotracker (Duffy and Avery 2013), or measure the formation of female gametes/zygotes using antibodies against the gamete-zygote surface protein Pfs25 (Bolscher et al., 2015; Miguel-Blanco et al., 2015) or specifically assess male gametocyte ability to produce flagellated gametes (Ruecker et al., 2014). The major drawbacks in the current assays include the need to use gametocyte cultures highly purified from asexual parasites (D'Alessandro et al., 2013) or from uninfected red blood cells, or both (Lelievre et al., 2012), long incubation and assay times imposed by the slow decay of the enzymatic or transgenic reporter activity in unhealthy or dead mature gametocytes (D'Alessandro et al., 2013) or by the slow accumulation of sufficient signal intensity (Duffy

and Avery 2013). The existing assays able to quantify female gamete formation, all based on Pfs25 antibody, require high number of parasites, which limits throughput (Bolscher et al., 2014), and/or additional 16h-24h incubation of activated gametocytes/gametes to achieve adequate signal intensities of fluorescent labelled Pfs25 antibodies (Ruecker et al., 2014; Bolscher et al., 2014; Miguel-Blanco et al., 2015).

In order to address the need for a high throughput assay to measure the viability of the quiescent mature gametocytes we developed a simple and robust phenotypic assay, solely based on the fact that only viable mature stage V gametocytes are able to form gametes. After compound treatment, mature gametocytes are triggered to undergo gametogenesis and multiple imaging readouts are measured within two hours, including both the total gametocyte numbers and the fraction of those, alive, able to “round up”. Importantly, our high-throughput compatible assay is optimized for use with non-transgenic parasites, allowing the screening of mature gametocytes from any laboratory line or field isolate.

## Methods

***P. falciparum* culture and gametocytogenesis.** The strains 3D7A and 3D7-PFL1675c/ULG8-GFP were cultured *in vitro* as described by Trager and Jensen (Trager and Jensen 1976) with minor modifications. Briefly, parasites were maintained in human type O-positive RBCs at 5% haematocrit (Hct) in RPMI 1640 medium supplemented with 25 mM HEPES (Sigma), 50 µg/ml hypoxanthine and with the addition of either 10% (v/v) naturally clotted heat-inactivated O+ human serum (Interstate Blood Bank, Inc.) and 5 nM WR99210 (Jacobus Pharmaceuticals) for 3D7-PFL1675c/ULG8-GFP, or 5% AB human serum (Sigma) and 2.5 mg/ml Albumax II (Gibco) for 3D7A. The cultures were maintained at 37°C in a standard gas mixture consisting of 5% O<sub>2</sub>, 5% CO<sub>2</sub> and 90% N<sub>2</sub>.

At Day-3 of the induction protocol, mid stage trophozoite parasites were isolated on a CS magnetic column (MACS) and VarioMACS separator (Miltenyi Biotec). Fresh RBCs were added to the isolated trophozoites to reach a final parasitemia of 2%, and the hct reduced to 1.25%. After overnight shaking, the Day-2 culture was put under nutritional stress overnight, by keeping the cultures at a high parasitemia of 9% at 2.5% hct and providing only a partial (3/4) exchange of medium. Resulting trophozoite parasites, Day-1, were adjusted to 2% - 3% parasitaemia and shaken overnight. Gametocyte cultures were maintained in medium supplemented with 50 mM N-acetylglucosamine (NAG; Sigma-Aldrich) in order to clear residual asexual parasites and obtain a virtually pure gametocyte culture. At Day 4, 3D7-PFL1675c/ULG8-GFP gametocytes were isolated on a CS magnetic column, resuspended in T-25 flasks at 2.5% hct, >50% parasitaemia and cultivated in a hypoxia workstation (Bugbox, Ruskin Intl), until fully mature stage V gametocytes (Day 14). 3D7A gametocytes used in the non-transgenic assay were diluted with fresh blood to a final gametocytemia of 10% and maintained at 2.0 - 2.5% hct in a standard incubator, with daily change of pre-warmed culture medium until use (stage V; day 12 of gametocytogenesis).

Gametogenesis was measured by treating samples with 50 µM xanthurenic acid (XA; Sigma-Aldrich) in exflagellation buffer (RPMI 1640 with 20 mM HEPES, 4 mM sodium bicarbonate, pH 8.0). After 10 min incubation at room temperature, the numbers of macrogametes and non-activated female gametocytes were determined using Giemsa smears. Specific inhibition of rounding-up was achieved by incubating samples with 5 µM CMPD-2 (kind gift from Dr. D.A. Baker, London School of Hygiene & Tropical



Medicine) for 10 min at room temperature. Cultures showing an activation of 95% or above on day 12 were used in the assay.

**Anti-malarial compound stock preparations and handling.** A panel of 39 antimalarial compounds (see Table S1 for complete details) was prepared as 10 mM / 100% DMSO stock solutions from solids. For IC<sub>50</sub> determination, DMSO compound stocks were serially diluted in 384-well deep well polypropylene storage plates (Axygen), across the plate. The dilutions made resulted in three concentrations per log dose for each compound tested (14 points, final concentration range 10 µM – 0.5 nM). All dilutions were in 4% DMSO, of which 5 µl were stamped into the assay plate, using a Minitrak (PerkinElmer) liquid handler, to a final DMSO concentration of 0.4% v/v. The antimalarials were tested in three biological replicates.

The MMV Malaria Box was received as 10 mM stocks in 100% DMSO. Compounds were reformatted into 384-well format while being pre-diluted twofold into 100% DMSO. DMSO-diluted stocks were stored at –20°C and once thawed were not repeat freeze-thawed in order to maintain the integrity of the compounds. On the day of assays, stocks were further diluted 25 fold in water and finally 10 fold into culture, to obtain a final screening concentration of 5 µM at 0.4% DMSO. The MMV Malaria Box was screened at a single dose of 5 µM, in two biological replicates. MMV Malaria Box hits were manually cherry-picked, serially diluted as described above and tested in dose-response (14 points, range 10 µM – 0.5 nM) in three biological replicates.

**Assay Development: Proof of Principle.** As proof of principle, the initial assay was developed using a 96 well plate format with 3D7-PFL1675c/ULG8-GFP transgenic parasites. Mature gametocyte cultures were plated in 96 wells imaging plates (Ibidi, Germany), in a final volume of 100 µL per well. To test the relationship between the automated gamete count and the initial gametocyte density per well, gametocytes were seeded at different initial densities (1,250 – 90,000 per well). The rounding-up process was activated 48 hours post-incubation by the addition of 5 µL XA (50 µM final concentration). Gamete numbers were measured in 20 wells using a Scan<sup>R</sup> automated imaging cytometry station (Olympus, Japan). Briefly, microplates were imaged with a UPLSAPO 20X N.A. 0.75 (Olympus, Japan) and a filter cube consisting of 470-90nm excitation, 500nm dichromatic mirror and 520 nm long-pass emission. Gametocytes were seeded at a final average density of 40,000 / well, which allowed sampling of a statistically relevant number of events from a single 400x400 µm image field from each well. The Scan<sup>R</sup> Analysis software (v2.5.1) was used to detect and analyze gametocytes from each well. The 'edge' algorithm was used to segment images and shape and intensity thresholds were finely adjusted for each experimental session in order to exclude debris and poorly stained cells. Further area- and circularity-based gating of events allowed complete separation of elongated (gametocytes) versus round (gametes) parasites and compared to manually counted gametes using a haemocytometer. The number of identified parasites per well image (average ± SD) was plotted against the actual number of parasites per well using linear regression.

In a separate experiment, the speed of gametocyte rounding-up was determined by the addition of paraformaldehyde (PFA, 2% final concentration) at different time intervals after stimulation of mature gametocytes with XA and temperature shift.

As candidate positive controls specific for blocking the rounding up process even in presence of XA stimulation, we tested the specific PfPKG inhibitors CMPD-1 and CMPD-2 (McRobert et al., 2008; Taylor et al., 2010) in 8 points dose response.

**Acridine Orange Gamete (AO-GMT) assay.** For greater versatility, a HTS assay was designed which would allow the use of non-transgenic parasite strains, where gametocytes were stained with a fluorescent dye. For this assay, experimental compounds prepared as described above were dispensed in 384 black clear-bottom imaging plates (Viewplate, PerkinElmer) and added with 20  $\mu$ l of medium. In each AO-GMT assay plate the following in-plate controls were used: 5  $\mu$ M CMPD-2 (7 wells); 5  $\mu$ M Methylene Blue (MB; 7 wells); 0.4% DMSO (14 wells).

Plates were then pre-warmed at 37°C for a minimum of 30 minutes. 3D7A gametocytes on day 12 of gametocytogenesis from cultures showing acceptable rounding-up upon XA stimulation were seeded in the pre-warmed plates using a Multidrop (Thermo Scientific) 384 reagent dispenser to a final volume of 45  $\mu$ l and 0.1% hct (~40,000 gametocytes per well). Plates were sealed with gas-exchange membranes (Breathe Easy, Sigma) and immediately returned to standard incubation conditions (37°C; 5% O<sub>2</sub>, 5% CO<sub>2</sub> and 90% N<sub>2</sub>). Extreme care was taken in keeping handling time to a minimum and to ensure pre-warming of all tools and reagents at 37 °C before use.

After 48 hours incubation, plates were retrieved and brought to room temperature. Using a Bravo Automated Liquid Handling Platform (Agilent), half of the culture supernatant volume was slowly aspirated from each well and gently replaced with RPMI supplemented with 25 mM HEPES (Sigma) and 50  $\mu$ g/ml hypoxanthine, 80  $\mu$ M XA and 120 nM acridine orange base (AO; Sigma) to final in-well concentrations of XA and AO of 40  $\mu$ M and 60 nM, respectively. Plates were imaged after 2.5 hours light-protected incubation at room temperature (22.7  $\pm$  0.3 °C). The assay workflow is illustrated in Figure 2.

**Imaging data analysis.** Image acquisition and analysis was undertaken on an Opera QEHS micro-plate confocal imaging system (PerkinElmer). Four field images were taken from each well at 5  $\mu$ m from the bottom of the 384-wells imaging plates using a 20X water immersion objective using 488 nm excitation and 520/35 nm emission, and an exposure time of 280 - 400 msec.

A custom script based on the spot detection algorithm was developed using the high-volume image data storage and analysis system Columbus 2.5 (PerkinElmer). A first pass selection was used to filter out unwanted spots based on size (accepted range 45 – 100 px<sup>2</sup>) and background-corrected spot intensity (accepted range between the 5<sup>th</sup> and 95<sup>th</sup> percentile of DMSO and CMPD-2 pooled spot populations).

A second pass selection using a spot width-to-length cutoff of 0.65 allowed to discriminate between “spherical” fluorescent gametes, and crescent-shaped fluorescent gametocytes within the selected spot population. With these specifications, it took approximately 20 minutes to screen one full plate.

The use of both a ‘full kill’ (MB) and a ‘no round-up’ (CMPD-2) control in each plate, together with the shape-recognition script allow the simultaneous quantification of compound effects on the overall gametocyte population (irrespective of their ability to round-up, i.e. a “classical” fluorescence-based gametocytocidal assay), as well as to determine the impact on functional viability and efficiency of rounding-up.

Raw imaging data were exported to Excel 2010 (Microsoft) and reduction in gametes and total sexual form numbers, as well as inhibition of rounding-up were calculated as a percentage of the relevant positive and negative controls as below:

1:

$$\begin{aligned} & \% \text{ activated gametocyte / gamete inhibition} \\ & = 100 - \frac{\text{gamete no. sample} - \text{gamete no. CMPD-2}}{\text{gamete no. 0.4\% DMSO} - \text{gamete no. CMPD-2}} \times 100; \end{aligned}$$

2:

$$\% \text{ inhibition of rounding - up} = 100 - \frac{\text{RND}_{\text{sample}} - \text{RND}_{\text{CMPD-2}}}{\text{RND}_{\text{0.4\% DMSO}} - \text{RND}_{\text{CMPD-2}}} \times 100,$$

where RND is the proportion of female gamete in each well:

3:

$$\text{RND} = \frac{\text{gamete no. sample}}{\text{gamete no. sample} + \text{gametocyte no. sample}}$$

4:

$$\begin{aligned} & \% \text{ total gametocyte inhibition} = \\ & 100 - \frac{(\text{gametes+gametocytes})_{\text{sample}} - (\text{gametes+gametocytes})_{\text{MB}}}{(\text{gametes+gametocytes})_{\text{CMPD-2}} - (\text{gametes+gametocytes})_{\text{MB}}} \times 100. \end{aligned}$$

CMPD-2, an inhibitor of rounding up, which completely blocks activation but does not kill gametocytes, was used as either positive control for activated gametocyte numbers and rounding-up (no activation) vs 0.4% DMSO (max activation), as well as negative control for total parasite numbers (no kill and no activation) vs MB (full kill).

The assay quality was evaluated for each readout using the Z' parameter, defined as:

$$Z' = \frac{3 \times \sigma_{\text{neg}} + 3 \times \sigma_{\text{pos}}}{\text{avg}_{\text{neg}} - \text{avg}_{\text{pos}}}$$

where avg and  $\sigma$  represent the average and standard deviation of the signal obtained from at least 7 wells; and neg and pos represent the relevant negative (maximum signal) and positive (minimum signal) controls used for each readout.

Correlation between number of gametocyte per well determined by microscopy counts or identified by the light microscopy Scan<sup>R</sup> assay script were calculated using Excel 2010 (Microsoft). Correlation between total sexual form counts and gamete numbers obtained in the HTS confocal imaging assay was calculated using SPSS v.21 (IBM). Normalized % inhibitions were plotted against log  $\mu\text{M}$  concentration of each compound and IC<sub>50</sub> values were calculated using a variable slope, 4 parameter non-linear regression analysis in GraphPad Prism 5.0. IC<sub>50</sub> values were not calculated for compounds which did not reach maximal inhibition at the highest concentration tested.

**Standard Membrane Feeding Experiments.** Standard Membrane Feeding Experiments were performed as described previously (Zhang et al., 1999). Briefly, compounds were diluted in DMSO and RPMI1640 medium and combined with mature gametocytes from *P. falciparum* reporter strain NF54- $\Delta\text{Pf47-5'hsp70-GFP::Luc}$  to a final compound concentration of 1 and 10  $\mu\text{M}$  (0.1% DMSO) and incubated for 24 hours. Subsequently, the haematocrit was adjusted to 56% by adding fresh human red blood cells

(Sanquin, the Netherlands) and the bloodmeal was fed to 2 day old *Anopheles stephensi* mosquitoes. Eight days post-feeding, ten mosquitoes from each of the two vehicle control (0.1% DMSO) cages were dissected and the baseline oocyst intensity was determined by microscopy following staining of the midguts with 2% mercurochrome. In addition, twenty-four mosquitoes from each cage were homogenized and luciferase reporter activity was determined as described previously (Stone et al., 2014).

## Results

Healthy mature gametocytes of *P. falciparum* exposed to a drop in temperature and 40  $\mu$ M XA are readily triggered to undergo gamete formation. The first step of the process is the fast transition from the typical elongated shape of both male and female gametocytes to a spherical cell, still enclosed in its erythrocyte membrane (Figure 1). With the only assumption that this process requires the mature gametocyte to be alive, as it needs to sense the change in environment and to respond by modifying its cell shape, we hypothesized that effects of compounds on mature gametocyte viability could be phenotypically assessed from their ability to “round up” and that failure to undergo this developmental step would be predictive of the compounds’ transmission-blocking activity measured in experimental infections of mosquitoes. To this end we devised an imaging-based assay measuring the number of induced spherical activated gametocytes in a format suitable for high throughput screening of large compound libraries, and then compared the data from our assay with published or newly generated data on the transmission-blocking activity in the mosquito of the identified hits.

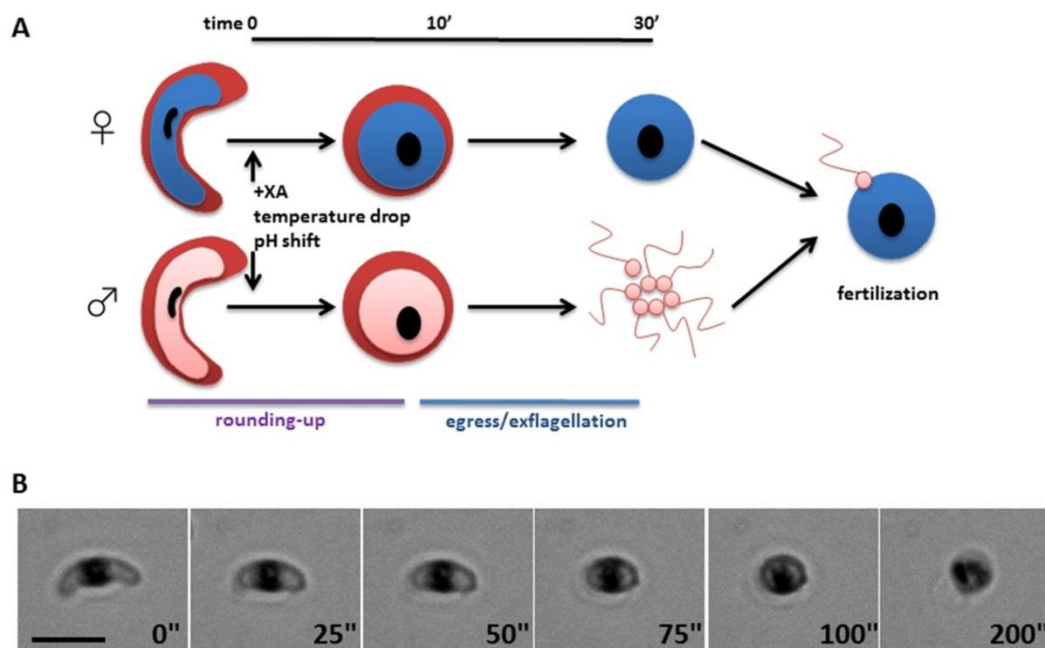


**Figure 1.** A. The mature gametocyte activation process (modified from Kuehn and Pradel 2010). B. Time lapse of gametocyte rounding-up.

**Establishing Proof of Principle for the rounding-up assay.** To establish the “rounding up” assay, a *P. falciparum* transgenic line expressing a GFP reporter under control of the flanking regions of parasite gene PFL1675c, abundantly transcribed in stage V gametocytes was initially used. This strain produces elongated mature gametocytes which are readily distinguishable, by fluorescence microscopy, from the spherical rounded up gametes (Figure 2A,B). Synchronous stage V gametocytes were obtained in 96 wells microtiter plates<sup>18</sup> to develop a proof-of-principle assay (GFP-GMT) in which GFP detection of elongated gametocytes and of induced spherical gametes was achieved with a Scan<sup>^</sup>R (Olympus, Germany) modular epifluorescence microscope-based imaging platform. Script parameters were specifically optimized (see methods for full details) to identify the fluorescent cells and subsequently enable spherical gametes to be distinguished from elongated gametocytes. In this protocol, each fluorescent parasite was identified by calculating background-corrected fluorescence intensity and an edge segmentation parameter, which defined the object for further analysis as a region of interest (ROI). For each ROI, a circularity factor was then calculated to classify the object as a spherical rounded up gamete or as an elongated, non-activated gametocyte. Further area- and circularity-based gating parameters were incorporated to ignore signal from debris and poorly stained cells, and to specifically identify elongated gametocytes and round gametes, importantly generating image galleries of the individual objects for post-assay quality control inspections.

A linear relationship was observed between the number of gametocytes per well, as determined by manual haemocytometer counts, compared to the automated script estimation. An  $r^2$  value of 0.98 was obtained and linearity was maintained from 1250 to 80,000 gametocytes per well (Figure 2C).

In establishing the gametogenesis induction protocol, a time course was performed to define the minimum time necessary to achieve a satisfactory rounding up efficiency before image acquisition. These experiments showed that 10 minutes are sufficient to achieve rounding up of 80% of the induced gametocytes (Figure 2D).

In order to introduce a reliable baseline control of non-activated gametocytes, we tested two specific inhibitors of the gametocyte rounding up process, Compound 1 and Compound 2 (CMPD-1 and -2). These are potent inhibitors of the *P. falciparum* cGMP-dependent Protein Kinase G (PKG), previously described to block the gametocyte transition from crescent to spherical shape (CMPD-1  $IC_{50}$  = 5.8 nM against recombinant PfPKG) (McRobert et al., 2008). Mature gametocytes were activated with XA in presence or absence of increasing concentrations of CMPD-1 and CMPD-2; parasites were fixed with 2% paraformaldehyde after 10 minutes and the plate imaged. Results (Figure 2E) confirmed a higher inhibitory activity of CMPD-2 ( $IC_{50}$  = 0.07  $\mu$ M) compared to CMPD-1 ( $IC_{50}$  = 0.47  $\mu$ M) (McRobert et al., 2008; Taylor et al., 2010), and the former was chosen as the reference rounding-up inhibitor in the assay.

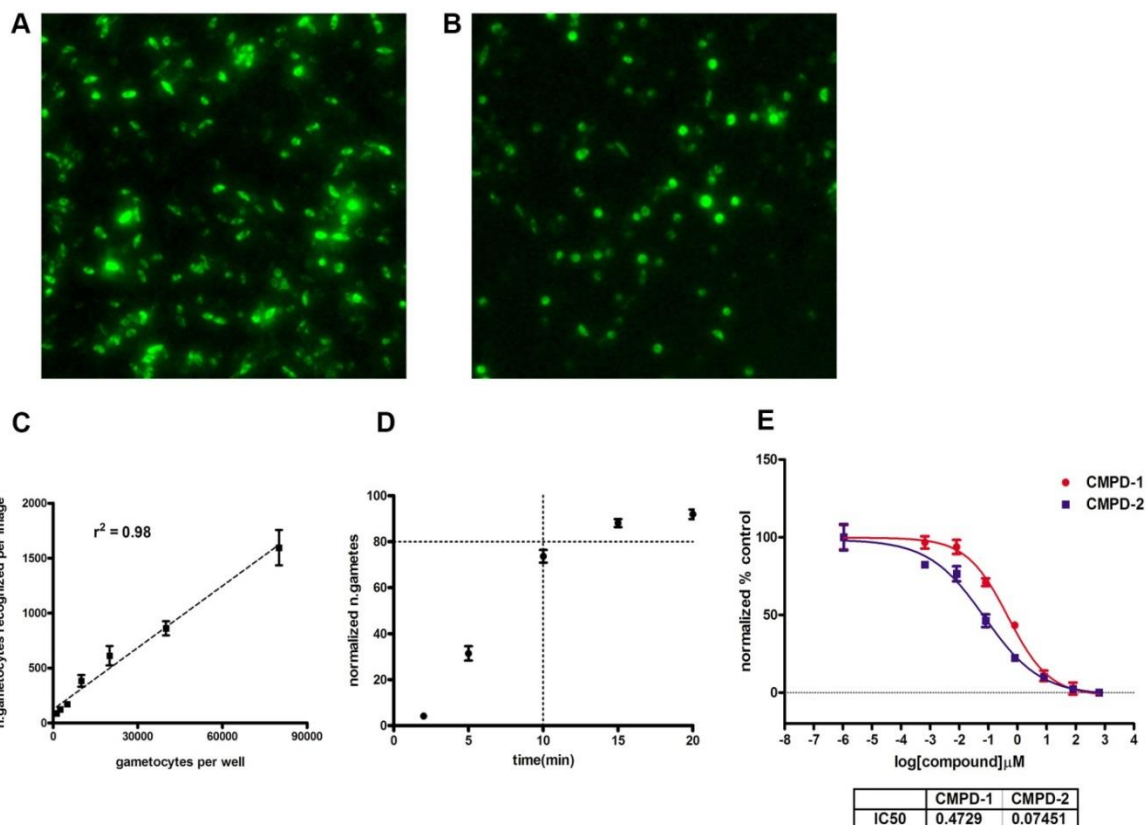


**Figure 2.** A, B. Representative images of fluorescent gametocytes (A) and gametes (B) from the parasite line 3D7-PFL1675c/ULG8-GFP. C. Linearity plot of the number of gametocyte per well determined by microscopy counts or identified by the assay script after Scan<sup>^</sup>R station automated cytometry imaging. D. Kinetic of rounding-up efficiency in a gamete activation time course with 3D7-PFL1675c/ULG8-GFP gametocytes. E. Dose-response analysis of the action of CMPD-1 and 2 inhibitors on rounding-up of 3D7-PFL1675c/ULG8-GFP gametocytes.

**Assay miniaturization and scale-up for HTS.** To develop an assay not reliant on transgenic gametocytes but potentially applicable to any parasite line or clinical isolate, the assay protocol optimised for proof of principle was modified to introduce a straightforward step for parasite labelling with the fluorescent dye, Acridine Orange (AO). AO has been previously demonstrated to have very low anti-plasmodial activity, compared to other fluorescent dyes (Joanny et al., 2012). The final AO concentration of 60 nM utilized in our assay is 51-fold lower than its reported  $\text{IC}_{50}$  against 3D7 stage V gametocytes (Gebru et al., 2014). The introduction of an additional full-kill positive control treatment, the potent gametocytocidal compound, Methylene blue (MB) (Adjalley et al., 2011), allowed the assay to simultaneously measure the gametocytocidal and rounding-up inhibitory effects of compounds (Figure 3A). Importantly, the AO gamete (AO-GMT) assay was adapted to 384 well format for HTS. In all assay runs, the in-plate controls consisted of 5  $\mu\text{M}$  MB and 5  $\mu\text{M}$  CMPD-2 as positive controls (7 wells each) and 0.4% DMSO as the negative control (16 wells). The average  $\pm$  SEM  $Z'$  values for gamete numbers (CMPD-2 as positive control) and total gametocyte numbers (MB as positive control) were  $0.69 \pm 0.02$  and  $0.66 \pm 0.02$ , respectively ( $n = 12$ ). The DMSO control showed an average %CV of  $8.0\% \pm 0.004\%$  ( $n = 12$ ). The performance of the assays was extremely stable from the first to last plates with high within-plate reproducibility (Figure 3B). The final flow chart of the AO-GMT assay is illustrated in Figure 4.

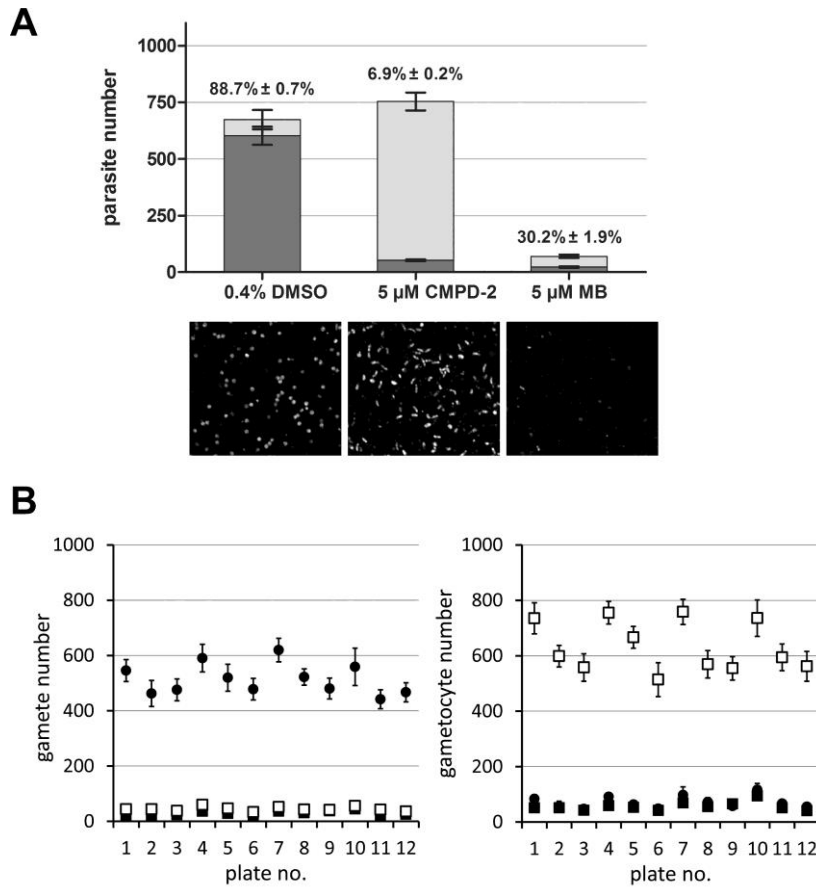


**Figure 3.** A. Quantitative comparison ( $n = 17$ ) and exemplar images of positive and negative controls *P. falciparum* 3D7A parasite populations, obtained from the Opera High Content Screening system. Dark bars = activated gametocyte numbers; light bars = total gametocyte numbers. Error bars represent SEM; percentages above bars indicate % rounding-up.

B. AO-GMT assay in-plate control data. Spots identified by the script as gametes (left panel) and gametocytes (right panel) in wells treated with 0.4% DMSO (closed circles); 5  $\mu\text{M}$  methylene blue (close squares) or 5  $\mu\text{M}$  CMPD-2 (open squares). Average numbers  $\pm$  SEM. Error bars in positive controls are masked by symbols in some cases due to their small size.

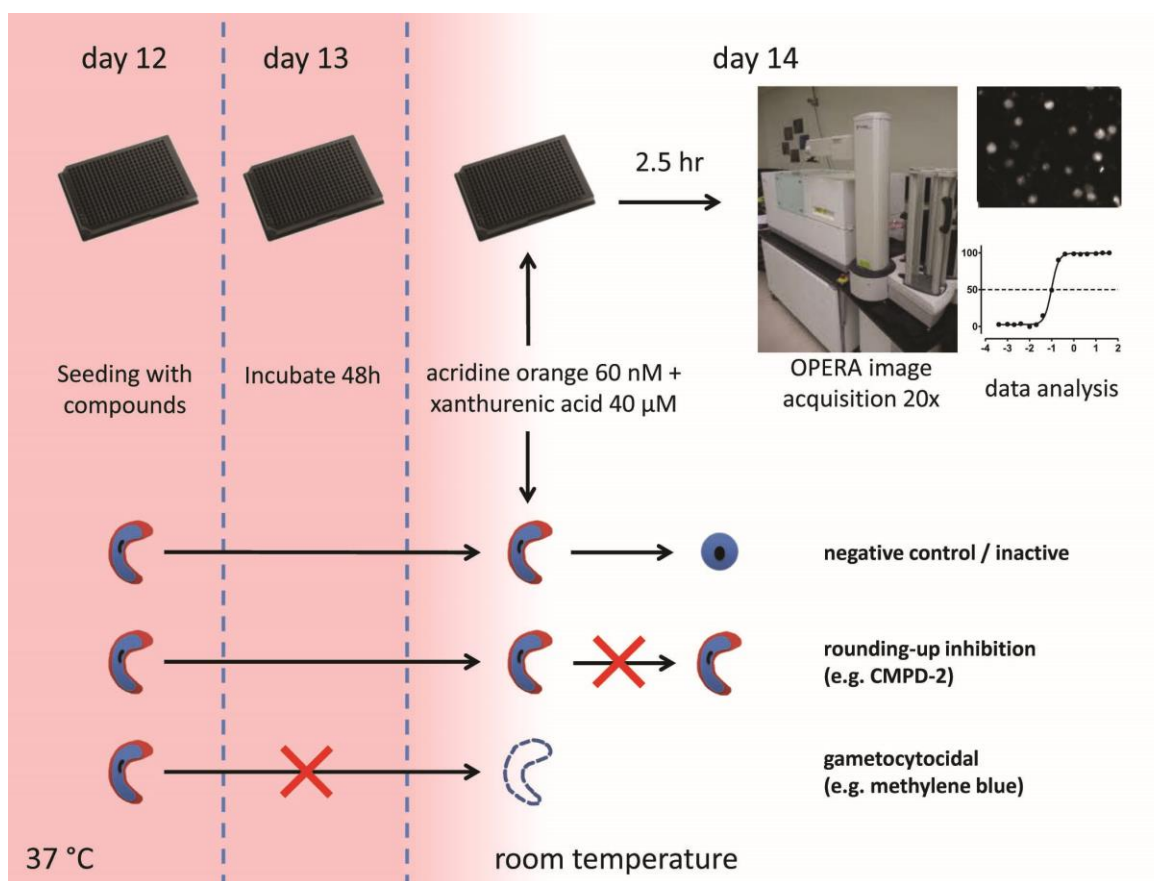


**Figure 4.** Workflow of the AO-GMT assay and the underlying parasite biology.

**Activity of current anti-malarial compounds on mature gametocytes.** The AO-GMT imaging assay was used to screen a set of 39 known antimalarial drugs belonging to different chemical classes and acting via different mechanisms on asexual parasites, whose activities have been recently tested against multiple malaria parasite species and stages (Delves et al., 2012) and on *P. falciparum* gamete formation (Ruecker et al., 2014; Bolscher et al., 2015; Sun et al., 2014).

Compounds were tested in dose-response at a maximum concentration of 10  $\mu\text{M}$  for 48h. In brief, results showed that very few compounds affected gametocyte numbers and viability with an  $\text{IC}_{50}$  value below 5  $\mu\text{M}$  (Table 1). The low number of active compounds identified is in agreement with previous published assays (Ruecker et al., 2014; Bolscher et al., 2015; Sun et al., 2014). Analysis of the inhibition readouts at 10  $\mu\text{M}$  showed, as expected, a broad correlation between activity on gametes and on total gametocytes.



| class             | compound             | gamete formation |        |                     |       | total sexual forms |        |                     |       | proportion of rounding-up |        |                               |      |
|-------------------|----------------------|------------------|--------|---------------------|-------|--------------------|--------|---------------------|-------|---------------------------|--------|-------------------------------|------|
|                   |                      | IC50 (µM) ± SEM  |        | % inhibition† ± SEM |       | IC50 (µM) ± SEM    |        | % inhibition† ± SEM |       | EC50 (µM) ± SEM           |        | % of 0.4% DMSO control† ± SEM |      |
| 4-aminoquinolines | amodiaquine          |                  |        | 62.13               | 4.40  |                    |        | 53.58               | 5.88  |                           |        | 87.03                         | 3.69 |
| 4-aminoquinolines | AQ-13                | 3.15             | 0.65   | 88.09               | 2.59  | 3.50               | 0.38 * | 78.91               | 2.52  |                           |        | 83.77                         | 1.18 |
| 4-aminoquinolines | chloroquine          |                  |        | 63.72               | 3.78  |                    |        | 58.03               | 3.31  |                           |        | 92.01                         | 1.03 |
| 4-aminoquinolines | hydroxychloroquine   |                  |        | 60.62               | 5.12  |                    |        | 55.37               | 3.92  |                           |        | 92.56                         | 2.85 |
| 4-aminoquinolines | naphthoquine         | 1.14             | 0.23   | 89.47               | 0.12  | 1.60               | 0.22 * | 73.02               | 2.19  |                           |        | 60.12                         | 3.66 |
| 4-aminoquinolines | piperaquine          |                  |        | 16.73               | 2.19  |                    |        | 10.17               | 5.88  |                           |        | 96.22                         | 0.98 |
| 8-aminoquinoline  | diethylprimaquine    |                  |        | 20.96               | 6.12  |                    |        | 14.37               | 0.57  |                           |        | 95.32                         | 3.01 |
| 8-aminoquinoline  | NPC-1161B            | 2.76             | 0.34   | 104.02              | 0.93  | 3.15               | 0.18 * | 93.09               | 1.02  |                           |        | 60.28                         | 5.55 |
| 8-aminoquinoline  | primaquine           |                  |        | 53.31               | 2.92  |                    |        | 27.69               | 4.24  |                           |        | 69.46                         | 3.05 |
| 8-aminoquinoline  | tafenoquine          | 3.45             | 0.55   | 104.77              | 0.58  | 4.22               | 0.38 * | 95.42               | 0.37  |                           |        | 71.54                         | 9.15 |
| aminoalcohols     | halofantrine         |                  |        | 38.11               | 21.07 |                    |        | 34.01               | 17.10 |                           |        | 89.50                         | 5.87 |
| aminoalcohols     | lumefantrine         |                  |        | -4.82               | 1.74  |                    |        | 0.82                | 1.07  |                           |        | 99.06                         | 0.52 |
| aminoalcohols     | mefloquine (+ RS)    | 4.75             | 0.67 * | 86.10               | 2.42  |                    |        | 64.35               | 3.66  |                           |        | 52.30                         | 2.52 |
| aminoalcohols     | mefloquine (Racemic) | 5.11             | 1.18 * | 82.39               | 2.24  |                    |        | 58.49               | 1.04  |                           |        | 52.19                         | 5.68 |
| aminoalcohols     | quinine              |                  |        | 1.74                | 5.03  |                    |        | 5.54                | 3.56  |                           |        | 98.76                         | 0.58 |
| antilinoacridine  | pyronaridine         | 3.32             | 0.41 * | 106.85              | 0.42  | 3.96               | 0.34 * | 93.40               | 2.58  |                           |        | 23.87                         | 3.79 |
| antibiotics       | azithromycin         |                  |        | 16.75               | 7.83  |                    |        | 19.19               | 5.39  |                           |        | 98.24                         | 2.34 |
| antibiotics       | clindamycin          |                  |        | 3.65                | 6.95  |                    |        | 8.13                | 5.87  |                           |        | 99.75                         | 0.82 |
| antibiotics       | doxycyclin           |                  |        | -2.33               | 7.82  |                    |        | 3.51                | 6.46  |                           |        | 99.68                         | 0.95 |
| antibiotics       | fosmidomycin         |                  |        | -3.83               | 3.73  |                    |        | -5.75               | 8.28  |                           |        | 100.63                        | 0.60 |
| antibiotics       | tetracycline         |                  |        | -3.62               | 3.85  |                    |        | 0.82                | 3.07  |                           |        | 99.00                         | 0.59 |
| antibiotics       | thiostrepton         | 1.39             | 0.31   | 92.58               | 1.93  |                    |        | 39.98               | 3.62  | 1.97                      | 0.16 * | 18.55                         | 1.93 |
| antifolates       | chlorproguanil       | 3.08             | 0.42 * | 99.56               | 2.67  | 4.16               | 0.44 * | 87.82               | 3.97  |                           |        | 63.25                         | 0.21 |
| antifolates       | dapsone              |                  |        | -4.72               | 3.30  |                    |        | 1.46                | 3.10  |                           |        | 99.71                         | 0.48 |
| antifolates       | proguanil            |                  |        | 50.93               | 7.71  |                    |        | 44.13               | 5.73  |                           |        | 87.23                         | 3.68 |
| antifolates       | pyrimethamine        |                  |        | 7.72                | 6.63  |                    |        | 5.51                | 5.75  |                           |        | 100.33                        | 0.50 |
| antifolates       | trimethoprim         |                  |        | 14.51               | 3.48  |                    |        | 12.03               | 2.24  |                           |        | 101.07                        | 0.45 |
| diamidines        | pentamidine          |                  |        | 68.34               | 3.44  |                    |        | 55.52               | 2.47  |                           |        | 98.27                         | 0.70 |
| endoperoxides     | artemether           |                  |        | 44.26               | 7.09  |                    |        | 38.73               | 5.54  |                           |        | 99.84                         | 0.45 |
| endoperoxides     | artemisinin          |                  |        | 35.40               | 11.73 |                    |        | 32.35               | 10.02 |                           |        | 100.47                        | 1.25 |
| endoperoxides     | artemisono           |                  |        | 61.65               | 3.28  |                    |        | 27.22               | 1.64  |                           |        | 75.03                         | 2.76 |
| endoperoxides     | artesunate           |                  |        | 62.97               | 9.48  |                    |        | 49.67               | 8.42  |                           |        | 90.27                         | 2.05 |
| endoperoxides     | dihydroartemisinin   |                  |        | 64.32               | 4.79  |                    |        | 53.68               | 3.70  |                           |        | 93.17                         | 1.53 |
| naphthoquinones   | atovaquone           |                  |        | 54.82               | 1.13  |                    |        | 25.91               | 3.95  |                           |        | 56.86                         | 1.63 |
| others            | cycloheximide        |                  |        | 62.10               | 4.32  |                    |        | 17.36               | 4.34  |                           |        | 48.58                         | 3.15 |
| others            | methylene blue       | 0.17             | 0.04   | 108.60              | 0.20  | 0.28               | 0.04   | 100.24              | 0.20  | 0.91                      | 0.18 * | 76.40                         | 3.78 |
| sulfonamides      | sulfadiazine         |                  |        | 1.29                | 7.52  |                    |        | 0.03                | 7.11  |                           |        | 81.65                         | 2.22 |
| sulfonamides      | sulfadoxine          |                  |        | -1.85               | 1.72  |                    |        | 1.65                | 2.54  |                           |        | 65.65                         | 1.37 |
| sulfonamides      | sulfamethoxazole     |                  |        | -4.20               | 3.38  |                    |        | -6.58               | 6.01  |                           |        | 16.56                         | 2.82 |

† activity at 10 µM shown

\* IC<sub>50</sub> value to be considered as approximate (maximal inhibition plateau not reached)

**Table 1.** Activity of a panel of antimalarial drugs and compounds on gametes, total sexual forms and rounding-up efficiency.

Generally, active compounds showed a higher activity on gamete inhibition with respect to gametocyte viability (Figure 5), an observation likely explained by the higher sensitivity of the functional viability readout. Five compounds, namely thiostrepton, cycloheximide, artemisono, atovaquone and primaquine, were found to reduce gamete numbers more than total parasite numbers at this concentration (Table 1).

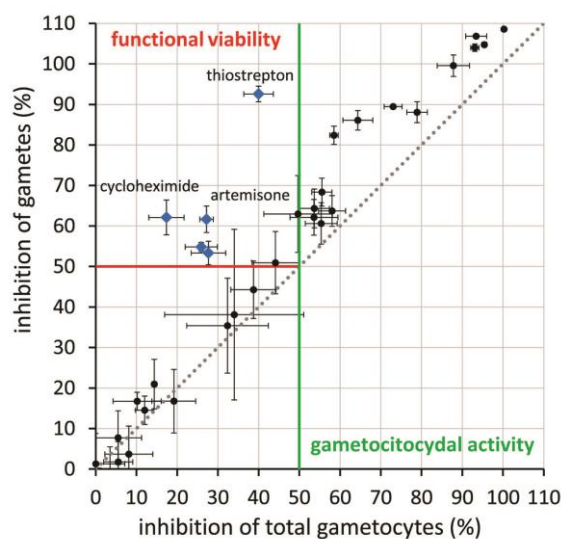


**Figure 5.** A. Activity of 39 current and candidate antimalarial drugs on mature *P. falciparum* 3D7A gametocytes and their rounding-up process. Scatterplot of activities of all compounds. Compounds were tested at 10 µM concentration. Red and green lines represent 50% activity thresholds for functional viability and total gametocytes readout, respectively. Five

compounds showing a higher inhibition on gametes than on total gametocytes are shown as blue squares (thiostrepton, cycloheximide, artemisone, atovaquone and primaquine).

Methylene blue represented the only compound from the panel tested which exhibited strong inhibitory activity against mature gametocytes, with an  $IC_{50}$  of  $0.17 \pm 0.04 \mu\text{M}$  for gametes and  $0.28 \pm 0.04 \mu\text{M}$  for total gametocytes, in agreement with previous reports (Ruecker et al., 2014; Bolscher et al., 2015; Duffy and Avery 2013; Miguel-Blanco et al., 2015; Adjalley et al., 2011; Sun et al., 2014; Spangenberg et al., 2013). Antimalarial drugs belonging to the 4-aminoquinoline, 8-aminoquinoline and antifolate classes have previously been shown to have poor late stage gametocytocidal activity *in vitro* (Ruecker et al., 2014; Bolscher et al., 2015; Duffy and Avery 2013; Miguel-Blanco et al., 2015; Spangenberg et al., 2013). As expected, our AO-GMT assay detected activity for most of these compounds only at concentrations above  $2.5 \mu\text{M}$ . Only naphthoquine displayed moderate  $IC_{50}$  values in similar ranges for gametes and total sexual forms of  $1.14 \pm 0.23$  and  $1.60 \pm 0.22 \mu\text{M}$ . Pyrimethamine, reported to selectively target male gametogenesis (Ruecker et al., 2014; Delves et al., 2013), was inactive in our female gamete assay. Among the aminoalcohols only mefloquine (both racemic and +RS) reduced gamete numbers, with an estimated  $IC_{50}$  of  $\sim 5 \mu\text{M}$ , similar to other recent reports on female gamete assays (Ruecker et al., 2014; Bolscher et al., Miguel-Blanco et al., 2015). No specific effect on rounding-up efficiency was observed. Of the seven antibiotic-like compounds tested, only thiostrepton and cycloheximide demonstrated activity against gamete formation. Thiostrepton was the most potent, with an  $IC_{50}$  of  $1.39 \pm 0.31 \mu\text{M}$  on rounded forms. Interestingly, upon treatment with the two compounds at  $10 \mu\text{M}$ , 92.6% and 62.1% gamete inhibition were observed, respectively, however total gametocyte counts were only slightly reduced, demonstrating that these compounds mainly affected the rounding-up process itself (thiostrepton RND  $EC_{50} \sim 1.97 \pm 0.16 \mu\text{M}$ ). Previous work has pointed out that endoperoxides have inhibitory effect on *P. falciparum* sexual stages, although with large assay-related differences (Ruecker et al., 2014; Bolscher et al., 2015; Duffy and Avery 2013; Miguel-Blanco et al., 2015; Spangenberg et al., 2013). In our 48h AO-GMT assay none of the five endoperoxides tested fully inhibited gametes or gametocytes at  $10 \mu\text{M}$ , however artemisone and artesunate reached 50% gamete inhibition at  $5 \mu\text{M}$ .

**Phenotypic Screening of the Medicines for Malaria Venture Malaria Box.** Medicines for Malaria Venture (MMV) has assembled a “Malaria Box” of 390 compounds with antimalarial activity against asexual blood stage parasites (Spangenberg et al., 2013) and made it freely available to the research community for use in the identification of new antimalarial targets and for screening against other parasite stages, as well as against unrelated organisms.

Given the amount of transmission blocking data rapidly accumulating on this focused library (Medicines for Malaria Venture 2015), the MMV Malaria Box was chosen to further validate the AO-GMT assay. Compounds were screened at  $5 \mu\text{M}$  with a 48 h incubation on stage V gametocytes. A strong linear correlation ( $r^2 = 0.957$ ) was observed between the inhibition values obtained by the two assay readouts, namely efficiency of gamete rounding up and total number of sexual forms after compound incubation, suggesting that a compound’s gametocytocidal activity is quantitatively described by either parameter. However, a scatter plot of the values from these readouts shows that with increasing

gametocytocidal activity an increasing number of compounds reduced gamete numbers more than total sexual forms (visible as outliers in Figure 6A). This observation confirms the higher sensitivity of the functional readout over the total count, as already observed with reference antimalarial drugs. The overall comparison of the two assay readouts also indicated that none of the Malaria Box compounds exclusively affected gamete formation without reducing total gametocyte numbers at the same time, i.e. no compound showed an activity similar to that of the CMPD-2 control.

Primary screening identified 37 hits with > 50% inhibitory activity on gamete formation. Of these, three compounds were immediately excluded from the active hit list due to autofluorescence or clearly visible artifacts detected upon inspection of the screening images.

The majority of the hits detected at the 5  $\mu$ M screening dose were gametocyte/gamete inhibitors (24 compounds, 71% of the total hits), while fewer compounds showed a gamete-biased activity (i.e. decreased the rounding-up efficiency to a higher degree than they reduced total parasite numbers; 10 hits, 29% of the total) (Figure 6B). Of the gamete-biased hits, MMV000760, MMV000787, MMV007907 and MMV396797 showed gamete vs. total gametocyte inhibitions of 69.0% vs. 38.8%, 66.2% vs. 42.0%, 77.1% vs. 48.1% and 88.1% vs. 51.9%, respectively. These results indicate that such compounds, while killing a proportion of the gametocyte population at 5  $\mu$ M, also cause sterilization of the remaining, otherwise viable population.

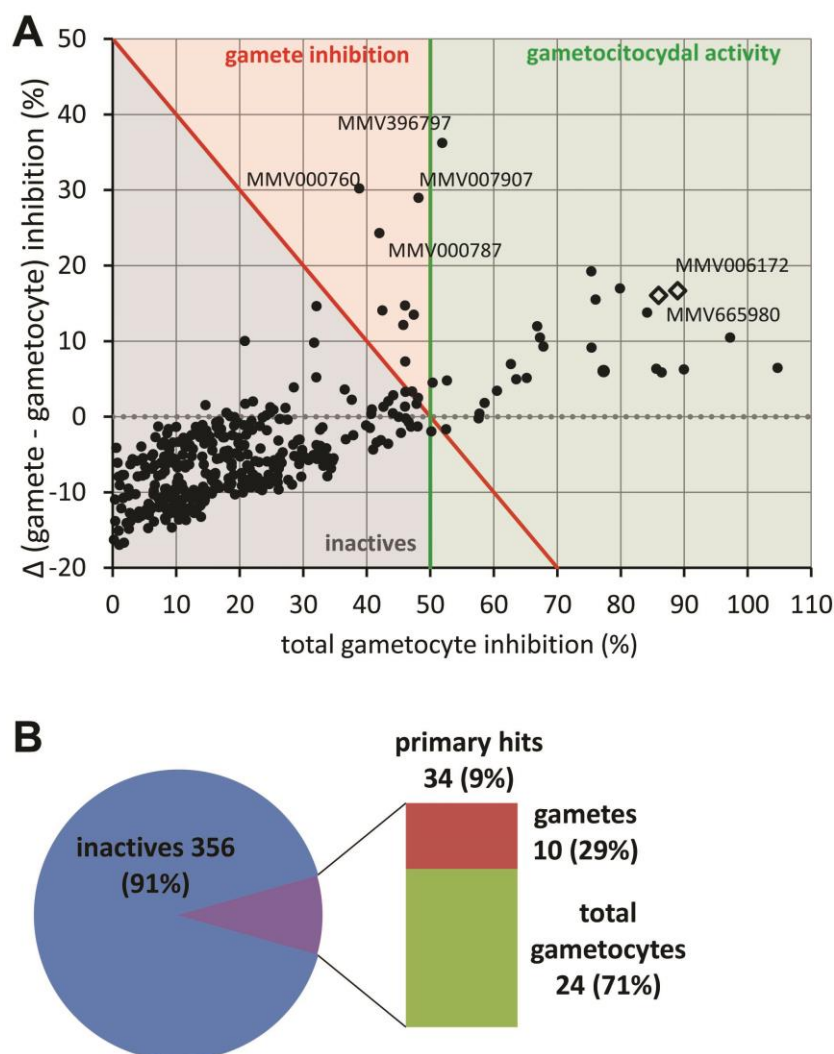


**Figure 6.** A. Scatterplot of activity on gamete formation and gametocytes for the entire MMV Malaria Box. Spots are total gametocyte percent inhibition values (X axis) and difference between gamete inhibition and corresponding X value (Y axis) of two biological replicates; red and green lines represent 50% activity thresholds for functional viability and total gametocytes readout, respectively. Dotted gray line indicates gamete and gametocyte inhibition equipotency. White diamonds correspond to the two compounds with the most potent gametocytocidal activity in subsequent dose-response tests. Compounds were screened at 5  $\mu\text{M}$  concentration. B. Overview of screening outcomes; see Supplementary Table S2 for the complete dataset.

The inhibitory activity of the twenty four anti-gametocyte/gamete hits was confirmed in follow-up dose-response experiments (Table 2), using fresh stock concentrates. The most potent inhibitors of gamete formation were MMV006172 and MMV665980, with submicromolar  $\text{IC}_{50}$  values of  $0.455 \pm 0.040 \mu\text{M}$  and  $0.809 \pm 0.100 \mu\text{M}$ , respectively. Twelve more confirmed hits, while still completely inhibiting gamete formation at the highest concentration of 5  $\mu\text{M}$ , showed a lower potency with  $\text{IC}_{50}$  values in the range of 1.1 – 2.9  $\mu\text{M}$ . The rest of the confirmed hits only reached inhibition values between 50% and 85% at the highest concentration, and therefore an  $\text{IC}_{50}$  value was not calculated.

| compound name | Set        | gametes                      |                      |                              |                      | total sexual forms           |                      |                      |       | proportion of rounding-up |       |
|---------------|------------|------------------------------|----------------------|------------------------------|----------------------|------------------------------|----------------------|----------------------|-------|---------------------------|-------|
|               |            | IC <sub>50</sub> (μM)‡ ± SEM | % inhibition † ± SEM | IC <sub>50</sub> (μM)‡ ± SEM | % inhibition † ± SEM | IC <sub>50</sub> (μM)‡ ± SEM | % inhibition † ± SEM | % of control † ± SEM | ± SEM |                           |       |
| MMV006172     | Probe-like | 0.455                        | 0.040                | 107.33                       | 1.67                 | 0.405                        | 0.090                | 103.30               | 0.52  | 15.12                     | 8.96  |
| MMV665980     | Probe-like | 0.809                        | 0.100                | 99.00                        | 2.52                 |                              |                      | 74.82                | 5.98  | 16.19                     | 2.75  |
| MMV019918     | Drug-like  | 1.063                        | 0.167 *              | 95.67                        | 2.03                 | 0.825                        | 0.123 *              | 88.47                | 1.82  | 44.99                     | 4.34  |
| MMV000448     | Probe-like | 1.095                        | 0.117 *              | 105.67                       | 1.45                 | 0.643                        | 0.121 *              | 104.08               | 0.58  | 30.45                     | 8.09  |
| MMV665941     | Probe-like | 1.553                        | 0.276 *              | 90.67                        | 1.86                 | 0.843                        | 0.265 *              | 90.84                | 3.05  | 74.57                     | 3.22  |
| MMV007591     | Probe-like | 1.731                        | 0.148                | 98.33                        | 4.37                 | 1.504                        | 0.269 *              | 98.32                | 5.68  | 53.14                     | 10.91 |
| MMV667491     | Probe-like | 2.354                        | 0.215 *              | 98.67                        | 2.33                 | 1.710                        | 0.427 *              | 93.21                | 1.03  | 43.33                     | 10.42 |
| MMV665830     | Probe-like | 2.469                        | 0.205 *              | 87.67                        | 3.84                 | 2.043                        | 0.403 *              | 84.31                | 2.55  | 65.52                     | 6.83  |
| MMV396797     | Drug-like  | 2.635                        | 0.113 *              | 93.00                        | 2.65                 |                              |                      | 69.86                | 5.88  | 29.36                     | 2.08  |
| MMV000787     | Probe-like | 2.693                        | 0.172 *              | 86.00                        | 0.58                 |                              |                      | 52.57                | 1.94  | 29.09                     | 0.47  |
| MMV019690     | Probe-like | 2.711                        | 0.124 *              | 93.33                        | 2.60                 | 2.252                        | 0.429 *              | 91.54                | 1.58  | 59.44                     | 9.76  |
| MMV006169     | Probe-like | 2.718                        | 0.271 *              | 88.67                        | 7.26                 | 1.710                        | 0.427 *              | 92.75                | 7.96  | 77.61                     | 8.75  |
| MMV019555     | Probe-like | 2.768                        | 0.176 *              | 89.33                        | 0.33                 |                              |                      | 79.63                | 1.75  | 46.61                     | 3.45  |
| MMV666597     | Probe-like | 2.926                        | 0.269 *              | 95.00                        | 6.56                 | 1.927                        | 0.422 *              | 94.67                | 4.37  | 63.97                     | 16.32 |
| MMV000788     | Drug-like  |                              |                      | 80.00                        | 2.52                 |                              |                      | 52.24                | 1.37  | 37.14                     | 2.12  |
| MMV396794     | Drug-like  |                              |                      | 80.00                        | 4.16                 |                              |                      | 77.83                | 1.82  | 68.81                     | 10.62 |
| MMV006429     | Drug-like  |                              |                      | 75.00                        | 8.62                 |                              |                      | 73.56                | 4.76  | 73.16                     | 12.17 |
| MMV665878     | Drug-like  |                              |                      | 74.67                        | 4.91                 |                              |                      | 68.77                | 2.38  | 65.04                     | 5.16  |
| MMV007907     | Drug-like  |                              |                      | 74.00                        | 5.13                 |                              |                      | 52.50                | 3.35  | 45.41                     | 5.62  |
| MMV000963     | Drug-like  |                              |                      | 73.33                        | 6.01                 |                              |                      | 73.44                | 5.51  | 75.53                     | 3.75  |
| MMV000662     | Drug-like  |                              |                      | 71.33                        | 7.54                 |                              |                      | 70.55                | 6.25  | 73.43                     | 6.57  |
| MMV396749     | Drug-like  |                              |                      | 57.00                        | 5.13                 |                              |                      | 55.22                | 2.36  | 77.27                     | 1.66  |
| MMV665969     | Probe-like |                              |                      | 56.33                        | 3.48                 |                              |                      | 51.39                | 1.20  | 74.19                     | 2.18  |
| MMV306025     | Drug-like  |                              |                      | 50.67                        | 12.33                |                              |                      | 55.53                | 9.26  | 83.65                     | 5.31  |

\* IC<sub>50</sub> value to be considered as approximate (maximal inhibition plateau not reached)

† activity at 5 μM shown

‡ IC<sub>50</sub> values were calculated only for compounds whose inhibition at 5 μM reached at least 85%

**Table 2.** Activity of the confirmed AO-GMT hits from the MMV Malaria Box on *P. falciparum* 3D7A gamete formation and gametocytes.

Five of the 8 confirmed hits with an IC<sub>50</sub> below an arbitrary threshold of 2.5 μM (MMV665980, MMV019918, MMV000448, MMV665941, MMV667491) have been recently shown to be efficient transmission blocking compounds in dose-response Standard Membrane Feeding Assay (SMFA) experiments (data available at ChEMBL: <http://www.ebi.ac.uk/chemblntd>). The remaining three compounds (MMV006172, MMV007591 and MMV005830) had never been previously tested by this assay. We therefore assessed the transmission reducing potential of these compounds by SMFA performed on mature gametocytes treated for 24 h at 1 and 10 μM. Microscopic analyses of midguts of mosquitoes in the vehicle control cages showed a baseline infection of 2.8 oocysts on average per mosquito. Analyses of luminescence signals showed that all compounds reduced oocyst intensities by more than 85% at 10 μM (Figure 7). The most potent hit in our assay, MMV006172, was also the most active in SMFA, resulting in a complete block of infection intensity and prevalence at 10 μM, and near complete block at 1 μM (99,8% inhibition of oocyst intensity and 98% inhibition of oocyst prevalence). Next, MMV007591 completely blocked infection intensity and prevalence at 10 μM and at 1 μM resulted in 80% and 62% reduction of intensity and prevalence, respectively. Finally, MMV005830 was the least effective, resulting in 85% and 69% reduction of intensity and prevalence, respectively, at the highest concentration tested of 10 μM. At 1 μM, no significant reduction was present. In conclusion, these results collectively demonstrate that all the AO-GMT assays confirmed hits tested in SMFA

possessed transmission blocking activity in the mosquito. The SMFA and the AO-GMT assay results are therefore in excellent agreement, and provided strong evidence for the predictive power of our phenotypic assay.

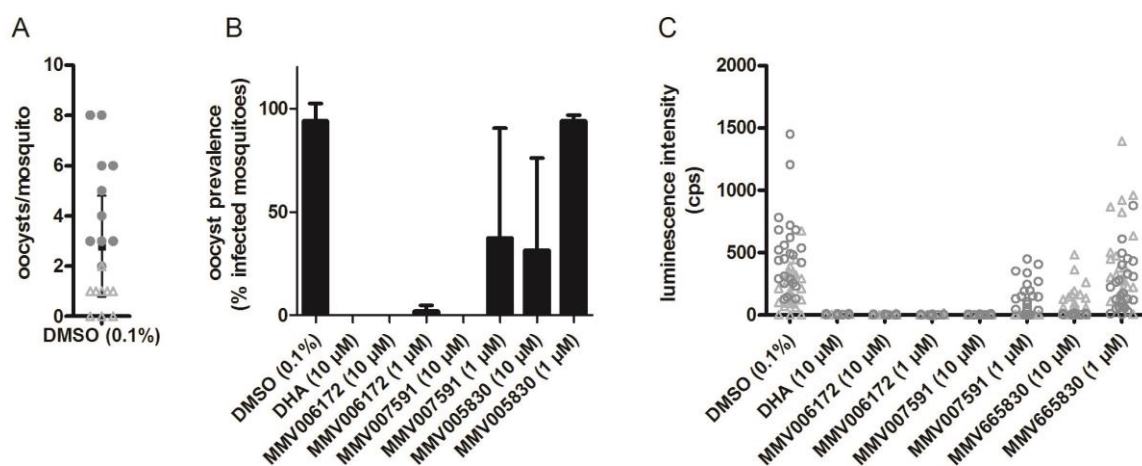


**Figure 7.** Transmission-reducing activity of three confirmed MMV Malaria Box hits. (A) SMFA showed a baseline mean oocyst density of 2.8 mosquitoes per midgut. (B) Luminescence-based assessment of oocyst prevalence (% infected mosquitoes). The figure shows average prevalence determined from two independent feeds. Error bars indicate standard deviations. (C) Luminescence-based assessment of oocyst intensity. The figure shows luminescence counts in individual mosquitoes from replicate feeds (open circles and triangles). Lines and error bars indicate the average and standard error of the mean.

## Discussion

This study addressed the need for high throughput assays (HTS) to predict the effect of compounds on the mature gametocyte stages of *P. falciparum* to identify molecules able to block the transmission of the parasite from infected humans to mosquitoes. Stage V gametocytes persist in the circulation for several weeks and play an essential role for the continuation of the *P. falciparum* parasite life cycle and thus malaria, making them an attractive drug target. However, the apparently quiescent nature of these parasites has proven to be the main obstacle in the development of assays capable of reliably monitoring their infectivity, thus leaving the SMFA approach as the only functional assay to evaluate compound transmission blocking activity. Although the throughput of this assay has been improved by use of luminescent reporter parasites (Stone et al., 2014), its capacity is still too limited for screening of very large compound libraries. Therefore, there is a need for assays with higher throughput that can preselect compounds for subsequent validation in the SMFA.

As the mature gametocyte is highly responsive to environmental changes, ready to suddenly transform into a gamete, we used the first event in gametocyte activation (the “rounding up”) as the most sensitive and fastest phenotypic readout of our assay, which in addition makes it specific to measure the functional viability of the mature gametocytes. Our results indicate that a high level of gametocyte activation is efficiently and reproducibly obtained from highly synchronous, mature stage V gametocytes in 384 well plates.

Solely based on the ability to count and distinguish elongated gametocytes and spherical gametes, our imaging based assay has been validated using reference antimalarial drugs and a pilot screen of a small focused library (390 compounds MMV Malaria Box). The protocol, initially performed on GFP-expressing transgenic parasites, was adapted to assess mature gametocytes of any genetic background by labelling the parasites with the inexpensive AO stain. The imaging protocol and scripts specific for this assay were developed for use on a confocal high-content imaging system, in conjunction with high-throughput liquid handling equipment, to obtain a HTS assay. This approach extends the use of the high content HTS approach recently proposed for asexual (Duffy and Avery 2012) and sexual parasites (Duffy and Avery 2013; Miguel-Blanco et al., 2015) taking advantage of the unique morphology of *P. falciparum* gametocytes and gametes.

In the HTS adaptation of the AO staining assay, the time elapsing between gametocyte activation and automated image acquisition is of the order of 1-2 h. This makes the AO-GCT assay particularly suited to monitor the viability of female gametocytes, as the activated male gametocytes maintain a spherical shape only for about 10 minutes (Sinden et al., 1978), after which they quickly progress to divide into flagellated microgametes, undetected by our assay. As the sex ratio in *Plasmodium* 3D7A gametocytes is strongly female biased, with male gametocytes representing about 1/7 of the total gametocytes (Schwank et al., 2010), the AO-GMT assay is nevertheless reliably monitoring compound activity on the vast majority of the gametocyte population. The assay is however versatile as the protocol can accommodate a cell fixation step after 10 minutes from gamete activation, which, although not practical in HTS of large chemical libraries, enables the imaging of all (male and female) round forms in follow-up experiments on small number of compounds of interest. The comparison of the AO-GMT assay with the two published assay approaches monitoring female gamete formation (Ruecker et al., 2014; Bolscher et al., 2015; Miguel-Blanco et al., 2015) indicates that our assay does not require expensive detection reagents such as labelled antibodies and/or chemoluminescent immunoassay detection kits, neither the long incubation times after gamete activation (16 to 24 h), necessary for those reagents to achieve satisfactory fluorescence intensity on the gamete surface (Table 3). Importantly, image acquisition within a short time after the induction of gametogenesis ensures that the phenotypic readout truly reflects compound effects on the mature gametocyte, rather than possible confounding effects on female gamete viability. In addition, this is the first assay with the capability to simultaneously count elongated gametocytes and activated gametocytes / female gametes in the same well. Our assay can therefore uniquely distinguish between sterilizing compounds that inhibit gametocyte rounding-up without affecting total sexual forms and gametocytocidal compounds, as well as partial, dose-related effects (Figure 4). This feature can contribute to the identification of sterilizing compounds with arguably different mechanisms of action compared to gametocytocidal compounds. So far, however, none of the tested antimalarial compounds possessed a female sterilizing activity devoid of inhibition of total gametocytes. Moreover, we found that total gametocytes count is an equivalent predictor of compound activity as gamete formation.

| Assay                          | AO-GMT assay                      | GFP-GMT assay     | female assay <sup>14</sup> | dual M/F assay <sup>13</sup> | female assay <sup>20</sup> |
|--------------------------------|-----------------------------------|-------------------|----------------------------|------------------------------|----------------------------|
| reagent for readout            | Acridine Orange                   | GFP               | conjugated Mabs            | conjugated Mabs              | conjugated Mabs            |
| time after compound incubation | 2h                                | 10min             | 16h                        | 20min + 24h                  | 24h                        |
| plate format                   | 384 wells                         | 384 wells         | 384 wells                  | 96 wells                     | 384 wells                  |
| gcytes/well                    | $4 \times 10^4$                   | $4 \times 10^4$   | $2 \times 10^5$            | NA                           | $8 \times 10^3$            |
| readout(s)                     | gametocytes and female gametes    | spherical gametes | female gametes             | male and female gametes      | female gametes             |
| z'                             | 0.69 (gametes) 0.66 (gametocytes) | 0.76              | 0.72                       | 0.43 (male) 0.36 (female)    | 0.7                        |

**Table 3.** Comparison of existing assay approaches and parameters with our AO-GMT (confocal microscopy-based, HTS) and GFP-GT (light microscopy-based, proof of principle) assays.

Overall, the protocol strength is the use of a straightforward, rapid and fully automated HTS approach. After a single magnetic purification step on day 4 of gametocytogenesis, ~40,000 parasites/well are seeded and incubated with compounds in 384-wells imaging plates for 48h, followed by exposure to XA and AO in a single automated step without washes, and by automated readout acquisition after only 2h incubation at room temperature. The high-content imaging-based assay has the advantage that the fluorescent microscopy output is a direct measurement of compound effect on individual gametes/gametocytes and not of the total contents of a well, minimizing the interference of background effects. Moreover, the fluorescence signal is specific of parasites, as uninfected erythrocytes lack of nucleic acids reactive to the fluorescent marker. Finally, the possibility to store and review the images provides an important quality control and allows for the quick elimination of false positives/artifacts. At our optimized AO-GMT assay conditions, the current cost of testing a 20,000 compound library is comparable or lower to that of the other gametocytocidal assays available at Griffith, and the current screening capability is ~25,000 compounds per week.

The screening of the MMV Malaria Box with the AO-GMT assay identified 14 active compounds that showed an  $IC_{50} < 3 \mu M$ . Eight of the most potent compounds were tested in SMFA for validation of their transmission reducing activity, and all of them proved to be active transmission blocking compounds. This confirmation provided solid evidence for the high predictive power of the AO-GMT readout. The two top ranking compounds exhibited submicromolar gametocytocidal  $IC_{50}$ . The most potent, MMV006172, with  $IC_{50} = 0.455 \mu M$  in our assay, had been previously identified as a late stage gametocytocidal compound with  $IC_{50}$  range between 0.420 and 2.6  $\mu M$  (Duffy and Avery 2013; Sanders et al., 2014; Sun et al., 2014; Bowman et al., 2014; D'Alessandro et al., 2015). Its transmission blocking activity was confirmed in our SMFA. Interestingly, this compound only caused a partial inhibition at 1  $\mu M$  in a previous female gamete formation assay (Ruecker et al., 2014), in which however a different assay format and compound exposure time were used. The observation that the longer incubation time in our assay leads to a complete female gametocytocidal effect is in keeping with previous observations



that presumed sex-specific effects relate to differences in kinetics rather than an absolute sex preference of gametocytocidal compound activity (Bolscher et al., 2015).

The second most potent hit, MMV665980, ( $IC_{50} = 0.809 \mu\text{M}$ ) had not been previously identified as a late stage gametocytocidal hit, however it was recently reported to reversibly inhibit (sterilize) male and female mature gametocytes, with  $IC_{50} = 0.614 \mu\text{M}$  against female gametes in carry-over format (Ruecker et al., 2014). Also in this case transmission-blocking activity was verified in SMFA ( $IC_{50} = 1.71 \mu\text{M}$ ). Three more compounds showing gametocytocidal activity below  $2 \mu\text{M}$  in our assay, namely MMV019918, MMV000448 and MMV665941, were previously identified in other gamete (Ruecker et al., 2014) and gametocyte assays (Duffy and Avery 2013; Sun et al., 2014), although with a wide range of potencies, and all confirmed to be transmission-blocking in SMFA. In conclusion, our assay identified and confirmed the activity of all previously reported female gamete inhibitors from the MMV Malaria Box, and all hits from our assay that underwent SMFA validation confirmed their transmission-reducing activity in the mosquito without false positive hits.

Our work showed that it is possible to combine a functional readout on a cell type, the mature *P. falciparum* gametocytes, whose quiescent metabolism makes it an elusive drug target, with a practicable, cheap, fast and fully automated HTS protocol.

Our assay significantly accelerates the possibility to screen very large libraries of compounds to identify quality hits with very high likelihood of showing transmission blocking activity in the gold standard mosquito infectivity assay.

### Authorship statement

In this project I produced and characterized the 3D7-PFL1675c/ULG8 transgenic line, used for the establishment of the “rounding-up” assay.

### References

Adjalley, S.H., Johnston, G.L., Li, T., Eastman, R.T., Eklund, E.H., Eappen, A.G., et al. (2011). Quantitative assessment of *Plasmodium falciparum* sexual development reveals potent transmission-blocking activity by methylene blue. *Proc Natl Acad Sci U S A* 108, E1214-23. doi: 10.1073/pnas.1112037108.

Billker, O., Lindo, V., Panico, M., Etienne, A.E., Paxton, T., Dell, A., Rogers, M., Sinden, R.E., and Morris, H.R. (1998). Identification of xanthurenic acid as the putative inducer of malaria development in the mosquito. *Nature*. 392, 289-292.

Bolscher, J. M., Koolen, K.M., van Gemert, G.J., van de Vegte-Bolmer, M.G., Bousema, T., Leroy, D., Sauerwein, R.W., and Dechering, K.J. (2015). A combination of new screening assays for prioritization of transmission-blocking antimalarials reveals distinct dynamics of marketed and experimental drugs. *J Antimicrob Chemother*. 70, 1357-66.

Bousema, T., Okell, L., Shekalaghe, S., Griffin, J.T., Omar, S., Sawa, P., Sutherland, C., Sauerwein, R., Ghani, A.C., and Drakeley, C. (2010). Revisiting the circulation time of *Plasmodium falciparum*

gametocytes: molecular detection methods to estimate the duration of gametocyte carriage and the effect of gametocytocidal drugs. *Malar J.* 9, 136.

Bousema, T., and Drakeley, C. (2011). Epidemiology and infectivity of *Plasmodium falciparum* and *Plasmodium vivax* gametocytes in relation to malaria control and elimination. *Clinical microbiology reviews* 24, 377-410.

Bowman, J. D., Merino, E.F., Brooks, C.F., Striepen, B., Carlier, P.R., and Cassera, M.B. (2014). Antiapicoplast and gametocytocidal screening to identify the mechanisms of action of compounds within the malaria box. *Antimicrobial agents and chemotherapy.* 58, 811-819.

Skinner-Adams, T.S., Gardiner, D.L., and Trenholme KR. (2013). *Plasmodium falciparum* gametocytes: with a view to a kill. *Parasitology.* 140, 1718-34.

Cevenini, L., Camarda, G., Michelini, E., Siciliano, G., Calabretta, M.M., Bona, R., et al. (2014). Multicolor bioluminescence boosts malaria research: quantitative dual-color assay and single-cell imaging in *Plasmodium falciparum* parasites. *Anal Chem.* 86, 8814-21. doi: 10.1021/ac502098w.

Chevalley, S., Coste, A., Lopez, A., Pipy, B., and Valentin, A. (2010). Flow cytometry for the evaluation of anti-plasmodial activity of drugs on *Plasmodium falciparum* gametocytes. *Malar J* 9, 49.

D'Alessandro, S., Silvestrini, F., Dechering, K., Corbett, Y., Parapini, S., Timmerman, M., Galastri, L., Basilico, N., Sauerwein, R., Alano, P., and Taramelli, D. (2013). A *Plasmodium falciparum* screening assay for anti-gametocyte drugs based on parasite lactate dehydrogenase detection. *J. Antimicrob. Chemother.* 68, 2048-2058.

D'Alessandro, S., Corbett, Y., Ilboudo, D.P., Misiano, P., Dahiya, N., Abay, S.M., Habluetzel, A., Grande, R., Gismondo, M.R., Dechering, K.J., Koolen, K.M., Sauerwein, R.W., Taramelli, D., Basilico, N., and Parapini, S. (2015). Salinomycin and other ionophores as new class of antimalarial drugs with transmission blocking activity. *Antimicrob Agents Chemother.* 59, 5135-44.

D'Alessandro, S. et al. (2015). *ASTMH annual meeting.* 128.

Delves, M., Plouffe, D., Scheurer, C., Meister, S., Wittlin, S., Winzeler, E.A., Sinden, R.E., and Leroy, D. (2012). The activities of current antimalarial drugs on the life cycle stages of *Plasmodium*: a comparative study with human and rodent parasites. *PLoS Med.* 9, e1001169.

Delves, M., Ruecker, A., Straschil, U., Lelièvre, J., Marques, S., López-Barragán, M.J., Herreros, E., and Sinden, R.E. (2013). Male and female *Plasmodium falciparum* mature gametocytes show different responses to antimalarial drugs. *Antimicrobial agents and chemotherapy.* 57, 3268-3274.

Dondorp, A. M., Nosten, F., Yi, P., Das, D., Phyo, A.P., Tarning, J., Lwin, K.M., Ariey, F., Hanpithakpong, W., Lee, S.J., Ringwald, P., Silamut, K., Imwong, M., Chotivanich, K., Lim, P., Herdman, T., An, S.S., Yeung, S., Singhasivanon, P., Day, N.P., Lindegardh, N., Socheat, D., and White, N.J. (2009). Artemisinin resistance in *Plasmodium falciparum* malaria. *N Engl J Med.* 361, 455-467.

Duffy, S., and Avery, V. M. (2012). Development and optimization of a novel 384-well anti-malarial imaging assay validated for high-throughput screening. *The American journal of tropical medicine and hygiene.* 86, 84-92.

Duffy, S., and Avery, V. M. (2013). Identification of inhibitors of *Plasmodium falciparum* gametocyte development. *Malar J.* 12, 408.

Eichner, M., Diebner, H.H., Molineaux, L., Collins, W.E., Jeffery, G.M., and Dietz, K. (2001). Genesis, sequestration and survival of *Plasmodium falciparum* gametocytes: parameter estimates from fitting a model to malariatherapy data. *Transactions of the Royal Society of Tropical Medicine and Hygiene.* 95, 497-501.

Gebru, T., Mordmuller, B., and Held, J. (2014). Effect of fluorescent dyes on in vitro-differentiated, late-stage *Plasmodium falciparum* gametocytes. *Antimicrobial agents and chemotherapy.* 58, 7398-7404.

Joanny, F., Held, J., and Mordmuller, B. (2012). In vitro activity of fluorescent dyes against asexual blood stages of *Plasmodium falciparum*. *Antimicrobial agents and chemotherapy.* 56, 5982-5985.

Karunamoorthi, K. (2011). Vector control: a cornerstone in the malaria elimination campaign. *Clin Microbiol Infect.* 17, 1608-1616.

Lelievre, J. Almela, M.J., Lozano, S., Miguel, C., Franco, V., Leroy, D., and Herreros E. (2012). Activity of clinically relevant antimalarial drugs on *Plasmodium falciparum* mature gametocytes in an ATP bioluminescence "transmission blocking" assay. *PLoS One.* 7, e35019.

Lucantoni, L., Duffy, S., Adjalley, S. H., Fidock, D. A., and Avery, V. M. (2013). Identification of MMV malaria box inhibitors of *Plasmodium falciparum* early-stage gametocytes using a luciferase-based high-throughput assay. *Antimicrobial agents and chemotherapy.* 57.

McRobert, L., Taylor, C.J., Deng, W., Fivelman, Q.L., Cummings, R.M., Polley, S.D., Billker, O., and Baker, D.A. (2008). Gametogenesis in malaria parasites is mediated by the cGMP-dependent protein kinase. *PLoS Biol.* 6, e139.

Medicines For Malaria Venture (MMV). *Malaria Box results*, <<http://www.mmv.org/research-development/malaria-box-results>> (2015).

Miguel-Blanco, C. Lelièvre, J., Delves, M.J., Bardera, A.I., Presa, J.L., López-Barragán, M.J., Ruecker, A., Marques, S., Sinden, R.E., and Herreros, E. (2015). Imaging-based HTS assay to identify new molecules with transmission-blocking potential against *P. falciparum* female gamete formation. *Antimicrobial agents and chemotherapy*. 59, 3298-305.

Mok, S., Ashley, E.A., Ferreira, P.E., Zhu, L., Lin, Z., Yeo, T., Chotivanich, K., Imwong, M., Pukrittayakamee, S., Dhorda, M., Nguon, C., Lim, P., Amaratunga, C., Suon, S., Hien, T.T., Htut, Y., Faiz, M.A., Onyamboko, M.A., Mayxay, M., Newton, P.N., Tripura, R., Woodrow, C.J., Miotto, O., Kwiatkowski, D.P., Nosten, F., Day, N.P., Preiser, P.R., White, N.J., Dondorp, A.M., Fairhurst, R.M., and Bozdech, Z. (2015). Drug resistance. Population transcriptomics of human malaria parasites reveals the mechanism of artemisinin resistance. *Science*. 347, 431-435.

Peatey, C. L., Skinner-Adams, T.S., Dixon, M.W., McCarthy, J.S., Gardiner, D.L., and Trenholme, K.R. (2009). Effect of antimalarial drugs on *Plasmodium falciparum* gametocytes. *J Infect Dis*. 200, 1518-1521.

Petersen, I., Eastman, R., and Lanzer, M. (2011). Drug-resistant malaria: molecular mechanisms and implications for public health. *FEBS Lett*. 585, 1551-1562.

Ruecker, A., Mathias, D.K., Straschil, U., Churcher, T.S., Dinglasan, R.R., Leroy, D., Sinden, R.E., and Delves, M.J. (2014). A male and female gametocyte functional viability assay to identify biologically relevant malaria transmission-blocking drugs. *Antimicrobial agents and chemotherapy*. 58, 7292-7302.

Sanders, N. G., Sullivan, D. J., Mlambo, G., Dimopoulos, G., and Tripathi, A. K. (2014). Gametocytocidal screen identifies novel chemical classes with *Plasmodium falciparum* transmission blocking activity. *PLoS One*. 9, e105817.

Schwank, S., Sutherland, C. J., and Drakeley, C. J. (2010). Promiscuous expression of alpha-tubulin II in maturing male and female *Plasmodium falciparum* gametocytes. *PLoS One*. 5, e14470.

Sinden, R. E., Canning, E. U., Bray, R. S., and Smalley, M. E. (1978). Gametocyte and gamete development in *Plasmodium falciparum*. *Proceedings of the Royal Society of London. Series B, Biological sciences*. 201, 375-399.

Spangenberg, T., Burrows, J.N., Kowalczyk, P., McDonald, S., Wells, T.N., and Willis, P. (2013). The open access malaria box: a drug discovery catalyst for neglected diseases. *PLoS One*. 8, e62906.

Stone, W.J., Churcher, T.S., Graumans, W., van Gemert, G.J., Vos, M.W., Lanke, K.H., et al. (2014). A Scalable Assessment of *Plasmodium falciparum* Transmission in the Standard Membrane-Feeding Assay, Using Transgenic Parasites Expressing Green Fluorescent Protein-Luciferase. *J Infect Dis*. 210, 1456-63.

Sun, W., Tanaka, T.Q., Magle, C.T., Huang, W., Southall, N., Huang, R., Dehdashti, S.J., McKew, J.C., Williamson, K.C., and Zheng, W. (2014). Chemical signatures and new drug targets for gametocytocidal drug development. *Scientific reports*. 4, 3743.

Tanaka, T. Q., and Williamson, K. C. (2011). A malaria gametocytocidal assay using oxidoreduction indicator, alamarBlue. *Mol Biochem Parasitol*. 177, 160-163.

Taylor, C. J., McRobert, L., and Baker, D. A. (2008). Disruption of a *Plasmodium falciparum* cyclic nucleotide phosphodiesterase gene causes aberrant gametogenesis. *Mol Microbiol*. 69, 110-118.

Taylor, H. M., McRobert, L., Grainger, M., Sicard, A., Dluzewski, A.R., Hopp, C.S., Holder, A.A., and Baker, D.A. (2010). The malaria parasite cyclic GMP-dependent protein kinase plays a central role in blood-stage schizogony. *Eukaryot Cell*. 9, 37-45.

Trager, W., and Jensen, J. B. (1976). Human malaria parasites in continuous culture. *Science*. 193, 673-675.

Wang, Z., Liu, M., Liang, X., Siriwat, S., Li, X., Chen, X., Parker, D.M., Miao, J., and Cui, L. (2014). A flow cytometry-based quantitative drug sensitivity assay for all *Plasmodium falciparum* gametocyte stages. *PLoS One*. 9, e93825.

WHO. *World Malaria Report*,  
<[http://www.who.int/malaria/publications/world\\_malaria\\_report\\_2014/report/en/](http://www.who.int/malaria/publications/world_malaria_report_2014/report/en/)> (2014).

Zhang, J. H., Chung, T. D., and Oldenburg, K. R. (1999). A simple statistical parameter for use in evaluation and validation of high throughput screening assays. *Journal of biomolecular screening*. 4, 67-73.

# Enlightening the malaria parasite life cycle: bioluminescent Plasmodium in fundamental and applied research

Giulia Siciliano and Pietro Alano<sup>1</sup>

<sup>1</sup> Dipartimento di Malattie Infettive, Parassitarie ed Immunomediate, Istituto Superiore di Sanità, Rome, Italy

This work is published in *Frontiers in Microbiology*. 2015 May 11;6:391. doi: 10.3389/fmicb.2015.00391. Review.

**Abstract:** The unicellular protozoan parasites of the genus *Plasmodium* impose on human health worldwide the enormous burden of malaria. The possibility to genetically modify several species of malaria parasites represented a major advance in the possibility to elucidate their biology and is now turning laboratory lines of transgenic *Plasmodium* into precious weapons to fight malaria. Amongst the various genetically modified plasmodia, transgenic parasite lines expressing bioluminescent reporters have been essential to unveil mechanisms of parasite gene expression and to develop *in vivo* imaging approaches in mouse malaria models. Mainly the human malaria parasite *Plasmodium falciparum* and the rodent parasite *Plasmodium berghei* have been engineered to express bioluminescent reporters in almost all the developmental stages of the parasite along its complex life cycle between the insect and the vertebrate hosts. *Plasmodium* lines expressing conventional and improved luciferase reporters are now gaining a central role to develop cell based assays in the much needed search of new antimalarial drugs and to open innovative approaches for both fundamental and applied research in malaria.

## 1. Introduction

Half of the world population is at risk of malaria (WHO World Malaria Report 2013), the most common and severe parasitic mosquito-borne disease (White et al., 2014). Five species of the protozoan genus *Plasmodium* infect humans, with *Plasmodium falciparum* and *Plasmodium vivax* causing over 200 million cases/year and *P. falciparum* inflicting virtually all the 6-700,000 annual deaths (2013) recorded mainly in children of Sub-Saharan Africa.

The malaria parasite exhibits a complex life cycle involving an *Anopheles* mosquito and a vertebrate host [Figure 1]. When an infected female mosquito bites a human, the *Plasmodium* sporozoites travel to the liver and invade hepatocytes, where parasites replicate as hepatic schizonts until several thousand merozoites are produced and released in the bloodstream. In *P. vivax*, but not in *P. falciparum*, some liver parasites remain instead quiescent (hypnozoites), resuming replication and infection after several weeks or months. Upon erythrocyte invasion in the bloodstream *Plasmodium* parasites undergo asexual replication forming mature schizonts whose rupture releases merozoites that invade new erythrocytes. Some blood stage parasites differentiate instead into male and female gametocytes that, when ingested in the mosquito blood meal, are activated to produce gametes. Gamete fusion in the insect midgut produces a zygote which develops into a motile ookinete, traversing the gut wall and transforming into an oocyst, where thousands of sporozoites are produced. The life cycle is closed when sporozoites, migrated from the ruptured oocyst to the mosquito salivary glands, are injected in a new human host by the insect bite.

The pathogenesis of malaria is caused by the asexual blood stages. In the clinical manifestations of *P. falciparum* malaria, the ability of parasites to sequester in the microvasculature of several organs, including the brain, is a major cause of disease severity and of a fatal outcome (Milner et al., 2014; Miller et al., 2002). Consequently, the need to cure symptomatic patients traditionally drove efforts towards finding drugs targeting the asexual blood stage parasites, often underestimating the importance of eliminating also the sporozoite and gametocyte transmission stages or, in *P. vivax*, the hypnozoites. The recent concerning reports from South East Asia of a decreased sensitivity of some *P. falciparum* infections to frontline combination therapies based on artemisinin derivatives is now calling for renewed efforts to address this emergency in the frame of a global strategy to control malaria and eventually eradicate this deadly parasite.

It is possible to cultivate all asexual and sexual blood stages of *P. falciparum* *in vitro*, unlike *P. vivax*. Plasmodium species infecting rodents have been also intensely studied as mouse models of aspects of malaria, with *Plasmodium berghei* particularly exploited for its amenability to genetic manipulation. In contrast, transgenesis technology has been comparatively more troublesome in *P. falciparum*. This review aims to highlight the importance of Plasmodium transgenic parasites, particularly those engineered with bioluminescent reporters, both in the study of the fundamental biology of Plasmodium and in developing effective antimalarial treatments

Luciferase enzymes catalyze the light-producing chemical reactions of bioluminescent organisms, in which a luminogenic substrate (e.g. D-luciferin) is oxidized in the presence of ATP, yielding photons. These can be accurately measured by a luminometer with a sensitivity and a virtual absence of background that made bioluminescent reporters potent and versatile tools in biology (Smale, 2010). Luciferases hold a special place in the history of Plasmodium transgenesis: the first plasmid construct to be successfully transfected in malaria parasites contained a firefly (*Photynus pyralis*) luciferase gene whose expression, driven by the promoter of a parasite sexual stage-specific gene, was measured in ookinetes of the bird parasite *Plasmodium gallinaceum* (Goonewardene et al., 1993). Subsequently, luciferase reporters have been used to optimize transfection techniques in Plasmodium parasites (Hasenkamp et al., 2012; Epp et al., 2008), including the introduction of the luciferase from the sea pansy *Renilla reniformis*, where use of different substrates (D-luciferin and coelenterazine) enabled simultaneous detection of the two parasite produced reporters (Militello & Wirth 2003; Helm et al., 2010). Since the 1990's, with the stable genetic transformation of different species of Plasmodium (Waters et al., 1997), luciferase reporter genes greatly contributed to elucidate key aspects of malaria infection, from the parasite cellular biology, protein trafficking, gene function and drug resistance, in several developmental stages throughout the Plasmodium life cycle [Figure 1].

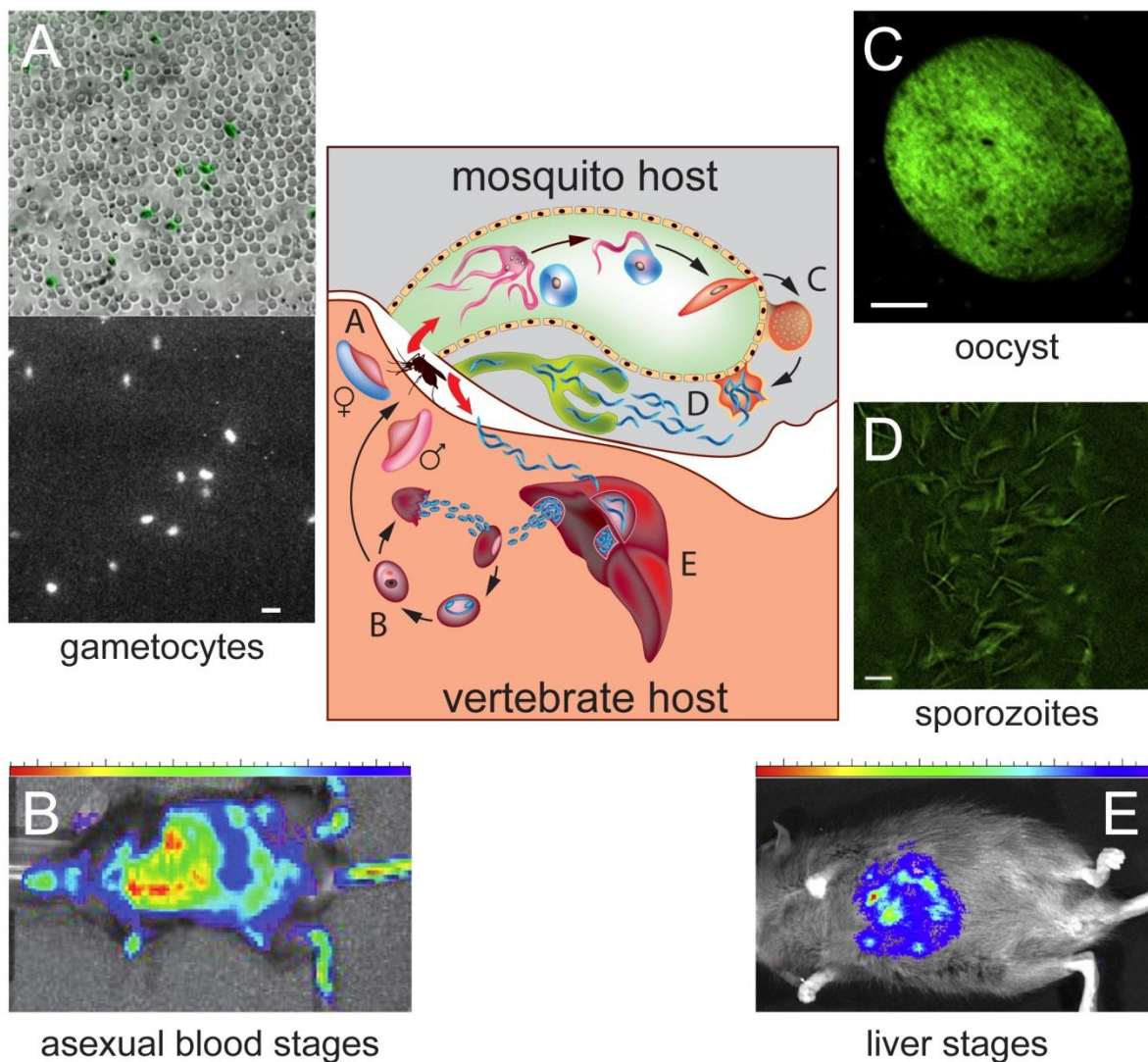


**Figure 1. Transgenic bioluminescent malaria parasites at different stages of their development in the vertebrate and mosquito hosts.** The central diagram represents the *Plasmodium* life cycle, showing the progression through the developmental stages of the parasites in the mosquito vector and in the vertebrate host. A) Bioluminescence imaging of individual *P. falciparum* gametocytes expressing a click beetle luciferase under a sexual stage-specific promoter. The bright field image shows immobilized gametocytes, highlighted in green, amongst uninfected erythrocytes; the dark field shows the bioluminescence signal of the gametocytes incubated with D-luciferin. Magnification bar: 15 $\mu$ m. (Adapted from Cevenini et al., 2014). B) Bioluminescence imaging of a mouse infected with asexual *P. berghei* parasites expressing a firefly luciferase-GFP fusion. Heatmap of the bioluminescent signal identifies the sites of accumulation of the parasites (Reproduced with permission from Claser et al., 2011). C) Fluorescence of a firefly luciferase-GFP fusion protein expressed in *P. falciparum* sporozoites contained in a oocyst and D) obtained from the dissection of infected mosquito salivary glands. Magnification bar: 5 $\mu$ m. E) *In vivo* bioluminescent signal obtained by transgenic *P. falciparum* liver stage parasites developing in the chimeric liver of a humanized mouse (C, D, E are reproduced with permission from Vaughan et al., 2014).



## **2. The Plasmodium life cycle marked by bioluminescent parasite developmental stages**

### **2.1 Plasmodium mosquito stages**

Parasite sexual stage development in the mosquito vector is crucial for the transmission of *Plasmodium*, and elucidating the biology of this process may therefore lead to design novel malaria transmission-blocking strategies. Some studies with bioluminescent parasites highlighted the importance of post-transcriptional regulation acting on stability and translation of several mRNAs, including those encoding major proteins of the gamete and ookinete surface (Mair et al., 2006). Assays with luciferase reporters were for instance fundamental to identify regulatory elements in the transcripts of the P25 and P28 surface proteins of *P. gallinaceum* and *P. falciparum* (Golightly et al., 2000; Oguariri et al., 2006).

Plasmodium parasites expressing luciferases also improved tool development for applied studies. A powerful bioassay to determine parasite ability to infect mosquitoes is based on feeding cultured Plasmodium gametocytes to mosquitoes, and it is used to measure effect of transmission blocking drugs or antibodies. This assay is however technically demanding and time consuming as the resulting oocysts need to be individually counted in dissected insects. After improvements by using *P. berghei* parasites expressing a Green Fluorescent Protein (GFP) in mosquito stages (Delves and Sinden, 2010), a transgenic line of the human parasite *P. falciparum* line expressing the firefly luciferase in oocysts was developed. In the resulting luminescence-based Standard Membrane Feeding Assay (SMFA) the mean luminescence intensity of individual and pooled mosquitoes accurately quantified mean oocyst intensity, eliminating the need for mosquito dissection and putting the basis for significant SMFA scalability (Stone et al., 2014).

Towards the end of parasite development in the mosquito, the sporozoites produced in the oocyst migrate to the insect salivary glands. Number of salivary gland sporozoites, the only mosquito stages infectious to a mammalian host, is an important index of Plasmodium mosquito development. The construction of a *P. berghei* line where a GFP-luciferase fusion is specifically expressed in sporozoites enabled establishment of a simple and fast assay of sporozoite loads from whole mosquitoes (Ramakrishnan et al., 2012).

### **2.2 Transmission from mosquitoes: sporozoites and liver stages**

Plasmodium sporozoites injected from an infected mosquito to a human or rodent host start their intracellular development into the liver hepatocytes. This clinically silent stage is the target for prophylactic or vaccine strategies, particularly against *P. vivax* long lasting hypnozoites.

Plasmodium liver stage development has been poorly explored compared to that of blood stages partly because the *in vivo* and *in vitro* analyses, respectively in mouse models and in cultured liver cells, are constrained by the necessity to sacrifice high numbers of mice or by inefficiency of sporozoite infection of cultured liver cells. Transgenic luciferase-expressing sporozoites improved detection strategies introducing bioluminescence imaging (BLI) and *in vivo* imaging system (IVIS) in the analysis of parasite liver stage development in live mice and in cultured hepatocytes. Real-time bioluminescence

imaging requires injection of the luciferin substrate in the mouse or in the dissected organ and an intensified charge-coupled photon counting video camera to measure photon emission (Franke-Fayard et al., 2006; Braks et al., 2013). BLI and IVIS using firefly or sea pansy luciferases have been used for real-time, live monitoring of the progression of rodent parasitic infection in the whole animal or in specific organs (Ploemen et al., 2009; Annoura et al., 2013; Manzoni et al., 2014) and to test activity of drugs targeting liver stage infection, using *P. yoelii* and *P. berghei* transgenic sporozoites in human liver HepG2 or Huh-7 cells and in whole mice (Mwakingwe et al., 2009; Ramalhete et al., 2011; Derbyshire et al., 2012; Lacrue et al., 2013; Marcisin et al., 2014; Li et al., 2014; Ramalhete et al., 2014; Zuzarte-Luis et al., 2014). To improve these approaches, identification of parasite promoters specifically activated in liver development was achieved in *P. berghei*, also in this case relying on use of transgenic luciferase-promoter fusions (Helm et al., 2010).

The ability to reliably quantify parasite infection in hepatocytes is essential in the development of malaria vaccines. To overcome limitations of qRT-PCR-based quantification, *P. berghei* parasites expressing a GFP-luciferase fusion were introduced to evaluate antimalarial immunity both *in vivo*, in mice where this was induced by sporozoites unable to proliferate after irradiation or chloroquine prophylaxis, and *in vitro* in Huh-7 human liver hepatoma cells (Ploemen et al., 2011; Miller et al., 2013). Luciferase expressing *P. berghei* and *P. falciparum* sporozoites were also used to assess adequacy of sporozoite attenuation, obtained this time by genetic mutation, respectively in *in vivo* murine malaria model and in primary human hepatocytes (Annoura et al., 2012; van Schaijk et al., 2014). These studies highlighted the role of cell mediated immunity mounting against the multiplication-deficient sporozoites. A role for antibody mediated immunity was instead shown by BLI of luciferase-expressing sporozoites of the human parasite *P. falciparum* in mice with a humanized liver, showing that infection in this organ was reduced by passive transfer of a monoclonal antibody targeting the sporozoite surface protein CSP (Sack et al., 2014). Finally, *P. berghei* and *P. yoelii* luciferase transgenic parasites were instrumental to evaluate modes of sporozoite administration, a critical bottleneck in immunization and challenge protocols (Ploemen et al., 2013).

### **2.3 From the liver to the blood: the asexual erythrocytic stages**

Maturation of the liver schizont releases thousands of merozoites that invade blood stream erythrocytes and starts the asexual, symptomatic blood stage infection. In *P. falciparum* the blood stage schizonts disappear from circulation as they adhere to host ligands on endothelial cells of the microvasculature in several organs, especially in the brain and in the placenta, through parasite proteins expressed on the infected erythrocyte surface, leading to severe pathogenesis such as cerebral malaria or adverse effects during pregnancy. As parasites are observed to accumulate in several organs, including the brain, also in the mouse malaria model, real-time BLI in whole mice or in dissected organs were conducted with *P. berghei* transgenic lines expressing luciferase under a constitutive or a schizont-specific promoter to identify the involved components of the immune system (Franke-Fayard et al., 2005; Amante et al., 2007; Spaccapelo et al., 2010; Claser et al., 2011; Pasini et al., 2013; Imai et al., 2014).

The need to elucidate the mechanisms of malaria pathogenesis directed research on the fundamental biology of parasite asexual development, one important aspect being how the parasite regulates its

gene expression. The extremely high A+T content of the Plasmodium genomes however prevented homology based identification of promoters, regulatory elements and parasite transcription factors, whereas luciferase reporters proved to be of paramount importance in functionally identifying gene promoters and regulatory regions (Horrocks and Kilbey 1996; Militello et al., 2004; Porter 2002; Hasenkamp et al., 2013). This work identified sequences functioning as bi-directional promoters, like the intergenic region of the *P. berghei* elongation factor-1 $\alpha$  (*ef-1 $\alpha$* ) gene (de Koning-Ward et al., 1999; Fernandez-Becerra et al., 2003) or the intron of the *P. falciparum* *var* genes (Epp et al., 2008), or evaluated whether specific promoters from one Plasmodium species were able (Fernandez-Becerra et al., 2003; Ozwara et al., 2003) or unable (Azevedo et al., 2007) to recruit the transcriptional machinery of a different malaria species. Importantly, luciferase expressing parasites were used to identify regulatory regions governing the expression of the *P. falciparum* polymorphic *var* genes encoding the parasite sequestration ligands, whose expression switch is responsible for parasite antigenic variation and immune evasion (Deitsch et al., 1999; Calderwood et al., 2003; Frank et al., 2006; Muhle et al., 2009). In summary, luciferase reporters not only contributed to identify functional elements involved in parasite gene regulation (López-Estraño et al., 2007; Gopalakrishnan and López-Estraño 2010; Bischoff et al., 2000; Patakottu et al., 2012; Zhang et al 2011; Militello et al., 2004), but also were essential to select specific promoters in the development of Plasmodium inducible expression systems (de Azevedo et al., 2012; Kolevzon et al., 2014) and to test new regulatory regions in chromosomally integrated luciferase cassettes (Weiwer et al., 2011; Ekland et al., 2011; Che et al., 2012; Khan et al., 2012; Hasenkamp et al., 2013).

A major effort in the fight against malaria, particularly *P. falciparum*, has been the screening for new antimalarial drugs, an endeavor that the appearance of artemisinin resistance in South East Asia makes dramatically urgent. In the past decades, *in vitro* methods measuring the incorporation of [<sup>3</sup>H]-labeled hypoxanthine and ethanalamine or the activity of parasite Lactate Dehydrogenase have been the standard for *P. falciparum* cell based assays and used in large drug screenings (Fidock, 2010). The demand for high-throughput, non-radioactive assays prompted to exploit also in Plasmodium the high sensitivity and virtual absence of background of luciferase reporters, until recently used in this field only to study expression of the *P. falciparum* multidrug resistance gene *pfmdr1* in drug treated parasites (Waller et al., 2003; Myrick et al., 2003). To this aim a *P. falciparum* line expressing the firefly luciferase under the *heat shock protein 86* (*pfhsp86*) gene promoter in asexual stages enabled establishment of a cell-based luciferase drug screening assay in 96w plates (Cui et al., 2008), subsequently adapted to 384w plate using 10<sup>5</sup>-10<sup>6</sup> parasites per well (Lucumi et al., 2010). Also *P. berghei* parasites expressing a firefly luciferase-GFP fusion were used for *in vitro* and *in vivo* bioluminescence drug assay, enabling use of animal models to test new drugs *in vivo* (Franke-Fayard et al., 2008; Lin et al., 2013).

## **2.4 Preparing departure from the blood: the gametocytes**

Plasmodium gametocytes are the parasite sexual stages responsible for the transmission from the vertebrate host to the mosquito. Male and female gametocytes are formed in the bloodstream and, in *P. falciparum*, they mature in 10 days through five developmental stages. Upon ingestion in the mosquito gut, mature gametocytes promptly differentiate into gametes and fertilization ensures parasite infection in the insect vector. A key priority in the present goal to globally eliminate malaria is

to identify new drugs targeting in the bloodstream both the asexual and the sexual stages of the parasite. However, the non-replicative nature of gametocytes imposed to develop specific cell based screening assays, different from those used for asexual stages. One problem is for instance that of false negative signals due to the persistence of fluorescent reporter or of parasite enzyme activities in unhealthy or dying gametocytes. *P. falciparum* lines expressing a GFP-firefly luciferase gene under gametocyte specific promoters were established (Adjalley et al., 2011) and used in high-throughput screening assays of compounds with anti-asexual stage activity (Lucantoni et al., 2013). Recently, luciferase-based gametocyte assays have been improved by replacing the commonly used commercial luciferase substrates with an ATP-free, non-lysing D-luciferin formulation, yielding assay readouts that more reliably monitored viability and sensitivity to compounds of the treated gametocytes (Cevenini et al., 2014). In this work, absence of parasite cell lysis and the introduction in *P. falciparum* of the use of a potent luciferase from *Pyrophorus plagiophthalmus* under a gametocyte promoter enabled to perform for the first time bioluminescence imaging at the level of single parasite cells, individually distinguishing live and dead *P. falciparum* gametocytes (Cevenini et al., 2014).

### **3. Multiplexing, subcellular localization, imaging: the future in the use of bioluminescence malaria parasites**

Virtually all stages of the complex life cycle of malaria parasites have been enlightened by the use in several studies of luciferase reporters. These engineered parasites provided key answers to fundamental biological questions and now represent important tools for drug screening. Novel potent reporters have already expanded the luciferase repertoire used in *P. falciparum* beyond the *P. pyralis* and Renilla enzymes (Cevenini et al., 2014; Azevedo et al., 2014), increasing sensitivity and enabling to further reduce parasite numbers in high-throughput screening assays, a nontrivial improvement when using specific stages (e.g. the gametocytes) whose cultivation is technically demanding. Nevertheless exploitation of the full potential of bioluminescent reporters in malaria research is just moving the first steps.

The possibility to tune luciferase emission properties, such as emission wavelength, kinetics or thermo- and pH-stability, via random or site-directed mutagenesis or use of enzyme natural variants, led to introduce multicolor bioluminescence in antimalarial drug screening. A green and a red light emitting luciferase from *P. plagiophthalmus* were expressed in *P. falciparum* immature and mature gametocytes, providing for the first time the possibility to simultaneously measure differential, stage specific effects of drugs in a dual-color luciferase assay, and opening the possibility to apply multicolor bioluminescence to any parasite stage in fundamental and applied studies. A dual expression system with distinct luciferases would for instance be valuable in cell based high-throughput screenings to readily identify and discard compounds active against the reporter rather than the target cell (Thorne et al., 2012), as they will most likely affect only one luciferase type.

Another promising application of luciferase reporters is through their fusion to specific signals used by the parasite to traffic proteins in different extracellular compartments of the infected erythrocyte. As protein export is uniquely regulated in the parasite and is essential for its survival, use of such fusions may be invaluable to screen for compounds targeting this process. Preliminary studies were conducted with the *P. pyralis* enzyme (Burghaus et al., 2001) and more recent work established *P. falciparum* lines

which express a brighter deep-sea shrimp luciferase equipped with sequences driving the reporter in the parasite cytoplasm or in erythrocyte compartments (Azevedo et al., 2014).

In another field of application, the achievement of single parasite cell bioluminescence imaging and the availability of luciferases whose red-shifted light emission is more efficiently detectable from blood and tissues are paving the road to significant progress in analyses of the host-parasite interplay. Co-cultures of different *P. falciparum* stages and human cell types *in vitro* can provide new insights of the physiology of asexual and sexual stage parasite sequestration. The increased sensitivity achieved in *in vivo* mouse imaging with a red-shifted luciferase expressed by the unicellular protozoan parasite *Trypanosoma brucei* (Van Reet et al., 2014) is promising in view of use also in Plasmodium infected mice. Importantly, the increasing availability of humanized mouse models for *P. falciparum* and *P. vivax* infections, supporting development of asexual and sexual blood stages and of liver stages (Kaushansky et al., 2014) and the use of *P. falciparum* transgenic lines with a luciferase expressed constitutively (Vaughan et al., 2012) or under stage-specific promoters are expected to answer many unsolved questions.

The wealth of biological information provided by the use of engineered bioluminescent malaria parasites, not to mention those not reviewed here expressing a variety of fluorescent reporters, has been and will most likely continue to be enormous. The confined use of these whole cell biosensors in laboratory settings does not pose regulatory concerns on environmental release. From their aseptic sites of utilization, these genetically modified parasites will nevertheless have the most significant impact in the real world, contrasting the unbearable burden of a worldwide devastating disease.

## Authorship statement

I read the cited papers and drafted the manuscript.

## References

Adjalley, S.H., Johnston, G.L., Li, T., Eastman, R.T., Eklund, E.H., Eappen, A.G., et al. (2011). Quantitative assessment of *Plasmodium falciparum* sexual development reveals potent transmission-blocking activity by methylene blue. *Proc Natl Acad Sci U S A*.108, E1214-23. doi: 10.1073/pnas.1112037108.

Amante, F.H., Stanley, A.C., Randall, L.M., Zhou, Y., Haque, A., McSweeney, K., et al. (2007). A role for natural regulatory T cells in the pathogenesis of experimental cerebral malaria. *Am J Pathol*. 171, 548-59.

Annoura, T., Ploemen, I.H., van Schaijk, B.C., Sajid, M., Vos, M.W., van Gemert, G.J., et al. (2012). Assessing the adequacy of attenuation of genetically modified malaria parasite vaccine candidates. *Vaccine*. 30, 2662-70. doi: 10.1016/j.vaccine.2012.02.010.

Annoura, T., Chevalley, S., Janse, C.J., Franke-Fayard, B., and Khan, S.M. (2013). Quantitative analysis of *Plasmodium berghei* liver stages by bioluminescence imaging. *Methods Mol Biol*. 923, 429-43

Azevedo, M.F., and del Portillo HA. (2007). Promoter regions of *Plasmodium vivax* are poorly or not recognized by *Plasmodium falciparum*. *Malar J.* 6, 20.

Azevedo, M.F., Nie, C.Q., Elsworth, B., Charnaud, S.C., Sanders, P.R., Crabb, B.S., et al. (2014). *Plasmodium falciparum* transfected with ultra bright NanoLuc luciferase offers high sensitivity detection for the screening of growth and cellular trafficking inhibitors. *PLoS One.* 9, e112571. doi: 10.1371/journal.pone.0112571

Bischoff, E., Guillotte, M., Mercereau-Puijalon, O., and Bonnefoy, S. (2000). A member of the *Plasmodium falciparum* Pf60 multigene family codes for a nuclear protein expressed by readthrough of an internal stop codon. *Mol Microbiol.* 35, 1005-16.

Braks, J., Aime, E., Spaccapelo, R., Klop, O., Janse, C.J., and Franke-Fayard, B. (2013). Bioluminescence imaging of *P. berghei* schizont sequestration in rodents. *Methods Mol Biol.* 923, 353-68

Burghaus, P.A., and Lingelbach, K. (2001). Luciferase, when fused to an N-terminal signal peptide, is secreted from transfected *Plasmodium falciparum* and transported to the cytosol of infected erythrocytes. *J Biol Chem.* 276, 26838-45.

Calderwood, M.S., Gannoun-Zaki, L., Wellems, T.E., and Deitsch, K.W. (2003). *Plasmodium falciparum* var genes are regulated by two regions with separate promoters, one upstream of the coding region and a second within the intron. *J Biol Chem.* 278, 34125-32.

Cevenini, L., Camarda, G., Michelini, E., Siciliano, G., Calabretta, M.M., Bona, R., et al. (2014). Multicolor bioluminescence boosts malaria research: quantitative dual-color assay and single-cell imaging in *Plasmodium falciparum* parasites. *Anal Chem.* 86, 8814-21. doi: 10.1021/ac502098w.

Claser, C., Malleret, B., Gun, S.Y., Wong, A.Y., Chang, Z.W., Teo, P., et al. (2011). CD8+ T cells and IFN- $\gamma$  mediate the time-dependent accumulation of infected red blood cells in deep organs during experimental cerebral malaria. *PLoS One.* 6, e18720. doi: 10.1371/journal.pone.0018720.

Che, P., Cui, L., Kutsch, O., Cui, L., and Li, Q. (2012). Validating a firefly luciferase-based high-throughput screening assay for antimalarial drug discovery. *Assay Drug Dev Technol.* 10, 61-8. doi: 10.1089/adt.2011.0378.

Cui, L., Miao, J., Wang, J., Li, Q., and Cui, L. (2008). *Plasmodium falciparum*: development of a transgenic line for screening antimalarials using firefly luciferase as the reporter. *Exp Parasitol.* 120, 80-7. doi: 10.1016/j.exppara.2008.05.003.

de Azevedo, M.F., Gilson, P.R., Gabriel, H.B., Simões, R.F., Angrisano, F., Baum, J., et al. (2012). Systematic analysis of FKBP inducible degradation domain tagging strategies for the human malaria parasite *Plasmodium falciparum*. *PLoS One.* 7, e40981. doi: 10.1371/journal.pone.0040981.

de Koning-Ward, T.F., Sperança, M.A., Waters, A.P., and Janse, C.J. (1999). Analysis of stage specificity of promoters in *Plasmodium berghei* using luciferase as a reporter. *Mol Biochem Parasitol.* 100,141-6.

Deitsch, K.W., del Pinal, A., and Wellems, T.E. (1999). Intra-cluster recombination and var transcription switches in the antigenic variation of *Plasmodium falciparum*. *Mol Biochem Parasitol.* 101, 107-16.

Delves, M.J., and Sinden, R.E. (2010). A semi-automated method for counting fluorescent malaria oocysts increases the throughput of transmission blocking studies. *Malar J.* 9, 35. doi:10.1186/1475-2875-9-35.

Derbyshire, E.R., Prudêncio, M., Mota, M.M., and Clardy, J. (2012). Liver-stage malaria parasites vulnerable to diverse chemical scaffolds. *Proc Natl Acad Sci U S A.* 109, 8511-6. doi: 10.1073/pnas.1118370109.

Ekland, E.H., Schneider, J., and Fidock, D.A. (2011). Identifying apicoplast-targeting antimalarials using high-throughput compatible approaches. *FASEB J.* 25, 3583-93. doi: 10.1096/fj.11-187401.

Epp, C., Raskolnikov, D., and Deitsch, K.W. (2008). A regulatable transgene expression system for cultured *Plasmodium falciparum* parasites. *Malar J.* 7, 86. doi: 10.1186/1475-2875-7-86.

Fidock, D.A. (2010). Drug discovery: Priming the antimalarial pipeline. *Nature.* 465, 297-298. doi: 10.1038/465297a.

Fernandez-Becerra, C., de Azevedo, M.F., Yamamoto, M.M., and del Portillo, H.A. (2003). *Plasmodium falciparum*: new vector with bi-directional promoter activity to stably express transgenes. *Exp Parasitol.* 103, 88-91.

Frank, M., Dzikowski, R., Costantini, D., Amulic, B., Berdougou, E., and Deitsch, K. (2006). Strict pairing of var promoters and introns is required for var gene silencing in the malaria parasite *Plasmodium falciparum*. *J Biol Chem.* 281, 9942-52.

Franke-Fayard, B., Djokovic, D., Dooren, M.W., Ramesar, J., Waters, A.P., Falade, M.O., et al. (2008). Simple and sensitive antimalarial drug screening in vitro and in vivo using transgenic luciferase expressing *Plasmodium berghei* parasites. *Int J Parasitol.* 38, 1651-62. doi: 10.1016/j.ijpara.2008.05.012.

Franke-Fayard, B., Janse, C.J., Cunha-Rodrigues, M., Ramesar, J., Büscher, P., Que, I., et al. (2005). Murine malaria parasite sequestration: CD36 is the major receptor, but cerebral pathology is unlinked to sequestration. *Proc Natl Acad Sci U S A.* 102, 11468-73.

Franke-Fayard, B., Waters, A.P., and Janse, C.J. (2006). Real-time in vivo imaging of transgenic bioluminescent blood stages of rodent malaria parasites in mice. *Nat Protoc.* 1, 476-85.

Golightly, L.M., Mbacham, W., Daily, J., and Wirth, D.F. (2000). 3' UTR elements enhance expression of Pgs28, an ookinete protein of *Plasmodium gallinaceum*. *Mol Biochem Parasitol.* 105, 61-70.

Goonewardene, R., Daily, J., Kaslow, D., Sullivan, T.J., Duffy, P., Carter, R., et al. (1993). Transfection of the malaria parasite and expression of firefly luciferase. *Proc Natl Acad Sci USA.* 90, 5234-6.

Gopalakrishnan, A.M., and López-Estraño, C. (2010). Role of cis-regulatory elements on the ring-specific hrp3 promoter in the human parasite *Plasmodium falciparum*. *Parasitol Res.* 106, 833-45. doi: 10.1007/s00436-010-1738-9.

Hasenkamp, S., Russell, K.T., and Horrocks, P. (2012). Comparison of the absolute and relative efficiencies of electroporation-based transfection protocols for *Plasmodium falciparum*. *Malar J.* 11, 210. doi: 10.1186/1475-2875-11-210.

Hasenkamp, S., Russell, K.T., Ullah, I., and Horrocks, P. (2013). Functional analysis of the 5' untranslated region of the phosphoglutamase 2 transcript in *Plasmodium falciparum*. *Acta Trop.* 127, 69-74. doi: 10.1016/j.actatropica.2013.03.007.

Hasenkamp, S., Sidaway, A., Devine, O., Roye, R., and Horrocks, P. (2013). Evaluation of bioluminescence-based assays of anti-malarial drug activity. *Malar J.* 12, 58. doi: 10.1186/1475-2875-12-58.

Helm, S., Lehmann, C., Nagel, A., Stanway, R.R., Horstmann, S., Llinas, M., et al. (2010). Identification and characterization of a liver stage-specific promoter region of the malaria parasite *Plasmodium*. *PLoS One.* 5, e13653. doi: 10.1371/journal.pone.0013653.

Horrocks, P., and Kilbey, B.J. (1996). Physical and functional mapping of the transcriptional start sites of *Plasmodium falciparum* proliferating cell nuclear antigen. *Mol Biochem Parasitol.* 82, 207-15.

Imai, T., Iwawaki, T., Akai, R., Suzue, K., Hirai, M., Taniguchi, T., et al. (2014). Evaluating experimental cerebral malaria using oxidative stress indicator OKD48 mice. *Int J Parasitol.* 44, 681-5. doi: 10.1016/j.ijpara.2014.06.002.

Kaushansky, A., Mikolajczak, S.A., Vignali, M., and Kappe, S.H. (2014). Of men in mice: the success and promise of humanized mouse models for human malaria parasite infections. *Cell Microbiol.* 16, 602-11. doi: 10.1111/cmi.12277.

Khan, T., van Brummelen, A.C., Parkinson, C.J., and Hoppe, H.C. (2012). ATP and luciferase assays to determine the rate of drug action in in vitro cultures of *Plasmodium falciparum*. *Malar J.* 11, 369. doi: 10.1186/1475-2875-11-369.

Kolevzon, N., Nasereddin, A., Naik, S., Yavin, E., and Dzikowski, R. (2014). Use of peptide nucleic acids to manipulate gene expression in the malaria parasite *Plasmodium falciparum*. *PLoS One.* 9, e86802. doi: 10.1371/journal.pone.0086802.

Lacrué, A.N., Sáenz, F.E., Cross, R.M., Udenze, K.O., Monastyrskyi, A., Stein, S., et al. (2013). 4(1H)-Quinolones with liver stage activity against *Plasmodium berghei*. *Antimicrob Agents. Chemother.* 57, 417-24. doi: 10.1128/AAC.00793-12.

Li, Q., O'Neil, M., Xie, L., Caridha, D., Zeng, Q., Zhang, J., et al. (2014). Assessment of the prophylactic activity and pharmacokinetic profile of oral tafenoquine compared to primaquine for inhibition of liver stage malaria infections. *Malar J.* 13, 141. doi: 10.1186/1475-2875-13-141.



Lin, J.W., Sajid, M., Ramesar, J., Khan, S.M., Janse, C.J., and Franke-Fayard, B. (2013). Screening inhibitors of *P. berghei* blood stages using bioluminescent reporter parasites. *Methods Mol Biol.* 923, 507-22.

López-Estraño, C., Gopalakrishnan, A.M., Semblat, J.P., Fergus, M.R., Mazier, D., and Haldar, K. (2007). An enhancer-like region regulates *hrp3* promoter stage-specific gene expression in the human malaria parasite *Plasmodium falciparum*. *Biochim Biophys Acta.* 1769, 506-13.

Lucantoni, L., Duffy, S., Adjalley, S.H., Fidock, D.A., and Avery, V.M. (2013). Identification of MMV malaria box inhibitors of *Plasmodium falciparum* early-stage gametocytes using a luciferase-based high-throughput assay. *Antimicrob Agents Chemother.* 57, 6050-62. doi: 10.1128/AAC.00870-13.

Lucumi, E., Darling, C., Jo, H., Napper, A.D., Chandramohanadas, R., Fisher, N., et al. (2010). Discovery of potent small-molecule inhibitors of multidrug-resistant *Plasmodium falciparum* using a novel miniaturized high-throughput luciferase-based assay. *Antimicrob Agents Chemother.* 54, 3597-604. doi: 10.1128/AAC.00431-10.

Mair, G.R., Braks, J.A., Garver, L.S., Wiegant, J.C., Hall, N., Dirks, R.W., et al. (2006). Regulation of sexual development of *Plasmodium* by translational repression. *Science.* 313, 667-9

Manzoni, G., Briquet, S., Risco-Castillo, V., Gaultier, C., Topçu, S., Ivănescu, M.L., et al. (2014). A rapid and robust selection procedure for generating drug-selectable marker-free recombinant malaria parasites. *Sci Rep.* 4, 4760. doi: 10.1038/srep04760.

Marcisin, S.R., Sousa, J.C., Reichard, G.A., Caridha, D., Zeng, Q., Roncal, N., et al. (2014). Tafenoquine and NPC-1161B require CYP 2D metabolism for anti-malarial activity: implications for the 8-aminoquinoline class of anti-malarial compounds. *Malar J.* 13, 2. doi: 10.1186/1475-2875-13-2.

Militello, K.T., Dodge, M., Bethke, L., and Wirth, D.F. (2004). Identification of regulatory elements in the *Plasmodium falciparum* genome. *Mol Biochem Parasitol.* 134, 75-88.

Militello, K.T., and Wirth, D.F. (2003). A new reporter gene for transient transfection of *Plasmodium falciparum*. *Parasitol Res.* 89, 154-7.

Miller, L.H., Baruch, D.I., Marsh, K., and Doumbo, O.K. (2002). The pathogenic basis of malaria. *Nature.* 415, 673-9.

Miller, J.L., Murray, S., Vaughan, A.M., Harupa, A., Sack, B., Baldwin, M., et al. (2013). Quantitative bioluminescent imaging of pre-erythrocytic malaria parasite infection using luciferase-expressing *Plasmodium yoelii*. *PLoS One.* 8, e60820. doi: 10.1371/journal.pone.0060820.

Milner, D.A. Jr., Whitten, R.O., Kamiza, S., Carr, R., Liomba, G., Dzamalala, C., et al. (2014). The systemic pathology of cerebral malaria in African children. *Front Cell Infect Microbiol.* 4, 104. doi: 10.3389/fcimb.2014.00104.

Myrick, A., Munasinghe, A., Patankar, S., and Wirth, D.F. (2003). Mapping of the *Plasmodium falciparum* multidrug resistance gene 5'-upstream region, and evidence of induction of transcript levels by antimalarial drugs in chloroquine sensitive parasites. *Mol Microbiol.* 49, 671-83.

Muhle, R.A., Adjalley, S., Falkard, B., Nkrumah, L.J., Muhle, M.E., and Fidock, D.A. (2009). A *var* gene promoter implicated in severe malaria nucleates silencing and is regulated by 3' untranslated region and intronic cis-elements. *Int J Parasitol.* 39(13), 1425-39. doi: 10.1016/j.ijpara.2009.05.001.

Mwakingwe, A., Ting, L.M., Hochman, S., Chen, J., Sinnis, P., and Kim, K. (2009). Noninvasive real-time monitoring of liver-stage development of bioluminescent *Plasmodium* parasites. *J Infect Dis.* 200, 1470-8. doi: 10.1086/606115.

Oguariri, R.M., Dunn, J.M., and Golightly, L.M. (2006). 3' gene regulatory elements required for expression of the *Plasmodium falciparum* developmental protein, Pfs25. *Mol Biochem Parasitol.* 146, 163-72.

Ozwarra, H., van der Wel, A., Kocken, C.H., and Thomas, A.W. (2003). Heterologous promoter activity in stable and transient *Plasmodium knowlesi* transgenes. *Mol Biochem Parasitol.* 130, 61-4.

Pasini, E.M., Braks, J.A., Fonager, J., Klop, O., Aime, E., Spaccapelo, R., et al. (2013). Proteomic and genetic analyses demonstrate that *Plasmodium berghei* blood stages export a large and diverse repertoire of proteins. *Mol Cell Proteomics.* 12, 426-48. doi: 10.1074/mcp.M112.021238.

Patakottu, B.R., Singh, P.K., Malhotra, P., Chauhan, V.S., and Patankar, S. (2012). In vivo analysis of translation initiation sites in *Plasmodium falciparum*. *Mol Biol Rep.* 39, 2225-32. doi: 10.1007/s11033-011-0971-3.

Ploemen, I., Behet, M., Nganou-Makamdop, K., van Gemert, G.J., Bijker, E., Hermsen, C., et al. (2011). Evaluation of immunity against malaria using luciferase-expressing *Plasmodium berghei* parasites. *Malar J.* 10, 350. doi: 10.1186/1475-2875-10-350.

Ploemen, I.H., Chakravarty, S., van Gemert, G.J., Annoura, T., Khan, S.M., Janse, C.J., et al. (2013). *Plasmodium* liver load following parenteral sporozoite administration in rodents. *Vaccine.* 31, 3410-6. doi: 10.1016/j.vaccine.2012.09.080.

Ploemen, I.H., Prudêncio, M., Douradinha, B.G., Ramesar, J., Fonager, J., van Gemert, G.J., et al. (2009). Visualisation and quantitative analysis of the rodent malaria liver stage by real time imaging. *PLoS One.* 4, e7881. doi: 10.1371/journal.pone.0007881.

Porter, M.E. (2002). Positive and negative effects of deletions and mutations within the 5' flanking sequences of *Plasmodium falciparum* DNA polymerase delta. *Mol Biochem Parasitol.* 122, 9-19.

Ramakrishnan, C., Rademacher, A., Soichot, J., Costa, G., Waters, A.P., Janse, C.J., et al. (2012). Salivary gland-specific *P. berghei* reporter lines enable rapid evaluation of tissue-specific sporozoite loads in mosquitoes. *PLoS One.* 7, e36376. doi: 10.1371/journal.pone.0036376.

Ramalhete, C., da Cruz, F.P., Lopes, D., Mulhovo, S., Rosário, V.E., Prudêncio, M., et al. (2011). Triterpenoids as inhibitors of erythrocytic and liver stages of Plasmodium infections. *Bioorg Med Chem.* 19, 7474-81. doi: 10.1016/j.bmc.2011.10.044.

Ramalhete, C., da Cruz, F.P., Mulhovo, S., Sousa, I.J., Fernandes, M.X., Prudêncio, M., et al. (2014). Dual-stage triterpenoids from an African medicinal plant targeting the malaria parasite. *Bioorg Med Chem.* 22, 3887-90. doi: 10.1016/j.bmc.2014.06.019.

Sack, B.K., Miller, J.L., Vaughan, A.M., Douglass, A., Kaushansky, A., Mikolajczak, S., et al. (2014). Model for *in vivo* assessment of humoral protection against malaria sporozoite challenge by passive transfer of monoclonal antibodies and immune serum. *Infect Immun.* 82, 808-17. doi: 10.1128/IAI.01249-13.

Smale, S.T. (2010). Luciferase assay. *Cold Spring Harb Protoc.* 2010: doi: 10.1101/pdb.prot5421.

Spaccapelo, R., Janse, C.J., Caterbi, S., Franke-Fayard, B., Bonilla, J.A., Syphard, L.M., et al. (2010). Plasmeprin 4-deficient *Plasmodium berghei* are virulence attenuated and induce protective immunity against experimental malaria. *Am J Pathol.* 176, 205-17. doi: 10.2353/ajpath.2010.090504.

Stone, W.J., Churcher, T.S., Graumans, W., van Gemert, G.J., Vos, M.W., Lanke, K.H., et al. (2014). A Scalable Assessment of *Plasmodium falciparum* Transmission in the Standard Membrane-Feeding Assay, Using Transgenic Parasites Expressing Green Fluorescent Protein-Luciferase. *J Infect Dis.* 210, 1456-63. doi: 10.1093/infdis/jiu271.

Thorne, N., Shen, M., Lea, W.A., Simeonov, A., Lovell, S., Auld, D.S., et al. (2012). Firefly luciferase in chemical biology: a compendium of inhibitors, mechanistic evaluation of chemotypes, and suggested use as a reporter. *Chem Biol.* 19, 1060-72. doi: 10.1016/j.chembiol.2012.07.015.

Van Reet, N., Van de Vyver, H., Pyana, P.P., Van der Linden, A.M., and Büscher, P. (2014). A panel of *Trypanosoma brucei* strains tagged with blue and red-shifted luciferases for bioluminescent imaging in murine infection models. *PLoS Negl Trop Dis.* 8, e3054. doi: 10.1371/journal.pntd.0003054.

van Schaijk, B.C., Ploemen, I.H., Annoura, T., Vos, M.W., Lander, F., van Gemert, G.J., et al. (2014). A genetically attenuated malaria vaccine candidate based on *P. falciparum* b9/slarp gene-deficient sporozoites. *Elife.* 3. doi: 10.7554/eLife.03582.

Vaughan, A.M., Mikolajczak, S.A., Camargo, N., Lakshmanan, V., Kennedy, M., Lindner, S.E., et al. (2012). A transgenic *Plasmodium falciparum* NF54 strain that expresses GFP-luciferase throughout the parasite life cycle. *Mol Biochem Parasitol.* 186, 143-7. doi: 10.1016/j.molbiopara.2012.10.004.

Waller, K.L., Muhle, R.A., Ursos, L.M., Horrocks, P., Verdier-Pinard, D., Sidhu, A.B., et al. (2003). Chloroquine resistance modulated *in vitro* by expression levels of the *Plasmodium falciparum* chloroquine resistance transporter. *J Biol Chem.* 278, 33593-601.

Waters, A.P., Thomas, A.W., van Dijk, M.R., and Janse, C.J. (1997). Transfection of malaria parasites. *Methods.* 13, 134-47.

Weiwer, M., Mulrooney, C., Massi, D., Heidebrecht, R., Wiegand, R., Lukens, A.K., et al. (2011). ML238: An Antimalarial Small Molecule of a Unique Structural Class. *Probe Reports from the NIH Molecular Libraries Program*.

White, N.J., Pukrittayakamee, S., Hien, T.T., Faiz, M.A., Mokuolu, O.A., and Dondorp, A.M. (2014). Malaria. *Lancet*. 383, 723-35. doi: 10.1016/S0140-6736(13)60024-0.

WHO World Malaria Report 2013  
([http://www.who.int/malaria/publications/world\\_malaria\\_report/en/](http://www.who.int/malaria/publications/world_malaria_report/en/))

Zhang, X., Tolzmann, C.A., Melcher, M., Haas, B.J., Gardner, M.J., Smith, J.D., et al. (2011). Branch point identification and sequence requirements for intron splicing in *Plasmodium falciparum*. *Eukaryot Cell*. 10, 1422-8. doi: 10.1128/EC.05193-11.

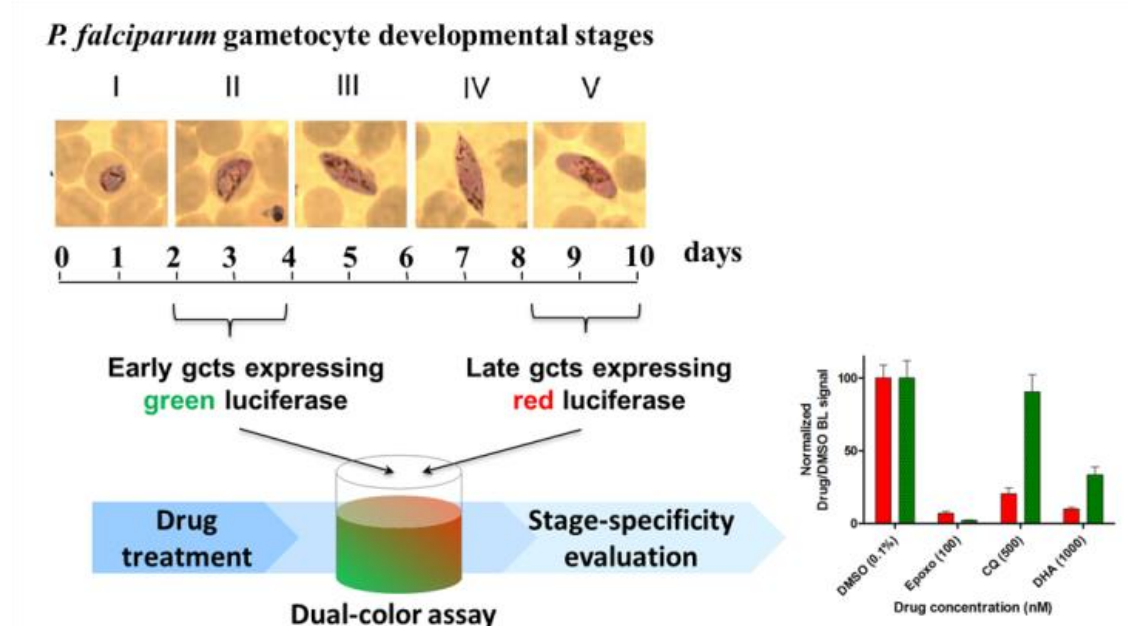
Zuzarte-Luis, V., Sales-Dias, J., and Mota, M.M. (2014). Simple, sensitive and quantitative bioluminescence assay for determination of malaria pre-patent period. *Malar J*. 13, 15. doi: 10.1186/1475-2875-13-15.

# Multicolor bioluminescence boosts malaria research: quantitative dual-color assay and single-cell imaging in *Plasmodium falciparum* parasites

Luca Cevenini<sup>‡1,2</sup>, Grazia Camarda<sup>‡3#</sup>, Elisa Michelini<sup>1,2</sup>, **Giulia Siciliano**<sup>3</sup>, Maria Maddalena Calabretta<sup>2</sup>, Roberta Bona<sup>4</sup>, T. R. Santha Kumar<sup>5</sup>, Andrea Cara<sup>4</sup>, Bruce R. Branchini<sup>6</sup>, David A. Fidock<sup>5,7</sup>, Aldo Roda<sup>1,2</sup>, Pietro Alano<sup>3</sup>.

1 INBB, Istituto Nazionale di Biostrutture e Biosistemi, 00136 Rome, Italy. 2 Department of Chemistry "G. Ciamician", University of Bologna, 40126 Bologna, Italy. 3 Dipartimento di Malattie Infettive, Parassitarie ed Immunomediate, Istituto Superiore di Sanità, 00161 Rome, Italy. 4 Dipartimento Farmaco, Istituto Superiore di Sanità, 00161 Rome, Italy. 5 Department of Microbiology and Immunology, Columbia University Medical Center, New York 10032, NY, USA. 6 Department of Chemistry, Connecticut College, New London, CT 06320, USA. 7 Division of Infectious Diseases, Department of Medicine, Columbia University Medical Center, New York 10032, NY, USA.

This work is published in Analytical Chemistry. 2014 Sep 2;86(17):8814-21. doi: 10.1021/ac502098w. Epub 2014 Aug 15.



**Abstract:** New reliable and cost-effective anti-malarial drug screening assays are urgently needed to identify drugs acting on different stages of the parasite *Plasmodium falciparum*, and particularly those responsible for human-to-mosquito transmission, i.e. the *P. falciparum* gametocytes. Low  $Z'$  factors, narrow dynamic ranges and/or extended assay times are commonly reported in current gametocyte assays measuring gametocyte-expressed fluorescent or luciferase reporters, endogenous ATP levels, activity of gametocyte enzymes or redox dependent dye fluorescence. We hereby report on a dual-luciferase gametocyte assay with immature and mature *P. falciparum* gametocyte stages expressing red and green-emitting luciferases from *Pyrophorus plagiophthalmus* under the control of the parasite

sexual stage specific *pfs16* gene promoter. The assay was validated with reference antimalarial drugs and allowed to quantitatively and simultaneously measure stage-specific drug effects on parasites at different developmental stages. The optimized assay, requiring only 48h incubation with drugs and using a cost-effective luminogenic substrate, significantly reduces assay cost and time in comparison to state-of-the-art analogous assays. The assay had a Z' factor of  $0.71\pm 0.03$  and it is suitable for implementation in 96- and 384-well microplate formats. Moreover, the use of a non-lysing D-luciferin substrate significantly improved the reliability of the assay and allowed to perform, for the first time, *P. falciparum* bioluminescence imaging at single-cell level.

## Introduction

Malaria still represents the deadliest parasitic infection afflicting humans worldwide, with *Plasmodium falciparum* causing the most severe form of the disease. In the goal to globally eliminate malaria it is increasingly recognized that anti-parasite interventions need to target not only the pathogenic asexual forms of the parasite but also the *Plasmodium* developmental stages responsible for transmission between the human and the Anopheles hosts. Such reinvigorated efforts include the challenge of revising high throughput (HTS) drug screening approaches, currently tailored against the *Plasmodium* replicative asexual blood stages, in order to identify compounds active against multiple stages of the malarial parasite life cycle. This is particularly important at a time where no safe drug is available against *P. falciparum* transmission stages and reports have established the emergence of parasite resistance to the frontline artemisinin drugs.

*P. falciparum* gametocytes are the parasite sexual stages responsible for the human-to-mosquito transmission. These are formed in the human bloodstream where they undergo a ten-day multi-stage development showing remarkable morphological (Hawking et al., 1971) and physiological (Silvestrini et al., 2010) differences that distinguish early and mature stages. The non-replicative nature of these sexual blood stages and their long maturation time constrained so far the ability of the recently developed gametocyte assays to sensitively and reliably monitor compound effects on gametocyte viability, mainly because activity of fluorescent or endogenous parasite enzyme reporters tends to persist in the unhealthy drug treated gametocytes (D'Alessandro et al., 2013). Current cell based reporter assays against these parasite stages generally show suboptimal robustness, require long assay time and expensive reagents, and do not provide information about stage-specificity of target drugs.

Bioluminescence (BL) is the emission of light in living organisms in which an enzyme, generally called luciferase, catalyses the oxidation of a specific substrate, luciferin, with a release of photons in the visible spectrum. Luciferase genes cloned from different organisms are used in several bioanalytical applications thanks to peculiar characteristic of BL reactions such as high quantum yield, high signal-to noise ratio and the possibility to multiplex assays using luciferases emitting at different wavelengths. As luciferases do not require post-translational modifications for activity and are not toxic to cells even at high concentrations, these enzymes have been successfully exploited as reporters in a variety of ultrasensitive cell-based assays (Cevenini et al., 2013; Ekström et al., 2013). The possibility to tune luciferase emission properties such as emission wavelength and kinetics or thermo- and pH-stability (Michelini et al., 2009) via random or site-directed mutagenesis opens the avenue to significantly improve *P. falciparum* HTS luciferase assays, so far restricted to the use of the *Photinus pyralis* wild type

enzyme (Che et al., 2012; Hasenkamp et al., 2012; Adjalley et al., 2011; Lucantoni et al., 2013; Tanaka et al., 2013). Improvements can be achieved by combining luciferases emitting at different wavelength under the control of different regulatory sequences to monitor multiple molecular targets or signaling events, resulting in increased information from the same cell/well and reduced assay cost/time. Also, the introduction of a second, constitutively expressed luciferase in the same cell can provide an internal viability control to correct the analytical signal, improving assay reliability and robustness. Moreover, the possibility to monitor in real-time the BL signal emitted by a single parasite by non-invasive BL imaging offers tremendous potential for clarifying mechanisms of action of target drugs.

In this work the combination of multicolor bioluminescence and use of an optimized luminogenic substrate are reported for the first time in *P. falciparum* to quantitatively and simultaneously assess the viability of parasites at different developmental stages in a format scalable to HTS and to introduce single-cell imaging methodology in the study of this parasite.

## Experimental section

**Parasite cultures and transfection.** The *P. falciparum* 3D7A line (Walliker et al., 1987) was cultured in human 0+ erythrocytes, kindly provided by Prof. G. Girelli, Dipartimento di Biopatologia Umana, University of Rome “La Sapienza”, at 5% haematocrit under 5% CO<sub>2</sub>, 2% O<sub>2</sub>, 93% N<sub>2</sub> (Trager and Jensen 1976). Cultures were grown in medium containing RPMI 1640 medium (Gibco) supplemented with 25 mM Hepes, 50 µg/ml hypoxanthine, 0.25 mM NaHCO<sub>3</sub>, 50 µg/ml gentamicin sulphate and 10% pooled heat-inactivated 0+ human serum. Ring stage parasites at 3–5% parasitaemia were transfected by electroporation with 80–100 µg of transfection vectors using the following conditions: voltage, 0.31 kV; capacitance, 960 µF; resistance to infinity (Fidock and Wellems 1997). Following transfection, parasites were maintained in drug free medium for 24h; at this time, positive selection was initiated by the addition 1.2 µg/ml of blasticidin (BSD) to select the parasites stably maintaining the episomal constructs.

Production of transgenic lines with stably integrated luciferase cassettes in the *pfelo1* locus was attempted equipping the luciferase cassettes with *pfelo1* homology regions for Zinc Finger Nuclease (ZFN)-mediate genome editing (Straimer et al., 2012). The episome-containing transgenic parasites were transfected with ZFN expression plasmid and double selection started after 24h by adding 1.2 µg/ml of BSD and 2.5nM WR99210. After 7 days of selection, parasites were allowed to recover in the absence of any drug. Southern blot analysis of the resulting parasites with *pfelo1*- and *bsd*-specific probes on parental parasites and on parasites containing the episomal plasmids before and after transfection of the ZFN plasmids revealed however that successful disruption of the *pfelo1* locus was mediated by integration of the entire plasmid via homologous recombination through the *pfelo1* 3' homology region.

**Plasmid construction.** The multistep procedure to obtain pCR2.1 vectors carrying myc-tagged luciferase expression cassettes equipped with Bbx1 attB sites under the expression control of the *pfs16* regulatory regions was as follows. First, attB-site adaptor, flanked by HindIII-SacI restriction site, was obtained by annealing oligonucleotides #1-attBsite-dir (all oligonucleotides used in this work are listed in Supplementary Table S1) and #2-attBsite-rev, digested and inserted into the HindIII-SacI digested pCR2.1, producing pCR2.1-attB plasmid. Upstream *pfs16* regulatory regions were PCR amplified with

primer pairs #3-pfs16-5'UTR-dir and #4-pfs16-5'UTR-rev for PpyWT, PpyRE10, PpyGRTS, and LitRE6, and primers #3-pfs16-5'UTR-dir and #5-pfs16-5'UTR-rev2 for CBG99 and CBR, and cloned into SacI-BamHI digested pCR2.1-attB after SacI-BamHI digestion, producing pCR2.1-attB-5'pfs16A and pCR2.1-attB-5'pfs16B. The above different reverse primers were needed to introduce a myc-tag sequence in frame with downstream luciferases to be cloned. Downstream *pfs16* regulatory regions were PCR amplified with primers #6-pfs16-3'UTR-dir and #7-pfs16-3'UTR-rev and cloned into pCR2.1-attB-5'pfs16 after XbaI-ApaI digestion, producing pCR2.1-attB 5'-3'pfs16A and pCR2.1-attB 5'-3'pfs16B. PpyWT, PpyRE10, and PpyGRTS, from pGEX expression plasmid were inserted into pCR2.1-attB-5' 3'pfs16A via BamHI-NotI cloning; LitRE6, from pCMV plasmid was inserted into pCR2.1-attB-5' 3'pfs16A via BamHI-XbaI cloning. CBG99 and CBR were obtained from pCBG99-basic and pCBR-basic vectors (Promega) and cloned into pCR2.1-attB-5' 3'pfs16B via NcoI-XbaI.

The procedure to produce constructs able to mediate the chromosomal integration of the luciferase cassettes was as follows. First, a unique HindIII site in the pDC2 backbone site was disrupted by HindIII digestion and a Klenow fill-in reaction. An attB site was inserted by overlapping PCR between *pfelo1* gene homology regions (HRs) as follows. As above, a HindIII site in *pfelo1* HR-I was mutated by amplifying HRI using primers #8-pfelo1HR-I-dir and #9-pfelo1-HR-I-rev1, ligating it into pGEM-T plasmid (Promega). The resulting plasmid was linearised by HindIII digestion, filled-in with Klenow polymerase, re-ligated and used as template for PCR amplification with above primer #8-pfelo1HR-I-dir and #10-pfelo1-HR-I-rev2. The latter contained, in 5' to 3' direction, stop codon, HindIII and attB sites. HR-II PCR amplification was performed with primers #11-pfelo1-HR-II-dir and #12-pfelo1-HR-II-rev. The former contained, 5' to 3', attB and HindIII sites. HR-I and HR-II PCR products were gel purified and mixed together in a PCR mix lacking primers and subjected to 5 cycles of amplification to generate a full-length HR-I-HindIII-attB- HindIII -HR-II template. Then, above primers #8-pfelo1HR-I-dir and #12-pfelo1-HR-II-rev were added to get the final PCR product, which was digested with ApaI-BamHI, gel purified and inserted into AvrII-BamH I digested pDC22-(mutHindIII) vector, producing the *pfelo1*-attB donor plasmid. Digestion of the latter plasmid with HindIII released the attB site which was replaced by the HindIII-HindIII attB-containing luciferase cassette from the pCR2.1 vectors (Figure 1).

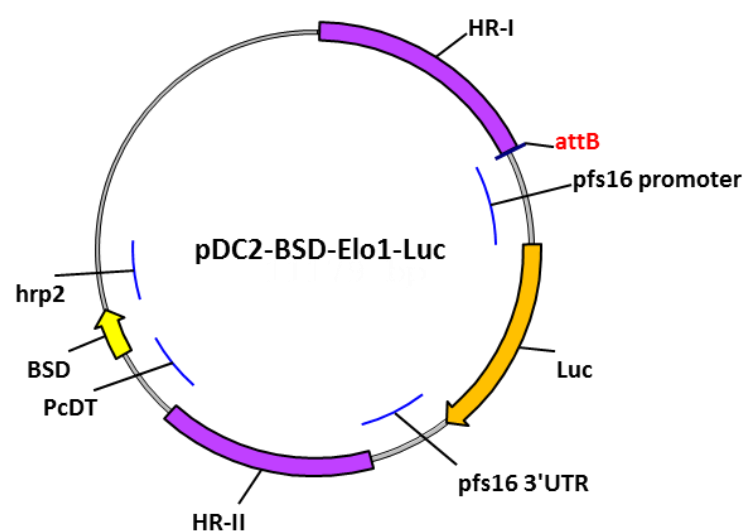




**Figure 1.** Representative map of the plasmids containing the luciferase reporter genes under the expression control of the *P. falciparum* gametocyte-specific gene *pfs16*. Representative luciferase coding sequence (Luc) flanked by promoter and 3' untranslated region (3'UTR) of gene *pfs16*. Homology regions (HR) I and II of gene *pfelo1*. Coding sequence of the blasticidine S-deaminase (BSD) gene flanked by promoter of the *P. chabaudi* dihydrofolate reductase-thymidylate synthase gene (PcDT) and the 3'UTR of the *P. falciparum* histidine rich protein 2 gene (*hrp2*).

**Plasmid copy number determination by SYBR-Green Real-Time PCR.** The *bsd* selectable marker (primers #13-*bsd-fw* and #14-*bsd-rev*) was used along with the *pfeba175* gene (primers #15-*pfeba175-fw* and #16-*pfeba175-rev*) as a control for genome numbers. Genomic DNA was extracted from asexual cultures of episomal transfectants expressing the different luciferases alongside with parental 3D7 parasites using the Bioline Blood DNA kit. DNA (50ng in 2 $\mu$ l) was added to a 13 $\mu$ l PCR mix containing 3.7 $\mu$ l water, 7.5 $\mu$ l PCR Sybrgreen Master Mix and 0.9 $\mu$ l of each primer (final concentration 300nM). Real-time assays were performed using ABI Prism 7500 Real-time PCR System (Applied Biosystems, Foster City, CA) and 7500 Software v2.0.5. The PCR parameters were as follows: 20 sec at 95 $^{\circ}$ C followed by 40 cycles of 95 $^{\circ}$ C for 15 sec and 58 $^{\circ}$ C for 30 sec. Fluorescent product was detected at the last step of each cycle. Plasmid copy numbers were determined against reference amplification titration curves of plasmid ( $10^2$  to  $10^7$  copies) in 25ng of 3D7 genomic DNA for *bsd* and of 3D7 genomic DNA (1.25 to 100ng) in  $10^7$  plasmid copies for *eba175*. All samples and controls were run in triplicate, normalized as plasmid copy number/genome and expressed as fold variation compared to PpyWT luciferase (Figure 2).

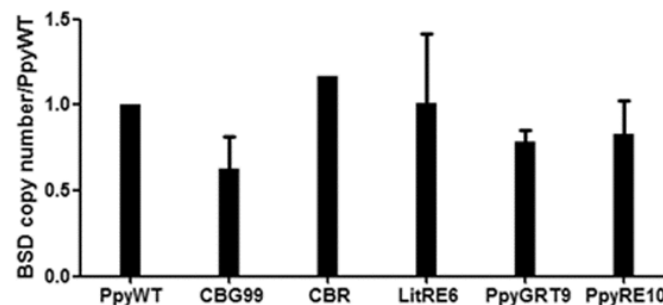


**Figure 2.** Relative copy number of the six luciferase expression plasmids in the *P. falciparum* transgenic lines. SYBR-Green Real-time PCR experiments were performed as described, amplifying the plasmid *bsd* and the parasite *pfeba175* gene sequences to determine plasmid copy number per parasite genome. Results of two independent experiments are expressed as fold over the PpyWT plasmid copy number (mean  $\pm$  SD).

**Southern blot analysis.** Genomic DNA from the different parasite lines was analyzed as follows. Genomic DNA samples, 3 $\mu$ g, were digested with AflIII and EcoRI, electrophoresed on a 0.8% agarose gel and transferred onto a Nytran nylon membrane. Hybridization of the membrane was performed at 54 $^{\circ}$ C with a 639 bp [ $^{32}$ P]-labeled *pfelo1* probe that was PCR amplified from 3D7 genomic DNA using primers

#17*elo1*probe-fwd and #18*elo1*probe-rev. The membrane was stripped in hot 0.1% SDS and hybridized at 54°C with a 389 bp [<sup>32</sup>P]-labeled *bsd* probe amplified by PCR with primer #19*bsd*-probe-fw and #20*bsd*-probe-rev from plasmid pDC2-*elo1*-CBG99 (Figure 3).

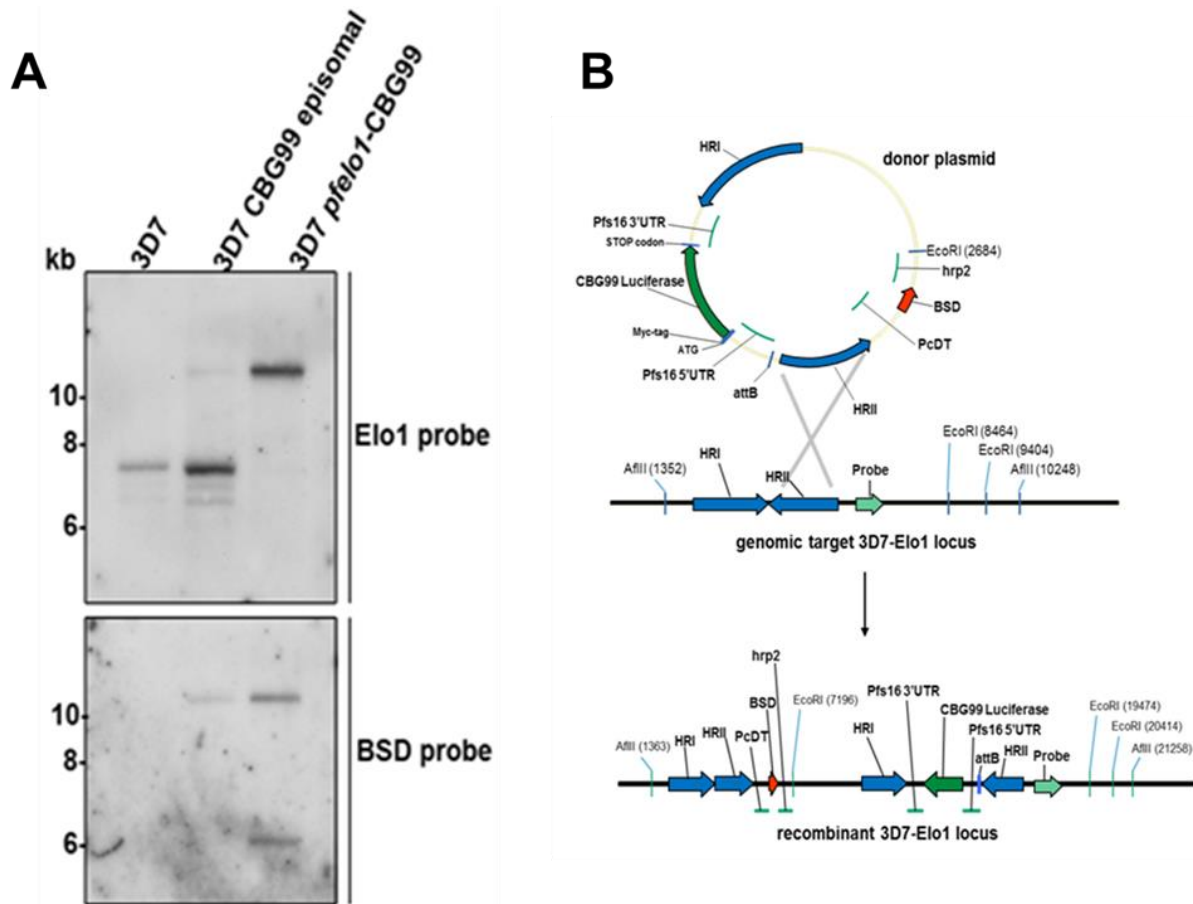


**Figure 3.** A) Southern blot analysis of genomic DNA extracted from parasites of the parental line 3D7, of the 3D7 derived line episomally maintaining the *pfs16*-CBG99 plasmid and of the parasite line after single crossover plasmid integration. Genomic DNAs were digested with AflIII and EcoRI. B) Diagram of the *pfs16*-CBG99 integration plasmid, of the target *pfe1o1* locus and of the resulting modified locus.

***P. falciparum* gametocyte drug treatments.** Drug assays were performed on gametocytes at different stage of maturation. For early (stage II) gametocytes, induced cultures were treated 48h with 50mM N-acetyl-glucosamine (NAG) to eliminate asexual stages before drug treatment. Late (IV-V) stage gametocytes had been NAG-treated 96h at the onset of gametocytogenesis and then allowed to mature. Drug treatments were performed in 100µl final volume in 96w culture plates at a final hematocrit of 1%. In these cultures gametocytemias were routinely ranging from 1 to 2.5% for episomal transgenic parasites and from 2 to 3.5% for 3D7*elo1*-*pfs16*-CBG99. Drugs were dissolved in dimethyl sulfoxide (DMSO), except for chloroquine, which is soluble in water. Control samples were treated with DMSO at the highest concentration present in treated samples, which never exceeded 0.1%.

**Immunofluorescence analysis.** Mixed stage gametocyte smears were fixed with acetone for 5 min at room temperature, blocked with PBS/3% BSA for 30 min and incubated with a rabbit anti-Pfg27

antibody (Olivieri et al., 2009)(1:500 in 1xPBS 2% BSA) to label all gametocytes and with a mouse anti-myc antibody (ab32, Abcam) (1:200 in 1xPBS 2% BSA). After incubation and washes in 1XPBS, slides were incubated with a 1:200 dilution of affinity purified, rhodamine-conjugated and FITC-conjugate secondary antibody against rabbit and mouse IgG respectively (Figure 4).

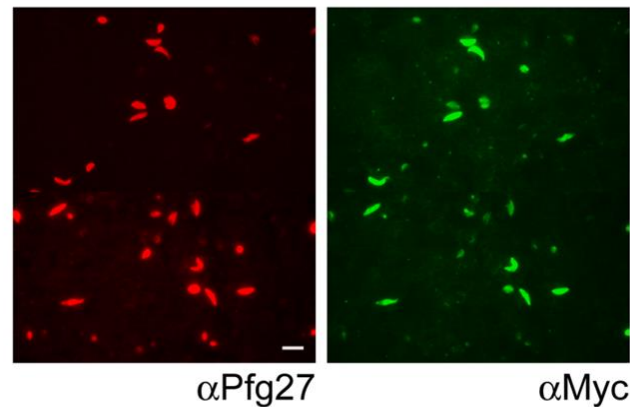


**Figure 4.** Immunofluorescence analysis of 3D7elo1-pfs16-CBG99 gametocytes. Immunofluorescence analysis of 3D7elo1-pfs16-CBG99 gametocytes with antibodies specific for the Myc tag sequence fused to the CBG99 luciferase and for the gametocyte-specific protein Pfg27. Magnification bar is 10 $\mu$ m.

**Luciferase assays.** Comparison of luciferase activities from the six episome-expressing transgenic parasites was performed on stage III gametocytes after Percoll purification (Carter et al., 1989). Frozen aliquots of equal numbers of gametocytes were resuspended in ice with 100 $\mu$ l of PBS just prior to luminometric measurements, transferred to 96w white plates, and 100 $\mu$ l of Britelite™ plus Reporter Gene Assay System (Perkin-Elmer) added. Total light outputs were recorded using a Microplate Scintillation and Luminescence CounterTopCount NXT™ (Perkin-Elmer) over a 20min-period in 3sec-intervals. Equivalent samples were also read using a Varioskan Flash multimode reader (Thermo Fisher). Luminescence measurements were expressed as signal to noise ratio with respect to untransfected 3D7 control parasite samples.

Commercial substrates Britelite™, Neolite™ and Steady-lite™ were from PerkinElmer, One-Glo™, Steady-Glo® and Bright-Glo™ from Promega. Frozen pellets of gametocyte expressing CBG99 luciferase were used to compare bioluminescence emission kinetics. Briefly, 100 $\mu$ l of the same aliquot of resuspended gametocytes were transferred to a 96-well white microtiter plate and 100 $\mu$ l of each substrate were added simultaneously with a multichannel pipette. Bioluminescence emissions were acquired for 45min with 300ms integration time using a Varioskan reader. All samples were tested in triplicate and performed at least three times. Luciferase assays after drug-treatment experiments were performed after transferring samples to 96-well white microplates. Different D-luciferin concentrations and buffer compositions were tested and the optimal substrate was 0.5mM D-luciferin (final concentration) in citrate buffer 0.1M, pH 5.5. Substrate (1mM D-luciferin) was added directly to the

samples at a 1:1 ratio and plates were read within 2 min after addition. Luminescence measurements were performed as described above.

**Bioluminescence single-cell imaging.** Single cell bioluminescence imaging was performed on control (DMSO 0.1%) or drug treated gametocytes (epoxomicin 100nM, chloroquine 500nM). After 48h incubation, gametocytes (100µl at 0.1% HCT) were transferred to a clear bottom 96-well microplate (ibidi GmbH) coated with Cell-Tak cell and tissue adhesive (BD Biosciences) according to manufacturer's instructions and allowed to adhere for 30min at 37°C. BL imaging was performed using an inverted microscope (Olympus CK40) connected to an electron multiplying charge coupled device (EM-CCD) camera (ImagEM-X2, Hamamatsu). BL images were acquired for 10 minutes with 40X objective (UApo, Olympus) after addition of 100µl of D-luciferin 1mM. All the setup was enclosed in a custom-built dark box to shield from ambient light. Images were processed with HImage software (v4.1.5.12, Hamamatsu) applying a cosmic ray removal option (threshold 10,000) and brightness/contrast adjusted with normal linear function.

**Dual-luciferase gametocyte assays.** The dual-reporter assays have been performed using CBG99 and CBR expressing parasites (1% hematocrit), at stage II and stage V of development, mixed in a 1:10 ratio, respectively, in order to compensate for the different BL signals from the two enzymes. Gametocyte mixed populations were seeded in 96-well plate and treated for 48h with 500nM chloroquine (CQ), 100nM epoxomicin (Epoxo) or DMSO 0.1% (control). By adding BL substrate emissions kinetics were acquired for 15min (300ms integration time) with Varioskan Flash using both F545 (510-580nm) and F615 (590-640nm) high transmittance band-pass emission filters. Raw BL intensities taken from 5 to 10 min were elaborated with ChomaLuc™ calculator19 to unmix BL emission (corrected BL) of the green- and red-emitting gametocytes. The mean value of each corrected BL kinetic is plotted and normalized with respect to DMSO control.

| #  | Name                     | Sequence (5'-3')  | Sites        |
|----|--------------------------|---|--------------|
| 1  | attB site dir            | ggggaagcttCGGCTTGTTCGACGACGGCGGTCTCCGTCGTCAGGATC<br>ATCgagctcgggg                   | HindIII-SacI |
| 2  | attB site rev            | ccccgagctcGATGATCCTGACGACGGAGACCGCCGTCGTCGACAAG<br>CCGagcttcccc                     | HindIII-SacI |
| 3  | <i>pfs16</i> 5' UTR dir  | ggggGAGCTCCTACTGTACTTTTTTTGGAC  | SacI         |
| 4  | <i>pfs16</i> 5' UTR rev1 | ggggGGATCCCATGGTAGGTCTTCTTCTGATATTAGTTTTTGTTTC<br>CATGTTGAAGAAAGTATAAATAGAAAAATGGC  | BamHI        |
| 5  | <i>pfs16</i> 5' UTR rev2 | ggggGGATCCCATGGtTAGGTCTTCTTCTGATATTAGTTTTTGTTTC<br>CATGTTGAAGAAAGTATAAATAGAAAAATGGC | BamHI        |
| 6  | <i>pfs16</i> 3' UTR dir  | ggggTCTAGAGATGAAGGAGACGAAGGAGATG  | XbaI         |
| 7  | <i>pfs16</i> 3' UTR rev  | ggggggggccaagcttTATTTAGAGGTGAGGACTATG   | ApaI         |
| 8  | <i>pfelo1</i> HR-I dir   | gggatccACATGAATAAACTATTCACCCC   | BamHI        |
| 9  | <i>pfelo1</i> HR-I rev1  | TCCACACGTATATATCGGAGG   |              |
| 10 | <i>pfelo1</i> HR-I rev2  | GATCCTGACGACGGAGACCGCCGTCGTCGAAAGCCGAAGCTTCT<br>Atccacagtatatatcggagg               |              |

|    |                          |   |      |
|----|--------------------------|---|------|
| 11 | <i>pfelo1</i> HR-II dir  | GTCGACGACGGCGGTCTCCGTCGTCAGGATCATCGCGGAAGCTT<br>atttggtacagttgattatgg |      |
| 12 | <i>pfelo1</i> HR-II rev  | TCGGGCCCCGATTGCTTTTTTCATTTTTTCCCTC                                    | Apal |
| 13 | <i>bsd</i> fw            | TTGTCTCAAGAAGAATCCAC  |      |
| 14 | <i>bsd</i> rev           | TAGAGAGAGCTGCGCTGGCG  |      |
| 15 | <i>pfeba175</i> fw       | TGGATAACACCAGTGAAGAACTACAG  |      |
| 16 | <i>pfeba175</i> rev      | CAATATCTTCATATTCCTTAGTAAGCG   |      |
| 17 | <i>elo1</i> probe-fw     | ACAGGCCGAGAAAATAAAGGAGAATGGC  |      |
| 18 | <i>elo1</i> probe-rev    | CGGCATCTTGTTCTTGTACCATAACAATG   |      |
| 19 | 19 <i>bsd</i> -probe-fw  | GCACCTTTGTCTCAAGAAGAATCCACCC  |      |
| 20 | 19 <i>bsd</i> -probe-rev | GCCCTCCCACACATAACCAGAGGGGCAGC   |      |

**Table 1.** List and sequence of the oligonucleotide primers used in the work.

## Results and discussion

**Expression of green- and red- emitting luciferases in *P. falciparum*.** A panel of six ATP-dependent luciferases derived from different bioluminescent species or obtained by rational mutagenesis were selected according to their enzymatic properties (Table 1) and expressed for the first time in the malaria parasite. The repertoire of luciferases used so far as reporters in malaria parasites is to our knowledge restricted to the *Renilla* and the *P. pyralis* enzymes, with only the latter luciferase being used in HTS and live imaging applications. Selected luciferases were the green wild-type *Photinus pyralis* enzyme (PpyWT) (Branchini et al., 2007), a red-shifted emission variant (PpyRE10) (Branchini et al., 2010), a mutant with green-shifted emission and increased thermal stability (PpyGRTS) (Branchini et al., 2007), a red-emitting variant of the firefly *Luciola italica* (LitRE6) (Maguire et al., 2012), and the green- and red-emitting luciferases from the click beetle *Pyrophorus plagiophthalmus* (CBG99 and CBR) (Wood et al., 1989).

*P. falciparum* parasites were transfected with plasmid constructs in which the promoter and 3' untranslated region (UTR) of the gametocyte specific gene *pfs16* (Figure 1) were used to specifically drive cytoplasmic expression of the above luciferases from the onset of sexual differentiation (stage I) through the ten-day long maturation to stage V gametocytes (Hawking et al., 1971). Six transgenic parasite lines were selected for blasticidin resistance and real-time PCR experiments determined that plasmid copy number differed at most twofold between these lines (Figure 2).

| Reporter gene (Organism)                       | In vitro BL emission <sup>a</sup> ( $\lambda_{\max}$ nm) | Half-life (37°C) | pH dependent emission | Half bandwidth (nm) <sup>b</sup> |
|--|--|------------------|-----------------------|----------------------------------|
| PpyWT<br>( <i>Photinus pyralis</i> )           | 557  | 0.26 h           | Yes                   | 66                               |
| PpyGRTS<br>( <i>Photinus pyralis</i> )         | 548  | 10.5 h           | No                    | 62                               |
| PpyRE10<br>( <i>Photinus pyralis</i> )         | 617  | 3.6 h            | No                    | 42                               |
| LitRE6<br>( <i>Luciola italica</i> )           | 610  | 9.6 h            | No                    | 70                               |
| CBG99<br>( <i>Pyrophorus plagiophthalmus</i> ) | 537  | > 5 h            | No                    | 65                               |
| CBR<br>( <i>Pyrophorus plagiophthalmus</i> )   | 613  | > 5 h            | No                    | 62                               |

<sup>a</sup> Bioluminescence emission spectra measured in Hek293 cell lines.

<sup>b</sup> Bandwidths (nm) of emission spectra were measured at 50% of the intensity at the maximum wavelength.

**Table 2.** Properties of luciferases selected for expression in *Plasmodium falciparum*.

In order to identify the most active luciferases in view of the development of a dual-color assay, BL emissions were measured from equal number of purified stage III gametocytes of the six transgenic lines. The comparison of the BL signals from the different luciferase-expressing gametocytes revealed in our hands that the green- and the red-emitting *P. plagiophthalmus* enzymes provide BL signals significantly higher than the other tested luciferases and display stable emission kinetics (Figure 5a). Although the emission spectra of these luciferases show a remarkable overlap, the distance between the two  $\lambda_{\max}$  of approximately 76nm, combined with the use of appropriate emission filters and a spectral unmixing algorithm (Almond et al., 2003), are adequate to successfully establish a dual-luciferase gametocyte assay in which contribution of each luciferase can be sensitively and robustly determined. In addition, these reporters exhibit pH-independent emission and glow-type emission kinetics, making them the best candidates for the implementation of the dual-color assay.

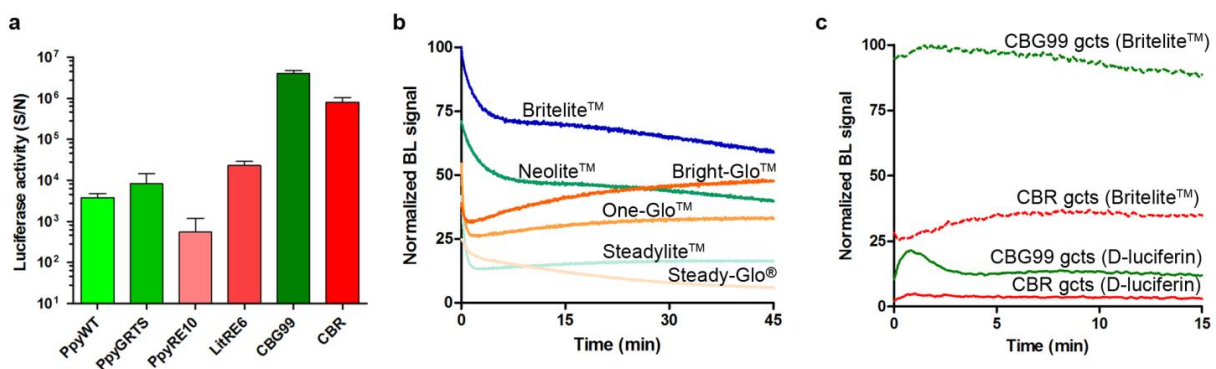


**Figure 5.** Luciferase selection and characterization (a) BL emission intensities of same amount ( $2.5 \times 10^5$ ) of purified stage III transgenic gametocytes expressing the luciferases indicated (with Britelite™ substrate). (b) Normalized emission kinetics obtained with CBG99 expressing gametocytes ( $4 \times 10^4$  gametocytes/well) using different commercial substrates. (c) Comparison of BL intensities and kinetic profiles obtained with transgenic gametocytes expressing CBG99 or CBR luciferase using Britelite™ or D-luciferin substrates. In (b) and (c) the highest BL signal is set as 100%.

**Improvement in luciferase assay performance on the non-proliferating parasite sexual stages.** The need to identify novel drugs active against *P. falciparum* gametocytes recently prompted much work to establish cell-based assays against such parasite stages. To improve current assays, the effect of several BL commercial substrates on the assay analytical performance was evaluated. Emission kinetics of the gametocyte-expressed CBG99 luciferase in a 45-minute window showed that the highest and most stable BL signal was obtained using Britelite™ (Figure 5b). However, as commercial substrates generally contain additives (luciferase inhibitors, lysing components, ATP) to enhance and stabilize the bioluminescent signal, a home-made D-luciferin solution was developed as an alternative substrate to better reflect the viability of the gametocytes in drug screening assays, avoiding artifactual BL emission in the treated cells. Gametocytes expressing the CBG99 or the CBR luciferase were incubated with Britelite™ or with a formulation of 0.5mM D-luciferin dissolved in 0.1M citrate buffer pH 5.5, optimized to enter cells in other eukaryotic and in prokaryotic systems (Michellini et al., 2008). Although the non-lysing D-luciferin substrate produced a lower BL signal than Britelite™, a stable signal was obtained from 5 to 15 minutes after substrate addition, with only 5% variability over 10 min (Figure 5c). In order to directly compare the performance of Britelite™ and D-luciferin substrates in faithfully monitoring parasite viability exposed to drug treatment, synchronous unpurified cultures (1% hematocrit, 2% gametocytemia) of stage II and stage IV gametocytes expressing CBG99 or CBR were exposed for 48h to a 100nM concentration of the reference gametocytocidal drug epoxomicin (Czesny et al., 2009).

Results showed that the decline in luciferase activity in the drug-treated gametocytes was significantly more pronounced using the D-luciferin substrate than Britelite™ in both gametocyte stages for both parasite lines (Figure 6a,b). At 48h, with D-luciferin, residual luciferase activity was virtually absent or <1% in early and late gametocytes respectively, whereas with Britelite™ it was  $37 \pm 5\%$  in early gametocytes and respectively  $57 \pm 4\%$  and  $72 \pm 6\%$  in the CBR- and CBG99-late stages. The robustness of this determination was indicated by a cumulative assay  $Z'$ -factor (Zhang et al., 1999) of  $0.92 \pm 0.09$  and was confirmed by the comparable epoxomicin  $IC_{50}$  values on early and late gametocyte stages obtained with the commercial and the D-luciferin substrates ( $12.5 \pm 0.4$  nM and  $14.3 \pm 0.6$  nM with D-luciferin and Britelite, respectively, on early and  $10.7 \pm 0.8$  nM and  $10.1 \pm 0.5$  nM with D-luciferin and Britelite, respectively, on late stages) (Figure 6c). Compared to the assays traditionally used to identify compounds blocking the multiplication of the parasite asexual stages, gametocyte assays face the challenge to reliably measure the ability of compounds to inhibit development or metabolism of such non-proliferating parasite stages. Low  $Z'$  factors, narrow dynamic ranges and/or extended assay times are commonly reported in current gametocyte cell-based assays measuring gametocyte-expressed fluorescent or luciferase reporters (Adjalley et al., 2011; Lucantoni et al., 2013; Buchholz et al., 2011; Wang et al., 2014), endogenous ATP levels (Lelièvre et al., 2012), activity of gametocyte enzymes (D'Alessandro et al., 2013) or redox dependent dye fluorescence (Tanaka et al., 2011; Duffy and Avery 2013). Such suboptimal performances are largely due to the persistence or slow decay of the above

reporters or signals in the non-dividing gametocytes, even when they are affected by the compound treatment.

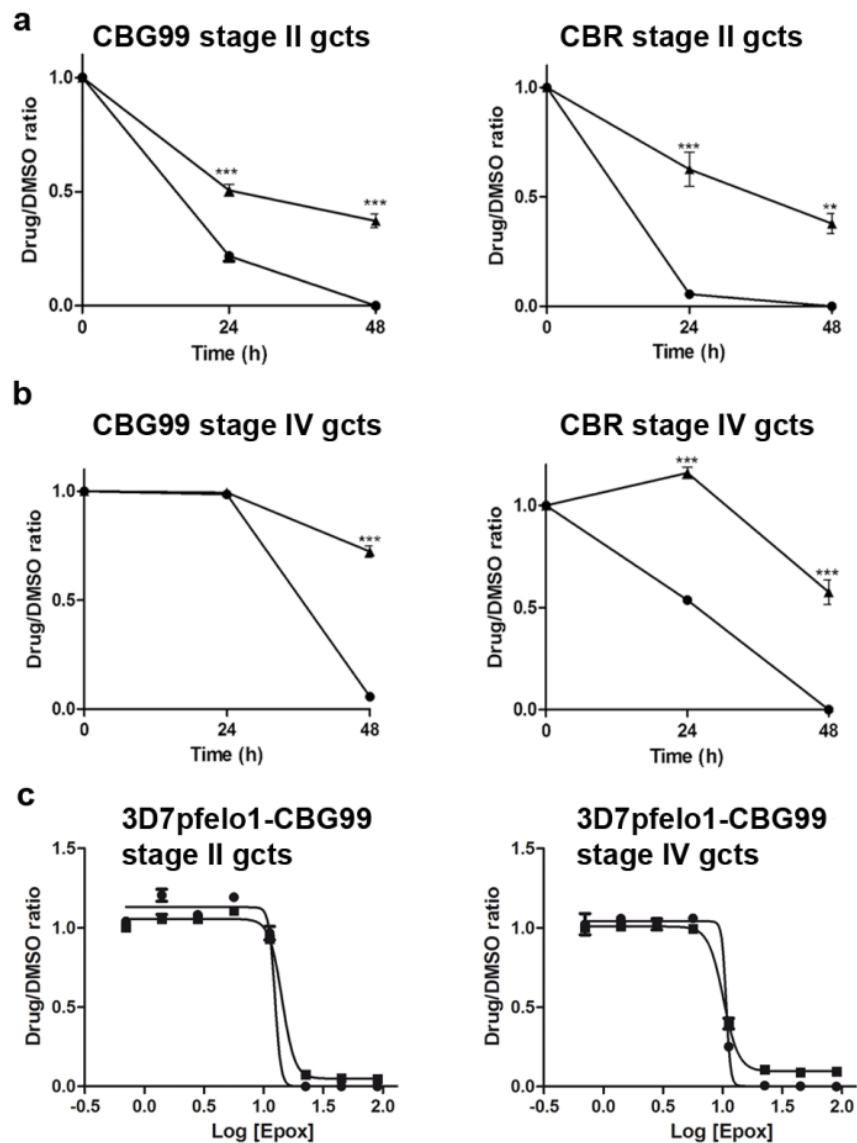


**Figure 6.** Bioluminescence in control and drug treated *P. falciparum* gametocytes (a) D-luciferin and Britelite™ performances in drug treatment assay. Bioluminescence from early stage gametocytes expressing CBG99 (left) and CBR (right) measured with D-luciferin (-●-) and Britelite™ (-▲-) at t=0, t=24h and t=48h. (b) Same experiment on stage IV gametocytes. Results are expressed as drug/DMSO ratio. Statistics are performed with the GraphPad Prism software. (c) Comparison of D-luciferin and Britelite™ performances in dose-response gametocytocidal assays. Early (left) and late (right) stage gametocytes expressing the CBG99 luciferase were treated for 72h with increasing doses of epoxomicin (0-90nM) before luciferase activity was measured with 0.5mM D- luciferin and Britelite™. IC50 values were calculated using the GraphPad Prism software.

The replacement of commonly used cell-lysing BL substrates with a formulation of non-toxic, non-lysing D-luciferin substrate solution resulted in assays where the BL signal rely both on the expression of



the luciferase reporter and, importantly, on the use of the parasite endogenous ATP, thus reliably reflecting the viability of the treated and untreated gametocytes. This improvement results in a cost-effective and less time-consuming protocol able to measure the drop to background level in gametocyte viability produced by epoxomicin in only 48h whereas as long as 144h are required in similar assays based on the gametocyte endogenous lactate dehydrogenase activity (D'Alessandro et al., 2013). Such an improvement was observed not only on the immature gametocytes but also on the late sexual stages, the ones freely circulating in the blood stream ready for uptake by the mosquito bite, whose apparently quiescent metabolic state makes the identification of inhibitory compounds particularly challenging.

**Single cell bioluminescence imaging in live *P. falciparum* parasites.** The possibility to use a non-lysing D-luciferin substrate to produce a BL signal from whole living parasites was here exploited to introduce BL imaging at the single-cell level, unprecedented in malaria parasites, to visualize live gametocytes of different stages. In order to perform these experiments a parasite line stably expressing the CBG99 luciferase from an integrated chromosomal locus was produced. A derivative of the *P. falciparum* 3D7 line was generated in which diagnostic Southern blot analysis (Figure 3) confirmed the integration of the *pfs16*-CBG99 cassette in the *P. falciparum* locus encoding the fatty acid elongase-1, *pfelo1*, dispensable for gametocyte, mosquito and liver stage development (Kumar and Fidock, unpublished observations). Immunofluorescence experiments on gametocytes of this line, named 3D7*elo1-pfs16*-CBG99, confirmed that the Myc-tagged luciferase reporter can be readily detected in >80% of the gametocytes (Figure 4).

Stage IV gametocytes from the 3D7*elo1-pfs16*-CBG99 line, immobilized in 96w plates, were incubated with 0.5mM D-luciferin and imaged with an optical microscope connected to an EM-CCD camera. Individual bioluminescent live gametocytes could be readily imaged and clearly distinguished from uninfected red blood cells (Figure 7a), representing to our knowledge the first report of single-cell BL imaging in a protozoan species. Stage IV gametocytes were then treated for 48h with 100nM epoxomicin, with 500nM chloroquine, which on such stages has a limited activity at high concentration, or with the DMSO vehicle. In this experiment no bioluminescent cells were detectable in the epoxomicin treated wells, weak BL signals were seen from gametocytes treated with chloroquine, whereas strong signals were detected on the metabolically active control parasites (Figure 7b). The failure to detect BL signals from morphologically recognizable gametocytes after drug treatment clearly indicates that the BL imaging signal is diagnostic of the viability of such cells. These results further confirmed that the use of a non-lysing D-luciferin substrate greatly improves the reliability of measuring luciferase reporter activity in the assessment of parasite viability.

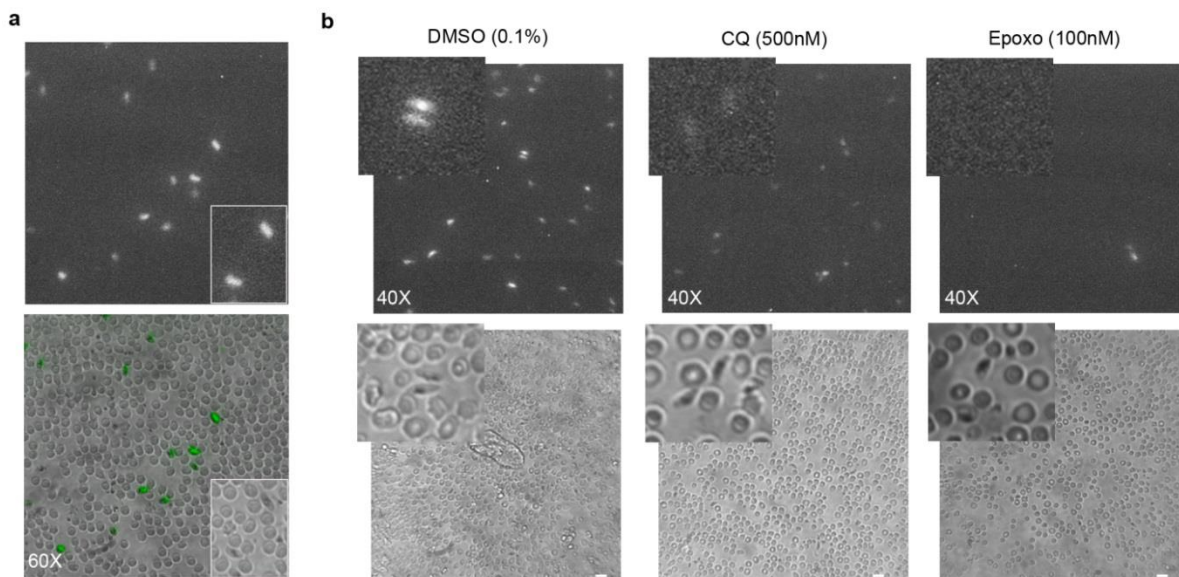


**Figure 7.** (a) Single gametocyte bioluminescence imaging of 3D7elo1-pfs16-CBG99 DMSO-treated gametocytes (60x objective, 10min acquisition). Magnification bar is 10  $\mu$ m. (b) BL imaging of control (0.1% DMSO) and drug-treated stage IV gametocytes (500nM chloroquine (CQ) and 100nM epoxomicin) (40x objective, 10min acquisition). Parts of the photographs showing representative gametocytes in the bright field and in the BL images are enlarged. Magnification bar is 10 $\mu$ m.

Imaging approaches based on the detection of transgenic BL cells are widely used in several biological systems, and have been exploited also in protozoan unicellular parasites such as *P. falciparum*, *P. berghei*, *Trypanosome cruzi* and *Leishmania* to detect parasite infections in whole animals. The availability of several luciferase variants whose emissions are optimized for detection from deep tissues is currently improving the sensitivity of such approaches to describe the patterns of sequestration in natural or engrafted mouse tissues by populations of parasites (Claser et al., 2014; Vaughan et al., 2012; Lewis et al., 2014; Taylor et al., 2014).

**Development and validation of a dual-color stage-specific luciferase assay.** To fully exploit the potential of multicolor bioluminescence, the selected green and red luciferases were combined to develop a dual-color assay to quantitatively measure stage specific effects of drugs on gametocytes at different developmental stages. Only one report in the rodent *P. berghei* parasites describes a dual luciferase assay exploiting the fact that the two enzymes require different luminogenic substrates (Helm et al., 2010), whereas our approach is based on the use of the same BL substrate and on the ability to quantitatively distinguish the simultaneous emissions of two reporters at different wavelengths.

A sensitive and robust dual-color assay ideally requires two luciferases with comparable BL intensities and virtually non-overlapping emission spectra. Our test of different novel luciferases in *P. falciparum* was motivated by the fact that the significant red-shift emission, caused by slight pH and temperature changes, of the green PpyWT luciferase (Michelini et al., 2008), makes this reporter unsuitable for dual-color assays. Although the firefly red-emitting mutant PpyRE10, with the longest emission wavelength ( $\lambda_{max}$ =617nm) and the narrowest emission spectrum (half bandwidth of 42 nm), would have represented the ideal red-emitting partner of the green-emitting CBG luciferase ( $\lambda_{max}$ =537nm), the better performance of the CBR luciferase led us to develop the dual color BL assay with the *P. plagiophthalmus* enzymes.

Experiments were preliminarily performed to achieve an efficient spectral unmixing of the CBG99 and the CBR luciferase BL emissions. A green F545 (510-580 nm) and a red F615 (590-640 nm) high-transmittance bandpass emission filters were used for the simultaneous BL acquisition. The F545 filter allowed acquisition of about 65% of the CBG and only 5% of the CBR luciferase emission, whereas with the F615 filter about 70% of the red luciferase and 16% of the green one were detected (Figure 8).

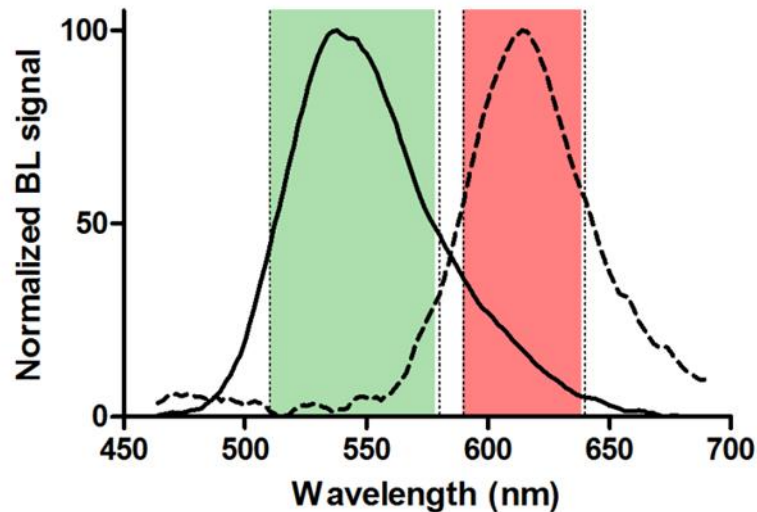


**Figure 8.** Bioluminescence emission spectra of the CBG99 (solid line) and CBR (dashed line) luciferases. Wavelengths intervals of the green F545 (510-580 nm) and red F615 (590-640 nm) bandpass filters used for the simultaneous acquisition of the two selected luciferases with Varioskan luminometer were highlighted. The F545 allows to acquire about the 65% of the CBG and only the 5% of the CBR luciferase emission, whereas the F615 filter detect about the 70% of the red luciferase and the 16% of the green one. Due to this significant overlap between BL emissions, the introduction of a spectral unmixing algorithm (such as Chroma-Luc™ calculator) is needed for quantitative and reliable luciferase activity determination.

Thanks to a spectral unmixing algorithm (Chroma-Luc™ calculator) (Almond et al., 2003) the overlap between BL emissions can be reliably calculated to achieve a quantitative determination of the specific BL contributions of the individual luciferases. Dual-color BL assays were then performed, with the above filter pair, on samples containing different proportions of CBG99- and CBR-expressing gametocytes. Results confirmed that the activities of the two luciferases within mixed gametocyte populations can be accurately quantified from the corrected green and red light emissions simultaneously recorded from the same well (Figure 9).

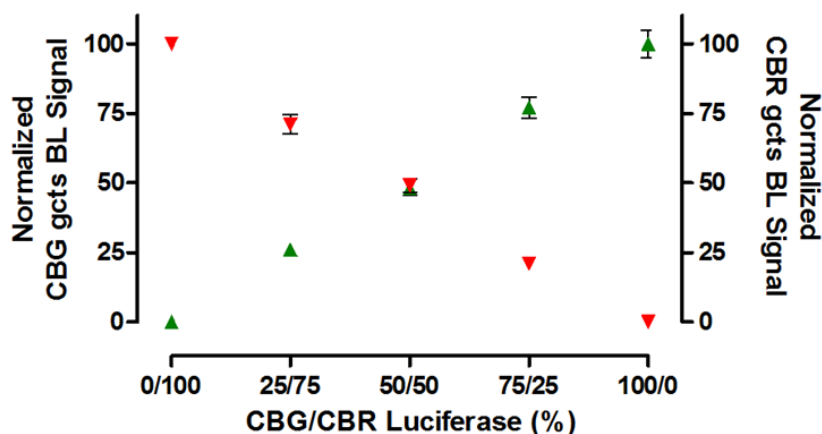


**Figure 9.** Spectral unmixing of CBG99- and CBR-luciferase expressing gametocytes. CBG99 and CBR expressing gametocytes were mixed in different proportions corresponding to the indicated percentages of CBG/CCR luciferase activities. BL acquisitions were performed with Varioskan luminometer using the F545 and F615 filters. Raw BL emissions were elaborated with the ChromaLuc™ calculator spreadsheet to extract the corrected BL emissions, i.e. the contribution to the total light output of the green and red light emitting gametocytes. The relative CBG99/CCR combinations were chosen to mimic effects of compounds active on both stages or active mainly on one stage, leading to inhibition thresholds of 50% or 75%, typically used in hit compound identification.

The ability of the dual-reporter assay to measure stage-specific drug effects was validated treating for 48h mixtures of stage II and of stage V gametocyte cultures with 500nM chloroquine, virtually inactive on mature gametocytes (Maguire et al., 2012), or 100 nM epoxomicin, killing all sexual stages (Czesny et al., 2009).

The dual assays calculated the specific emissions of the CBG99 and the CBR luciferases, which were respectively produced by early and by late gametocytes in one experiment (Figure 10 a) and by late and by early stages in the reciprocal experiment (Figure 10b). Results were that neither luciferase showed any activity after epoxomicin treatment, confirming that this drug efficiently killed both gametocyte stages. By contrast, in chloroquine-treated parasites only a minor decrease in activity was measured for either the red or the green luciferase when these were produced by the chloroquine-insensitive mature gametocytes, whereas a dramatic drop in activity of both luciferases was observed when these were expressed by the early gametocytes. The dual assay was also performed comparing the D-luciferin and the Britelite™ substrates, further supporting that assays using the non-lysing D-luciferin substrate formulation more faithfully reflect the differential stage-specific activity of these drugs and assess parasite viability (Figure 4c). Drugs killing all gametocyte stages or differentially active against immature and mature sexual stages validated the ability of the dual-color assay to quantitatively measure such stage-specific effects. The calculated assay Z' factor of  $0.71 \pm 0.03$  indicated an excellent robustness for scaling up to HTS formats. The use of a dual-color BL assay to monitor different parasite sexual stages provides a proof of principle that this approach can be used on other parasite stages, which has relevant implications for future strategies in the frame of malaria eradication.

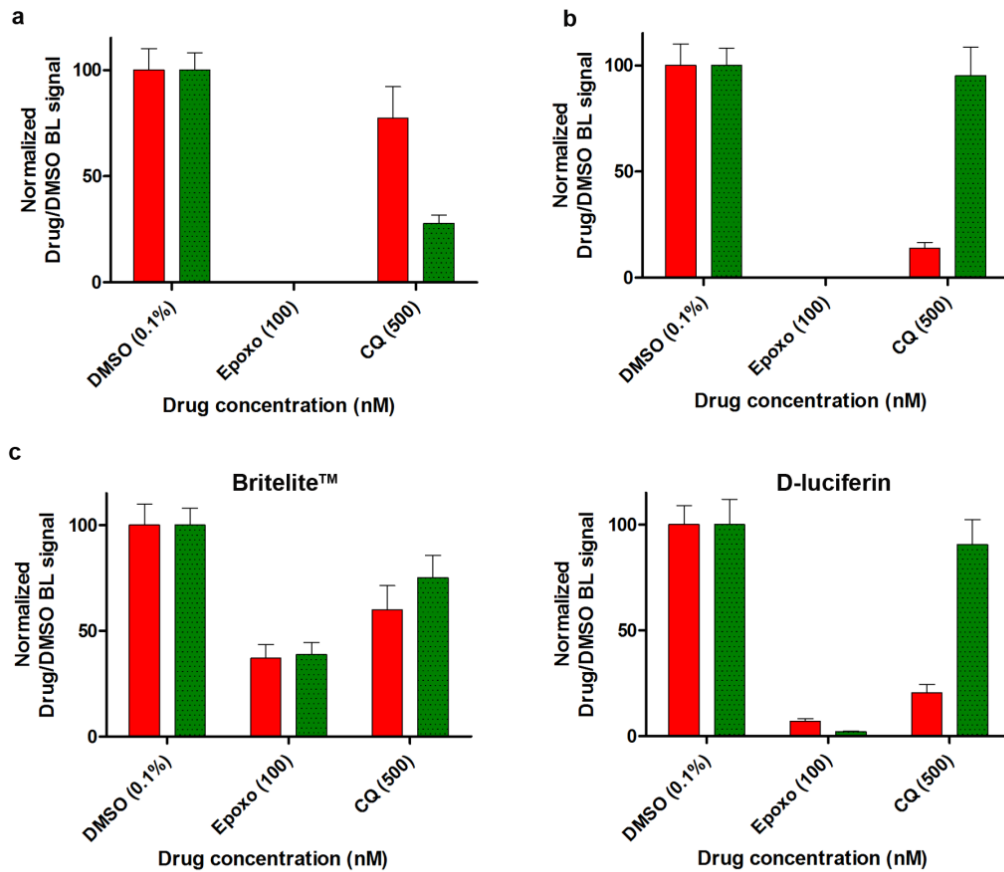


**Figure 10.** Dual-color gametocyte assay validation. **(a)** Dual-luciferase assay with early and mature gametocytes respectively expressing the CBG99 (green bar) and the CBR luciferase (red bar). BL intensities were acquired with a Varioskan luminometer using F545 and F615 optical filters. Raw BL measurements were spectrally unmixed with Chroma-Luc™ calculator and normalized with respect to DMSO control. **(b)** Reciprocal dual-color assay with mature and early stage gametocytes expressing the CBG99 and the CBR luciferase respectively. **(c)** Comparison of Britelite™ and D-luciferin performance in an independent dual-color assay using CBG99 mature stage and CBR early stage gametocytes.

## Conclusion

In this work we developed a robust, cost-effective, and reliable dual-color gametocyte assay that exploits, for the first time in malaria, the potentiality of multicolor bioluminescence. The assay provided superior analytical performance in comparison to previously reported assays with the potential of improving current drug screenings in terms of cost, time and sensitivity. We envisage that the same approach could be easily applied to develop new screening assays for identifying antimalarial drugs targeting different parasite stages. Besides, this methodology can be used for instance to simultaneously compare expression of stage-specific gene products, measure distinct cellular pathways, or evaluate the activity of an inducible or treatment-responsive promoter compared to a constitutive internal viability control, respectively driving the expression of the two luciferases in the same parasite.

Moreover, the single-cell BL imaging of the human malaria parasite *P. falciparum* opens the possibility to monitor in real time individual luciferase-expressing parasites in their stage-specific functional interactions with host tissues and cells and to assess how distinct cell types affect viability of specific parasite stages in *in vitro* and *ex vivo* settings. The concomitant significant development of affordable plate readers with customizable technical modules dedicated to multiplexing and BL imaging

will greatly facilitate the applicability of the approaches presented here both in the study of and in the fight against this deadly parasite.

## Authorship statement

I did the transfection experiments to produce the 3D7*elo1-pfs16*-CBG99 transgenic line of *P. falciparum* and performed its molecular characterization. .

## References

Adjalley, S.H., Johnston, G.L., Li, T., Eastman, R.T., Ekland, E.H., Eappen, A.G., Richman, A., Sim, B.K., Lee, M.C., Hoffman, S.L., and Fidock, D.A. (2011). Quantitative assessment of *Plasmodium falciparum* sexual development reveals potent transmission-blocking activity by methylene blue. *Proc. Natl. Acad. Sci. U S A.* 108, E1214-23.

Almond, B., Hawkins, E., Stecha, P., Garvin, D., Paguio, A., Butler, B., Beck, M., Wood, M., and Wood, K. (2003). Introducing Chroma-Luc technology. *Promega Notes.* 85, 11–14.

Branchini, B.R., Ablamsky, D.M., Murtiashaw, M.H., Uzasci, L., Fraga, H., and Southworth, T.L. (2007). Thermostable red and green light-producing firefly luciferase mutants for bioluminescent reporter applications. *Anal. Biochem.* 361, 253-262.

Branchini, B.R., Ablamsky, D.M., and Rosenberg, J.C. (2010). Chemically modified firefly luciferase is an efficient source of near-infrared light. *Bioconjugate Chem.* 21, 2023-2030.

Buchholz, K., Burke, T.A., Williamson, K.C., Wiegand, R.C., Wirth, D.F., and Marti, M. (2011). A high-throughput screen targeting malaria transmission stages opens new avenues for drug development. *J. Infect. Dis.* 203, 1445-1453.

Carter, R., Graves, P.M., Creasey, A., Byrne, K., Read, D., Alano, P., and Fenton, B. (1989). *Plasmodium falciparum*: an abundant stage-specific protein expressed during early gametocyte development. *Exp. Parasitol.* 69, 140-149.

Cevenini, L., Michelini, E., D'Elia, M., Guardigli, M., and Roda, A. (2013). Dual-color bioluminescent bioreporter for forensic analysis: evidence of androgenic and anti-androgenic activity of illicit drugs. *Anal. Bioanal. Chem.* 405, 1035-1045.

Che, P., Cui, L., Kutsch, O., Cui, L., and Li, Q. (2012). Validating a firefly luciferase-based high-throughput screening assay for antimalarial drug discovery. *Assay Drug Dev. Technol.* 10, 61-68.

Claser, C., Malleret, B., Peng, K., Bakocevic, N., Gun, S.Y., Russell, B., Ng, L.G., and Rénia, L. (2014). Rodent *Plasmodium*-infected red blood cells: imaging their fates and interactions within their hosts. *Parasitol. Int.* 63, 187-194.

Czesny, B., Goshu, S., Cook, J.L., and Williamson, K.C. (2009). The proteasome inhibitor epoxomicin has potent *Plasmodium falciparum* gametocytocidal activity. *Antimicrob. Agents Chemother.* 53, 4080-4085.

D'Alessandro, S., Silvestrini, F., Dechering, K., Corbett, Y., Parapini, S., Timmerman, M., Galastri, L., Basilico, N., Sauerwein, R., Alano, P., and Taramelli, D. (2013). A *Plasmodium falciparum* screening assay for anti-gametocyte drugs based on parasite lactate dehydrogenase detection. *J. Antimicrob. Chemother.* 68, 2048-2058.

Duffy, S., and Avery, V.M. (2013). Identification of inhibitors of *Plasmodium falciparum* gametocyte development. *Malar. J.* 12, 408.

Ekström, L., Cevenini, L., Michelini, E., Schulze, J., Thörngren, J.O., Belanger, A., Guillemette, C., Garle, M., Roda, A., and Rane, A. (2013). Testosterone challenge and androgen receptor activity in relation to UGT2B17 genotypes. *Eur. J. Clin. Invest.* 43, 248-255.

Fidock, D.A., and Wellems, T.E. (1997). Transformation with human dihydrofolate reductase renders malaria parasites insensitive to WR99210 but does not affect the intrinsic activity of proguanil. *Proc. Natl. Acad. Sci. U.S.A.* 94, 10931-10936.

Hasenkamp, S., Wong, E.H., and Horrocks, P. (2012). An improved single-step lysis protocol to measure luciferase bioluminescence in *Plasmodium falciparum*. *Malar. J.* 10, 11-42.

Hawking, F., Wilson, M.E., and Gammage, K. (1971). *Trans. R. Soc. Trop. Med. Hyg.* 65, 549-559.

Helm, S., Lehmann, C., Nagel, A., Stanway, R.R., Horstmann, S., Llinas, M., and Heussler, V.T. (2010). Identification and characterization of a liver stage-specific promoter region of the malaria parasite *Plasmodium*. *PLoS One.* 5, e13653.

Lelièvre, J., Almela, M.J., Lozano, S., Miguel, C., Franco, V., Leroy, D., and Herreros, E. (2012). Activity of clinically relevant antimalarial drugs on *Plasmodium falciparum* mature gametocytes in an ATP bioluminescence "transmission blocking" assay. *PLoS One.* 7, e35019.

Lewis, M.D., Fortes Francisco, A., Taylor, M.C., Burrell-Saward, H., McLatchie, A.P., Miles, M.A., and Kelly, J.M. (2014). Bioluminescence imaging of chronic *Trypanosoma cruzi* infections reveals tissue-specific parasite dynamics and heart disease in the absence of locally persistent infection. *Cell Microbiol.* doi: 10.1111/cmi.12297.

Lucantoni, L., Duffy, S., Adjalley, S.H., Fidock, D.A., and Avery, V.M. (2013). Identification of MMV malaria box inhibitors of plasmodium falciparum early-stage gametocytes using a luciferase-based high-throughput assay. *Antimicrob. Agents Chemother.* 57, 6050-6062.

Maguire, C.A., van der Mijn, J.C., Degeling, M.H., Morse, D., and Tannous, B.A. (2012). Codon-optimized *Luciola italica* luciferase variants for mammalian gene expression in culture and in vivo. *Mol. Imaging.* 11, 13-21.

Michelini, E., Cevenini, L., Mezzanotte, L., Ablamsky, D., Southworth, T., Branchini, B.R., and Roda, A. (2008). Combining intracellular and secreted bioluminescent reporter proteins for multicolor cell-based assays. *Photochem. Photobiol. Sci.* 2, 212-217.

Michelini, E., Cevenini, L., Mezzanotte, L., and Roda, A. (2009). Luminescent probes and visualization of bioluminescence. *Methods Mol. Biol.* 574, 1-13.

Olivieri, A., Camarda, G., Bertuccini, L., van de Vegte-Bolmer, M., Luty, A.J., Sauerwein, R., and Alano, P. (2009). The Plasmodium falciparum protein Pfg27 is dispensable for gametocyte and gamete production, but contributes to cell integrity during gametocytogenesis. *Mol. Microbiol.* 73, 180-193.

Silvestrini, F., Lasonder, E., Olivieri, A., Camarda, G., van Schaijk, B., Sanchez, M., Younis, S., Sauerwein, R., and Alano, P. (2010). Protein export marks the early phase of gametocytogenesis of the human malaria parasite Plasmodium falciparum. *Mol. Cell Proteomics.* 9, 1437-1448.

Straimer, J., Lee, M.C., Lee, A.H., Zeitler, B., Williams, A.E., Pearl, J.R., Zhang, L., Rebar, E.J., Gregory, P.D., Llinás, M., Urnov, F.D., and Fidock, D.A. (2012). Site-specific genome editing in Plasmodium falciparum using engineered zinc-finger nucleases. *Nat. Methods.* 9, 993-998.

Tanaka, T.Q., and Williamson, K.C. (2011). A malaria gametocytocidal assay using oxidoreduction indicator, alamarBlue. *Mol. Biochem. Parasitol.* 177, 160-163.

Tanaka, T.Q., Dehdashti, S.J., Nguyen, D.T., McKew, J.C., Zheng, W., and Williamson, K.C. (2013). A quantitative high throughput assay for identifying gametocytocidal compounds. *Mol. Biochem. Parasitol.* 188, 20-25.

Taylor, M.C., and Kelly, J.M. (2014). Optimizing bioluminescence imaging to study protozoan parasite infections. *Trends Parasitol.* 30, 161-162.

Trager, W., and Jensen, J.B. (1976). Human malaria parasites in continuous culture. *Science.* 193, 673-675.



Vaughan, A.M., Mikolajczak, S.A., Wilson, E.M., Grompe, M., Kaushansky, A., Camargo, N., Bial, J., Ploss, A., and Kappe, S.H. (2012). Complete Plasmodium falciparum liver-stage development in liver-chimeric mice. *J. Clin. Invest.* 122, 3618-3628.

Walliker, D., Quakyi, I.A., Wellems, T.E., McCutchan, T.F., Szarfman, A., London, W.T., Corcoran, L.M., Burkot, T.R., and Carter, R. (1987). Genetic analysis of the human malaria parasite Plasmodium falciparum. *Science.* 236, 1661-1666.

Wang, Z., Liu, M., Liang, X., Siriwat, S., Li, X., Chen, X., Parker, D.M., Miao, J., and Cui, L. (2014). A flow cytometry-based quantitative drug sensitivity assay for all Plasmodium falciparum gametocyte stages. *PLoS One.* 9, e93825.

Wood, K.V., Lam, Y.A., and McElroy, W.D. (1989). Introduction to beetle luciferases and their applications. *J. Biolumin. Chemilumin.* 1, 289-301.

Zhang, J.H., Chung, T.D., and Oldenburg, K.R. (1999). A Simple Statistical Parameter for Use in Evaluation and Validation of High Throughput Screening Assays. *J. Biomol. Screen.* 4, 67-73.

# Synergy of drugs affecting the redox equilibrium of *Plasmodium falciparum* mature gametocytes investigated with a bioluminescence assay specific for late sexual stages

Giulia Siciliano<sup>1</sup>, T. R. Santha Kumar<sup>2</sup>, Roberta Bona<sup>3</sup>, Grazia Camarda<sup>1#</sup>, Maria Maddalena Calabretta<sup>4</sup>, Luca Cevenini<sup>4</sup>, Katja Becker<sup>5</sup>, Elisabeth Davioud-Charvet<sup>6</sup>, Andrea Cara<sup>3</sup>, David A. Fidock<sup>2,7</sup>, Pietro Alano<sup>1</sup>.

1 Dipartimento di Malattie Infettive, Parassitarie ed Immunomediate, Istituto Superiore di Sanità, Rome, Italy. 2 Department of Microbiology and Immunology, Columbia University Medical Center, New York, USA. 3 Dipartimento Farmaco, Istituto Superiore di Sanità, Rome, Italy. 4 Department of Chemistry "G. Ciamician", University of Bologna, Bologna, Italy. 5 Biochemistry and Molecular Biology, Interdisciplinary Research Center, Justus Liebig University Giessen, Germany. 6 UMR 7509 Centre National de la Recherche Scientifique and University of Strasbourg, European School of Chemistry, Polymers and Materials (ECPM), Strasbourg, France. 7 Division of Infectious Diseases, Department of Medicine, Columbia University Medical Center, New York, USA.

This manuscript is in preparation for submission to the Journal of Infectious Diseases

**Abstract:** Killing the terminally differentiated mature (stage V) gametocytes of *Plasmodium falciparum*, responsible for humans to mosquito parasite transmission, is essential for malaria eradication. The non-dividing nature and the apparently low metabolism of these stages makes it challenging to identify targetable cellular processes and to reliably measure sensitivity to compounds of late gametocytes in drug screenings.

A *P. falciparum* line was developed in which the potent click beetle luciferase CBG99 is chromosomally integrated and transcriptionally regulated by the PFL1675c parasite promoter. This sequence was functionally selected for efficiently and specifically activating reporter expression in stage V gametocytes. Bioluminescence of mature gametocytes from this line is measured with a novel luciferase protocol using a non-lysing, ATP free D-luciferin substrate formulation. This improved assay sensitively and reliably monitors gametocyte viability and sensitivity to compounds.

The fact that the pro-oxidant drug methylene blue (MB) efficiently inhibits gametocyte development and transmission drove our attention to targeting the poorly described redox equilibrium of late gametocytes and to investigate MB mode of action. Drugs and compounds described to unbalance the parasite redox equilibrium in asexual parasites were tested alone and in combination with MB and IC<sub>50</sub> were measured on mature gametocytes. These experiments revealed that inhibitors of the parasite pentose phosphate pathway, producing most of the infected erythrocyte NADPH, are virtually ineffective on late gametocytes but, intriguingly, they potently synergize MB activity against these parasites.

This work identifies redox equilibrium as a promising drug target in mature gametocytes. Measuring gametocyte sensitivity to different pro-oxidant drug combinations will drive the design of the most appropriate transmission blocking treatment(s).

## Introduction

Malaria is the most severe parasitic mosquito-borne disease, with an enormous burden for human population, especially for poor communities in endemic countries.

According to the last estimates, 200 million cases of malaria occurred globally in 2013 leading to 600 000 deaths, mostly caused by the parasite *Plasmodium falciparum*, with 90% of the cases located in Africa and with 78% of the annual deaths occurring in children aged under 5 years, with pregnant women at higher risk (WHO World Malaria Report 2014).

The symptoms of the disease are due to the asexual cycle of *P. falciparum* parasites, causing fever, anemia, acidosis, renal failure and cerebral and placental malaria, with the latter symptoms causing coma and death, and mother and fetal death, respectively, in the most serious cases (Tilley et al; 2011).

Responsible of parasite transmission from the human host to the *Anopheles* mosquito vector are the mature gametocytes, the sexual parasite forms that, in *P. falciparum*, develop in 10-12 days in the human host and, once ingested with the blood meal, are activated to become female and male gametes into the mosquito midgut, where fertilization and subsequent maturation of the zygote occur. The zygote produces an ookinete, which further transform into an oocyst, leading to sporozoites ready to infect another human host during the next mosquito bite.

The necessity of eradicating *P. falciparum* malaria in the World has been recently focusing the attention on finding drugs able to kill the transmittable mature gametocytes. An obstacle along this path proved to be that, in contrast to asexual parasites and, partly, to early stage gametocytes, mature gametocytes are insensitive to virtually all anti-malarial drugs (Adjalley et al. PNAS 2011), possibly because they appear as quiescent, low metabolically active cells (Delves et al. 2013, Sinden et al. 1978).

With the exception of primaquine, that besides killing *P. vivax* asexual stages is active also on *P. falciparum* gametocytes, although it is not totally safe in humans (Butterworth et al., 2013) and the only drug described to be efficiently active against *P. falciparum* gametocytes at different maturation stages is methylene blue (MB) (Adjalley et al. 2011). MB is a heterocyclic aromatic compound whose mechanism of action against the malaria parasites is controversial with the most commonly accepted model being that this molecule acts as a redox cyler, accepting electrons from the flavoprotein glutathione reductase (GR) (Ehrhardt et al., 2013) . GR is responsible for the production of the reducing agent glutathione, whose pathway is very important for the parasite detoxification from the free oxygen species mainly deriving from hemoglobin digestion in the infected red blood cell (Tripathi et al., 2007), described to occur in all asexual stages of *P. falciparum* and also during gametocyte development, until the gametocyte reaches stage IV of maturation (Hanssen et al., 2012).

The fact that the pro-oxidant drug MB efficiently inhibits gametocyte development and parasite transmission to the vector drove our attention to the poorly described redox equilibrium of late stage gametocytes as a promising new target, and to investigate the mode of action of MB.

The non-dividing nature and the apparently low metabolism of mature gametocytes make it challenging to identify targetable cellular processes in these cells. In addition, the same features make it difficult to reliably measure sensitivity to compounds of late gametocytes in drug screenings. To overcome this problem, and to develop a tool enabling to investigate this and other similar questions on late gametocyte drug sensitivity, we developed a transgenic line in which the potent click beetle luciferase CBG99 (Cevenini et al., 2014) is chromosomally integrated and transcriptionally regulated by a newly identified late gametocyte-specific promoter. This sequence was functionally selected for efficiently and specifically activating reporter gene expression in stage V gametocytes.

Use of this transgenic line enabled us to quantitatively measure effects on mature gametocytes of a panel of drugs and compounds described to unbalance the parasite redox equilibrium in asexual parasites. Effects of combination of compounds, targeting different enzymes involved in redox balance, were also investigated. This work leads to reveal that the action of MB on stage V gametocyte can be potently synergized by simultaneously inhibiting the pentose phosphate pathway.

## Materials and Methods

**Parasite cultures and transfections.** The *P. falciparum* 3D7A (Walliker et al., 1987) and NF54<sup>attB</sup> (Adjalley et al., 2011) lines were cultured in human 0+ erythrocytes, kindly provided by Prof. G. Girelli, Dipartimento di Biopatologia Umana, University of Rome “La Sapienza”, at 5% haematocrit under 5% CO<sub>2</sub>, 2% O<sub>2</sub>, 93% N<sub>2</sub> (Trager et al., 1976). Cultures were grown in medium containing RPMI 1640 medium (Gibco) supplemented with 25 mM Hepes, 50 µg/ml hypoxanthine, 0.25 mM NaHCO<sub>3</sub>, 50 µg/ml gentamicin sulphate and 10% pooled heat-inactivated 0+ human serum. Ring stage parasites at 3–5% parasitaemia were transfected by electroporation with 80–100 µg of transfection vectors using a BioRad electroporator with the following conditions: voltage, 0.31 kV; capacitance, 960 µF; resistance to infinity (Fidock et al., 1997).

Production of the transgenic lines expressing GFP under control of candidate gene regulatory sequences (Upregulated in Late Gametocytes, ULG) carried by episomal plasmids was obtained by transfecting the *P. falciparum* 3D7A with the pASEX-ULG-GFP plasmids described below and in Figure 1. Following transfection, parasites were maintained in drug free medium for 24h; at this time, positive selection was initiated by adding 2.5 nM WR99210.

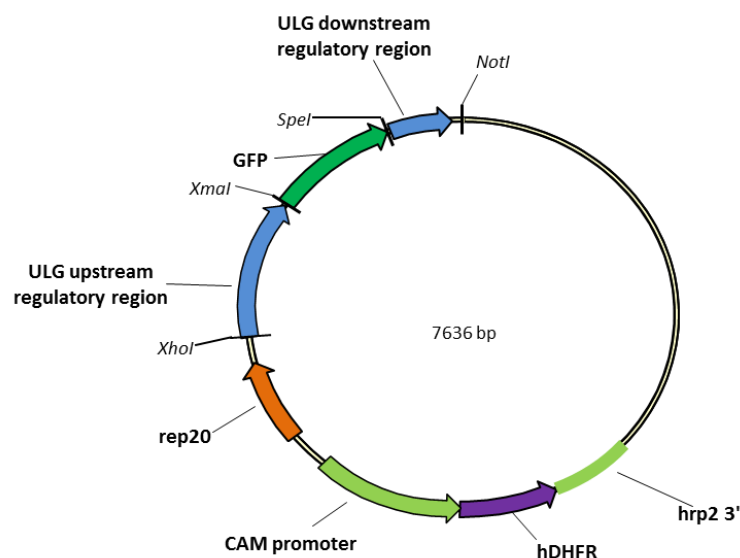


**Figure 1.** Map of a representative pASEX-ULG-GFP plasmid containing the GFP reporter gene flanked by the *P. falciparum* ULG upstream and downstream regulatory regions. The plasmid contains the human dihydrofolate reductase (*hDHFR*) gene, flanked by the calmodulin (*CAM*) promoter and the histidine rich protein 2 (*hrp2*) gene 3' UTR as the WR99210 selection marker. The *rep20* sequence facilitates plasmid segregation in daughter cells (O'Donnell et al., 2002).

Production of the transgenic line with a stably integrated CBG99 luciferase under the expression control of the pfULG8 regulatory regions was obtained transfecting plasmid pCR2.1-attP-FRT-

hDHFR/GFP-ULG8-CBG99 (Figure 2), which contained an *attP* site for Bbx1 mediated integration (Nkumah et al., 2006) in the parasite line NF54<sup>attB</sup> of *P. falciparum*. These parasites contain a Bbx1 *attB* site in the *cg6* gene. Plasmid pCR2.1-*attP*-FRT-hDHFR/GFP-ULG8-CBG99 was co-transfected with a plasmid expressing the *integrase* gene (pINT plasmid; Adjalley et al., 2011). Double selection started 24h after transfection by adding 250 µg/ml of G418 and 2.5nM of WR99210. After 6 days of double selection, parasites were treated only with 2.5nM of WR99210 and after other 3 days parasites were allowed to recover in the absence of any drug.

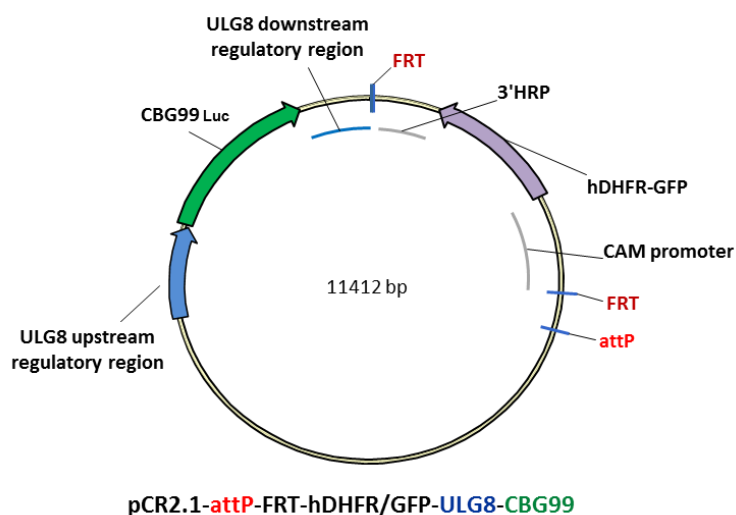


**Figure 2.** Map of the pCR2.1-*attP*-FRT-hDHFR/GFP-ULG8-CBG99 plasmid. The plasmid contains the CBG99 luciferase gene flanked by the *P. falciparum* ULG8 upstream and downstream regulatory regions, the selection cassette constituted by the *hDHFR* (human dihydrofolate reductase) coding sequence fused to that of the *GFP* (Green Fluorescent Protein) gene, flanked by the calmodulin promoter (*CAM*) and the histidine rich protein 2 (*hrp2*) gene 3' UTR. The *FRT* sequences flanking the selection cassette enable the removal of the selection cassette using the FLP recombinase enzyme (van Schaijk et al., 2010). The *attP* site mediates the integration of the plasmid into an *attB* site through activity of a Bbx-1 integrase enzyme (Adjalley et al., 2011).

**Plasmid construction.** The multistep cloning strategy to obtain the pASEX-ULG-GFP vectors carrying a GFP expression cassette under the ULG regulatory regions was as follows. The pASEX-GFP plasmid The downstream regulatory regions of genes *pfs28*, *mal8p1.16* and ULG1-8 were PCR amplified using the primer pairs #3 and #4, #7 and #8, #11 and #12, #15 and #16, #19 and #20, #23 and #24, #27 and #28, #31 and #32, #35 and #36, #39 and #40 in Table 1.

| # | Primer name                      | Sequence (5'-3')                                  | Sites |
|---|----------------------------------|---|-------|
| 1 | pfs28 upstream sequence dir      | gggCTCGAGATATATATTTTTAAATGGTAAATTATCAAGG          | XhoI  |
| 2 | pfs28 upstream sequence rev      | gggCCCGGGTGTATTCATTGTATAAAAACTAAAAATATAAAATAATAAG | XmaI  |
| 3 | pfs28 downstream sequence dir    | gggACTAGTATATATATATATATATATAGTCATATGATTTGC        | SpeI  |
| 4 | pfs28 downstream sequence rev    | gggGCGGCCGCATTTTTATGAATATATACTCAACC               | NotI  |
| 5 | mal8.p1.16 upstream sequence dir | gggCTCGAGTCTCTATATACTATGGAATATGTGC                | XhoI  |
| 6 | mal8.p1.16 upstream sequence rev | gggCCCGGGTCTTAACATTGCGTGGGATTAATATTTAATG          | XmaI  |

|    |                                    |  |      |
|----|------------------------------------|--|------|
| 7  | mal8.p1.16 downstream sequence dir | gggACTAGTCAAAAAAAAAATAAAATTTGAATAAATTGG        | SpeI |
| 8  | mal8.p1.16 downstream sequence rev | gggGCGGCCGCACAAATGTAATCAATGATTATATGAAGTGGG     | NotI |
| 9  | ULG1 upstream sequence dir         | gggCTCGAGGGAAGTAAAGATAAAGAAAGTGAACG            | XhoI |
| 10 | ULG1 upstream sequence rev         | gggCCCGGGATAATTCATTACTAGGAATTATAAAG            | XmaI |
| 11 | ULG1 downstream sequence dir       | gggACTAGTAAAGAAATTCGTATAAAAAATTTATGTTGC        | SpeI |
| 12 | ULG1 downstream sequence rev       | gggGCGGCCGCATTATATACATACTTCAAATATACG           | NotI |
| 13 | ULG2 upstream sequence dir         | gggCTCGAGCGTTTTTAAATGGTTATTAGAAAATCCG          | XhoI |
| 14 | ULG2 upstream sequence rev         | gggCCCGGGACTTTCATGTCTGTTCTGTTATGTTATC          | XmaI |
| 15 | ULG2 downstream sequence dir       | gggACTAGTGATGGAAGAATATTATATGAGTG               | SpeI |
| 16 | ULG2 downstream sequence rev       | gggGCGGCCGCAAAAACCACGAATAAATAATACGCC           | NotI |
| 17 | ULG3 upstream sequence dir         | gggCTCGAGTTAATAAAGCTTGTTCATAATTTCTAGG          | XhoI |
| 18 | ULG3 upstream sequence rev         | gggCCCGGGCGATTACTTGCAGGTAATGTAGCCATTG          | XmaI |
| 19 | ULG3 downstream sequence dir       | gggACTAGTTAAGATATAATCTTGAATAGAACAGC            | SpeI |
| 20 | ULG3 downstream sequence rev       | gggGCGGCCGCTTTTTCAAATGTCTATAAAGAGC             | NotI |
| 21 | ULG4 upstream sequence dir         | gggCTCGAGGCTCTTTATATCCATCACATCCATTAGC          | XhoI |
| 22 | ULG4 upstream sequence rev         | gggCCCGGGTTAAACATTTTTACTATAATTAATAAAC          | XmaI |
| 23 | ULG4 downstream sequence dir       | gggACTAGTGGAAGAAGATAATAAATGATG                 | SpeI |
| 24 | ULG4 downstream sequence rev       | gggGCGGCCGCATAATATACAAAACATCTGAGG              | NotI |
| 25 | ULG5 upstream sequence dir         | gggCTCGAGTTCACTATATTAAGGTGGAAGACTCC            | XhoI |
| 26 | ULG5 upstream sequence rev         | gggCCCGGGATACATCATGTACAGAAATAATGGAATGACAG      | XmaI |
| 27 | ULG5 downstream sequence dir       | gggACTAGTAAGGTCATATAAAAAGGAATATAAAAATTAC       | SpeI |
| 28 | ULG5 downstream sequence rev       | gggGCGGCCGCATTGTTTTATTTTATCCCTAGGG             | NotI |
| 29 | ULG6 upstream sequence dir         | gggCTCGAGCCAGAACAAAATAAAGACTGAACAAGG           | XhoI |
| 30 | ULG6 upstream sequence rev         | gggCCCGGGCGAAACATTTTTTATTAATAAAAATAGGAACAATTAG | XmaI |
| 31 | ULG6 downstream sequence dir       | gggACTAGTTTATTTATTTAATAAATTATGAAAAATAGTGG      | SpeI |
| 32 | ULG6 downstream sequence rev       | gggGCGGCCGCTGTAAGGTGCTTGTGAAGGATTTGCGC         | NotI |
| 33 | ULG7 upstream sequence dir         | gggCTCGAGATACATATAATACAAAATTTACGCACC           | XhoI |
| 34 | ULG7 upstream sequence rev         | gggCCCGGGATAGGACATCTTAAATTTATTTGTATATATGACAG   | XmaI |
| 35 | ULG7 downstream sequence dir       | gggACTGAGCATTTTATACGATAAAATGTATAAGATTATG       | SpeI |
| 36 | ULG7 downstream sequence rev       | gggGCGGCCGCTCTAAATATACAGTGTGTACTACTCC          | NotI |
| 37 | ULG8 upstream sequence dir         | gggCTCGAGCAACAGTAAAAATAAATGAATAAAAAAACC        | XhoI |
| 38 | ULG8 upstream sequence rev         | gggCCCGGGGAAAGACATTTCAAAAAATATAAAAAAATTAC      | XmaI |
| 39 | ULG8 downstream sequence dir       | gggACTAGTTATATATAATAACAATACAATATATTATACC       | SpeI |
| 40 | ULG8 downstream sequence rev       | gggGCGGCCGCAAAATTATTTTATTATATATTTTGTAGATAGCC   | NotI |

**Table 1.** List of primers used to amplify the ULG upstream and downstream regulatory regions.

These PCR amplification products (sizes and gene names are indicated in Table 2) were cloned into a SpeI-NotI digested pASEX-GFP plasmid (Pace et al., 2006), producing intermediate pASEX-GFP constructs containing these downstream late regulatory regions. The upstream genomic regions of the *pfs28*, *mal8p1.16* and ULG1-8 genes were PCR amplified using the primer pairs #1 and #2, #5 and #6, #9 and #10, #13 and #14, #17 and #18, #21 and #22, #25 and #26, #29 and #30, #33 and #34, #37 and #38 of Table 1. These fragments (sizes and gene names are indicated in Table 2) were cloned into the above intermediate plasmids after XhoI-XmaI digestion to produce the final pASEX-ULG-GFP, pASEX-*pfs28*-GFP and pASEX- *mal8p1.16*-GFP constructs.

| Gene name                  | Code | Bp upstream region | Bp downstream region |
|----------------------------|------|--------------------|----------------------|
| PF3D7_1030900/pfs28        | -    | 1620               | 670                  |
| PF3D7_0828000/mal8p1.16    | -    | 1519               | 784                  |
| PF3D7_1338800 /mal13p1.195 | ULG1 | 1529               | 718                  |
| PF3D7_1362600/mal13p1.312  | ULG2 | 1340               | 668                  |
| PF3D7_0816800/mal8p1.76    | ULG3 | 1608               | 815                  |
| PF3D7_0303900/pfc0176c     | ULG4 | 1590               | 835                  |
| PF3D7_0506400/pfe0315c     | ULG5 | 1387               | 835                  |
| PF3D7_1214500 /pfl0700w    | ULG6 | 1466               | 691                  |
| PF3D7_1221400/pfl1030w     | ULG7 | 1700               | 769                  |
| PF3D7_1234700/pfl1675c     | ULG8 | 1034               | 661                  |

**Table 2.** Names and sizes of the regulatory regions selected.

The multistep cloning strategy to obtain the PCR2.1-attP-FRT-hDHFR/GFP-ULG8-CBG99 plasmid was as follows. The pCR-2.1-pfs16-CBG99 plasmid (Cevenini et al., 2014) was digested with NcoI-XbaI and the NcoI site was blunted by fill in using the Klenow polymerase according to manufacturer instructions (New England Biolab) to remove the CBG99 luciferase coding sequence, which was inserted in the SmaI-SpeI digested pASEX-ULG8-GFP plasmid to replace the GFP coding sequence and to produce plasmid pASEX-ULG8-CBG99. The hDHFR/GFP selection cassette flanked by the FRT sites was obtained digesting with SmaI-ScaI plasmid MV129-Pf36p-DXO-hDHFR-GFP (van Schaijk et al., 2010) and was inserted into a SnaBI-EcoRV digested pCR2.1-attP plasmid (Nkrumah et al. 2006) to produce plasmid pCR2.1-attP-FRT-hDHFR/GFP. Finally, the pASEX-ULG8-CBG99 plasmid was digested with XhoI-NotI and the ULG8-CBG99 cassette was inserted into the XhoI-NotI digested pCR2.1-attP-FRT-hDHFR/GFP plasmid, forming the pCR2.1-attP-FRT-hDHFR/GFP-ULG8-CBG99 plasmid.

**Southern blot analysis.** This is still ongoing at Columbia University of New York.

**Time course of CBG99 luciferase activity in gametocyte development.** The NF54-cg6-hDHFR/GFP-ULG8-CBG99 parasite culture was induced to undergo gametocyte production by parasite overgrowth. At 48h after N-acetyl-glucosamine (NAG) treatment to eliminate residual asexual stage parasites, stage I/II gametocytes were partially purified from uninfected erythrocytes with a 60% Percoll density gradient centrifugation (Kariuki et al., 1998) and were incubated in complete medium until maturation. Aliquots of  $1 \times 10^5$  purified gametocytes from stage I/II to stage V were collected and frozen daily for a total of 13 days. To measure bioluminescence, the gametocyte pellets were resuspended in 100 $\mu$ l of 1X PBS supplemented with protease inhibitors (Complete™) and, after the addition of 100 $\mu$ l of Britelite Plus™ substrate (Perkin Elmer), luciferase activity of each sample was measured for 30 seconds on a Lumat LB 9501 Tube Luminometer.

**Luciferase assays on stage V gametocytes.** Gametocytes from the NF54-cg6-hDHFR/GFP-ULG8-CBG99 culture at stage V of maturation were exposed to different concentration of different compounds. Asexual cultures grown under conditions to induce gametocyte production were treated with N-Acetylglucosamine (NAG) for 96 hours at the onset of gametocytogenesis to clear asexual parasites. After NAG treatment gametocytes were purified from uninfected erythrocytes on MACS Separation Columns CS (Miltenyi Biotec) and allowed to mature. To calculate the IC<sub>50</sub>s, compounds (Table 3) serial dilutions were prepared and dispensed in 96-well plates in a final volume of 100  $\mu$ L per well. Synchronous  $1 \times 10^5$  stage V gametocytes (day X after NAG) were re-suspended in 100  $\mu$ L of complete medium and incubated with the compounds at 37°C for the time indicated. To calculate the IC<sub>50</sub> of MB on mature gametocytes in presence of a fixed dose of different compounds, MB was dispensed in 96-well plates as described above. Synchronous  $1 \times 10^5$  stage V gametocytes were re-suspended in 100  $\mu$ L of complete medium with 1 $\mu$ M of the different compounds and incubated with MB at 37°C., cell viability was evaluated by measuring luciferase activity of each sample for one second on a Varioskan™ Flash Multimode Reader (Thermo Scientific) after addition of 0.5 nM of D-Luciferin. The percentage viability was calculated as a function of drug concentration and curve fitting was obtained by non-linear regression analysis (GraphPad Prism 6.0).

| Code          | Name   |
|---------------|--|
| MB            | Methylene blue   |
| ML304         | (R)-N-((1-ethylpyrrolidin-2-yl)methyl)-4-methyl-11-oxo-10,11-dihydrodibenzo[b,f][1,4]thiazepine-8-carboxamide (PfGluPho inhibitor) |
| JB047         | Plasmodione (P_TM29)   |
| MB030         | 6-fluoro-analogue of P_TM29  |
| MB017         | Benzoylmenadione (P_TM29 metabolite I)   |
| M5            | Menadione derivative (GR inhibitor)  |
| P_TM22        | Menadione derivative (GR inhibitor)  |
| Paracetamol   | Acetaminophen (GSH depletor)   |
| Ascorbic acid | Vitamin C  |



|      |   |
|------|---|
| AG16 | Nam-based dual drug affecting the NADPH balance |
|------|---|

**Table 3.** List of codes and full names of the compounds used in this study.

## Results

**Development of a *P. falciparum* reporter line expressing luciferase specifically and efficiently in mature gametocytes.** To functionally identify parasite regulatory regions able to efficiently and specifically upregulate gene expression in late gametocytes, quantitative microarray data from time courses of asexual and sexual development were inspected (Le Roche et al., 2003; Young et al., 2005) (Figure 3). Pairs of upstream and downstream genomic regions were selected from eight genes whose transcripts preferentially accumulated in late stage gametocytes, which were called ‘Upregulated in Late Gametocytes’ (ULG1-8). Flanking regions were also obtained from genes *pfs28* (Eksi et al., 2008) and *mal8p1.16*, encoding a rhomboid protease (Adjalley et al., 2011), as these are the only two genes whose promoters have been used so far to express reporter genes in *P. falciparum* late stage gametocytes. Ten plasmids were altogether produced as described in Materials and methods (Table 1, Figure 1, Table 2) in which the above parasite regulatory sequences were used to drive GFP expression from episomal plasmids transfected in ten 3D7 derivative lines. FACS analysis of GFP expression in early and late stage gametocytes of the transgenic lines revealed that the pfULG8 regulatory regions combined the highest degree of stage specificity with the highest efficiency of expression compared to the genomic flanking regions from the other ULG candidates and importantly performed better than both reference late gametocyte promoters *pfs28* and *mal8p1.16*. In the pfULG8-GFP gametocytes GFP expression increased five-fold in late stage V compared to the immature stage II/III gametocytes (Figure 4a).

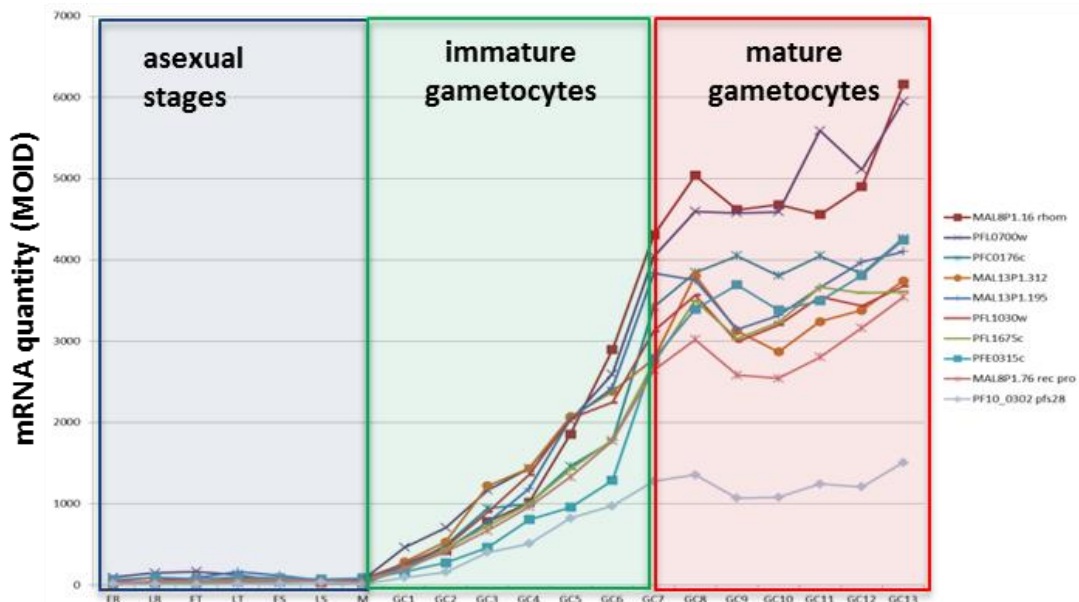


**Figure 3.** Transcript abundance of the eight ULG candidate genes and of the *pfs28* and the *mal8p1.16* genes mRNAs during the asexual cycle and gametocytogenesis. Microarray expression values (Match-Only Integral Distribution, MOID) are compiled from the time course analysis described in Le Roch et al., 2003 and Young et al., 2005. Parasite stages are ER: early

rings, LR: late rings, ET: early trophozoites, LT: late trophozoites, ES: early shizonts, LS: late shizonts, GC 1-13: gametocytogenesis day 1-13.

The ULG8 gene regulatory regions were therefore used to obtain a parasite line in which they could similarly regulate expression of a luciferase reporter, in this case stably integrated in the parasite's genome. The ULG8 regions were engineered to flank the *Phyrophorus plagiophthalmus* CBG99 luciferase gene as described, which was recently shown to be a potent bioluminescent reporter in all gametocyte stages (Cevenini et al., 2014). To produce such reporter line the plasmid containing the ULG8-CBG99 expression cassette was inserted into the *cg6* gene of a *P. falciparum* NF54<sup>attB</sup> line, by the co-transfection of this plasmid with a plasmid expressing the integrase of the Bxb1 mycobacteriophage (Nkrumah et al., 2006), generating the NF54-cg6-hDHFR/GFP-ULG8-CBG99 line (Figure 4b). To evaluate the reporter activity of the newly generated line, gametocytogenesis was induced and luciferase activity was measured daily on gametocytes from stage II to stage V. The profile of bioluminescence from the synchronized gametocytes clearly showed a significant increase in luciferase activity starting from the appearance of stage V gametocytes (Figure 4c). As in the ULG8-GFP gametocytes, the NF54-cg6-hDHFR/GFP-ULG8-CBG99 line, where the luciferase cassette is chromosomally integrated, showed a similar stage specificity of reporter activation in late sexual stages, with a similar five-fold increase in luciferase activity compared to the immature (stage II-III) gametocytes. Importantly to the use in compound screenings, the kinetic analysis of luciferase expression in stage V gametocytes from this line is characterized by a high stability, over 60 minutes (Figure 4d).

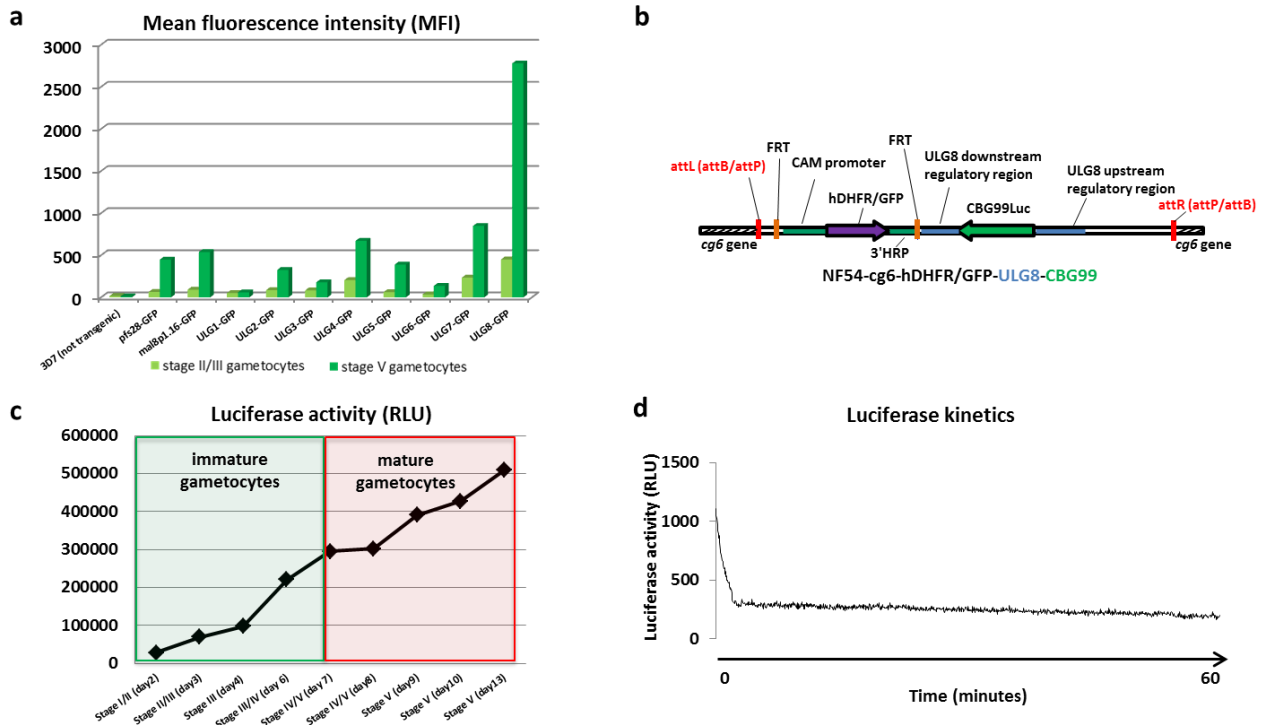


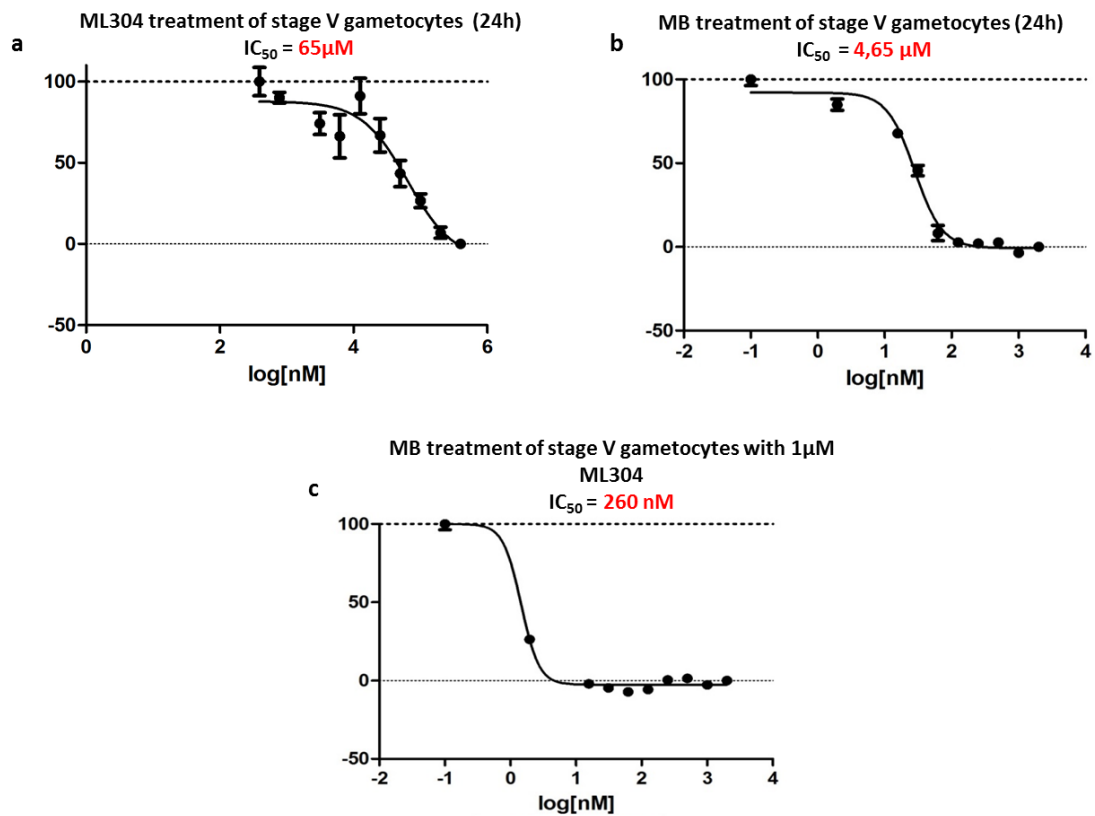
**Figure 4.** Development of a *P. falciparum* reporter line expressing luciferase specifically and efficiently in mature gametocytes. (a) Histograms representing the Mean Fluorescent Intensity (MFI) of the GFP reporter expressed under control of the ULG, the *pfs28* and the *mal8p1.16* regulatory regions in early (stage II/III) and late (stage V) gametocytes. (b) Structure of the ULG8-CBG99 luciferase cassette integrated in the *cg6* gene of the NF54<sup>attB</sup> *P. falciparum* line. From left to right, *attL*: attB/attP sequence resulting from the Bxb-1 mediated recombination of the attP-containing plasmid into the *cg6* attB site

(Nkrumah et al., 2006); *FRT*: FLP recognition sequence; *CAM*: calmodulin; *hDHFR*: human dihydrofolate reductase; *GFP*: green fluorescent protein; *hrp*: histidine rich protein; *attR*: attP/attB sequence resulting from the Bbx-1 mediated recombination of the attP-containing plasmid into the cg6 attB site. (c) CBG99 luciferase activity during gametocytogenesis of the transgenic *P. falciparum* line expressing the CBG99 luciferase under control of the ULG8 regulatory regions. (d) Kinetics of luciferase activity of the CBG99 reporter produced in stage V gametocytes of the NF54-cg6-hDHFR/GFP-ULG8-CBG99 line .

**Assessment of the activity of drugs affecting the redox equilibrium on *P. falciparum* mature gametocytes.** As Methylene blue (MB), a compound described to perturb the parasite redox equilibrium, was reported to block *P. falciparum* transmission killing mature gametocytes (Adjalley et al., 2011), we evaluated its action with the newly established assay described above, and we investigated the activity of additional drugs and compounds described to affect different aspects of the redox equilibrium of the human malaria parasite (Table 3).

One compound was described to specifically inhibit the glucose-6-phosphate dehydrogenase 6-phosphogluconolactonase (PfGluPho), a bifunctional enzyme that catalyses the first two steps of the pentose phosphate pathway (PPP), responsible for the production of most of the NADPH in erythrocytes infected by asexual parasites. This probe, the (*R*)-N-((1-ethylpyrrolidin-2-yl)methyl)-4-methyl-11-oxo-10,11-dihydrodibenzo[*b,f*][1,4]thiazepine-8-carboxamide (ML304) shows >420 fold selectivity against the human G6PD and a micromolar activity against asexual *P. falciparum* parasites (Maloney et al., 2010).

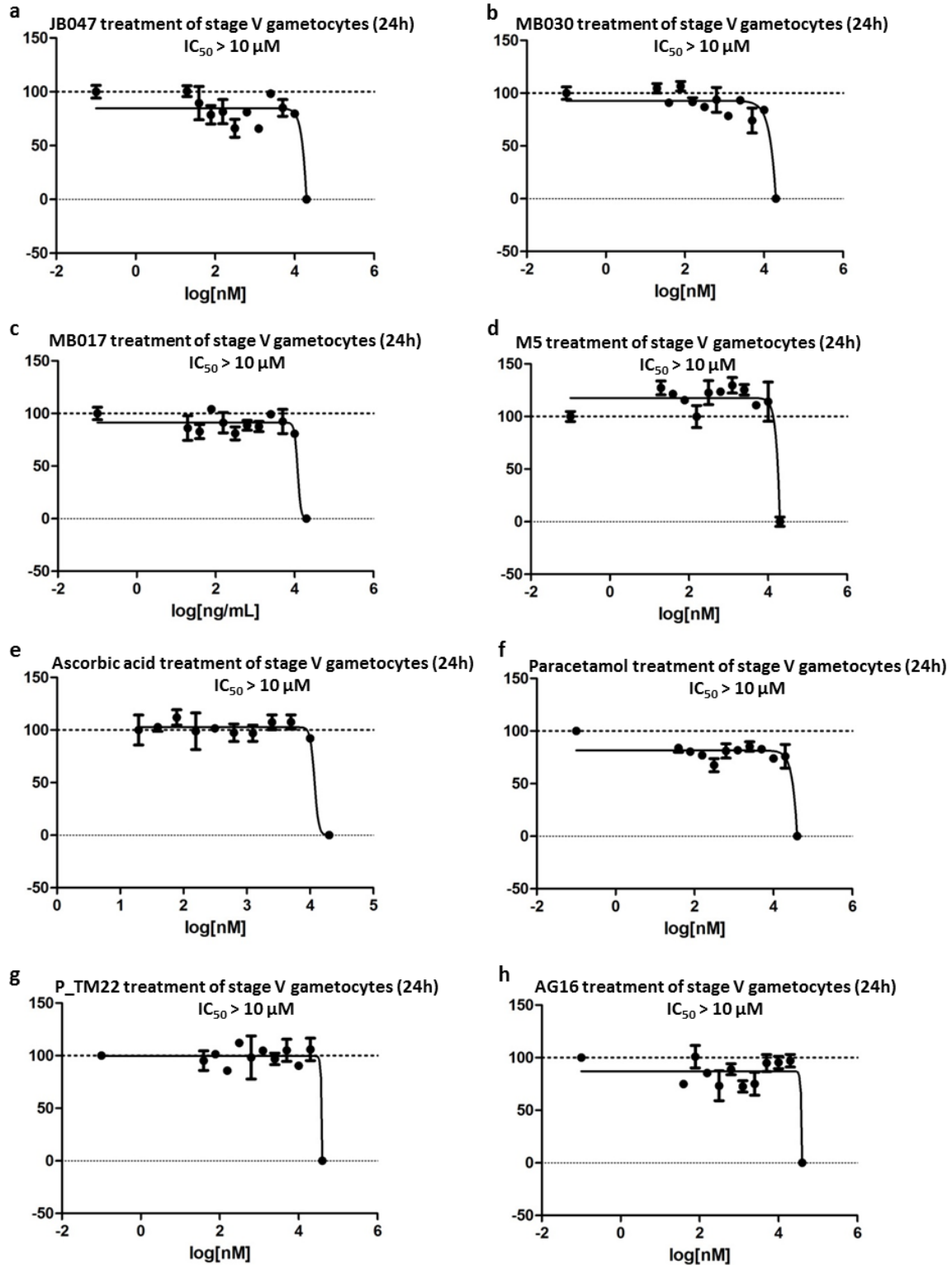
The activity of MB and ML304 on mature *P. falciparum* gametocytes after a 24h treatment was markedly different, as we observed an IC<sub>50</sub> of 4.65 μM for MB and of 65μM for ML304 (Figure 5a, b). Intriguingly, when an MB dose response curve was obtained on mature gametocytes in presence of a fixed concentration of 1μM of ML304 we observed a 20-fold decrease in the IC<sub>50</sub> of MB compared to that of MB alone, suggesting a synergistic activity of the two compounds on stage V gametocytes of *P. falciparum* (Figure 5c).



**Figure 5.** Dose response curves on treated stage V gametocytes and  $IC_{50}$ s values of **a.** ML304, **b.** Methylene Blue and **c.** Methylene Blue and 1microM ML304.

We tested the activity on mature gametocytes of other compounds known to kill asexual blood stages of *P. falciparum* by unbalancing the redox equilibrium as described in Table 3.

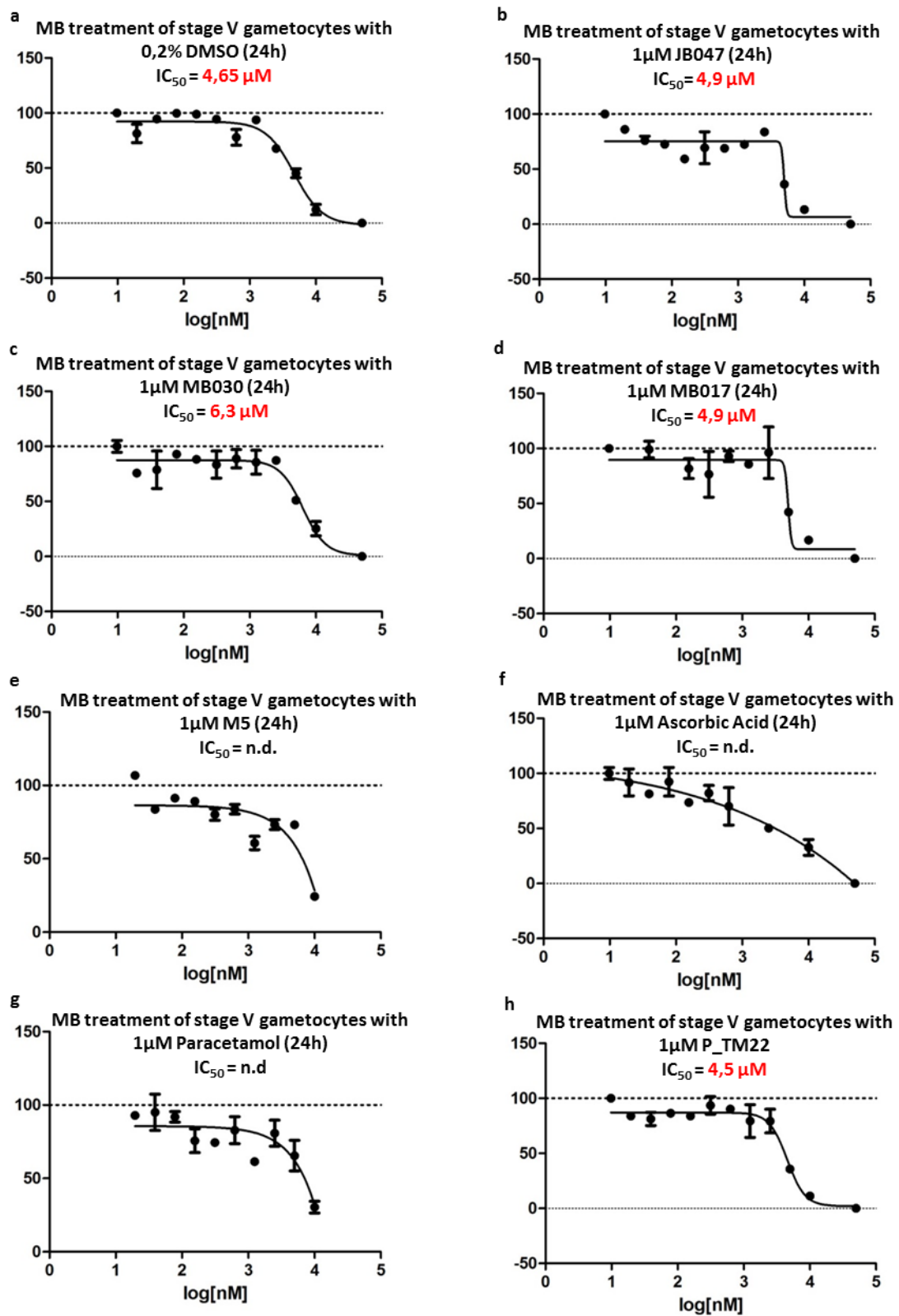
Dose response curves obtained with these compounds on mature gametocytes after 24 hours of treatment showed that none of them had any obvious activity on mature gametocytes (Figure 6 a-h).



**Figure 6:** Dose response curves on stage V gametocytes after treatment with different compounds known to perturb the redox equilibrium of *P. falciparum* asexual stages by different mechanisms (listed in Table 3).

To investigate possible synergistic actions of the above compounds with MB, as it was the case for ML304, we produced dose response curves of MB in presence of these compounds at a concentration of  $1 \mu M$ . In these experiments we observed that the  $IC_{50}$  values of MB in combination with the different

compounds didn't decrease compared to the  $IC_{50}$  of MB alone, indicating that none of them was producing synergistic effects with MB (Figure 7a-i).



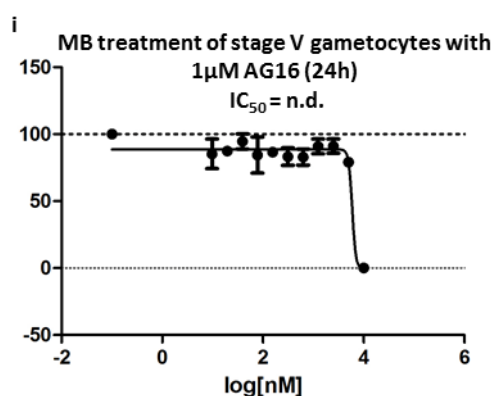


**Figure 7:** Dose response curves of MB on stage V gametocytes alone or in combination with a fixed dose (1  $\mu$ M) of compounds known to perturb the redox equilibrium of *P. falciparum* asexual stages. n.d.: not determined.

In fact, it was noticeable that some of the combination treatments appeared to decrease MB activity, making it impossible to determine the MB IC<sub>50</sub>, and suggesting that they had an antagonistic effect on MB activity. Further analysis will elucidate this possibility.

## Discussion and conclusions

This work aimed to study the poorly described redox equilibrium of mature gametocytes as a promising new target for anti-transmission drugs and to investigate the mode of action of MB.

After the first evidence that MB is a potent antimalarial, with an IC<sub>50</sub> in the nanomolar range on asexual blood stages (Atamna et al., 1996), this compound was described as an active inhibitor of the *P. falciparum* glutathione reductase (GR) (Farber et al., 1998). Subsequently, the interaction of MB with the human or Plasmodium GR was better elucidated, describing MB as a redox cycling substrate of the *P. falciparum* GR enzyme (Buchholz et al., 2007) whose activity catalyzed the reduction of MB by NADPH. The resulting reduced form of MB is then oxidized by O<sub>2</sub>. These reactions lead to the production of reactive oxidative species, such as H<sub>2</sub>O<sub>2</sub>, which are toxic for the parasite. Furthermore, they lead to the consumption of both O<sub>2</sub> and NADPH. In *P. falciparum* most of the NADPH is produced by the bifunctional enzyme glucose-6-phosphate dehydrogenase 6-phosphogluconolactonase (PfGluPho) (Preuss et al., 2012), which catalyzes the first two steps of the pentose phosphate pathway (PPP) (Preuss et al., 2012). This enzyme is structurally different from its human counterpart glucose-6-phosphate dehydrogenase (G6PD) (Preuss et al., 2012). NADPH is used by the parasite to counteract its oxidative stress: it is used by GR to reduce glutathione that, once reduced (GSH), participates in many detoxification cellular pathways (Tripathi et al., 2007; Gallo et al., 2009; Jortzik and Becker 2012). Most of the toxic oxygen species derives from parasite's hemoglobin digestion (Tripathi et al., 2007), described to occur in all asexual stages of *P. falciparum* and during gametocyte development, until the gametocyte reaches stage IV of maturation (Hanssen et al. 2012).

Although redox metabolism of the malaria parasite is not expected to be active in mature gametocytes, considering that hemoglobin digestion doesn't occur in this stage of gametocytogenesis, indirect evidence that some level of redox activity occur also in this stage has been provided (Tanaka and Williamson 2011).

To further support the hypothesis that redox metabolism is active in late gametocytes is the observation that MB is active not only against asexual blood stage parasites and early stage gametocytes but also against stage V gametocytes (Adjalley et al., 2011). The rationale of our effort to elucidate the mechanism of action of MB on mature gametocytes was that this work could reinforce the evidence of an active redox metabolism in this stage, importantly resulting in making this metabolic pathway an attractive target for anti-transmission drugs.

For this purpose we used the newly developed NF54-cg6-hDHFR/GFP-ULG8-CBG99 transgenic line that expresses the potent *Phyrophorus plagiotalamus* CBG99 luciferase gene (Cevenini et al., 2014) under control of the regulatory regions of gene PFL1675c to upregulate its expression in late stage of gametocytogenesis. These regulatory regions were selected from a functional analysis of different candidates as so far none of the *P. falciparum* transgenic lines expressing reporter genes during gametocytogenesis had the feature of specifically upregulating reporter expression in mature gametocytes. The line we developed for this work is therefore uniquely suitable for performing cell-based assays specific to test the activity of compounds against mature gametocytes by bioluminescence.

We decided to test different compounds described to perturb the redox metabolism of *P. falciparum* asexual blood stages and to investigate their activity alone and in combination with MB. These included two compounds described to affect the NADPH balance (ML304 and AG16, the former blocking the activity of the PfGluPho (Maloney et al., 2010)); three compounds of the family of benzoylmenadione (JB047, MB030 and MB017) which, as MB, act as redox cycler for the GR enzyme (Muller et al., 2011; Ehrhardt et al., 2013; Bielitzka et al., 2015); two menadione derivative compounds (M5 and P\_TM22), which act as GR inhibitor (Biot et al., 2004; Muller et al., 2011); paracetamol, which is a glutathione depletory, and ascorbic acid.

Results of assays where mature gametocytes were exposed to the individual compounds showed that, after a treatment of 24 hours, the only compound that showed an IC<sub>50</sub> below 10 µM was MB (IC<sub>50</sub> = 4.65 µM). Also when tested in single 1 microM dose in combination with MB these compounds didn't decrease MB IC<sub>50</sub>, with the remarkable exception of ML304, that was able to decrease the IC<sub>50</sub> of MB of about 20 fold. This dramatic decrease suggests that ML304 ability to affect NADPH levels helps MB activity as a redox cycler, which highlights the presence of an active redox metabolism in the mature transmission stages of *P. falciparum* and also suggests that the mechanism of action of MB in these stages is similar to that active in asexual blood stages.

The fact that ML304 alone has almost no effect on mature gametocytes compared to its ability to kill asexual blood stages with IC<sub>50</sub> values of about 600nM can be explained considering that the PfGluPho, the ML304 target, is a key enzyme providing precursors of nucleic acid biosynthesis, a pathway necessary for the asexual replicating parasites and unnecessary for the non-replicating mature gametocytes.

The fact that the other compounds tested alone didn't show any activity against *P. falciparum* mature gametocytes could be explained considering that these are less active against the parasite's asexual blood stages compared to ML304 (Muller et al., 2011; unpublished results). These compounds did not show any ability to synergize the activity of MB and in some cases they even appeared to act as MB antagonists. This feature, as in the case of M5, could be due to compound ability to inhibit GR (Bielitzka



et al., 2015), preventing in this way its role in reducing the redox cyler MB and producing the toxic oxygen species active in killing the parasites.

In conclusion, this work reveals with the use of a specific cell-based assay that activity of the redox cyler compound MB can be potentiated by co-treating *P. falciparum* late gametocytes with another compound reducing level of a critical effector of parasite detoxification pathways such as NADPH. These results confirm and expand the notion that redox metabolism is active on mature gametocytes and that its importance as a drug target is not restricted to asexual stages or immature gametocytes. The demonstration that it can be targeted by combination of drugs affecting synergistically different pathways of the parasites' redox equilibrium gives an important opportunity for the development of new *P. falciparum* anti-transmission drugs.

### Authorship statement

I preformed all the experiments of this project, with the exception of Southern blot analysis. Roberta Bona and Grazia Camarda participated to the construction of the GFP-expressing plasmids; T. R. Santha Kumar transfected the PCR2.1-attP-FRT-hDHFR/GFP-ULG8-CBG99 plasmid and is performing the Southern blot analysis; Maddalena Calabretta and Luca Cevenini participated to the construction of the PCR2.1-attP-FRT-hDHFR/GFP-ULG8-CBG99 plasmid; Katja Becker and Elisabeth Davioud-Charvet provided us the compounds used in the experiments.

### References

Adjalley, S.H., Johnston, G.L., Li, T., Eastman, R.T., Ekland, E.H., Eappen, A.G., Richman, A., Sim, B.K., Lee, M.C., Hoffman, S.L., and Fidock, D.A. (2011). Quantitative assessment of Plasmodium falciparum sexual development reveals potent transmission-blocking activity by methylene blue. *Proc Natl Acad Sci U S A*. 108, 1214-23.

Atamna, H., Krugliak, M., Shalmiev, G., Deharo, E., Pescarmona, G., and Ginsburg, H. (1996). Mode of antimalarial effect of methylene blue and some of its analogues on Plasmodium falciparum in culture and their inhibition of *P. vinckei petteri* and *P. yoelii nigeriensis* in vivo. *Biochem Pharmacol*. 51, 693-700.

Bielitza, M., Belorgey, D., Ehrhardt, K., Johann, L., Lanfranchi, D.A., Gallo, V., Schwarzer, E., Mohring, F., Jortzik, E., Williams, D.L., Becker, K., Arese, P., Elhabiri, M., and Davioud-Charvet, E. (2015). Antimalarial NADPH-Consuming Redox-Cyclers As Superior Glucose-6-Phosphate Dehydrogenase Deficiency Copycats. *Antioxid Redox Signal*. 22, 1337-51.

Biot, C., Bauer, H., Schirmer, R.H., and Davioud-Charvet, E. (2004). 5-substituted tetrazoles as bioisosteres of carboxylic acids. Bioisosterism and mechanistic studies on glutathione reductase inhibitors as antimalarials. *J Med Chem*. 47, 5972-83.

Buchholz, K., Schirmer, R.H., Eubel, J.K., Akoachere, M.B., Dandekar, T., Becker, K., and Gromer S. (2007). Interactions of methylene blue with human disulfide reductases and their orthologues from *Plasmodium falciparum*. *Antimicrob Agents Chemother.* 52, 183-91.

Cevenini, L., Camarda, G., Michelini, E., Siciliano, G., Calabretta, M.M., Bona, R., Kumar, T.R., Cara, A., Branchini, B.R., Fidock, D.A., Roda, A., and Alano, P. (2014). Multicolor bioluminescence boosts malaria research: quantitative dual-color assay and single-cell imaging in *Plasmodium falciparum* parasites. *Anal Chem.* 86, 8814-21.

Delves, M.J., Ruecker, A., Straschil, U., Lelièvre, J., Marques, S., López-Barragán, M.J., Herreros, E., and Sinden RE. (2013). Male and female *Plasmodium falciparum* mature gametocytes show different responses to antimalarial drugs. *Antimicrob Agents Chemother.* 57, 3268-74.

Ehrhardt, K., Davioud-Charvet, E., Ke, H., Vaidya, A.B., Lanzer, M., and Deponte, M. (2013). The antimalarial activities of methylene blue and the 1,4-naphthoquinone 3-[4-(trifluoromethyl)benzyl]-menadione are not due to inhibition of the mitochondrial electron transport chain. *Antimicrob Agents Chemother.* 57, 2114-20.

Eksi, S., Suri, A., and Williamson, K.C. (2008). Sex- and stage-specific reporter gene expression in *Plasmodium falciparum*. *Mol Biochem Parasitol.* 160, 148-51.

Fidock, D.A., and Wellems, T.E. (1997). Transformation with human dihydrofolate reductase renders malaria parasites insensitive to WR99210 but does not affect the intrinsic activity of proguanil. *Proc. Natl. Acad. Sci. U.S.A.* 94, 10931-10936.

Gallo, V., Schwarzer, E., Rahlfs, S., Schirmer, R.H., van Zwieten, R., Roos, D., Arese, P., and Becker, K. (2009). Inherited glutathione reductase deficiency and *Plasmodium falciparum* malaria--a case study. *PLoS One.* 4, e7303.

Hanssen, E., Knoechel, C., Dearnley, M., Dixon, M.W., Le Gros, M., Larabell, C., and Tilley L. (2012). Soft X-ray microscopy analysis of cell volume and hemoglobin content in erythrocytes infected with asexual and sexual stages of *Plasmodium falciparum*. *J Struct Biol.* 177, 224-32.

Jortzik, E., and Becker, K. (2012). Thioredoxin and glutathione systems in *Plasmodium falciparum*. *Int J Med Microbiol.* 302, 187-94.

Kariuki, M.M., Kiara, J.K., Mulaa, F.K., Mwangi, J.K., Wasunna, M.K., and Martin, S.K. (1998). *Plasmodium falciparum*: purification of the various gametocyte developmental stages from in vitro-cultivated parasites. *Am J Trop Med Hyg.* 59, 505-8.

Le Roch, K.G., Zhou, Y., Blair, P.L., Grainger, M., Moch, J.K., Haynes, J.D., De La Vega, P., Holder, A.A., Batalov, S., Carucci, D.J., and Winzeler, E.A. (2003). Discovery of gene function by expression profiling of the malaria parasite life cycle. *Science*. 301, 1503-8.

Maloney, P., Hedrick, M., Peddibhotla, S., Hershberger, P., Milewski, M., Gosalia, P., Li, L., Preuss, J., Sugarman, E., Hood, B., Suyama, E., Nguyen, K., Vasile, S., Sergienko, E., Salanawil, S., Stonich, D., Su, Y., Dahl, R., Mangravita-Novo, A., Vicchiarelli, M., McAnally, D., Smith, L.H., Roth, G., Diwan, J., Chung, T.D.Y., Pinkerton, A.B., Bode, L., and Becker, K. (2010). A 2nd Selective Inhibitor of *Plasmodium falciparum* Glucose-6-Phosphate Dehydrogenase (PfG6PDH) - Probe 2. *Probe Reports from the NIH Molecular Libraries Program [Internet]. Bethesda (MD): National Center for Biotechnology Information (US)*.

Müller, T., Johann, L., Jannack, B., Brückner, M., Lanfranchi, D.A., Bauer, H., Sanchez, C., Yardley, V., Deregnacourt, C., Schrével, J., Lanzer, M., Schirmer, R.H., and Davioud-Charvet, E. (2011). Glutathione reductase-catalyzed cascade of redox reactions to bioactivate potent antimalarial 1,4-naphthoquinones - a new strategy to combat malarial parasites. *J Am Chem Soc*. 133, 11557-71.

Nkrumah, L.J., Muhle, R.A., Moura, P.A., Ghosh, P., Hatfull, G.F., Jacobs, W.R. Jr, and Fidock, D.A. (2006). Efficient site-specific integration in *Plasmodium falciparum* chromosomes mediated by mycobacteriophage Bxb1 integrase. *Nat Methods*. 3, 615-21.

O'Donnell, R.A., Freitas-Junior, L.H., Preiser, P.R., Williamson, D.H., Duraisingh, M., McElwain, T.F., Scherf, A., Cowman, A.F., and Crabb, B.S. (2002). A genetic screen for improved plasmid segregation reveals a role for Rep20 in the interaction of *Plasmodium falciparum* chromosomes. *EMBO J*. 21, 1231-9.

Pace, T., Olivieri, A., Sanchez, M., Albanesi, V., Picci, L., Siden Kiamos, I., Janse, C.J., Waters, A.P., Pizzi, E., and Ponzi M. (2006). Set regulation in asexual and sexual *Plasmodium* parasites reveals a novel mechanism of stage-specific expression. *Mol Microbiol*. 60, 870-82.

Preuss, J., Jortzik, E., and Becker, K. (2012). Glucose-6-phosphate metabolism in *Plasmodium falciparum*. *IUBMB Life*. 64, 603-11.

Preuss, J., Maloney, P., Peddibhotla, S., Hedrick, M.P., Hershberger, P., Gosalia, P., Milewski, M., Li, Y.L., Sugarman, E., Hood, B., Suyama, E., Nguyen, K., Vasile, S., Sergienko, E., Mangravita-Novo, A., Vicchiarelli, M., McAnally, D., Smith, L.H., Roth, G.P., Diwan, J., Chung, T.D., Jortzik, E., Rahlfs, S., Becker, K., Pinkerton, A.B., and Bode, L. (2012). Discovery of a *Plasmodium falciparum* glucose-6-phosphate dehydrogenase 6-phosphogluconolactonase inhibitor (R,Z)-N-((1-ethylpyrrolidin-2-yl)methyl)-2-(2-fluorobenzylidene)-3-oxo-3,4-dihydro-2H-benzo[b][1,4]thiazine-6-carboxamide (ML276) that reduces parasite growth in vitro. *J Med Chem*. 55, 7262-72.

Sinden, R. E., Canning, E. U., Bray, R. S., and Smalley, M. E. (1978). Gametocyte and gamete development in *Plasmodium falciparum*. *Proceedings of the Royal Society of London. Series B, Biological sciences*. 201, 375-399.

Tanaka, T. Q., and Williamson, K. C. (2011). A malaria gametocytocidal assay using oxidoreduction indicator, alamarBlue. *Mol Biochem Parasitol*. 177, 160-163.

Trager, W., and Jensen, J.B. (1976). Human malaria parasites in continuous culture. *Science*. 193, 673-675.

Tripathi, T., Rahlfs, S., Becker, K., and Bhakuni, V. (2007). Glutathione mediated regulation of oligomeric structure and functional activity of *Plasmodium falciparum* glutathione S-transferase. *BMC Struct Biol*. 7, 67.

van Schaijk, B.C., Vos, M.W., Janse, C.J., Sauerwein, R.W., and Khan, S.M. (2010). Removal of heterologous sequences from *Plasmodium falciparum* mutants using FLPe-recombinase. *PLoS One*. 5, e15121.

Walliker, D., Quakyi, I.A., Wellems, T.E., McCutchan, T.F., Szarfman, A., London, W.T., Corcoran, L.M., Burkot, T.R., and Carter, R. (1987). Genetic analysis of the human malaria parasite *Plasmodium falciparum*. *Science*. 236, 1661-1666.

WHO World Malaria Report 2014  
([http://www.who.int/malaria/publications/world\\_malaria\\_report/en/](http://www.who.int/malaria/publications/world_malaria_report/en/))

Young, J.A., Fivelman, Q.L., Blair, P.L., de la Vega, P., Le Roch, K.G., Zhou, Y., Carucci, D.J., Baker, D.A., and Winzeler, E.A. (2005). The *Plasmodium falciparum* sexual development transcriptome: a microarray analysis using ontology-based pattern identification. *Mol Biochem Parasitol*. 2005. 143, 67-79.

# PfMDR1 mutations protect *Plasmodium falciparum* asexual blood stages and mature gametocytes against a piperazine-containing antimalarial.

Caroline L Ng<sup>1\*</sup>, Giulia Siciliano<sup>2</sup>, Marcus C Lee<sup>1†</sup>, Mariana J Almeida<sup>1</sup>, Selina E Bopp<sup>3†</sup>, Lucia Bertuccini<sup>4</sup>, Sergio Wittlin<sup>5</sup>, Rachel Kasdin<sup>1</sup>, Victoria C Corey<sup>3</sup>, Amelie LeBihan<sup>6</sup>, Elizabeth A Winzeler<sup>3</sup>, Pietro Alano<sup>2</sup>, and David A Fidock<sup>1,7</sup>.

1. Department of Microbiology and Immunology, Columbia University Medical Center, New York, NY, USA. 2. Dipartimento di Malattie Infettive, Parassitarie ed Immunomediate, Istituto Superiore di Sanità, Rome, Italy. 3. Pediatric Pharmacology and Drug Discovery, University of California San Diego, San Diego, CA, USA. 4. Dipartimento Tecnologie e Salute, Parassitarie ed Immunomediate, Istituto Superiore di Sanità, Rome, Italy. 5. Medical Parasitology and Infection Biology, Swiss Tropical and Public Health Institute, Basel, Switzerland. 6. Actelion Pharmaceuticals Ltd., Allschwil, Switzerland. 7. Division of Infectious Diseases, Department of Medicine, Columbia University Medical Center, New York, NY, USA.

†Present addresses:

Marcus C Lee

Malaria Programme, Wellcome Trust Sanger Institute, Wellcome Trust Genome Campus, Cambridge CB10 1SA, United Kingdom

Selina E Bopp

Department of Immunology and Infectious Diseases, Harvard School of Public Health, Boston, MA, USA

This work is submitted to Molecular Microbiology.

**Abstract:** ACT-451840 is a piperazine-containing antimalarial compound developed by Actelion Pharmaceuticals Ltd. with support from the Medicines for Malaria Venture. This compound is an exquisitely potent inhibitor of *Plasmodium falciparum* asexual (IC<sub>50</sub> <1 nM) and sexual (IC<sub>50</sub> < 4 nM) blood stage parasites. Single-step drug-selection studies yielded resistant asexual blood stage parasites with 3 to 100-fold shifts in IC<sub>50</sub> values compared to the sensitive parental line. Whole-genome tiling arrays and Illumina-based sequencing of ACT-451840-selected mutants led us to identify single nucleotide polymorphisms (SNPs) in *pfmdr1*. This gene encodes a digestive vacuole (DV)-resident membrane protein known to alter susceptibility to a variety of antimalarials, whose modes of action are related to inhibition of heme detoxification inside the DV. Using CRISPR-Cas9 based *pfmdr1* gene editing, we confirmed that PfMDR1 point mutations mediated resistance. Parasites harboring distinct mutations were found to have a slight fitness cost *in vitro*. We also observed potent activity of ACT-451840 on mature *P. falciparum* gametocytes. Unexpectedly, stage V gametocytes harboring Cas9-introduced *pfmdr1* mutations acquired resistance to this compound, suggesting that PfMDR1 can impart resistance to compounds active against mature gametocytes. The potent asexual and gametocytocidal properties of this compound merit further investigation.

## Introduction

Malaria exacts a large toll globally, and is a significant burden in developing countries. This infectious disease has a reported incidence of 198 million world-wide, and claims 584,000 lives per year, mostly children under the age of five (WHO, 2014). Artemisinin-based combination therapies are currently recommended as first-line treatment for uncomplicated *P. falciparum* malaria infections (WHO, 2015). Alarming, there have been reports that patients treated with artemisinin monotherapy or artemisinin-combination therapy in Western Cambodia, the Thai-Myanmar border, and across Myanmar show a delay in parasite clearance (Dondorp et al., 2009; Phyo et al., 2012; Tun et al., 2015; Ashley et al., 2014), which has been interpreted to signify the emergence of artemisinin resistance. Mutations in the kelch propeller domain (PF3D7\_1343700) were identified in whole-genome sequencing of a lab-derived artemisinin-resistant strain and Cambodian parasite isolates (Ariey et al., 2014), and proved to confer resistance to artemisinin by genetic manipulation (Straimer et al., 2015). In light of these reports, it is imperative to innovate our antimalarial drug pipeline to produce drugs that have a novel mechanism of action.

ACT-451840 is a potent piperazine-containing compound that targets all three stages (rings, trophozoites, and schizonts) of blood-stage asexual parasites (LeBihan et al., manuscript in preparation). This promising compound shows a good safety and tolerability profile, and there were no serious adverse events in Phase I clinical trials (Bruderer et al., 2015). We sought to determine its mode of action to explore how best to pair this agent in combination therapy should it advance clinically.

In previous work, PfMDR1 was shown to bind ACT-213615 (a preceding compound in this chemical family) in heterologous expression assays, and was implicated in modulating parasite susceptibility to this compound (Brunner et al., 2013). PfMDR1 is a 162254 Da multimembrane-spanning protein member of the ATP-binding cassette (ABC) superfamily that resides on the digestive vacuole (DV) membrane. The protein is composed of two halves, each containing six transmembrane domains (TMD) and one nucleotide-binding domain (NBD). The NBD is situated in the parasite cytoplasm, and because ATP conversion happens in the cytoplasm, it is thought that this ABC transporter facilitates solute movement into the DV. The active site of PfMDR1 can bind and transport a variety of substrates that are structurally and functionally diverse (Higgins 2007), and is reflected by PfMDR1's ability to mediate resistance to a variety of antimalarials, including lumefantrine, mefloquine, artesunate, quinine, and chloroquine (Reed et al., 2000; Sidhu et al., 2006; Veiga et al., 2011; Sanchez et al., 2008).

In this study, we identify and confirm the role of PfMDR1 in ACT-451840 resistance. Our results reinforce the central role of PfMDR1 in mediating sensitivities to drug in both asexual and sexual parasite stages.

## Experimental Procedures

**Generation of ACT-451840-resistant parasites.** Dd2, 7G8, and NF54 strains were cultured at 4% hematocrit as previously described (Fidock et al., 1997). Clonal lines of all three strains were subjected to single-step selection. NF54 was also subjected to step-wise selection. For single-step selections, parasites were cultured in 1.7 nM ACT-451840 (7G8,  $6 \times IC_{50}$ ) or 2.7 nM ACT-451840 (Dd2,  $4 \times IC_{50}$  and

NF54,  $5 \times IC_{50}$ ). Parasites ranging from  $2 \times 10^4$  to  $2 \times 10^9$  were exposed to media containing appropriate drug concentrations. For the first six days, media was changed every 24 hours and parasitemia closely monitored, ensuring against parasite overgrowth. Then, media was changed every 48 h and cultures were monitored for any parasite recrudescence. The experiment was carried out to 60 days, or until parasites recrudesced, whichever was earlier. For the step-wise selection, parasites were exposed to  $1 \times IC_{90}$ . At each step, when parasites recrudesced, drug concentration was increased two-fold to a final concentration of  $16 \times IC_{90}$  (12.8 nM).

**Whole Genome Microarray.** Parasite genomic DNA were prepared and hybridized to Affymetrix Pf microarray chips as described (Dharia et al., 2009). The PfGenominator software was used to extract meaning from raw data. SNP detection for Dd2 samples was set with a cut off for the p-value of  $10^{-5}$ . SNP detection for 7G8 and NF54 samples were decreased to a cut off p-value of  $10^{-8}$ .

**In vitro assessment of resistance levels.** To determine the level of ACT-451840 resistance generated, ACT-451840-resistant parasite lines were subjected to *in vitro* SYBR-green-based drug assays as described in (Ekland et al., 2011), except that parasites were assayed at 72 h post-drug exposure.  $IC_{50}$  values were obtained by non-linear regression analyses (GraphPad Prism 6.0).

**Whole Genome Microarray.** Genomic DNA isolated from parental and ACT-451840-resistant lines in 7G8, Dd2, and NF54 using phenol-chloroform extraction was fragmented and hybridized against a *P. falciparum* microarray containing 4.8 million tiled 25-mer probes (Dharia et al., 2009). The PfGenominator software was used to extract meaning from raw data. SNP detection for Dd2 samples was set with a cut off for the p-value of  $10^{-5}$ . SNP detection for 7G8 and NF54 samples were decreased to a cut off p-value of  $10^{-8}$ .

**Whole Genome Sequencing.** Genomic DNA isolated from parental and ACT-451840-resistant lines using phenol-chloroform extraction was fragmented by sonication, and subjected to paired-end Illumina-based multiplex sequencing according to manufacturer's protocol.

**PfMDR1 allele typing.** Genomic DNA was obtained from parasites using QIAGEN DNeasy Blood & Tissue Kit, according to manufacturer's protocol. *pfmdr1* was PCR amplified and sequenced.

**Fitness Assays.** ACT-451840-resistant lines and the wild-type counterparts were mixed in a 1:1 ratio. Genomic DNA was harvested regularly every 2 to 3 days, using QIAGEN DNeasy according to manufacturer's protocol. The proportion of wild-type to mutant parasite was determined by pyrosequencing polymorphic *pfmdr1* sites (Zhou et al., 2006). Single nucleotide polymorphisms within codons 807, 841, and 921 of *pfmdr1* were examined in Dd2, 7G8, and NF54 pairs, respectively. Pyrosequencing was performed on a Qiagen Pyrosequencing PSQ 96.

**Introduction of *pfmdr1* mutations via CRISPR-Cas9.** The pDC2-CAM-Cas9-hDHFR-chRNA plasmid contained the guide RNA, the Cas9 enzyme, and the hDHFR selectable marker. The cognate pDC2-cam-

T7RNAPol-bsd-pfmdr1<sub>M841I/M924I</sub> plasmid contained a template with silent mutations at the guide RNA, the M841I/M924I mutations, and the blasticidin selectable marker. NF54 parasites co-transfected with the pDC2-CAM-Cas9-hDHFR-chRNA and pDC2-cam-T7RNAPol-bsd-pfmdr1 plasmids were cultured under 2.7 nM ACT-451840 for 60 days, or selected with 2.5 nM WR99210 and 2 µg ml<sup>-1</sup> blasticidin for 6 days, then cultured in drug-free media.

**Gametocyte susceptibility to ACT-451840.** Gametocytes from Dd2 MDR1 WT, Dd2 MDR1 A807V, NF54 MDR1 WT, and NF54 MDR1<sup>Cas9</sup>M841I/M924I at different stages of maturation were exposed to different concentrations of ACT-451840. For early (stage II) gametocytes, induced cultures treated for 48 hours with 50 mM *N*-acetyl-glucosamine (NAG; Sigma Aldrich) to eliminate asexual stages were then purified from uninfected erythrocytes with a 60% Percoll density gradient centrifugation (Kariuki, 1998). Mature (stage V) gametocytes were NAG-treated for 96 hours at the onset of gametocytogenesis, purified from uninfected erythrocytes on MACS Separation Columns CS (Miltenyi Biotec) and then allowed to mature. ACT-451840 was dispensed in 96-well plates and serial dilutions were prepared in a final volume of 100 µL per well. Synchronous 1 × 10<sup>5</sup> early and late stage gametocytes were re-suspended in 100 µL complete medium, and incubated with the drug at 37°C. The compound was washed out 48 hours later, and after an additional 72 hours, cell viability was measured using a parasite lactate dehydrogenase (pLDH) assay {D'Alessandro, 2013 #16}. The percentage viability was calculated as a function of drug concentration and curve fitting was obtained by non-linear regression analysis (GraphPad Prism 6.0).

**Transmission electron microscopy.** Gametocytes at stages IV and V of maturation were Percoll-purified and processed as described (Kariuki, 1998). Cells were fixed with 2.5% glutaraldehyde, 2% paraformaldehyde and 2 mM CaCl<sub>2</sub> in 0.1 M sodium cacodylate buffer (pH 7.4) overnight at 4°C. Parasites were washed in cacodylate buffer and postfixed with 1% OsO<sub>4</sub> in 0.1 M sodium cacodylate buffer for 1 hour at room temperature, treated with 1% tannic acid in 0.05 M cacodylate buffer for 30 min and rinsed in 1% sodium sulphate in 0.05 cacodylate for 10 min. Fixed specimens were washed, dehydrated through a graded series of ethanol solutions (30 to 100% ethanol) and embedded in Agar 100 (Agar Scientific Ltd., U.K.). Ultrathin sections obtained by a MT-2B Ultramicrotome (UC6 - Leica) were stained with uranyl acetate and lead citrate and examined by an EM 208 Philips electron microscope.

**LysoTracker staining.** Gametocytes at stage II/III of maturation were purified from uninfected erythrocytes on MACS Separation Columns CS (Miltenyi Biotec). 1 × 10<sup>5</sup> gametocytes at stage II, III, IV and V were loaded with 100 nM of the acidotropic fluorescent dye LysoTracker Red DND-99 in complete medium and incubated for 2 hours at 37°C. During the last 15 minutes 10 µg ml<sup>-1</sup> of Hoechst 33258 were added for nuclei staining. The parasites were washed twice and a Leica DMRB microscope was used to visualize live samples. Fluorescence images were acquired using a Leica DFC340 FX camera through a Leica PL FLUOTAR 100x objective. Filters used to detect LysoTracker Red DND-99 were: EX: 515-560, EM: 590 long-pass filter. Filters used to detect Hoechst 33258 were: EX: 340-380, EM 425 long-pass filter.



## Results

**Generation of ACT-451840-resistant parasites.** ACT-451840 is a potent inhibitor of both multi-drug resistant and sensitive *P. falciparum* strains, with IC<sub>50</sub> values in the low nanomolar range (7G8: 0.3 nM; Dd2: 0.7 nM; NF54: 0.6 nM). To select for resistance, we subjected these *P. falciparum* strains at a range of inocula ( $2 \times 10^6$  –  $2 \times 10^9$ ) to constant selective pressure at  $4\text{--}6 \times \text{IC}_{50}$  concentrations. For Dd2 we also tested inocula of  $2 \times 10^4$  and  $2 \times 10^5$  parasites. The minimum inoculum for resistance (MIR) for 7G8 and NF54 was determined to be  $2 \times 10^7$  (2 of 3 flasks in each experiment), whereas the MIR for Dd2 was  $10^6$  (1 of 6 flasks). Parasites were recovered after 17–22 days, although parasites were also seen to emerge as late as day 61 (Table S1). NF54 was also subjected to step-wise selection in which parasites were exposed to  $1 \times \text{IC}_{90}$  (0.8 nM). When parasites recrudesced and grew to  $\geq 3\%$  parasitemia at this concentration, drug pressure was increased by a factor of 2, until a final concentration of  $16 \times \text{IC}_{90}$ . Parasites that recrudesced at  $16 \times \text{IC}_{90}$  (12.8nM) were selected for further analyses.

**Whole-genome Pf tiling microarray and Illumina-based paired-end genome sequencing identify PfMDR1 mutations.** Genomic DNA isolated from parental and ACT-451840-resistant lines in 7G8, Dd2, and NF54 using standard phenol-chloroform extraction was fragmented by DnaseI treatment and hybridized against a *P. falciparum* microarray containing 4.8 million tiled 25-mer probes (Dharia et al., 2009). This work identified a whole host of SNPs in PF3D7\_0523000 (multidrug resistance protein, PfMDR1) in mutant lines on all strain backgrounds (7G8, Dd2 and NF54). These SNPs were confirmed by Sanger sequencing. We note that the multidrug resistant Dd2 strain has three copies of *pfmdr1*, whereas the drug-resistant 7G8 and drug-sensitive NF54 strains carry a single copy. These novel *pfmdr1* mutations were all distinct from mutations at amino acid positions 86, 184, 1034, 1042, and 1246 that are frequently observed in field isolates and that are known to modulate parasite susceptibility to lumefantrine and related drugs (Reed et al., 2000; Sidhu et al., 2006; Veiga et al., 2011).

These novel PfMDR1 mutations cluster mainly in the latter half of the molecule, either in the loop between transmembrane domains (TMD) 5 and 6 or in TMD 6, 7, 8, 9, or 12 (Figure 1). We also observed that on a drug-resistant background, A807V and A807T yielded similar levels of resistance (8.0 and 8.4 nM in 7G8 and Dd2, respectively). On a drug-sensitive background, A807P was three-fold more resistant than A807V (65.0 nM compared to 20.2 nM, Figure 2A and Table 1). This suggests that the level of resistance was dependent on the parental PfMDR1 haplotype or genetic differences elsewhere in the parasite genomes.

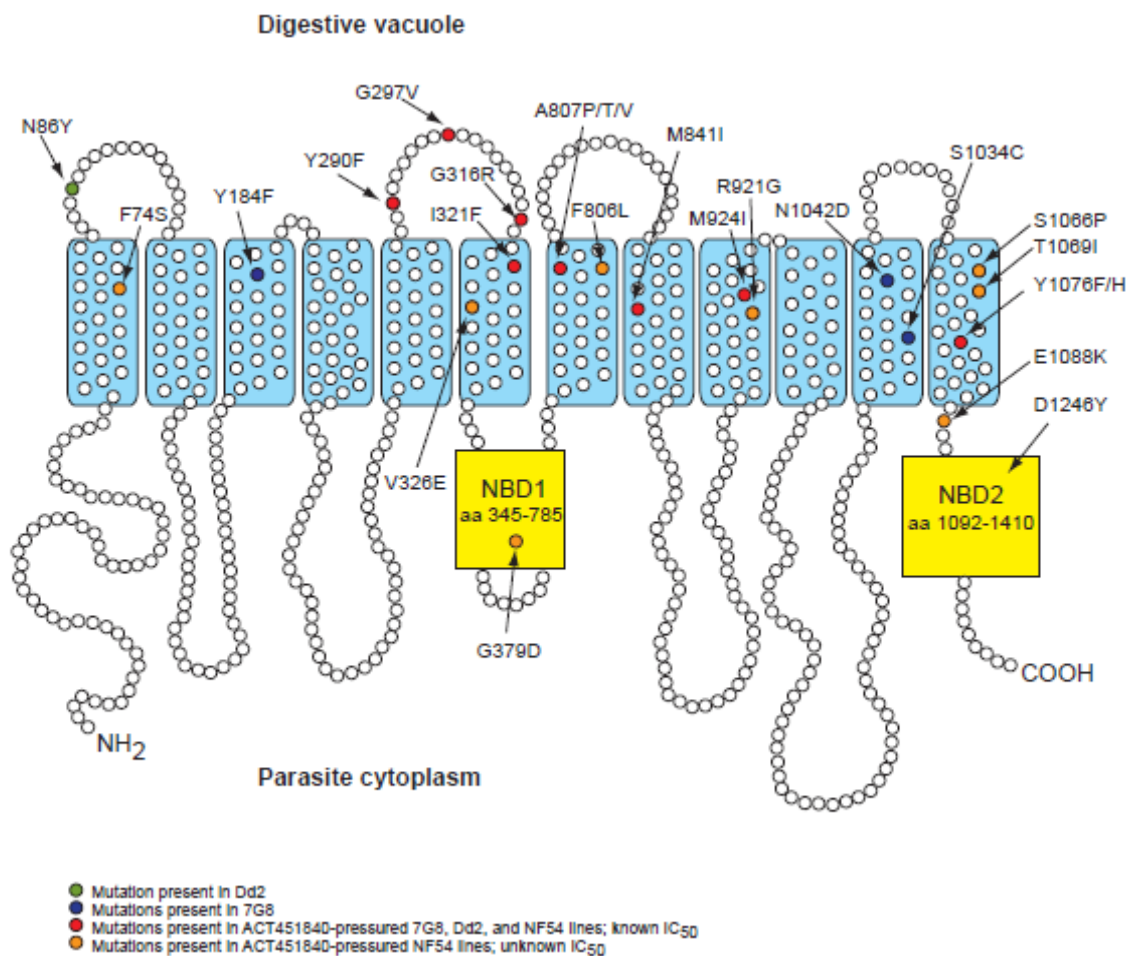


**Figure 1.** Diagram of PfMDR1: Diagram showing ACT-451840-resistance conferring mutations in PfMDR1. Common polymorphisms are shown in green (Dd2: N86Y) and blue (7G8: Y184F, S1034C, N1042D, D1246Y). Polymorphisms selected for by ACT-451840 and confirmed phenotypically by IC<sub>50</sub> determination are indicated in red (Y290F, G297V, G316R, I321F, A807P, A807T, A807V, M841I, M924I, Y1076F, Y1076H); polymorphisms selected for by ACT-451840 but not confirmed phenotypically are indicated in orange (F74S, V326E, G379D, F806L, R921G, S1066P, T1069I, E1088K). NBD = nucleotide binding domain.

Illumina-based paired-end whole genome sequencing did not identify SNPs in any other gene in all three genetic backgrounds. CNVs were not called in the whole genome sequencing due to a lack of sequencing depth. No CNVs were found to associate with ACT-451840 resistance in the tiling array analysis.

**Phenotyping ACT-451840 resistant parasites.** Clones were obtained from a subset of resistant lines by limiting dilution. Dose-response assays with these resistant clones demonstrated a 11- to 100-fold shift compared to the parental lines (Figure 2A and Table 1). PfMDR1 G316R, A807T, and M841I mutations examined on the 7G8 background, which carries PfMDR1 mutations Y184F, S1034C, N1042D, and D1246Y, showed similar levels of resistance to ACT-451840 (8 – 9.6 nM). We saw comparable IC<sub>50</sub> values in mutants (MDR1 A807V, M841I, and Y1076F) on the Dd2 background, which harbors a PfMDR1 N86Y mutation (8.4 – 10.6 nM). In the NF54 background, which has wild-type PfMDR1, we observed a

wide range in sensitivities to ACT-451840 with IC<sub>50</sub> values from 6.7 nM (NF54 MDR1 I321F) to 65 nM (NF54 MDR1 A807P).

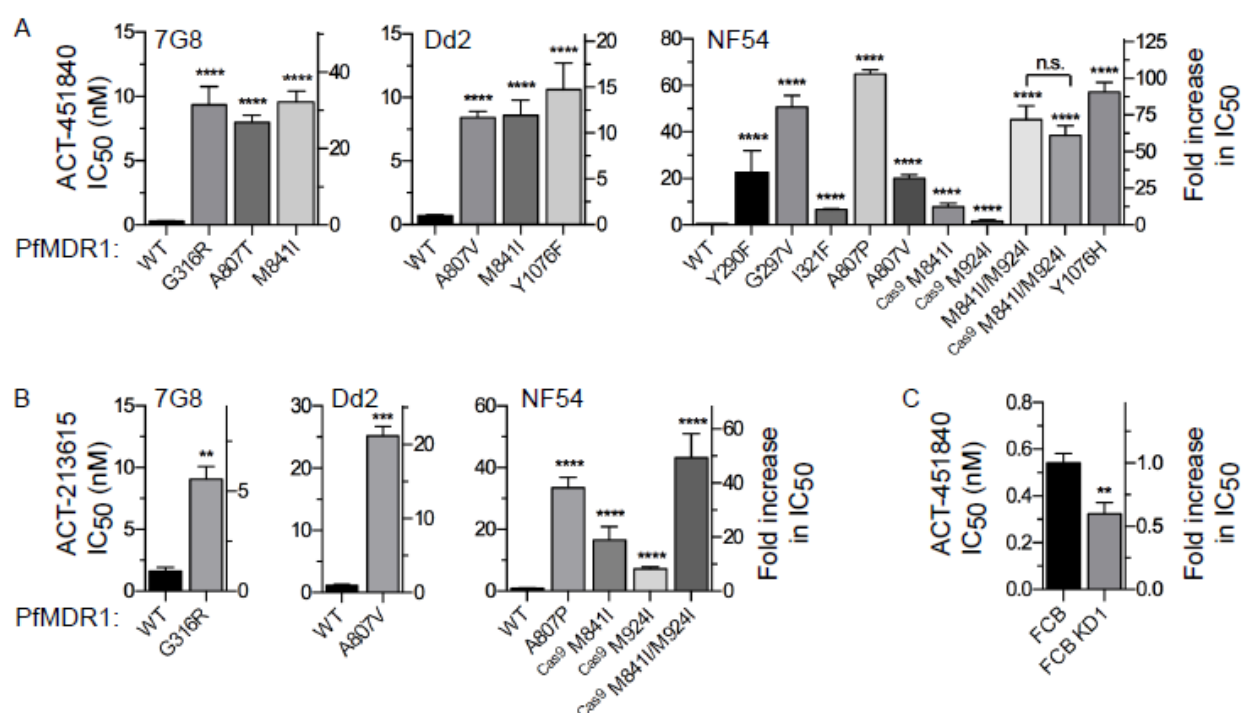


**Figure 2.** *P. falciparum* resistance to ACT-451840 and ACT-213615. (A) ACT-451840 potency on 7G8, Dd2, and NF54 ACT-451840-resistant lines. (B) Cross-resistance to ACT-213615 in ACT-451840-resistant lines. (C) ACT-451840 sensitivity displayed by FCB and FCB KD1 lines. Bar graphs display mean  $\pm$  S.E.M. Student's t-test was performed comparing resistant to parental lines, unless otherwise indicated. \*\* indicates  $P < 0.01$ , \*\*\* indicates  $P < 0.001$ , \*\*\*\* indicates  $P < 0.0001$ , and n.s. indicates no statistically significant difference between conditions.

| Parasite                        | MeanIC <sub>50</sub> values $\pm$ SEM (nM) | Number of assays | p-value  | Clones | IC <sub>50</sub> fold change |
|---------------------------------|--|------------------|----------|--------|------------------------------|
| 7G8 MDR1 WT                     | 0.3 $\pm$ 0.02                             | 10               | -        | Yes    | 1                            |
| 7G8 MDR1 G316R                  | 9.4 $\pm$ 1.4                              | 15               | < 0.0001 | Yes    | 31                           |
| 7G8 MDR1 A807T                  | 8.0 $\pm$ 0.6                              | 18               | < 0.0001 | Yes    | 27                           |
| 7G8 MDR1 M841I                  | 9.6 $\pm$ 0.8                              | 16               | < 0.0001 | Yes    | 32                           |
| Dd2 MDR1 WT                     | 0.7 $\pm$ 0.08                             | 13               | -        | Yes    | 1                            |
| Dd2 MDR1 A807V                  | 8.4 $\pm$ 0.5                              | 20               | < 0.0001 | Yes    | 12                           |
| Dd2 MDR1 M841I                  | 8.6 $\pm$ 1.2                              | 3                | < 0.0001 | Yes    | 12                           |
| Dd2 MDR1 Y1076F                 | 10.6 $\pm$ 2.1                             | 5                | < 0.0001 | Yes    | 15                           |
| NF54 MDR1 WT                    | 0.6 $\pm$ 0.04                             | 14               | -        | Yes    | 1                            |
| NF54 MDR1 Y290F                 | 22.7 $\pm$ 9.1                             | 2                | < 0.0001 | Yes    | 38                           |
| NF54 MDR1 G297V                 | 50.7 $\pm$ 5.0                             | 4                | < 0.0001 | No     | 85                           |
| NF54 MDR1 I321F                 | 6.7 $\pm$ 0.3                              | 3                | < 0.0001 | No     | 11                           |
| NF54 MDR1 A807P                 | 65.0 $\pm$ 1.7                             | 3                | < 0.0001 | Yes    | 108                          |
| NF54 MDR1 A807V                 | 20.2 $\pm$ 1.4                             | 4                | < 0.0001 | No     | 34                           |
| NF54 MDR1 <sup>Cas9</sup> M841I | 7.7 $\pm$ 1.6                              | 2                | < 0.0001 | No     | 13                           |
| NF54 MDR1 <sup>Cas9</sup> M924I | 1.8 $\pm$ 0.3                              | 3                | < 0.0001 | Yes    | 3                            |
| NF54 MDR1 M841I/M924I           | 45.4 $\pm$ 5.9                             | 4                | 0,0005   | Yes    | 76                           |

|                                       |            |   |          |     |    |
|---------------------------------------|------------|---|----------|-----|----|
| NF54 MDR1 <sup>Cas9</sup> M841I/M924I | 38.5 ± 4.2 | 4 | < 0.0001 | Yes | 64 |
| NF54 MDR1 Y1076H                      | 57.1 ± 4.1 | 8 | < 0.0001 | No  | 95 |

**Table 1.** Level of ACT-451840 resistance generated in 7G8, Dd2, and NF54 backgrounds. IC<sub>50</sub> values were calculated from 72 h dose-response data measured by flow cytometry of parasites stained with SYBR Green and Mitotracker Deep Red. Values indicate mean ± SEM, shown in nM. Significance was determined by Student's t-test.

**Confirmation of PfMDR1 involvement.** Prior studies with a related compound from this chemical series suggest that this class of agents might directly bind to PfMDR1 and thus inhibit its function (Brunner et al., 2013). Our results showed that resistance to ACT-451840 imparted cross-resistance to ACT-213615, implying that both compounds act in a similar manner (Figure 2B). We also examined ACT-451840 potency against the parasite line FCB, which has two copies of *pfmdr1*, and the isogenic line FCB KD1, which was genetically modified to disrupt one of the two *pfmdr1* copies (Sidhu et al., 2006). FCB KD1 was significantly more susceptible to ACT-451840 (Figure 2C), implicating a role for *pfmdr1* copy number in modulating parasite susceptibility to this compound.

**CRISPR-Cas9-mediated genetic engineering.** To demonstrate that mutations in *pfmdr1* are sufficient to confer ACT-451840 resistance, we genetically engineered the PfMDR1 double mutation M841I/M924I into wild-type NF54 parasites. These studies utilized the CRISPR-Cas9 system (Figure 3 and Table 2), which has been shown to effectively edit *Plasmodium spp.* genomes (Wagner et al., 2014; Ghorbal et al., 2014; Zhang et al., 2014). The Cas9 enzyme is directed to its target site via guide RNAs to allow site-specific sequence editing. Eight different guide RNAs were chosen by visually scanning the *pfmdr1* gene for GN<sub>18</sub>GG sequences. The distance between gRNA target sequences and the desired mutations varied from 15 base pairs away up to 708 base pairs away. Using tools designed by the Broad Institute and Harvard University, we determined that the gRNAs chosen had Doench scores between 0.094 and 0.779 (<http://www.broadinstitute.org/rnai/public/analysis-tools/sgrna-design>) (Doench et al., 2014), and verified that these gRNAs did not have off target sites elsewhere in the genome (<https://chopchop.rc.fas.harvard.edu/>). The guide RNA is carried on a plasmid that also expresses the Cas9 enzyme. A separate donor plasmid carries a 1.5 kb region of homology containing silent mutations at the binding site to prevent Cas9 from further inducing double-stranded breaks once editing is successful. Plasmids with guide RNAs targeting various target Cas9 cut sites were co-transfected with the cognate plasmids harboring silent binding site mutations by electroporation into infected erythrocytes as described (Fidock et al., 1997).

| gRNA | Sequence                | Protected sequence      | Distance (#nt) away |      | Doensch score | Editing success |
|------|-------------------------|-------------------------|---------------------|------|---------------|-----------------|
|      |                         |                         | 2523                | 2772 |               |                 |
| 1    | GCTTATAAAGACTCAGATACAGG | GCGTACAAGGATAGCGACACGGG | 354                 | 603  | 0.256         | 0 of 2          |
| 2    | GATCAAGATAAAAATACCCCAGG | GACCAGGACAAGAACACTCCGGG | 114                 | 111  | 0.383         | 1 of 2          |
| 3    | GATGTACATTTATTAACCGGG   | GACGTGCACTTGTGAAGACTGG  | 162                 | 63   | 0.280         | 0 of 2          |
| 4    | GTTAATACAGCTGCAACAATTGG | GTCAACACGGCCGCGACGATAGG | 264                 | 15   | 0.097         | 0 of 2          |
| 5    | GCTTCCTGTATTAACCTTGG    | GCCTCTTGATCAAGAACGAGGG  | 420                 | 171  | 0.238         | 0 of 2          |
| 6    | GCTATTGATTATAAAAATAAAGG | GCGATCGACTACAAGAACAAGGG | 510                 | 261  | 0.094         | 0 of 2          |
| 7    | GGATCCTTCTTAATTAAGAGG   | GGGAGTTTTTTGATCAAGAGGGG | 621                 | 372  | 0.779         | 0 of 2          |
| 8    | GGAAAATTAATGTCCTTAAAGG  | GGCAAGTTGATGAGTTGAAGGG  | 708                 | 459  | 0.215         | 3 of 4          |

**Table 2.** Guide RNAs design for the CRISPR-Cas9 system. Initial G of GN<sub>18</sub>GG is shown in red; protospacer adjacent motif is shown in blue; silent binding site substitutions are shown in green.

In the first set of transfections, all eight pairs of plasmids were transfected into NF54 parasites, in two biological replicates. These transfections were cultured in 2.7 nM ACT451840-containing media to select for a gain of resistance. We microscopically observed parasites in eleven of the sixteen transfections, but only three out of those incorporated the silent binding site mutations and the introduced mutations (~ 20% editing efficiency). The other eight positive transfections had spontaneous mutations in *pfmdr1* resulting in amino acid substitutions at Y290F (2 transfectants), G379D, A807V, A807P, R921G, and S1066P (2 transfectants), but no silent binding site mutations. Of the three successful transfections, one was targeted to guide RNA 2 and captured only one of the mutations, M841I. The remaining two successful transfections were targeted to guide RNA 8 and captured both mutations M841I and M924I. These three transfections did not have any *pfmdr1* mutations other than those introduced.

Because of the 100% success rate observed with guide RNA 8, we selected this guide RNA to optimize transfection and selection parameters. To examine whether transfections required direct selection with ACT-451840 to incorporate these mutations, we electroporated parasites and maintained these with 2.5 nM WR99210 and 2 µg ml<sup>-1</sup> blasticidin for six days, followed by culturing in drug-free media. One of two transfections was successful in capturing the binding site mutations and one of the introduced mutations, PfMDR1 M924I. This demonstrates that selection for plasmids alone can be sufficient to incorporate the desired mutations.

To confirm that these events were dependent on Cas9 activity, parasites were transfected only with the donor plasmid (and not the Cas9 plasmid). Neither transfection incorporated the *pfmdr1*-specific or binding site mutations. Therefore, the gene editing we observed was dependent on Cas9.

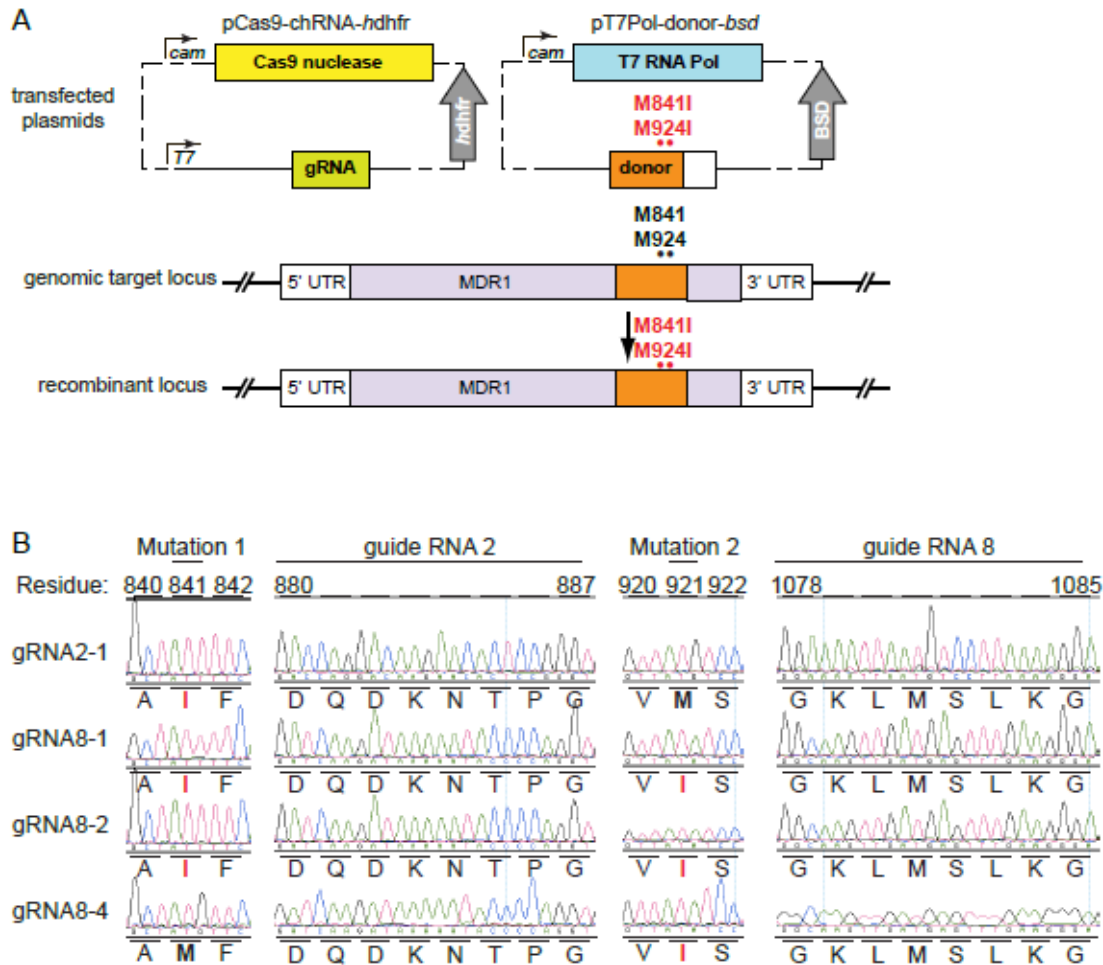


**Figure 3.** Genetic editing via CRISPR-Cas9. (A) The Cas9 enzyme is encoded on a plasmid that also expresses the guide RNA and a hDHFR selectable marker. The donor plasmid contains a template with silent mutations at the guide RNA, the PfMDR1 M841I/M924I double mutation, and the blasticidin selectable marker. (B) Electropherograms showing successful editing of PfMDR1 M841, M924I, and silent binding site mutations.

We confirmed that parasites engineered with the double mutation (NF54 MDR1<sup>Cas9</sup>M841I/M924I) and parasites that arose out of single-step selections harboring these mutations (NF54 MDR1 M841I/M924I) showed similar levels of ACT-451840 resistance (Figure 2A).

Since we have CRISPR-Cas9-generated parasites edited with M841I, M924I, or M841I/M924I, we can compare the contribution of each of these mutations to ACT-451840 resistance. Parasites harboring PfMDR1<sup>Cas9</sup>M841I or PfMDR1<sup>Cas9</sup>M924I mutations displayed similar levels of ACT451840 resistance (7.7 nM vs. 1.8 nM), but together the double mutation PfMDR1<sup>Cas9</sup>M841I/M924I was synergistic in ACT-451840 resistance (38.5 nM) (Figure 2A and Table 1). These relative ACT-451840 resistance levels translate to levels of cross-resistance to the related drug ACT-213615 (Figure 2B).

**Fitness Assays.** Pyrosequencing of *pfmdr1* alleles from parasites in direct co-competition assays between wild-type and mutant parasites showed that regardless of genetic background, the proportion

of wild-type allele increased over a 60-day period. The 7G8 MDR1 WT allele gained dominance over 7G8 MDR1 M841I with an average slope of 0.52. The Dd2 MDR1 WT allele outcompeted Dd2 MDR1 A807V with an average slope of 0.51. On the NF54 background, we observed a lesser degree of fitness cost associated with incorporating M841I/M924I double mutation, for the proportion of NF54 MDR1 WT allele increased only slightly over the MDR1<sup>Cas9</sup>M841I/M924I allele, demonstrating a slope of 0.13 (Figure 4).

Overall, wild-type parasites outgrew their *pfmdr1* mutant counterparts, indicating that mutations in PfMDR1 at positions A807V, M841I, and M841I/M924I confer a slight fitness cost.

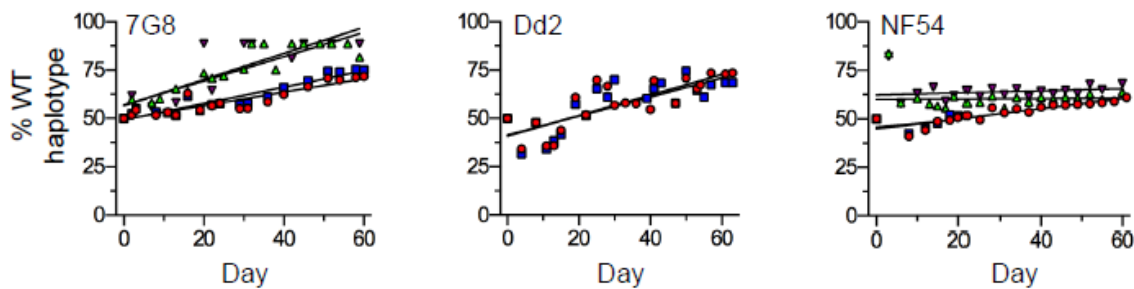


**Figure 4.** PfMDR1 haplotypes that mediate ACT-451840 resistance do not outcompete wild-type alleles. Parasite fitness was examined in co-cultures of wild-type and mutant strains of 7G8, Dd2, and NF54. Cultures were propagated for 60 days and DNA was sampled every 3 to 4 days. The relative nucleotide proportions of mutant vs. wild-type alleles were determined by pyrosequencing. Results are shown as the proportion of wild-type parasites in the culture. Experiments were performed at least twice per strain. Each symbol indicates a different run.

**Gametocyte susceptibility to ACT-451840.** Since ACT-451840 resistance is imparted by mutations in *pfmdr1*, and since the digestive vacuole is thought to be non-functional in stage V gametocytes (Hansen et al., 2012), we hypothesized that ACT-451840 might be active on early but not on late gametocytes, as seen with chloroquine, amodiaquine, and quinine (Sinden et al., 1982; Foote & Cowman 1994; Smalley et al., 1977; Klein et al., 1991). To test this hypothesis, we exposed early and late gametocytes from Dd2 MDR1 WT, Dd2 MDR1 A807V, NF54 MDR1 WT, and NF54 MDR1<sup>Cas9</sup>M841I/M924I to various concentrations of ACT-451840 and measured cell viability with the parasite lactate dehydrogenase (pLDH) assay (D'Alessandro et al., 2013). Experiments on wild-type parasites showed that ACT-451840 was active not only on the immature gametocytes but also on stage V gametocytes, with comparable IC<sub>50</sub> values (Dd2: 1.8 nM vs. 2.1nM; NF54: 1.8 nM vs. 3.9 nM) (Figure 5). When susceptibility to ACT-451840 in early and late gametocytes was compared between the wild-type and mutant lines, a dramatic increase in IC<sub>50</sub> was measured in immature (Dd2 1.8 nM vs. 208.9 nM; NF54: 1.8 nM vs. 883.6 nM) but also, importantly, in late gametocytes expressing mutant PfMDR1 (Dd2 2.1 nM vs. 383.0 nM; NF54: 3.9 nM vs. 973.6 nM) (Figure 5). This indicates that the mechanism conferring ACT-451840 resistance in asexual stages is also responsible for the decreased sensitivity to this compound observed in all stages of gametocyte development. In particular, the potent activity of ACT-451840 on stage V gametocytes is in sharp contrast to previous reports that mature gametocytes are generally refractory



to antimalarials (Peatey et al., 2009) and the involvement of PfMDR1 in this phenomenon contrasts with the notion that the digestive vacuole is no longer functional in stage V gametocytes.

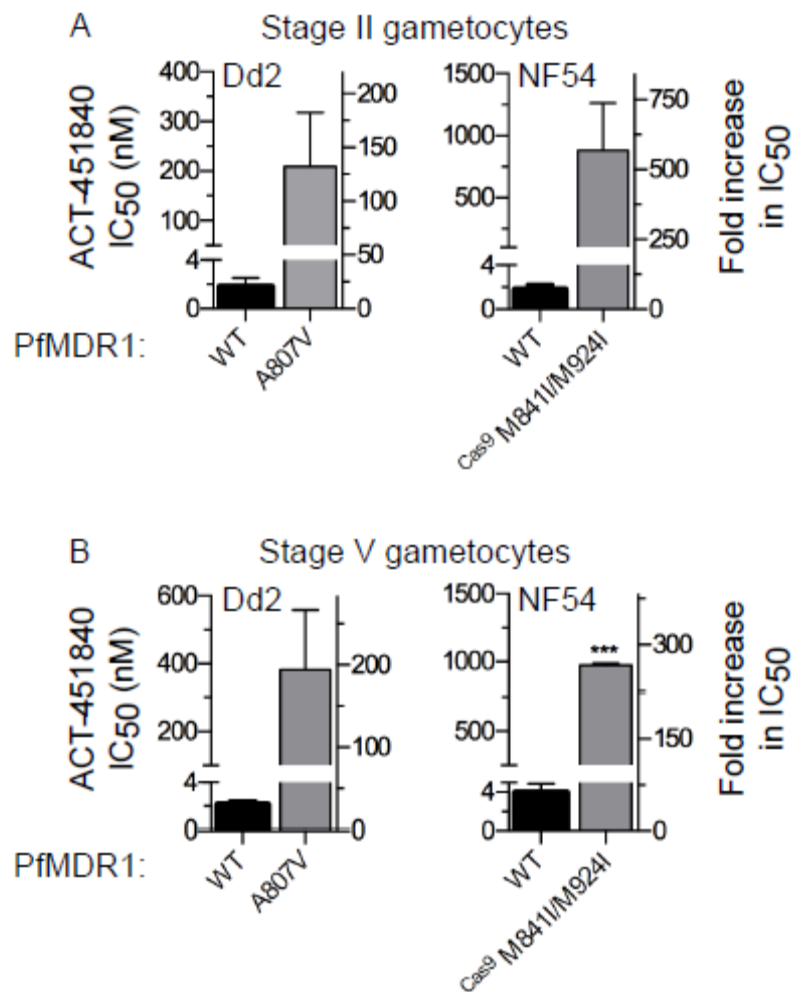


**Figure 5.** Gametocytes harboring mutant PfMDR1 haplotypes demonstrate resistance to ACT-451840. IC<sub>50</sub> values of ACT-451840 in (A) stage II and (B) stage V gametocytes derived from Dd2 and NF54 parental and mutant asexual blood stage parasites. Bar graphs display mean  $\pm$  S.E.M. Student's t-test was performed comparing mutant to wild-type lines. \*\*\* indicates  $p < 0.0005$ .

To address this point, this compartment was examined in ultrastructural sections from stage IV and stage V gametocytes. Results confirmed that multiple digestive vacuoles are readily detectable in the immature stage IV gametocytes (Figure 6A), and detection of a cytostome (see indent in Figure 6A) showed that at day 6-7 of sexual differentiation the erythrocyte cytoplasm surrounding the gametocyte is still actively endocytosed. Analysis of sections from stage V gametocytes showed that multiple digestive vacuoles, characterized by the presence of hemozoin crystals were readily detectable also in these stages (Figure 6B and C). The food vacuoles are clearly surrounded by a membrane, confirming that the subcellular site where PfMDR1 resides is structurally intact in these stages.

In a complementary approach the food vacuole was visualized in live gametocytes by staining with LysoTracker, a dye fluorescing in acidic lysosomal vesicles used to mark the food vacuole in *P. falciparum* asexual stages (Bohorquez et al., 2012). LysoTracker fluorescence, analyzed in gametocytes from stage II



to stage V of development, clearly resulted to be localized in correspondence of pigment granules in all stages of development (Figure 6D-G). This indicates that acidic food vacuoles are present throughout gametocyte development, and are still detectable in stage V gametocytes. Intriguingly, in the late stages, areas of LysoTracker fluorescence are devoid of hemozoin pigment, which may lead to speculate of possible rearrangements of this compartment in stage V gametocytes.

The above results altogether indicate that the compartment and the membranes where PfMDR1 is localized in asexual stages are present and maintain its characteristic acidic environment in *P. falciparum* sexual development including the stage V gametocytes. This supports the hypothesis that PfMDR1 is functional and mediates resistance to ACT-451840 in immature and mature sexual stages.

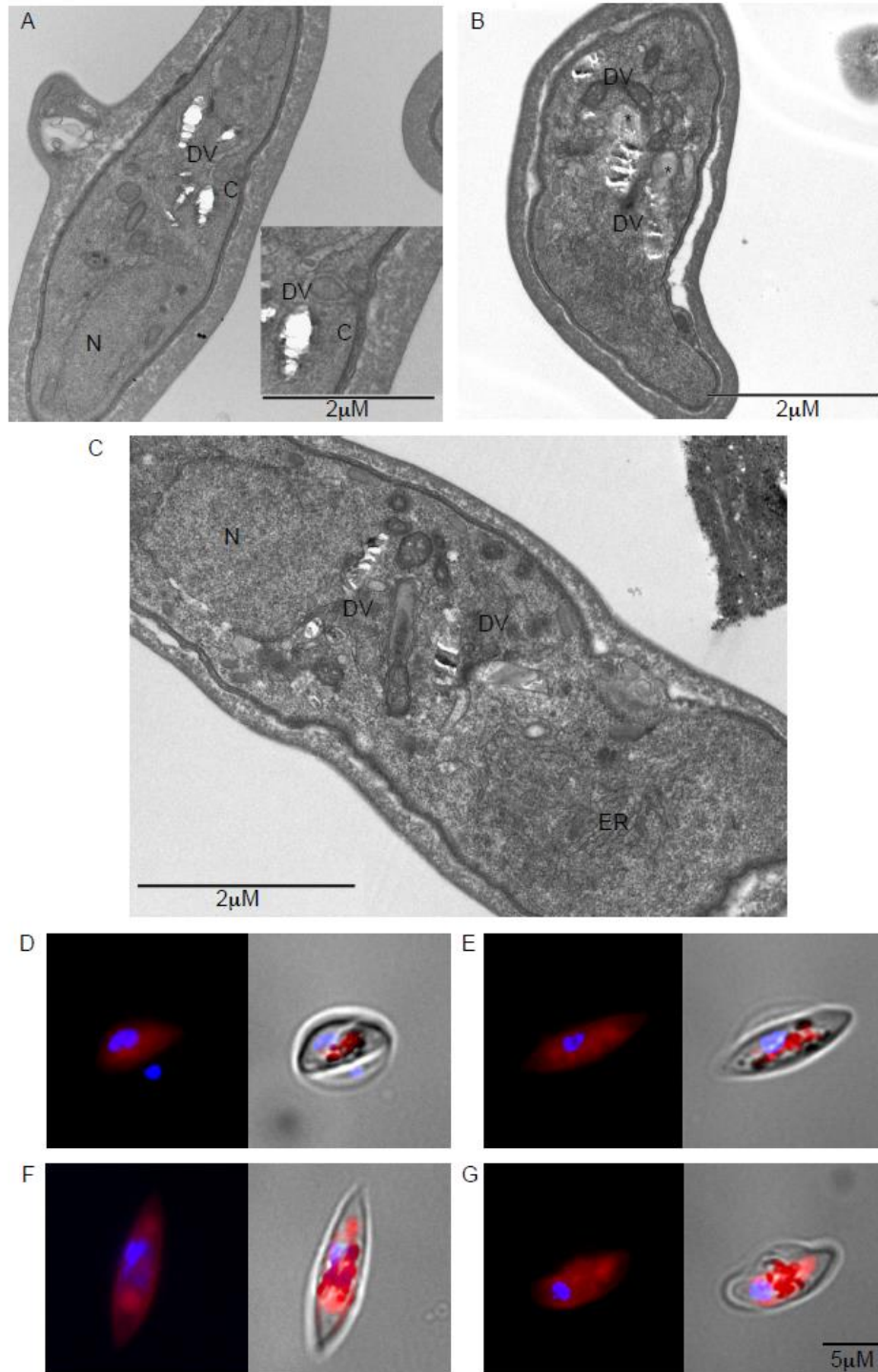


**Figure 6.** The digestive vacuole in gametocyte development. (A-C) Ultrastructural analysis of stage IV and stage V 3D7 gametocytes shows the active endocytosis of infected erythrocyte cytoplasm in stage IV gametocytes (A) through a cytotome (indent of panel A) and the accumulation of hemozoin in membrane surrounded vesicles constituting the fragmented food vacuole typical of gametocytes. In stage V gametocytes the hemozoin-containing vesicles are still present enclosed in a membrane (B, C). The asterisk (\*) indicates absence of hemozoin in digestive vacuole vesicles. C indicates cytotome, ER indicates endoplasmic reticulum, DV indicates digestive vacuole, and N indicates nucleus. Magnification bar: 2 μM. (D-G) LysoTracker staining of gametocytes at stage II (D), III (E), IV (F) and V (G) of maturation. A tight co-localization of LysoTracker fluorescence and dark haemozoin granules is evident in stage II and III gametocytes, whereas in stage IV and V areas of the acidic compartment are devoid of pigment granules. Magnification bar: 5 μM.

## Discussion

In this study, we show that PfMDR1 mediates resistance to ACT-451840, a potent piperazine-containing molecule. PfMDR1 is known to modulate sensitivities to a variety of antimalarials such as lumefantrine, quinine, and artemisinin, and chloroquine (Valderramos and Fidock 2006), and populations of parasites have been identified around the world that have evolved resistance to these drugs. It is therefore noteworthy that PfMDR1 polymorphisms that confer resistance to ACT-451840 and compounds in this chemical class do not confer cross-resistance to mefloquine, lumefantrine, halofantrine, quinine, monodesethyl amodiaquine, chloroquine, monodesethyl chloroquine, or artesunate. Furthermore, ACT-451840-resistant parasites were not rendered more fit compared to ACT-451840-sensitive parasites, indicating that they will likely be unable to outcompete sensitive parasites in the wild.

The majority of PfMDR1 mutations in ACT-451840-pressured parasites were found in the loop between TMD 5 and 6 that protrudes into the DV, or in the DV-facing portions of TMD 6 to 9 and TMD 12, suggesting that this region is important for ACT-451840 interaction. PfMDR1 is thought to orient on the DV membrane and efflux drug into the DV. Mutations in PfMDR1 may work to sequester drug in the DV and prevent its action in the cytoplasm of resistant lines, or, alternatively, PfMDR1 mutations may decrease drug influx into the DV-localized drug target.

In a 3D model of PfMDR1 (Patel et al., 2013), the loop between TMD 5 and TMD 6, as well as portions of TMD7 and TMD8 stick out into the DV. Y290F, G297V, and G316R lie in the loop between TMD 5 and TMD 6. Looking at mutations on the wild-type NF54 background, we see that mutations in this region result in high levels of resistance (NF54 MDR1 Y290F: IC<sub>50</sub> of 23 nM, a 38-fold increase over wild-type; NF54 MDR1 G297V: IC<sub>50</sub> of 51 nM, a 85-fold increase over wild-type). Compare these values to I321F, a nearby mutation buried in TMD 6, which displays an IC<sub>50</sub> of 7 nM, a mere 11-fold increase over wild-type.

The positional change matters, but so does the identity of the substitution. It is likely that position 807 in TMD 7 juts out into the DV. For this position, we have produced two different mutations: NF54 MDR1 A807P and NF54 MDR1 A807V. Although both these mutations yield resistance (a 108- and a 34-fold increase in IC<sub>50</sub> over wild-type values, respectively), the A807P mutation results in a three-fold increase in resistance compared to the A807V mutation (IC<sub>50</sub> of 65 nM vs. 20 nM). Alanine, valine, and proline are all non-polar, aliphatic molecules, but proline is known to introduce kinks in the beta sheet structure, thus causing a conformational change that might favor sequestration of drug away from its target.

The observation that hemoglobin digestion no longer takes place after gametocytes reach stage IV (Hanssen et al., 2012) may suggest that the digestive vacuole is not functional in stage V gametocytes. Indeed, *pfmdr1* transcripts were found to be down-regulated in late (stage V) gametocytes, as detected by strand-specific RNA-seq Illumina-based sequencing (Lopez-Barragan et al., 2011). Nevertheless, a proteomics analysis of synchronized parasites found comparable normalized emPAI values for PfMDR1 peptides in trophozoites, early (stage I/II) and late (stage V) gametocytes. This was in contrast to those of PfCRT, whose peptides were only found in trophozoites but not in sexual stages (Silvestrini et al., 2010). Measurable hemoglobin digestion and morphological evidence of cytostomes engulfing infected red blood cell cytoplasm in stage II-III gametocytes (Hanssen et al., 2012; Lanfrancotti et al., 2007) and in

stage IV gametocytes (this work) argue for the presence of an active food vacuole in early and mid stage gametocytes. The observation that ACT-451840 is a potent inhibitor of early and late gametocytes, and that mutant PfMDR1 confers resistance in these stages was therefore not surprising. In contrast, the observed activity of ACT-451840 against stage V gametocytes, and the significant increase in the IC<sub>50</sub> values conferred to late sexual stages by the PfMDR1 mutations, either selected for or engineered in the parasite genome, is in contrast with the current notion that digestive vacuole activity and hemoglobin digestion have ceased in late gametocytes. Ultrastructural and functional evidence based on LysoTracker staining indicates that in stage V gametocytes this compartment is present as several acidic vesicles surrounded by a membrane, representing the likely cellular sites where PfMDR1 resides. The observation that mutant PfMDR1 is able to confer a dramatic increase in resistance to ACT-451840 in these stages provides strong evidence that PfMDR1 is functional on these vesicles even after the end of hemoglobin digestion, when this protein may play a yet to be defined function.

These results argue against the notion that stage V gametocytes are metabolically quiescent. In this respect the observation that gametocytes are sensitive to inhibitors of the electron transport system such as antimycin A and cyanide (Krungskrai et al., 2000), indicate that the mitochondria of late gametocytes are still metabolically active.

### Authorship statement

I performed all the experiments on immature and mature gametocytes, except for the ultrastructural analysis.

### References

Ariey, F., Witkowski, B., Amaratunga, C., Beghain, J., Langlois, A.C., Khim, N., Kim, S., Duru, V., Bouchier, C., Ma, L., Lim, P., Leang, R., Duong, S., Sreng, S., Suon, S., Chuor, C.M., Bout, D.M., Ménard, S., Rogers, W.O., Genton, B., Fandeur, T., Miotto, O., Ringwald, P., Le Bras, J., Berry, A., Barale, J.C., Fairhurst, R.M., Benoit-Vical, F., Mercereau-Puijalon, O., and Ménard D. (2014). A molecular marker of artemisinin-resistant *Plasmodium falciparum* malaria. *Nature*. 505, 50-5.

Ashley, E.A., Dhorda, M., Fairhurst, R.M., Amaratunga, C., Lim, P., Suon, S., Sreng, S., Anderson, J.M., Mao, S., Sam, B., Sopha, C., Chuor, C.M., Nguon, C., Sovannaroeth, S., Pukrittayakamee, S., Jittamala, P., Chotivanich, K., Chutasmit, K., Suchatsoonthorn, C., Runchaoren, R., Hien, T.T., Thuy-Nhien, N.T., Thanh, N.V., Phu, N.H., Htut, Y., Han, K.T., Aye, K.H., Mokuolu, O.A., Olaosebikan, R.R., Folaranmi, O.O., Mayxay, M., Khanthavong, M., Hongvanthong, B., Newton, P.N., Onyamboko, M.A., Fanello, C.I., Tshefu, A.K., Mishra, N., Valecha, N., Phyto, A.P., Nosten, F., Yi, P., Tripura, R., Borrmann, S., Bashraheil, M., Peshu, J., Faiz, M.A., Ghose, A., Hossain, M.A., Samad, R., Rahman, M.R., Hasan, M.M., Islam, A., Miotto, O., Amato, R., MacInnis, B., Stalker, J., Kwiatkowski, D.P., Bozdech, Z., Jeeyapant, A., Cheah, P.Y., Sakulthaew, T., Chalk, J., Intharabut, B., Silamut, K., Lee, S.J., Vihokhern, B., Kunasol, C., Imwong, M., Tarning, J., Taylor, W.J., Yeung, S., Woodrow, C.J., Flegg, J.A., Das, D., Smith, J., Venkatesan, M., Plowe, C.V., Stepniewska, K., Guerin, P.J., Dondorp, A.M., Day, N.P., and White, N.J.; Tracking Resistance to Artemisinin Collaboration (TRAC). (2014). Spread of artemisinin resistance in *Plasmodium falciparum* malaria. *N Engl J Med*. 371, 411-23.

Bohórquez, E.B., Chua, M., and Meshnick, S.R. (2012). Quinine localizes to a non-acidic compartment within the food vacuole of the malaria parasite *Plasmodium falciparum*. *Malar J.* 11, 350.

Bruderer, S., Hurst, N., de Kanter, R., Miraval, T., Pfeifer, T., Donazzolo, Y., and Dingemans, J. (2015). First-in-humans study of the safety, tolerability, and pharmacokinetics of ACT-451840, a new chemical entity with antimalarial activity. *Antimicrob Agents Chemother.* 59, 935-42.

Brunner, R., Ng, C.L., Aissaoui, H., Akabas, M.H., Boss, C., Brun, R., Callaghan, P.S., Corminboeuf, O., Fidock, D.A., Frame, I.J., Heidmann, B., Le Bihan, A., Jenö, P., Mattheis, C., Moes, S., Müller, I.B., Paguio, M., Roepe, P.D., Siegrist, R., Voss, T., Welford, R.W., Wittlin, S., and Binkert, C. (2013). UV-triggered affinity capture identifies interactions between the *Plasmodium falciparum* multidrug resistance protein 1 (PfMDR1) and antimalarial agents in live parasitized cells. *J Biol Chem.* 288, 22576-83.

D'Alessandro, S., Silvestrini, F., Dechering, K., Corbett, Y., Parapini, S., Timmerman, M., Galastri, L., Basilico, N., Sauerwein, R., Alano, P., and Taramelli D. (2013). A *Plasmodium falciparum* screening assay for anti-gametocyte drugs based on parasite lactate dehydrogenase detection. *J Antimicrob Chemother.* 68, 2048-58.

Dharia, N.V., Sidhu, A.B., Cassera, M.B., Westenberger, S.J., Bopp, S.E., Eastman, R.T., Plouffe, D., Batalov, S., Park, D.J., Volkman, S.K., Wirth, D.F., Zhou, Y., Fidock, D.A., and Winzler EA. (2009). Use of high-density tiling microarrays to identify mutations globally and elucidate mechanisms of drug resistance in *Plasmodium falciparum*. *Genome Biol.* 10, R21.

Doench, J.G., Hartenian, E., Graham, D.B., Tothova, Z., Hegde, M., Smith, I., Sullender, M., Ebert, B.L., Xavier, R.J., and Root, D.E. (2014). Rational design of highly active sgRNAs for CRISPR-Cas9-mediated gene inactivation. *Nat Biotechnol.* 32, 1262-7.

Dondorp, A.M., Nosten, F., Yi, P., Das, D., Phyto, A.P., Tarning, J., Lwin, K.M., Ariey, F., Hanpithakpong, W., Lee, S.J., Ringwald, P., Silamut, K., Imwong, M., Chotivanich, K., Lim, P., Herdman, T., An, S.S., Yeung, S., Singhasivanon, P., Day, N.P., Lindegardh, N., Socheat, D., and White, N.J. (2009). Artemisinin resistance in *Plasmodium falciparum* malaria. *N Engl J Med.* 361, 455-67.

Ekland, E.H., Schneider, J., and Fidock, D.A. (2011). Identifying apicoplast-targeting antimalarials using high-throughput compatible approaches. *FASEB J.* 25, 3583-93.

Fidock, D.A., and Wellems, T.E. (1997). Transformation with human dihydrofolate reductase renders malaria parasites insensitive to WR99210 but does not affect the intrinsic activity of proguanil. *Proc. Natl. Acad. Sci. U.S.A.* 94, 10931-10936.

Foote, S.J., and Cowman, A.F. (1994). The mode of action and the mechanism of resistance to antimalarial drugs. *Acta Trop.* 56, 157-71.

Ghorbal, M., Gorman, M., Macpherson, C.R., Martins, R.M., Scherf, A., Lopez-Rubio, J.J. (2014). Genome editing in the human malaria parasite *Plasmodium falciparum* using the CRISPR-Cas9 system. *Nat Biotechnol.* 32, 819-21.

Hanssen, E., Knoechel, C., Dearnley, M., Dixon, M.W., Le Gros, M., Larabell, C., and Tilley L. (2012). Soft X-ray microscopy analysis of cell volume and hemoglobin content in erythrocytes infected with asexual and sexual stages of *Plasmodium falciparum*. *J Struct Biol.* 177, 224-32.

Higgins, C.F. (2007). Multiple molecular mechanisms for multidrug resistance transporters. *Nature.* 446, 749-57.

Kariuki, M.M., Kiara, J.K., Mulaa, F.K., Mwangi, J.K., Wasunna, M.K., and Martin, S.K. (1998). *Plasmodium falciparum*: purification of the various gametocyte developmental stages from in vitro-cultivated parasites. *Am J Trop Med Hyg.* 59, 505-8.

Klein, T.A., Tada, M.S., and Lima, J.B. (1991). Infection of *Anopheles darlingi* fed on patients with *Plasmodium falciparum* before and after treatment with quinine or quinine plus tetracycline. *Am J Trop Med Hyg.* 44, 604-8.

Krungkrai, J., Prapunwattana, P., and Krungkrai, S.R. (2000). Ultrastructure and function of mitochondria in gametocytic stage of *Plasmodium falciparum*. *Parasite.* 7, 19-26.

Lanfrancotti, A., Bertuccini, L., Silvestrini, F., and Alano, P. (2007). *Plasmodium falciparum*: mRNA co-expression and protein co-localisation of two gene products upregulated in early gametocytes. *Exp Parasitol.* 116, 497-503.

López-Barragán, M.J., Lemieux, J., Quiñones, M., Williamson, K.C., Molina-Cruz, A., Cui, K., Barillas-Mury, C., Zhao, K., and Su, X.Z. (2011). Directional gene expression and antisense transcripts in sexual and asexual stages of *Plasmodium falciparum*. *BMC Genomics.* 12, 587.

Patel, S.K., George, L.B., Prasanth Kumar, S., Highland, H.N., Jasrai, Y.T., Pandya, H.A., and Desai KR. (2013). A Computational Approach towards the Understanding of *Plasmodium falciparum* Multidrug Resistance Protein 1. *ISRN Bioinform.* 2013, 437168.

Peatey, C.L., Skinner-Adams, T.S., Dixon, M.W., McCarthy, J.S., Gardiner, D.L., and Trenholme, K.R. (2009). Effect of antimalarial drugs on *Plasmodium falciparum* gametocytes. *J Infect Dis.* 200, 1518-21.

Phyo, A.P., Nkhoma, S., Stepniewska, K., Ashley, E.A., Nair, S., McGready, R., ler Moo, C., Al-Saai, S., Dondorp, A.M., Lwin, K.M., Singhasivanon, P., Day, N.P., White, N.J., Anderson, T.J., and Nosten, F. (2012). Emergence of artemisinin-resistant malaria on the western border of Thailand: a longitudinal study. *Lancet*. 379, 1960-6.

Reed, M.B., Saliba, K.J., Caruana, S.R., Kirk, K., and Cowman AF. (2000). Pgh1 modulates sensitivity and resistance to multiple antimalarials in *Plasmodium falciparum*. *Nature*. 403, 906-9.

Sanchez, C.P., Rotmann, A., Stein, W.D., and Lanzer M. (2008). Polymorphisms within PfMDR1 alter the substrate specificity for anti-malarial drugs in *Plasmodium falciparum*. *Mol Microbiol*. 70, 786-98.

Sidhu, A.B., Uhlemann, A.C., Valderramos, S.G., Valderramos, J.C., Krishna, S., and Fidock DA. (2006). Decreasing pfmdr1 copy number in *Plasmodium falciparum* malaria heightens susceptibility to mefloquine, lumefantrine, halofantrine, quinine, and artemisinin. *J Infect Dis*. 194, 528-35.

Silvestrini, F., Lasonder, E., Olivieri, A., Camarda, G., van Schaijk, B., Sanchez, M., Younis Younis, S., Sauerwein, R., and Alano, P. (2010). Protein export marks the early phase of gametocytogenesis of the human malaria parasite *Plasmodium falciparum*. *Mol Cell Proteomics*. 9, 1437-48.

Sinden, R.E. (1982). Gametocytogenesis of *Plasmodium falciparum* in vitro: ultrastructural observations on the lethal action of chloroquine. *Ann Trop Med Parasitol*. 76, 15-23.

Smalley, M.E. (1977). *Plasmodium falciparum* gametocytes: The effect of chloroquine on their development. *Trans R Soc Trop Med Hyg*. 71, 526-9.

Straimer, J., Gnädig, N.F., Witkowski, B., Amaratunga, C., Duru, V., Ramadani, A.P., Dacheux, M., Khim, N., Zhang, L., Lam, S., Gregory, P.D., Urnov, F.D., Mercereau-Puijalon, O., Benoit-Vical, F., Fairhurst, R.M., Ménard, D., and Fidock DA. (2015). Drug resistance. K13-propeller mutations confer artemisinin resistance in *Plasmodium falciparum* clinical isolates. *Science*. 347, 428-31.

Tun, K.M., Imwong, M., Lwin, K.M., Win, A.A., Hlaing, T.M., Hlaing, T., Lin, K., Kyaw, M.P., Plewes, K., Faiz, M.A., Dhorda, M., Cheah, P.Y., Pukrittayakamee, S., Ashley, E.A., Anderson, T.J., Nair, S., McDew-White, M., Flegg, J.A., Grist. E.P., Guerin, P., Maude, R.J., Smithuis, F., Dondorp, A.M., Day, N.P., Nosten, F., White, N.J., and Woodrow, C.J. (2015). Spread of artemisinin-resistant *Plasmodium falciparum* in Myanmar: a cross-sectional survey of the K13 molecular marker. *Lancet Infect Dis*. 15, 415-21.

Valderramos, S.G., and Fidock, D.A. (2006). Transporters involved in resistance to antimalarial drugs. *Trends Pharmacol Sci*. 27, 594-601.

Veiga, M.I., Ferreira, P.E., Jörnham, L., Malmberg, M., Kone, A., Schmidt, B.A., Petzold, M., Björkman, A., Nosten, F., Gil, J.P. (2011). Novel polymorphisms in Plasmodium falciparum ABC transporter genes are associated with major ACT antimalarial drug resistance. *PLoS One*. 6, e20212.

Wagner, J.C., Platt, R.J., Goldfless, S.J., Zhang, F., and Niles, J.C. (2014). Efficient CRISPR-Cas9-mediated genome editing in Plasmodium falciparum. *Nat Methods*. 11, 915-8.

WHO World Malaria Report 2014

([http://www.who.int/malaria/publications/world\\_malaria\\_report/en/](http://www.who.int/malaria/publications/world_malaria_report/en/))

WHO World Malaria Report 2015

([http://www.who.int/malaria/publications/world\\_malaria\\_report/en/](http://www.who.int/malaria/publications/world_malaria_report/en/))

Zhang, C., Xiao, B., Jiang, Y., Zhao, Y., Li, Z., Gao, H., Ling, Y., Wei, J., Li, S., Lu, M., Su, X.Z., Cui, H., and Yuan J. (2014). Efficient editing of malaria parasite genome using the CRISPR/Cas9 system. *MBio*. 5, e01414-14.



## General discussion and conclusions

Malaria is a parasitic disease caused by five different Plasmodium species. *P. falciparum* is the most dangerous species causing annually most of the deaths for malaria in the world (WHO, 2015). The spread of the disease in the tropical areas is linked to the presence of the *Anopheles* mosquito, the obliged host of the parasite and vector of the disease between the different human hosts.

In the human host takes place the development of the parasite sexual transmission forms, the gametocytes, ingested by the mosquito during its blood-meal. The mechanisms driving gametocyte development from asexual blood stage parasites are still not completely clear, although they recently started to be elucidated (Kafsack et al., 2014). Gametocytogenesis takes place in 10-12 days during which parasites develop through five different maturation stages forming, in the first 6-7 days, immature gametocytes (stage I, II, III and IV) and then mature gametocytes (stage V) which, once in the mosquito, continue the parasite life cycle giving rise to the mosquito stages that will be injected in the blood of the next human host during the next mosquito bloodmeal.

Gametocytogenesis is a silent phenomenon. Gametocytes do not cause any symptoms, are sequestered in internal organs (Joice et al., 2014) as immature stages and, once they are mature, freely circulate in the human bloodstream for up to fifteen days, until they are ingested by the mosquito.

Drugs against malaria are typically directed only against the asexual blood forms of the parasite, due to the intention to cure the symptoms of this lethal disease. Very recently, the word “eradicating”, referred to malaria, started to be pronounced. One of the mechanisms necessary to eradicate malaria is to block the transmission from the human host to the mosquito killing gametocytes.

The debate on how to block malaria transmission started. The main questions regarding this point were as follows:

- What stage of gametocytogenesis must be hit, the immature, the mature gametocytes or both?
- How to determine, *in vitro*, if a compound is active against gametocytes?
- How to determine if hit gametocytes are still infective to the mosquito?
- Which compounds can be tested against gametocytes?

Theoretically killing immature gametocytes means blocking their development to mature gametocytes. It should be considered that immature gametocytes are not detectable in the human bloodstream during malaria infection but they are sequestered in internal organs, such as the spleen, the liver, the lungs but mostly the bone marrow. For these reasons, some sequestered immature gametocytes could escape from drug treatment to be released in circulation once mature, where they can play their role of being directly responsible for the transmission to the mosquito. Targeting mature gametocytes would mean targeting the forms directly infectious to the vector, once ingested by the mosquito. For this reason most of the attention focused on finding compounds able to specifically kill mature gametocytes, decreasing the priority towards compounds able to kill both early and late stage gametocytes.

Determining if a compound or a drug is active against gametocytes is more difficult than to determine if it is able to kill asexual blood stage parasites. This is mainly due to the non-replicating nature of gametocytes. Most of drug-screening assays on asexual blood-stages are typically based on the incorporation of intercalant dyes or radioactive isotopes in the newly replicated parasite DNA or on the detection of the activity of the parasite lactate dehydrogenase (pLDH), in both cases measuring parasite proliferation, a parameter which cannot be used on gametocytes.

The development of *Plasmodium* transgenic lines expressing reporter genes during their asexual life cycle changed the drug-screening assay methods. This first happened thanks to parasite transgenic lines expressing fluorescent proteins, as the Green Fluorescent Protein (GFP) and then thanks to parasite transgenic lines expressing enzymes as luciferases, able to convert the energy from using a specific chemical substrate (luciferin) into light, measured by a luminometer.

*P. falciparum* transgenic lines improved high throughput screening assays (HTS) allowing to screen a large number of compounds against asexual blood stage parasites, especially as the parasite resistance to many common antimalarial drugs became an urgent problem and finding new active drugs is a priority.

In order to perform HTS assays on gametocytes it became important how to evaluate if a gametocyte is dead or useless after the treatment with a specific compound, together with the necessity of making this evaluation fast, efficient and suitable for large scale use.

One of the problems is that, from a morphological point of view, a dead gametocyte usually looks like a healthy one. From this point of view, transgenic lines expressing fluorescent proteins are not suited for gametocyte HTS assays, because proteins such as the GFP are characterized by a long half-life and are detectable also in a dead cell.

In this scenario, enzymatic and functional or phenotypic cell-based assays have been chosen to develop and perform HTS assays on immature and mature gametocytes. The contribution of my laboratory involved the development of two enzymatic assays using transgenic gametocytes expressing luciferase reporter genes and one functional assay that does not need any parasite transgenic line, and that can be used to test compounds on lines of any genotypes, including gametocytes from drug resistant lines or field isolates from patients.

The idea to develop a dual color luciferase assay stemmed from the idea that (i) it would be important to screen for drugs active against both immature and mature gametocytes and (ii) luciferases naturally exist, and can be modified to emit light at different wavelengths (i.e. different colors); in addition, luciferases can be also modified to have a more stable activity at a given temperature or pH.

In addition, we wanted to explore more bioluminescent enzymes, as only the luciferases from the firefly *Photinus pyralis* or from the sea pansy *Renilla reniformis* had been, until our work, commonly used in Plasmodium.

We selected two luciferases from the clickbeetle *Phyrophorus plagiotalamus*, natural variants of this enzyme able to emit a red colored (CBR) or a green colored light (CBG99). When these reporters were transfected in the malaria parasites, these two luciferases demonstrated a higher efficiency in *P. falciparum* than the one commonly used in malaria. Put under the transcriptional control of the upstream and the downstream regulatory regions of the *pfs16* gene, parasites express these enzymes during all stages of gametocytogenesis. This allowed us to mix immature gametocytes expressing CBR

and mature gametocytes expressing CBG99, or the opposite, in order to test at the same time the ability of compounds to kill gametocytes at different stages of maturation. In this assay the viability of gametocytes is measured by a luminometer equipped with specific filters that specifically acquire each colored light (Cevenini et al., 2014) and by an algorithm that calculate the activity of the individual luciferases from the two population of parasites. Testing control drugs able to kill early stage gametocytes (e.g. chloroquine) or both early and late stage gametocytes (e.g. epoxomicin) demonstrated the validity of this innovative assay.

In this work we addressed another important issue: many commercial luciferase substrate kits contain not only the enzyme substrate luciferin, but also lysing solutions, ATP, signal enhancers and stabilizers, which together increase luciferase activity. As this could possibly result in detecting luciferase activity also from a dead cell, we introduced the idea to use, as luciferase substrate, D-luciferin in the absence of any of the above substances. This was done in order to more reliably monitor the viability of cells that will emit light only when express the luciferase but also only when it will use its own ATP for luciferase activity (not the one from the kit), indicating in this way that it is alive.

The dual color luciferase assay, together with the use of D-luciferin substrate, is very innovative in malaria but can be applied to many other parasites, both for applicative and fundamental research studies.

The dual color assay presented above uses two different *P. falciparum* transgenic lines expressing two different luciferases under the same promoter, *pfs16*, active during all gametocytogenesis. To develop assays highly specific for late stage gametocytes, we were interested in identifying a promoter active only in mature gametocytes of *P. falciparum*. Our purpose was to develop a transgenic line expressing under such specific promoter the potent CBG99 luciferase described above (Cevenini et al., 2014).

To identify this type of promoter from *P. falciparum*, we used transcriptomic analysis to select ten possible candidate genes whose transcripts were absent during asexual blood stages of development, while started to be expressed during gametocytogenesis and reached maximum accumulation in mature gametocytes. We were aware that from these data on mature mRNA we could not exactly know when the respective promoters started to be active during gametocytogenesis and also of the fact that they could be translationally repressed in mature gametocytes, being translated only in gametes (Mair et al., 2006).

We cloned the 5' upstream and the 3' downstream regions of the ten genes driving GFP expression in ten different plasmids, with which we transfected *P. falciparum* parasites. The evaluation of the GFP expression on early and late stage gametocytes allowed us to select a pair of regulatory regions (those of the *pf1675c/ULG8* gene) which resulted to be efficiently active only in mature gametocytes. We used this pair of genomic regions to drive CBG99 luciferase expression in a construct which was integrated in a *P. falciparum* locus as a chromosomally integrated cassette. Importantly, the resulting *P. falciparum* transgenic line showed the same pattern of luciferase expression and activity as the one we observed in the plasmid selection process for the episomally expressed GFP.

The development of this ULG8-CBG99 transgenic line is innovative and important in HTS assays, giving the opportunity to test drugs and compounds specifically against mature gametocytes of *P. falciparum*, the stages directly responsible of the transmission from the human host to the mosquito.

We next tested if mature gametocytes, after pharmacological treatments, were still infective to the *Anopheles* mosquito. The Standard Membrane Feeding Assay (SMFA) consists in feeding mosquitoes with blood infected by mature gametocytes, which were previously treated with a selected drug. Seven to twelve days later, fed mosquitoes are dissected and examined by microscopy for the presence of oocysts (Mulder B et al., 1999). Although many advantages were achieved using transgenic parasites first expressing a GFP (Stone et al., 2014) and then expressing a luciferase (Stone et al., 2015), this assay is not suitable for HTS, being very laborious, time consuming and expensive. Finding an alternative assay is one of the priorities in the investigation for anti-transmission drugs.

As alternative to the SMFA, functional assays evaluating the ability of gametocytes to form gametes after drug treatments *in vitro* have been developed. One of these assays is the dual gamete formation assay, developed in 2014 at the Imperial College of London by the group of Michel Delves (Ruecker et al., 2014). This assay, which is high throughput in the 96-well plate format, consists in treating mature gametocytes with a compound and in evaluating the ability of female gametocytes to form female macrogametes and of male gametocytes to exflagellate, after addition of the proper stimulus (XA, xanthurenic acid).

Limitations of this assay are due to the necessity of using an antibody for detecting female gametes and to the difficulty and the inaccuracy in automatically counting the male exflagellation centers, which are visible only for a few minutes.

We developed a functional imaging assay based on the assumption that only healthy female mature gametocytes are able to mature in macrogametes. This assay, developed for HTS in a 384-well plate format, gives the opportunity to identify compounds active against mature gametocytes by automatically counting banana shape gametocytes and round shaped macrogametes, after the treatment with a compound and the addition of XA, using a Scan<sup>R</sup> automated imaging cytometry station. Importantly this assay simultaneously identifies compounds killing gametocytes and those making them unable to transform into gametes.

Although this assay was developed using a transgenic line (pfl1675c/ULG8-GFP) it does not necessarily need using a transgenic line. The assay was improved by staining the parasites before image acquisition with the fluorescent dye acridine orange (AO), an inexpensive fluorescent dye that allows the instrument to count fluorescent gametocytes and gametes.

The assay, with its unique features, allows not only to test compound activity against mature gametocytes, but also to test their ability, after the treatment, to mature in those forms necessary into the mosquito to be fertilized by male microgametes. Furthermore, the assay does not need staining by antibody, reducing both costs and time, and does not need any transgenic line, being suitable for the screening of mature gametocytes from any laboratory line or field isolate.

Importantly, all the assays mentioned above, could be used in a complementary approach to evaluate compounds activity in anti-transmission HTS assays, comparing the  $IC_{50}$  resulting from the most promising compounds with the  $IC_{50}$  of the same compounds obtained by the SMFA, which still remains the best non-HTS assay for testing anti-transmission compounds.

We demonstrated to have enough assays to test compounds against gametocytes, especially against mature gametocytes.

The next question concerned which compounds, and how many, should be tested. The assays described above allow testing entire libraries of compounds, being urgent the necessity to block *P. falciparum* transmission. The compounds selected by different companies, may be either or not active also against the asexual blood stage parasites, although those able to cure malaria symptoms were the first selected to be tested against mature gametocytes. Unfortunately, most of the compounds active against asexual blood stage parasites and against immature gametocytes, are inactive against mature stage V gametocytes (Adjalley et al., 2011), and the only drug able to kill *P. falciparum* mature gametocytes (i.e. primaquine) shows side effect when used in humans.

One explanation for the reason why many compounds active against asexual blood stages and immature gametocytes of *P. falciparum* are inactive against mature gametocytes may reside in the possibility that stage V gametocytes have a different/slower metabolism than other stages of development of the parasites. This insensitivity against many drugs made mature stage V gametocytes being considered as apparently quiescent cells. Thus, finding metabolic pathways active in mature gametocytes means challenging the current view of their quiescence, approaching to block *P. falciparum* transmission.

A step forward was the finding that methylene blue (MB) kills mature stage V gametocytes of *P. falciparum* (Adjalley et al., 2011). MB was demonstrated to act in asexual blood stage parasites as a redox cyler: it counteracts the redox balance of the parasite being reduced by the enzyme glutathione reductase (GR), consuming all NADPH and O<sub>2</sub> and generating oxygen species toxic for the parasite (Ehrhardt et al., 2013).

*P. falciparum* GR uses NADPH, mostly produced by the pentose phosphate pathway (PPP), to reduce glutathione, that once reduced (GSH), participate to counteract the oxidative stress deriving from the haemoglobin digestion of the parasite. Because of haemoglobin digestion was demonstrated not to occur in mature stage V gametocytes (Hanssen et al., 2012), we hypothesized that either MB has other mechanisms of action than the one described above, or that mature gametocytes still have active redox metabolic pathways to counteract oxidative stress resulting from something different from haemoglobin digestion.

To understand the mechanism of action of MB on mature stage V gametocytes, we decided to use the Pfl1675c/ULG8-CBG99 line and the bioluminescent assay that we specific developed for mature gametocytes. We tested the activity of different compounds known to counteract the redox metabolism of the parasites both in comparison and in combination with MB. None of the compounds we tested was able to kill mature gametocytes after a 24 hours treatment but intriguingly the ML304 resulted able to synergize the activity of MB on mature stage V gametocytes, decreasing its IC<sub>50</sub> of about 20 fold. The ML304 is a probe described to block, on asexual blood stage parasites, the activity of the *P. falciparum* glucose-6-phosphate dehydrogenase 6-phosphogluconolactonase (PfGluPho) (Maloney et al., 2010), a bifunctional enzyme that catalyzes the first two steps of the PPP, necessary for NADPH production. This probe is completely inactive against the human G6PD.

This work is still ongoing and we still have to answer many questions. So far, the results we obtained confirmed that the redox metabolism is still active in mature stage V gametocytes and that it is a target of MB also in mature gametocytes of *P. falciparum*. We also demonstrated that it is possible to decrease the IC<sub>50</sub> of an active compound by a combination treatment on mature gametocytes (synergy).

In another project, we tested on both immature and mature gametocytes of *P. falciparum* the activity of a piperazine-containing compound, the Actelion-451840 (Act-451840) that showed a high activity against asexual blood stage parasites. David Fidock's group found that the target of this compound is the multidrug resistance protein 1 of *P. falciparum* (PfMDR1), selecting and generating Act-451840 resistant parasites: they observed, in asexual blood stage parasites, that the resistance was due to different point mutations on the gene coding for this protein. Mutations in *pfmdr1*, different from that giving resistance to the Act-451840, are associated to *P. falciparum* resistance to others antimalarials as chloroquine.

PfMDR1 resides on the membrane of the digestive vacuole of the parasites, which is the site where haemoglobin digestion occurs. As mentioned above, haemoglobin digestion was demonstrated to occur during all asexual parasite development and during gametocytes until stage IV of gametocyte maturation (Hanssen et al., 2012).

By testing the activity of Act-451840 on both early and late stage gametocytes of two different lines of *P. falciparum* (one line resistant to chloroquine and one wild-type line) we found that the drug was active not only against immature but also against mature gametocytes. The surprise was linked to the fact that we found a drug which was very active against mature gametocytes, with an IC<sub>50</sub> comparable to the one shown for asexual blood stages. We demonstrated also that mutant lines in the *pfmdr1* gene maintained resistance to the Act-451840 in both early and mature stage gametocytes, as shown for the asexual stage parasites. This evidence coupled to our demonstration that the site where PfMDR1 resides is still present in stage V gametocytes, suggested an unexpected function of the PfMDR1 protein in mature stage V gametocytes that could be addressed by a family of drugs against mature gametocytes.

All this work aimed at providing significant innovations for the important necessity to find drugs able to block *P. falciparum* transmission. The development of different enzymatic and functional assays gave us the opportunity to test different compounds.

An important and interesting conclusion of this long journey is a starting point: we found active pathways in mature gametocytes that can be suitable targets for anti-transmission drugs, challenging the current view of an apparently quiescence of these transmission stage parasites.

## References

Adjalley, S.H., Johnston, G.L., Li, T., Eastman, R.T., Ekland, E.H., Eappen, A.G., Richman, A., Sim, B.K., Lee, M.C., Hoffman, S.L., and Fidock, D.A. (2011). Quantitative assessment of Plasmodium falciparum sexual development reveals potent transmission-blocking activity by methylene blue. *Proc Natl Acad Sci U S A*. 108, 1214-23.

Cevenini, L., Camarda, G., Michelini, E., Siciliano, G., Calabretta, M.M., Bona, R., Kumar, T.R., Cara, A., Branchini, B.R., Fidock, D.A., Roda, A., and Alano, P. (2014). Multicolor bioluminescence boosts malaria research: quantitative dual-color assay and single-cell imaging in Plasmodium falciparum parasites. *Anal Chem*. 86, 8814-21.

Ehrhardt, K., Davioud-Charvet, E., Ke, H., Vaidya, A.B., Lanzer, M., and Deponte, M. (2013). The antimalarial activities of methylene blue and the 1,4-naphthoquinone 3-[4-(trifluoromethyl)benzyl]-

menadione are not due to inhibition of the mitochondrial electron transport chain. *Antimicrob Agents Chemother.* 57, 2114-20.

Hanssen, E., Knoechel, C., Dearnley, M., Dixon, M.W., Le Gros, M., Larabell, C., and Tilley L. (2012). Soft X-ray microscopy analysis of cell volume and hemoglobin content in erythrocytes infected with asexual and sexual stages of *Plasmodium falciparum*. *J Struct Biol.* 177, 224-32.

Joice, R., Nilsson, S.K., Montgomery, J., Dankwa, S., Egan, E., Morahan, B., Seydel, K.B., Bertuccini, L., Alano, P., Williamson, K.C., Duraisingh, M.T., Taylor, T.E., Milner, D.A., and Marti, M. (2014). *Plasmodium falciparum* transmission stages accumulate in the human bone marrow. *Sci Transl Med.* 6, 244.

Kafsack, B.F., Rovira-Graells, N., Clark, T.G., Bancells, C., Crowley, V.M., Campino, S.G., Williams, A.E., Drought, L.G., Kwiatkowski, D.P., Baker, D.A., Cortés, A., and Llinás, M. (2014). A transcriptional switch underlies commitment to sexual development in malaria parasites. *Nature.* 507, 248-52.

Mair, G.R., Braks, J.A., Garver, L.S., Wiegant, J.C., Hall, N., Dirks, R.W., Khan, S.M., Dimopoulos, G., Janse, C.J., and Waters, A.P. (2006). Regulation of sexual development of *Plasmodium* by translational repression. *Science.* 313, 667-9.

Maloney, P., Hedrick, M., Peddibhotla, S., Hershberger, P., Milewski, M., Gosalia, P., Li, L., Preuss, J., Sugarman, E., Hood, B., Suyama, E., Nguyen, K., Vasile, S., Sergienko, E., Salanawil, S., Stonich, D., Su, Y., Dahl, R., Mangravita-Novo, A., Vicchiarelli, M., McAnally, D., Smith, L.H., Roth, G., Diwan, J., Chung, T.D.Y., Pinkerton, A.B., Bode, L., and Becker, K. (2010). A 2nd Selective Inhibitor of *Plasmodium falciparum* Glucose-6-Phosphate Dehydrogenase (*Pf*G6PDH) - Probe 2. *Probe Reports from the NIH Molecular Libraries Program [Internet]. Bethesda (MD): National Center for Biotechnology Information (US).*

Mulder, B., Lensen, T., Tchuinkam, T., Roeffen, W., Verhave, J.P., Boudin, C., and Sauerwein R. (1999). *Plasmodium falciparum*: membrane feeding assays and competition ELISAs for the measurement of transmission reduction in sera from Cameroon. *Exp Parasitol.* 92, 81-6.

Ruecker, A., Mathias, D.K., Straschil, U., Churcher, T.S., Dinglasan, R.R., Leroy, D., Sinden, R.E., and Delves, M.J. (2014). A male and female gametocyte functional viability assay to identify biologically relevant malaria transmission-blocking drugs. *Antimicrobial agents and chemotherapy.* 58, 7292-7302.

Stone, W.J., Churcher, T.S., Graumans, W., van Gemert, G.J., Vos, M.W., Lanke, K.H., et al. (2014). A Scalable Assessment of *Plasmodium falciparum* Transmission in the Standard Membrane-Feeding Assay, Using Transgenic Parasites Expressing Green Fluorescent Protein-Luciferase. *J Infect Dis.* 210, 1456-63.

Stone, W.J., and Bousema, T. (2015). The Standard Membrane Feeding Assay: Advances Using Bioluminescence. *Methods Mol Biol.* 1325, 101-12.

WHO World Malaria Report 2015  
([http://www.who.int/malaria/publications/world\\_malaria\\_report/en/](http://www.who.int/malaria/publications/world_malaria_report/en/))



## Ringraziamenti

Credo che una grandissima fortuna sia alzarsi la mattina ed essere felici di andare a lavoro. Questo è sicuramente dovuto alla grande passione che si ha per quello che si fa, ma una gran parte la fanno le persone che si hanno intorno, con cui passiamo la maggior parte delle nostre giornate. A conclusione di questi 4 anni e mezzo passati in ISS, posso dire di essere stata davvero fortunata, e lo devo a tutti quelli che ora ringrazierò.

Il mio primo e più grande grazie va a **Pietro**. Grazie per tutta la fiducia che hai avuto in me e per tutto l'aiuto e gli insegnamenti che mi hai dato in questi anni. Ti ringrazio per tutto il tempo passato a parlarmi (e a raccontarmi) di "malaria" con quell'immensa passione negli occhi che non dimenticherò mai. Grazie davvero per il tuo contagioso entusiasmo, capace di rendere ogni esperimento e ogni progetto, anche il più ambizioso, possibili. Grazie per il modo in cui sei mentore e capo, senza far mai sentire nessuno inferiore a te, nonostante la tua enorme esperienza e capacità. Grazie per esserci sempre stato, pronto a rispondere alle mie domande senza mai farmi sentire meno importante di ciò che eri impegnato a fare in quel momento (è una cosa davvero rara). Grazie per avermi sempre spinto più in là di quelle che credevo fossero le mie capacità, dandomi sempre il coraggio di migliorarmi e di crescere. Grazie per avermi trattato più da collega che da dottoranda del tuo laboratorio. Grazie per tutte le volte che non hai voluto essere ringraziato e per tutte le volte che grazie lo hai detto (o pensato) tu.

Ringrazio **Andrea**. Grazie per avermi "scelta" quel settembre del 2011. Grazie a te ho potuto iniziare uno splendido progetto su malaria (che poi sono diventati tanti). Grazie di tutto il tempo che mi hai dedicato e all'interesse e alla passione che hai messo in un argomento per te nuovo. Grazie davvero tanto.

Ringrazio **Francesco**, a parimerito grande ricercatore e amico. Grazie per tutto il tuo aiuto, senza il quale sarebbe stato impossibile arrivare a questo punto. Grazie per il tuo modo di pensare e di lavorare (si vede che tu e Pietro lavorate insieme da tanti anni, siete matti uguali - in senso buono ovviamente), è davvero ammirevole. Grazie per essere stato sempre pronto a coinvolgermi, insegnarmi, parlarmi ed ascoltarmi, non solo per quello che riguarda il lavoro.

Un grazie di cuore va a **Pablo**. Grazie per le chiacchierate, per le passeggiate in giardino, per gli abbracci, la musica, le risate, i weekend in lab, le litigate, le discussioni, i thè (che per te sono sempre una cioccolata), i libri. Grazie per la tua Amicizia. Non avrei potuto desiderare un labmate migliore. E' stato bellissimo essere PhD students insieme.

Ringrazio **Valeria**. Perchè anche se sei arrivata dopo, è come se ci fossi stata sempre. Grazie per aver portato moltissima dolcezza (non solo nei meravigliosi dolci che fai) e amicizia. Per me è davvero bello sapere che ci sei, un'amica presente ogni giorno qualche stanza più in là.

Ringrazio **Merzad**, altro splendido labmate. E' sempre bello ridere e discutere con te e Pablo degli argomenti più vari (e anche di scienza, perchè no!).

Ringrazio **Roberta** e **Lina**. Grazie per avermi insegnato tanto appena arrivata (davvero molto di quello che so ora) e per essermi state vicine in un momento in cui era tutto nuovo e, come sapete, tutto un pò difficile.

Un immenso grazie va a **David**, il mio "capo americano". E' stato bellissimo ed importante per me il modo in cui mi hai accolto in laboratorio, trattandomi come se fossi lì da sempre e per sempre, dandomi

tutta la libertà e fiducia in quello che stavo facendo. Grazie per il modo in cui esalti sempre il nostro lavoro, anche pubblicamente. Grazie per le tue brillanti idee.

Ringrazio **Marta e Grazia**, ormai sulle loro strade lontane dal nostro gruppo. Siete sempre state un modello per me, e mi avete insegnato tanto, con grande serietà e passione.

Un grande grazie va a **Marta, Betta, Tommaso, Leonardo, Anna, Gabriella e Cecilia**. Siete fortissimi “gruppo Ponzi”. Fate parte di quelle persone che sono felice di vedere tutti i giorni.

Ringrazio **Becca, Andrew, Olivia, Caroline, Ori, Stan, Marcus, Nina, Philip e Kumar**. Avete reso la mia esperienza a New York ancora più indimenticabile.

Ringrazio **Sarah, Luca, Elisa e Maddalena**. Grazie per gli scambi di materiali ed idee che ci hanno coinvolto in questi anni di “progetto GAM”. Grazie per aver condiviso con me la vostra esperienza.

Ringrazio **Donatella e Robert**. Mi avete visto “crescere”, durante questo Dottorato, da un punto di vista più esterno e i vostri consigli e segni di approvazione mi hanno aiutato moltissimo e mi hanno sempre dato una grande forza. Avete fatto molto di più di quello che potete credere.

Infine ringrazio tutte le persone, esterne alla mia vita lavorativa, ma parte della mia vita, che hanno contribuito per più della metà a rendere questi anni ancora più meravigliosi. La maggior parte di voi c’era già prima, alcuni da sempre, e spero ci sarete ancora, sempre, a condividere ognuno i traguardi dell’altro. Voi tutti siete sempre la motivazione più grande per alzarsi col sorriso ogni mattina. Grazie!